4-23-2014 12:00 AM

Targeted Proteomics of Human Pluripotent Stem Cells

Kevin Gregory Kania
The University of Western Ontario

Supervisor
Gilles Lajoie
The University of Western Ontario Joint Supervisor
Lynne Postovit
The University of Western Ontario

Graduate Program in Biochemistry
A thesis submitted in partial fulfillment of the requirements for the degree in Master of Science

Targeted Proteomics of Human Pluripotent Stem Cells

(Thesis format: Monograph)

by

Kevin Gregory Kania

Graduate Program in Biochemistry

A thesis submitted in partial fulfillment
of the requirements for the degree of
Master of Science

The School of Graduate and Postdoctoral Studies
The University of Western Ontario
London, Ontario, Canada

Abstract

Human pluripotent stem cells (hPSCs) exhibit two unique characteristics: pluripotency and self-renewal. These properties are maintained by a series of complex signaling pathways, however, quantitative data for the respective proteins is lacking. Selected reaction monitoring (SRM) is a targeted, quantitative technique in mass spectrometry that is highly sensitive in peptide detection. In this thesis, an SRM protocol was developed in order to detect and quantify a defined set of proteins responsible for maintaining stem cell pluripotency. Two hESC differentiation protocols were validated for use as model systems within which to measure differential protein expression by SRM. SRM assays were generated for thirty-three proteins and tested on cell lysates. Wnt1 and β-catenin were shown to be upregulated during differentiation, while other proteins and peptides were detected but not quantifiable. The results of this study highlight the complexity of hPSC proteome and help further the understanding of the mechanisms responsible for pluripotency.

Keywords

proteomics, human embryonic stem cells, selected reaction monitoring, mass spectrometry, hESCs, hPSCs, differentiation.

Acknowledgments

Thanks to Dr. Lynne Postovit and Dr. Gilles Lajoie for giving me the opportunity to work in this lab. Your guidance and support have been invaluable.

Thanks to Paula Pittock for advice and aid in mass spectrometry and HPLC.

Thanks to Courtney Brooks for maintaining a steady stem cell culture.

Thanks to Dr. Cheryle Seguin for the support and the stem cells.

Thanks to Gabrielle Siegers and Kristin Chadwick for help in flow cytometry analysis.

Thanks to Michael, Scott, Krista, Alia, Guihua, Padmalaya, Jonathan, Dylan, and Miljan for the help, the conversation, and the company. Trivia nights ended too soon.

Table of Contents

List of Tables

List of Figures

List of Appendices

List of Abbreviations

4-OHT – 4-hydroxytamoxifen

ACN – acetonitrile

AQUA – absolute quantification

bFGF – basic fibroblast growth factor

B-ME – β-mercaptoethanol

BMP4 – bone morphogenic protein 4

BSA – bovine serum albumin

CA1K – CA1 Sox17/ERT2 Puro Clone K cells

CE – collision energy

CID – collision induced dissociation

CM – conditioned media

DAPI - 4',6-diamidino-2-phenylindole

DCM – dichloromethane

DDA – data-dependent acquisition

DKK1 – Dickkopf-related protein 1

DMEM – Dulbecco's Modified Eagle's Medium

DMSO – dimethyl sulfoxide

DP – declustering potential

DTT – dithiothreitol

DVL1 – Dishevelled-1

EDTA – ethylenediaminetetraacetic acid

ER^{T2} – human estrogen receptor

ESI – Electrospray Ionization

FACS – fluorescence activated cell sorting

FBS – fetal bovine serum

GAA – glacial acetic acid

hESC – human embryonic stem cell

HPLC – high performance liquid chromatography

hPSC – human pluripotent stem cell

IAA – iodoacetamide

iPSC – induced pluripotent stem cell

IRES – internal ribosome entry site

iTRAQ – isobaric tag for relative and absolute quantitation

MALDI – matrix-assisted laser desorption/ionization

MEF – mouse embryonic fibroblast

mESC – mouse embryonic stem cell

MRM – multiple reaction monitoring

MS – mass spectrometry

PBS – phosphate buffered saline

PTM – post-translational modification

Q1 – quadrupole 1

Q3 – quadrupole 3

RT – retention time

S/N – signal-to-noise

SCX – strong cation exchange

SD – standard deviation

SDS-PAGE – sodium dodecyl sulfate – polyacrylamide gel electrophoresis

SHH – Sonic hedgehog

SRM – selected reaction monitoring

SSEA1 - stage-specific embryonic antigen 1

SSEA3 - stage-specific embryonic antigen 3

SSEA4 - stage-specific embryonic antigen 4

1 Introduction

1.1 Human Pluripotent Stem Cells

Human pluripotent stem cells (hPSCs), which include human embryonic stem cells (hESCs) and induced pluripotent stem cells (iPSCs) possess two unique characteristics. They are pluripotent, that is, capable of differentiating into any of the three primary germ layers of mesoderm, endoderm, and ectoderm. Secondly, they are capable of self-renewal, meaning that they can proliferate indefinitely in culture while maintaining their pluripotency, provided the proper conditions are maintained.[1] Because of these properties, hPSCs are highly valued as a research tool for modeling *in vitro* differentiation and early human development, as well as showing great promise for use in regenerative medicine. In addition, hPSCs could be used as a model system for disease and search for treatments. However, the mechanisms responsible for stem cell pluripotency and self-renewal are still poorly understood, particularly at the protein level.

1.1.1 Human Embryonic Stem Cells

hESCs were first derived by Thomson *et al*. in 1998 from donated embryos generated from *in vitro* fertilization[2]. The inner cell mass of the pre-implantation blastocyst was extracted and plated on a feeder layer of γ-irradiated mouse embryonic fibroblasts (MEFs), which release cytokines and growth factors that promote pluripotency, and allowed to expand. The derived cells exhibited characteristics such as a high nucleus to cytoplasm ratio, high telomerase activity, and cell surface markers characteristic of undifferentiated nonhuman ESCs.[3] In addition, the colonies generated were not clonal expansions from a single cell, and were therefore heterogeneous while appearing uniform. Upon injection into severe combined immunodeficient (SCID) mice, hESCs generated teratomas, exhibiting the ability to generate mesoderm, endoderm and ectoderm. Since 1998, according to Fraga *et al.*, more than 1200 hESC lines have been derived worldwide. [4]

hESCs differ from mouse embryonic stem cells (mESCs) in several different characteristics.[5] While mESCs exhibit three-dimensional tightly packed colonies and a

doubling rate of 16 hours, hESCs colonies exhibit a flattened two-dimensional structure and a doubling time of about 36 hours.[6] In addition, while leukemia inhibitory factor (LIF) and bone morphogenic protein 4 (BMP4) are required to maintain mESC pluripotency, they are not sufficient to maintain hESC pluripotency, and BMP4, in fact, directs hESCs towards differentiation. [7] Surface marker SSEA1, which signifies pluripotency in mESCs, instead marks differentiation in hESCs. hESC cultures are technically difficult to maintain, and prone to spontaneous differentiation. hESCs exhibit poor survival upon dissociation, and cannot be expanded from the single cell state in the absence of Rho-associated kinase (ROCK) inhibitor, and as such, must be passaged in small clumps.[8] Basic fibroblast growth factor (bFGF) has been identified as a required factor in stem cell growth media. [9, 10] Typically, hESC culture media consists of a basal media such as DMEM, a protein source (KnockOut Serum Replacement) and self-renewal factors such as the aforementioned bFGF.

Due to the eventual push towards clinical use, there is a trend towards the use of hESC culture in defined and xeno-free conditions.[11] hESCs are frequently maintained in feeder-free conditions, in which instead of being plated on a MEF feeder layer, hESCs are plated on an alternate matrix. These matrices include products such as Matrigel® (BD) and Geltrex™ (Life Technologies), which are basement membranes derived from mouse Engelbreth-Holm-Swarm tumors. Consisting primarily of laminin, collagen IV and enactin, these basement membranes simulate the extracellular environment required to support these cells in tissues[12]. However, hPSC growth on these matrices require the use of either a defined medium such as mTeSR™, or hESC media conditioned on a MEF feeder layer in order to supply the growth factors required to maintain pluripotency. mTESR™ has been shown to maintain pluripotency in multiple hESC lines, including expression of factors such as Oct4, SSEA3, and SSEA4.[13]

1.1.2 Stem Cell Signaling/Important Pathways

Sox2, Oct4 and Nanog are transcription factors that are part of the core machinery of pluripotency in hESCs. [14, 15] These transcription factors both activate and repress target genes in vivo.[16] Although Oct4 is a pluripotency factor, different expression levels in the

presence of BMP4 can direct differentiation towards mesoderm or endoderm[17]. Nanog has been shown to repress endoderm differentiation. All three factors have been shown to be regulated by phosphorylation.[18] However, the network of proteins that control stem cell pluripotency and cell fate is markedly more complex, as seen in **Figure 1**.

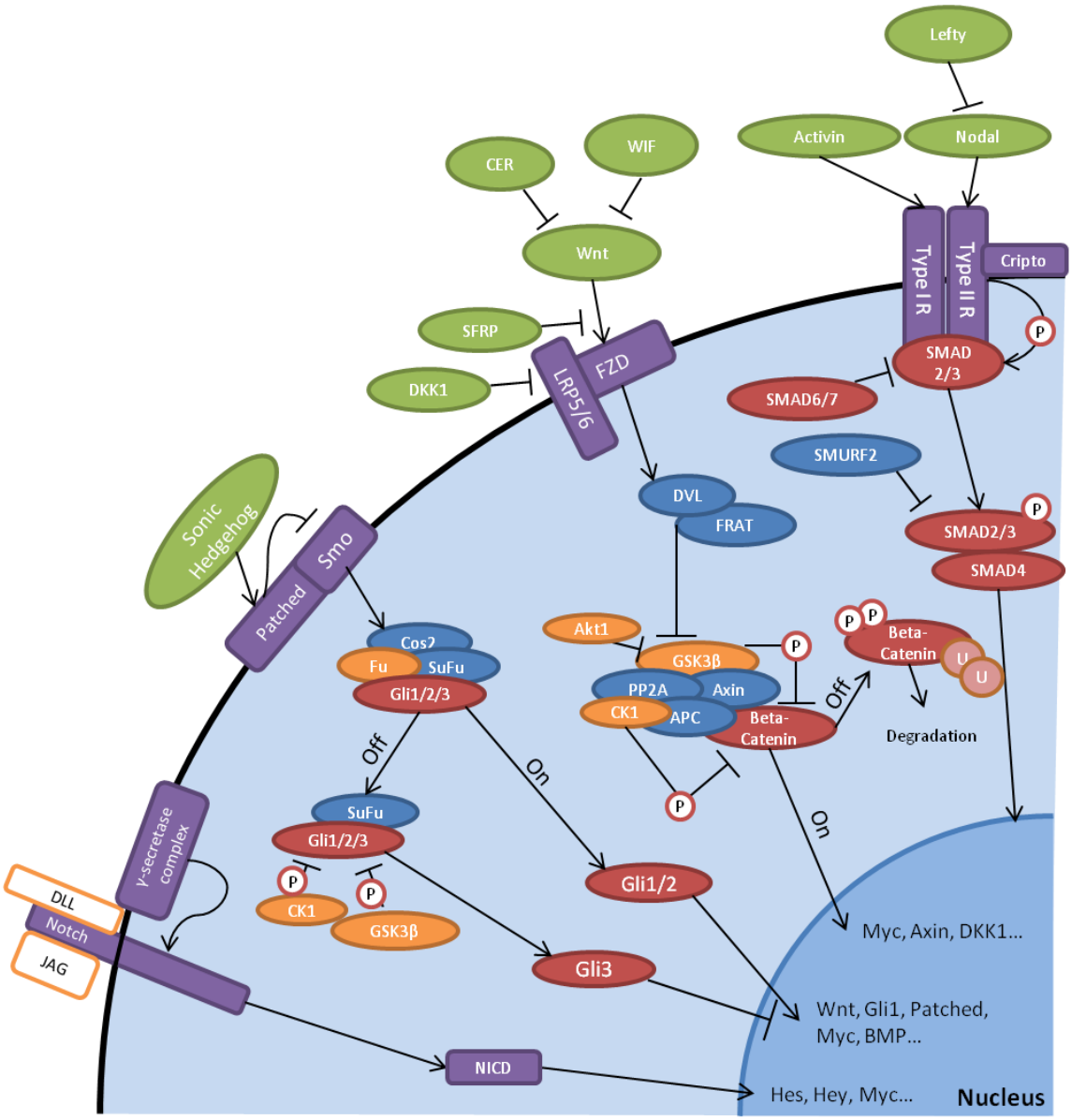

Figure 1. Stem cell signaling pathways. Notch, Hedgehog, Wnt, and Activin/Nodal signaling pathways are among those that play a role in maintaining pluripotency and stem cell fate. Transcriptional targets and crosstalk between proteins connect these pathways in a complex network that is still being elucidated. Figure adapted from Novus Biologicals.

In addition to the core machinery of transcription factors, the canonical Wnt, Nodal/Activin, Hedgehog, and Notch signaling pathways all play a role in maintaining the balance of stem cell pluripotency, with cross-talk between pathways further complicating characterization.[19]

The Wnt signaling pathway includes such proteins as Wnt1, Wnt2, Wnt3A, Wnt5A, Cerberus, WIF1, Frizzled, DKK1, Axin1, β-Catenin, APC, GSK3β, DVL1, Akt1, SFRP1, SFRP2 and FRAT1. Wnts are secreted developmental proteins that bind to Frizzled transmembrane receptors.[20] They are highly conserved across species and involved in embryogenesis patterning. When canonical Wnt signaling is inactive, the β-catenin destruction complex forms, resulting in the phosphorylation, ubiquitination and degradation of β-catenin. In the presence of Wnt signaling, the β-catenin destruction complex is disrupted, and β-catenin levels are allowed to accumulate. β-catenin translocates to the nucleus and acts as a co-activator for TCF/LEF transcription factors, activating the transcription of Wnt responsive genes such as Myc and DKK1.

The β-catenin destruction complex is made up of GSK3β, APC, Axin-1, PP2A, and CK1. GSK3β is a serine threonine protein kinase that is constitutively active. APC is a large tumor suppressor protein that is part of the β-catenin destruction complex. It also plays a role in cell migration, adhesion, transcriptional activation and apoptosis. SFRP1, SFRP2, and WIF-1 are Wnt inhibitors, previously identified to be secreted by hESCs.[21] DVL1 and FRAT-1 are positive regulators of Wnt signaling that inhibit GSK3B phosphorylation of β-catenin. Akt1 is a serine-threonine protein kinase that suppresses apoptosis by phosphorylation. It inhibits GSK3B to increase cell proliferation.

P53 is a tumor suppressor protein that plays many roles within cells, including acting as a cell cycle regulator and a role in cell division, differentiation or apoptosis.[22, 23] It can promote differentiation by suppressing Nanog.[24] CDKI1 aka p21 is a cyclin dependent kinase inhibitor controlled by P53 involved in regulation of the cell cycle at G1.

NOTCH signaling plays a key role in cell fate, affecting implementation of differentiation, proliferation, and apoptosis.[25] NOTCH is a transmembrane protein receptor for Jagged/Delta. Upon interaction, NOTCH is cleaved, and the intracellular

domain of the protein translocates to the nucleus and promotes transcription of downstream factors. Hes1 and Hey1 are transcription factors downstream of Notch signaling. Hes1 plays a role in cell proliferation and differentiation.[26] Hey1 plays a role in neuronal and cardiac differentiation.

Activin/Nodal signaling has been shown to be vital for maintenance of pluripotency. [27] Activin/Nodal signaling is required to maintain Nanog expression.[28] Nodal is a secreted protein that is responsible for formation of mesoderm and axial structures in the early embryo. It is not expressed in adult cells, except in certain cancers.[29] Lefty-1 is a member of the TGFβ family; it acts as an inhibitor of Nodal. Activin-A is a secreted homodimer that plays a role in cell fate and embryogenesis patterning. TDGF/Cripto-1 is a co-receptor for Nodal, also required for self-renewal and pluripotency.[30, 31] Cerberus is a secreted protein that acts as an inhibitor of the Wnt and Nodal pathways.[32]

Sonic hedgehog (SHH) signaling is involved in cell proliferation and early embryo patterning, and plays a role in hPSC differentiation.[33] Patched is a receptor for Sonic hedgehog that associates with and suppresses the activity of the protein Smoothened. Smoothened is a G-protein coupled receptor in tandem with Patched. SHH binding with Patched stops inhibition of Smoothened. GLI3 is a transcription factor that activates Patched expression during embryogenesis. It acts as both an activator and repressor of the Hedgehog signaling pathway. SUFU functions in concert with Sox2 and Oct4 in the Hedgehog pathway. It serves as a negative regulator of Sonic Hedgehog and β-catenin, and sequesters GLI3.

Though these signaling pathways have been summarized, quantitative data at the protein level is lacking. The crosstalk and effect of each pathway is largely affected by protein expression levels, and many of these proteins are present at low abundance, resulting in difficult detection by methods such as mass spectrometry. Nodal, Cripto and Lefty have been shown to be highly expressed components of TGFβ signaling that support the pluripotent state[34]. Small changes in Activin/Nodal signaling have also been shown to direct cell fate towards cardiac differentiation[35]. Singh *et al.* have shown that Akt activation is important to hESC self-renewal through suppression of the canonical Wnt

signaling pathway[36]. Upon activation and dimerization through Nodal or Activin signaling, Smad2/3 has been shown to maintain the pluripotent state by regulation of Nanog expression, but its activity can be affected by the crosstalk between PI3K/Akt, Raf/Mek/Erk, Wnt and GSK3B signaling.[36] In the absence of PI3K/Akt signaling, Wnt signaling is no longer suppressed and β-catenin can direct Smad2/3 to activate genes promoting differentiation, such as the mesendoderm marker MixL1. β-Catenin and Wnt signaling has been shown to be both antagonistic and key to maintenance of pluripotency, whereby large amounts of Wnt signaling results in high β-catenin expression promoting differentiation, though a basal level of β-catenin is necessary to sustain pluripotency.[37]

1.1.3 Induced Pluripotent Stem Cells

While hESCs proved to be a valuable tool, the requirement of human embryos in order to generate new cell lines has led to ethical questions and practical concerns that place limits on embryonic stem cell research. In 2006, the Yamanaka group identified four factors that enabled the reprogramming of fully differentiated somatic cells into the pluripotent state.[38] By introducing the factors Sox2, Klf4, Oct4 and c-Myc via retroviral transduction, MEFs began to exhibit stem-cell like morphology and markers. In addition, injection into nude mice resulted in generation of tissues. These derived cells were named induced pluripotent stem cells (iPSCs). One year later, the first human iPSCs were generated using the same four factors, dubbed the "Yamanaka Factors".[39] For this research, Shinya Yamanaka was jointly awarded the 2012 Nobel Prize for Physiology or Medicine with John Gurdon for discovering that mature cells can be reprogrammed to pluripotency. Concurrently, the Thomson group also developed a method to generate iPSC lines using Oct4, Sox2, Nanog and Lin28 as their reprogramming factors.[40] In addition to avoiding the need for destruction of human embryos to obtain new pluripotent cell lines, iPSCs present other research opportunities. The possibility of generating patient or disease specific cell lines could lead to more clinical relevance, and generating more genetically diverse lines would prove to be far simpler.[41, 42]

1.1.4 Variation among cell lines

Due to the variation inherent in the process of hPSC derivation and the overall inefficiency in iPSC reprogramming, it is important that cell lines be well characterized.[43, 44] Many studies have looked at characterization of cell lines, at transcriptional, epigenetic and proteomic levels. Bock *et al*. characterized 20 hESC and 12 IPSC lines by DNA methylation and gene expression, finding that variation between cell lines can affect differentiation potential[45]. By characterizing gene expression or methylation sites that deviated from the reference distribution, the group was able to develop a score card predicting a cell line's ability to differentiate into particular lineages. Similarly, a test set of iPSCs derived from different individuals was found to have differing capacities for neural differentiation[46]. Another study found that iPSCs and hESCs expressed highly similar proteomes, but some metabolic, antigen processing, and cell adhesion proteins were found to be differentially expressed.[47]

Before any therapeutic use for hPSCs is developed, we must better understand the microenvironment surrounding them, as well as their individual properties and capacity for differentiation. Though hPSCs are pluripotent and able to differentiate into any cell in the body, harnessing that ability requires a profound understanding of the signaling pathways at play. For instance, treatment of hPSCs with BMP4 will lead to differentiation; however, time of exposure affects the type of differentiation that will occur. Short-term exposure to BMP4 promotes mesoderm progenitor development, but this also requires FGF and Nodal/Activin signaling.[48] If that BMP4 signal is not inhibited, a feedback loop forms instead promoting the formation of trophoblast and extraembryonic endoderm.[49-51] In contrast, Seguin *et al.* have developed a CA1 cell line expressing a Sox17/ERT2 transgene that, when induced with tamoxifen, will promote differentiation towards a stable definitive endoderm precursor state that maintains expression of pluripotency markers Oct4 and Nanog.[52, 53] Differentiation protocols such as these would be aided by a tool that could elucidate subtle changes in protein expression that are occurring.

1.2 Mass Spectrometry

Mass spectrometry (MS) is a method of determining quantity, structure and composition of compounds by measuring the mass-to-charge ratio (*m/z*) of ions. Mass spectrometers consist of three main parts: an ionization source, a mass analyzer, and a detector. The ionization source ionizes the analyte. Two "soft" methods of ionization are commonly used in proteomic analysis, matrix-assisted laser desorption/ionisation (MALDI) and electrospray ionization (ESI). MALDI involves sample spotted on a plate and crystallized in a matrix, and ionized using a laser. Typically, this results in singly charged ions with a mass of [M+H]. Proteins can be identified by a technique known as Peptide Mass Fingerprinting (PMF), in which peptides generated from an enzymatic, typically trypsin, digest are detected and compared to a database. In the case of ESI, the analyte is sprayed out of an electrically charged tip in droplets, which are desolvated and sent into the mass analyzer. Compared to MALDI, ESI typically results in multiply charged ions, usually doubly or triply charged in the case of peptides. One particular benefit of ESI is that it can be easily integrated (i.e. on-line) with High Performance Liquid Chromatography (HPLC), allowing for chromatographic separation and more effective analysis of protein samples, as well as easier automation of protocols. The mass analyzer separates ions according to their *m/z* ratio, and the abundance of ions is measured by the detector. There are many types of mass analyzers, including Time-Of-Flight (TOF), Quadrupole (Q), Ion Trap (IT), and Orbitrap. Multiple mass analyzers can be combined to form a hybrid instrument that allows for tandem mass spectrometry (MS/MS). MS/MS allows for sequence data to be obtained from peptides by introducing a fragmentation step between multiple levels of MS scans. The fragmentation produces *m/z* peaks in the MS/MS scan that correspond to the difference in amino acid residues, from which the peptide sequence can be obtained. The data obtained is commonly analyzed using bioinformatics software, including search databases such as MASCOT and OMSSA, which use predictive algorithms to match MS data against a protein database in order to identify proteins in the sample.[54, 55] PEAKS is a *de novo* sequencing and database searching suite, with the unique feature of being able to combine searches from different tools.[56] It relies heavily on mass accuracy, resolution, and spectral quality. The Trans-Proteomic Pipeline provides a number of tools for working with MS/MS data, including the ability to convert

vendor specific files to the open mzXML or mzML format, as well as validation, identification and quantification analysis of the data set.[57, 58] Despite the power of LC – MS/MS, it has several shortcomings. Sequencing speed limits the amount of peptides that can be identified in each run, and sample complexity may cause abundant peptides to mask detection of less abundant peptides.

1.2.1 Selected Reaction Monitoring

Selected reaction monitoring (SRM) is a targeted, quantitative technique used in mass spectrometry, possible only on triple quadrupole mass spectrometers, such as the 4000 QTRAP® (AB SCIEX, Framingham, MA).[59] Also known as multiple reaction monitoring (MRM), SRM has been used in drug identification and analysis of metabolites, and is increasingly being used in proteomics. [60, 61] It involves the use of peptide precursor and fragment ion pairs known as "transitions" to identify peptides and thus proteins. By monitoring multiple transitions per peptide and multiple peptides per protein, SRM can serve to identify proteins with a great deal of specificity and selectivity. Indeed, the technique is able to obtain quantitative data over a range of five levels of magnitude, with a limit of detection between 10-50 attomoles under optimal conditions, as opposed to low femtomole levels for other instruments.[61, 62] A schematic of the mechanism of SRM can be seen in **Figure 2**. The first quadrupole is set to filter for the precursor peptide ion at a defined *m/z*, while the second quadrupole serves as a collision cell where collision induced dissociation (CID) occurs. The third quadrupole is set to filter for the fragment ion generated at a defined *m/z*. The chromatograph of each transition, including retention time and signal intensity is recorded. At its simplest, SRM can be considered a double filter method, capable of focusing on the analyte of interest, cutting through a more complex sample.[63] It differs from other mass spectrometry techniques in that it is a targeted rather than a scanning technique. Whereas other MS techniques perform survey scans, selecting the top N most abundant ions for MS/MS, SRM detects solely the ions corresponding to the list of transitions input into the method. No full MS spectrum is taken. As a result, it scans for only the targets listed, and is typically used in a hypothesis-driven approach where only certain defined peptides and

proteins are monitored. Post-translational modifications that may change the *m/z* ratio of the transitions will not be detected unless specifically accounted for.

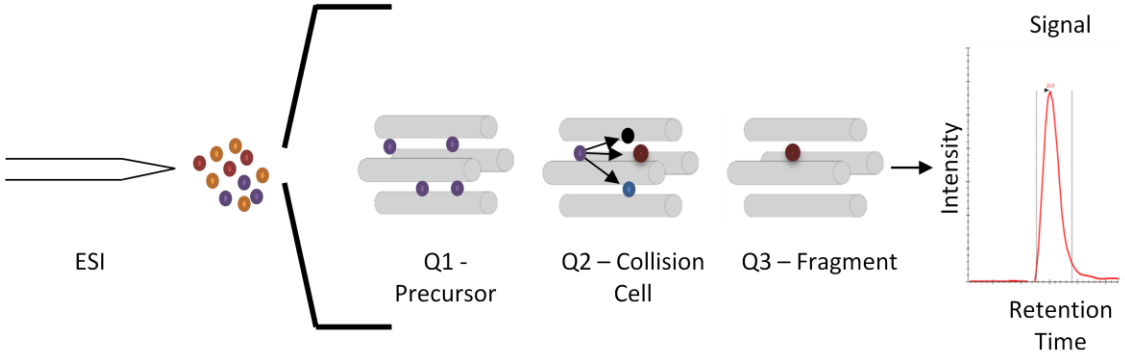

Figure 2. Schematic of SRM. A tryptic digest of protein sample is loaded and subjected to reverse-phase chromatography on a coupled HPLC system and ionized via electrospray ionization. The instrument scans for and detects peptide transitions based on a preloaded list of transitions. Precursor masses are selected in Q1, collision-induced dissociation occurs in Q2, while Q3 selects for the fragment mass. Intensity and retention time are recorded by the software. Figure adapted from Gstaiger and Aebersold, 2009.[64]

A proper SRM assay relies heavily upon reproducible chromatography. Numerous factors can affect the quality of chromatography, including changes in mobile phase, flow restriction, and the column temperature. Well-defined chromatographic peaks require a minimum of eight data points collected over the elution time. Effectiveness of an SRM assay therefore relies heavily upon the optimization of several factors. The dwell time refers to the time the instrument spends scanning for the individual transition, and as such, a higher dwell time correlates with a higher sensitivity. The cycle time refers to the time spent cycling through the entire list of transitions. If a given peptide has a chromatographic peak width of thirty seconds, in order to properly detect that peak, cycle time is limited to about 3.75 seconds in order to gather enough data points for a quantifiable peak. Thus, the maximum number of transitions that can be scanned at any given time are limited by both the cycle time and the dwell time.[65] Rather than cycle through the preset list of transitions throughout the entire sample run, a scheduled method may also be used. In a scheduled SRM method, each transition is associated with a predicted LC elution time, and as such is only scanned for in a pre-specified window around that time point. By doing this, transitions being scanned for concurrently are decreased, dwell time and thus sensitivity can increase, and more total transitions can be included in a single method, making more efficient use of instrument time. However, total number of transitions is also limited by the instrument itself. For the 4000 QTRAP®, a maximum of 1000 transitions can be included within a single scheduled method. Retention times can be predicted using software, or preferentially acquired manually through use of synthetic peptide standards.[66]

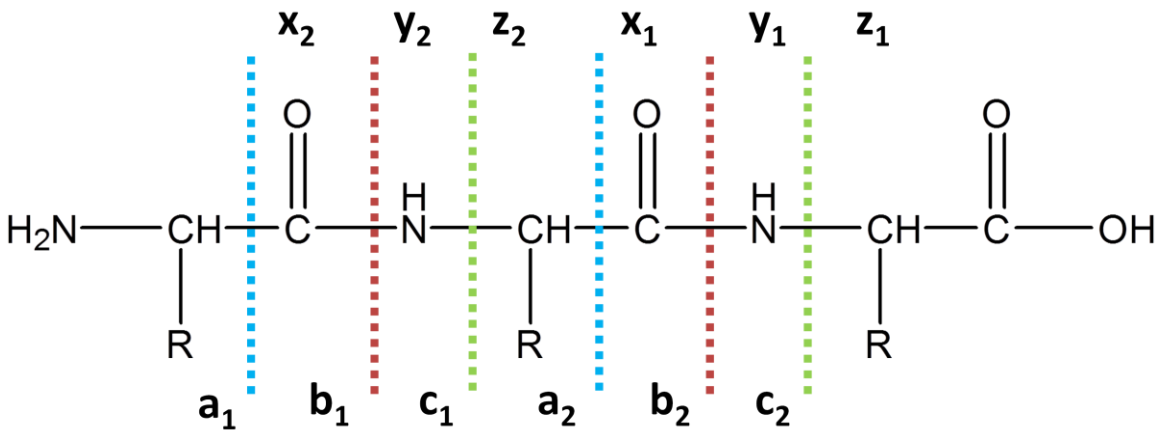

Figure 3. Potential fragment ions generated from peptide fragmentation. a,b,c ions refer to N-terminal fragments, while x,y,z refer to C-terminal fragments. In Collision Induced Dissociation (CID), b and y ions are typically observed.

When selecting peptide targets for SRM assays, several key criteria are necessary.[60] Most importantly, peptides should be "proteotypic," that is, both specific to the protein target and confidently and consistently identified by mass spectrometry. These peptides should reproducibly be obtained from the protease digest. Peptides should be kept to a residue length of between eight and twenty-five amino acids, and residues prone to oxidation such as methionine and tryptophan should be avoided. Doubly-charged precursors are preferred, unless there is a histidine present in the peptide sequence, making a triply-charged precursor more likely. CID usually results in peptides fragmenting at the peptide bond, generating y and b ions, as seen in **Figure 3**. Online repositories such as the Global Proteome Machine Database (GPMDB) and SRMAtlas contain libraries of both experimentally-derived and predicted transitions for peptides, serving as a helpful resource.[67, 68] However, due to the variation between instruments, it is best to select SRM targets based on own empirical data. In addition, many peptide fragmentation spectra deposited are for ion-trap instruments, which may differ from triple quadrupole fragmentation. Pure *in silico* predictions for protein and peptide targets may not be appropriate for SRM assays, as the given protein or peptide may not properly solubilize, ionize, or even be present after a tryptic digestion. Stergachis *et al*. developed a method where optimal proteotypic peptides are discovered through digestion of full-length proteins generated *in vitro* by cDNA clones[69]. This method could prove beneficial for generating assays for proteins present at low abundance that have not been observed via shotgun proteomics.

There are a variety of online tools that can be used in developing SRM assays, as reviewed by Cham *et al*.[70] Skyline is a publicly available program developed by the MacCoss lab of the University of Washington capable of generating, visualizing, and optimizing SRM protocols.[71] Transitions can be selected from spectral libraries obtained from sources such as Peptide Atlas, the Global Proteome Machine (GPM), and the National Institute of Standards and Technology (NIST), or from MS/MS data generated from the protein of interest. Methods can be refined by importing previously acquired SRM data and optimizing for collision energy. Collision energy optimization has been shown to significantly increase SRM signal.[72] SRM data such as retention time and peak

areas can also be exported for downstream analysis. Though SRM is limited to detecting the pre-selected transitions rather than discovering novel results and requires extensive optimization, it remains a powerful tool in hypothesis-driven research.

Because of the targeted nature of SRM and being a method of protein detection and quantification that does not require antibodies, proteomic studies using SRM are becoming more commonplace, in particular within yeast cells, mammalian cells, and human body fluids.[73] In 2009, Picotti *et al.* were able to characterize the full dynamic range of the proteome of *S. cerevisiae* using SRM, to the point of detecting proteins as low as 50 copies per cell.[74] Within an unfractionated yeast digest they were able to characterize a range of proteins covering 4.5 orders of magnitude. In addition, they were able to detect proteins that were previously unobserved in other proteomics experiments. In 2010, SRM was used by Murphy *et al.* to identify glycolytic proteins in cancer cells.[75] In 2010, Lopez *et al*. used SRM to verify putative protein biomarkers for Trisomy 21 in serum.[76] Lange *et al.* identified a set of virulence factors from *Streptococcus pyogenes* via SRM.[77]

Chen *et al.* used SRM to screen for members of the Wnt/ β-Catenin pathway in colon tissue samples and colon cancer cell lines, as the pathway is disregulated in this cancer.[78] Compared to results from Western blotting, differences in protein expression were easier to discern using SRM, with certain proteins, such as β-catenin, being capable of being detected in as few as 100 cells.

Apart from detection, SRM can also be used as a quantification tool. In order to estimate protein abundance in the microbe *Leptospira interrogans*, SRM was used.[79] Under what is known as the "best flyer" hypothesis, the most intense tryptic peptides for a protein should be constant throughout a whole proteome. As such, anchor point proteins were identified to generate a calibration curve. In an unfractionated, unlabeled sample, protein abundance changes were found for 39 proteins upon treatment with antibiotics. Bisson *et al.* combined SRM with affinity purification in order to characterize the signaling pathway surrounding the GRB2 adaptor protein within HEK293T cells.[80] Upon identifying GRB2-interacting proteins, SRM assays were generated. 90 of 108 GRB2-

associated proteins were detected by SRM. These SRM assays were later used to identify which proteins preferentially bound GRB2 SH2 or SH3 domains under various stimuli, thus greatly increasing the knowledge of the signaling dynamics surrounding the GRB2 adaptor. An SRM-based study was also performed quantifying the temporal phosphorylation profiles of the EGFR signaling network, taking advantage of SRM's reproducibility.[81] Due to its sensitivity and selectivity, SRM can be used in a wide variety of studies, and it would be particularly useful in characterizing a targeted list of signaling proteins within a complex background, such as a cell lysate.

1.2.2 Parallel Reaction Monitoring

An technique analogous to SRM known as parallel reaction monitoring (PRM), or targeted MS/MS, has recently been described for the high-resolution/high mass accuracy instrument the Q Exactive™ (Thermo). In place of the third quadrupole, an orbitrap mass analyzer is used.[82] Similar to SRM, pre-input targets are listed in the method, however, the orbitrap is capable of detecting all MS/MS fragments at once, thus eliminating the time consuming step of transition optimization. The Domon group was able to detect and quantify 770 yeast peptides in a single 60-minute experiment using this technique. [83] Using a synthetic peptide cocktail, the Coon group has shown that PRM provides comparable or, at times, better than SRM.[84] Though SRM is theoretically more sensitive than PRM due to a faster scan speed, the ability of PRM to obtain high-resolution data eliminates the chance of interfering ions confounding target detection.[85]

1.2.3 Quantitative Proteomics

The ultimate goal of SRM is quantitation. Although label-free quantification methods are widely used, reproducibility can be a concern, and without some sort of reference, comparison across sample acquisitions can be difficult.[86] Methods such as stable isotope labeling in with amino acids in cell culture (SILAC) and isobaric tag for relative and absolute quantitation (iTRAQ) are commonly used; however, these methods are examples of relative quantitation.[87-89] Each method has both advantages and disadvantages. An advantage of SILAC is that the label is incorporated upon protein synthesis, thus minimizing error further downstream in the workflow. However, it can

only be incorporated at the cellular level, it is expensive, and a great deal of optimization must take place in order to ensure 100% label incorporation. Methods such as iTRAQ are incorporated at the peptide level after a proteolytic digestion, and can allow for analysis of up to eight samples simultaneously.[89]

In order to achieve absolute quantitation, a known standard must be used. The absolute quantitation, or AQUA method involves synthesizing an isotopically labeled version of the target peptide, and spiking a known amount into the sample.[90] Typically the label is ^{13}C or ^{15}N, as these labels do not result in a shift in chromatographic retention time, unlike deuterium and ^{18}O containing compounds. Because of this, the synthetic peptide mimics the endogenous peptide in both retention time and fragmentation pattern, but differs in mass. The absolute amount of the target peptide can be obtained from the relative intensity of light to heavy transitions. The Gygi group confirmed the use of this method by quantifying a K-48 polyubiqitinated peptide. Using this method, the copy number per cell can be determined. Though effective, the synthesis of isotopically labeled peptides can become expensive if high amounts are required.

Alternately, there has been success using dimethyl labeling as a method of relative quantitation, as outlined in **Figure 4**.[91] Key advantages of this method are its ability to be incorporated post-digest, thus being compatible with all protein samples, its quick reaction time, and that it is inexpensive compared to other labeling techniques. A disadvantage is a slight shift in retention time compared to unlabeled peptides. Samples are treated with formaldehyde and sodium cyanoborohydride which introduces a dimethyl label to primary amines in a peptide, typically at the N- terminus and on the lysine side-chain. Using different isotopes of formaldehyde and sodium cyanoborohydride resulting in labels of varying masses, typically allowing for a light (+28 Da), medium (+32 Da), and heavy (+36 Da) label. By mixing these in a 1:1 ratio, up to three samples could be analyzed in a single mass spectrometry experiment.[92] Using this method, the Pinto lab was able to characterize the glycolytic proteome in MCF-7 breast cancer cells.[75] SRM assays specific to dimethyl-labeled targets were used to monitor changes in protein expression in both insulin-growth factor-1 stimulated MCF-7 cells, as well as across lung tumors of different levels of differentiation.

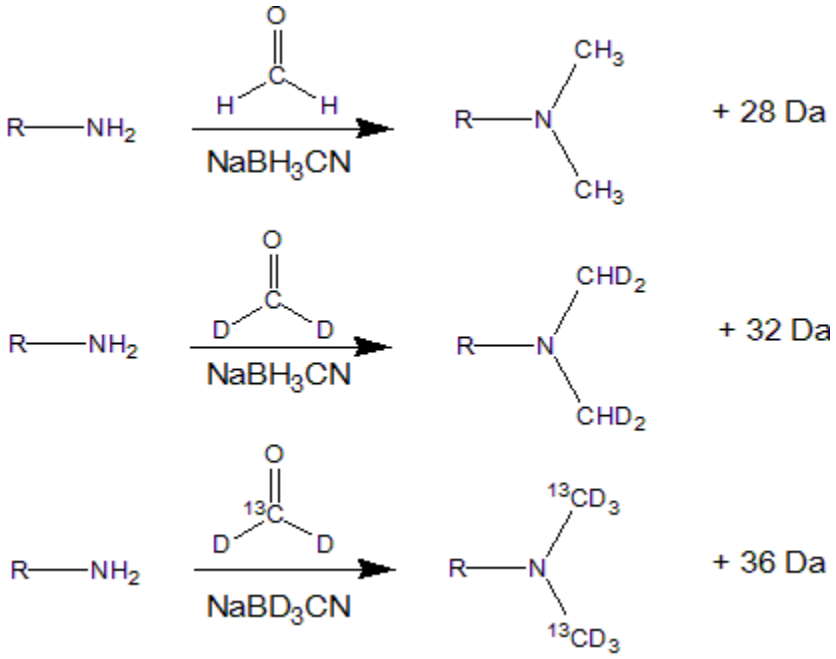

Figure 4. Dimethyl labeling of peptides. After tryptic digestion, peptides are treated with formaldehyde followed by incubation with sodium cyanoborohydride, introducing a dimethyl label to all primary amine groups present. Different isotopes of formaldehyde and sodium cyanoborohydride alter the size of the mass label introduced.

1.3 Proteomics and Stem Cells

The proteome is the full protein complement of a cell under a set of given conditions. Many studies investigating the transcriptome of hPSCs have been performed; however, protein expression is not always directly correlated to the level of transcript, due to post-transcriptional levels of regulation such as mRNA stability, protein degradation, protein processing, alternative splicing, and rates of translation.[93] Since proteins are the effectors of cellular processes, monitoring protein expression in addition to transcript is also important. A major advantage of the proteomic approach is the ability to identify and study many proteins with relatively little sample. Proteomic studies are frequently performed using a "bottom-up" or "shotgun" approach, in which proteins are enzymatically degraded to peptides, commonly using trypsin, and then analyzed by mass spectrometry. Alternately, "top-down" proteomics involves the study of whole intact protein mixtures by mass spectrometry. Due to the complexity of sample, there are usually additional fractionation techniques ahead of LC-MS, including strong cation exchange (SCX) or 1-D SDS-PAGE.[94] SCX fractionation followed by reverse-phase LC-MS is known as Multi-Dimensional Protein Identification Technology (MuDPIT).[95] Increasing the number of fractions often results in more protein identifications, however, it significantly increases instrument time. Using multiple fractionation techniques is complementary, and often results in increased protein coverage. Indeed, additional fractionation has been shown to be more effective than repeated analyses in terms of total number of proteins identified. [94, 96, 97] Ultra-long LC gradients have also been shown to increase identifications. Kocher *et al.* demonstrated the ability to detect 2761 proteins from an unfractionated HeLa cell lysate over the course of a single-run 10 hour gradient.[98] Longer gradient and column lengths generally increase peptide identification, but they generally reach a point of diminishing returns.[99]

Due to the complex nature of regulation and wide variety of proteins involved, proteomic studies of hPSCs have become increasingly common. Many levels of regulation are present, so studies targeting the hESC membrane, the extracellular matrix and secreted proteins have been conducted. The regulatory pathways and growth factors that govern hESC self-renewal and pluripotency are poorly defined, so Bendall *et al*. used a mass

spectrometry technique known as iterative exclusion in order to analyze MEF and hESC conditioned media.[100] Iterative exclusion involves injecting the same sample numerous times, but including all previous identifications on an exclusion list, thus making it more likely that low abundance proteins are identified on later injections. A large number of previously undetected secreted growth factors were identified, including Activin A, Lefty, and TGFβ, using this method.

Phosphorylation pathways have been shown to be important in hESC maintenance and critical in cell signaling.[101] Van Hoof *et al*. determined that the pluripotency-associated protein SOX2 becomes SUMOylated due to phosphorylation, suggesting that phosphorylation may play a role in regulation.[18] Rigbolt *et al*. conducted a temporal study characterizing the hESC phosphoproteome during differentiation.[102] Two methods of differentiation were used, treatment with phorbol 12-myristate 13 acetate (PMA) and culture in non-MEF-conditioned medium, in order to control for events specific to the treatment and those caused by cell differentiation. Using a combined quantitative proteomic and phosphoproteomic approach involving SCX, SILAC, and titanium dioxide phosphopeptide enrichment, 6521 proteins and 23 522 phosphorylation sites were profiled. It was found that numerous kinases, DNA methyltransferases and transcription factors relating to differentiation were regulated by phosphorylation, notably the transcriptional elongation complex PAF1, which binds to promoters of genes encoding Oct4 and Nanog. Given the complexity of the network of factors promoting pluripotency, a proteomics approach may be the best way to understand the interactions taking place.

Few hPSC studies involving SRM have been conducted. Yocum *et al.* used SRM to verify and quantify early markers of neural differentiation such as collapsin response mediator proteins 2 and 4 within hESCs grown in feeder-free conditions.[103] Protein markers such as cytokeratin-8 identified in earlier global experiments as well as proteins of significance such as Oct4 had SRM assays generated. Eight target proteins and 25 peptides were detected, though many targets that had not been detected in global experiments were also left undetected in SRM analysis, suggesting that the target selection and validation for SRM are highly important. This study also indicated that

SRM is a sensitive technique for detection of target proteins within hESCs. That sensitivity could be applied to obtain quantitative data for such targets.

1.4 Thesis Objectives and Rationale

Because of the complexity of the networks and mechanisms responsible for hPSC pluripotency, it would be beneficial to develop a targeted method capable of detecting and quantifying a defined set of stem cell signaling proteins simultaneously. Transcriptome studies have been performed, RNA transcript does not directly correspond to protein expression, therefore it is important to analyze the proteome as well. Many of these proteins have not been detected or quantified by conventional MS analysis. The dynamic range and sensitivity of SRM might be able to overcome the sensitivity or detection issues responsible for this.

In this thesis, an SRM protocol is developed with the intent of detecting and quantifying the proteins and cell signaling factors responsible for maintenance of stem cell pluripotency. This will provide a method capable of characterizing the "protein fingerprint" of stem cell cultures, and serve as a starting point to analyze changes in protein expression upon differentiation. We hypothesize this SRM protocol will provide quantitative information on the expression of a curated set of pluripotency-related proteins upon differentiation.

The objectives of this thesis are as follows. Firstly, two cell differentiation models within which protein expression changes could be analyzed were characterized. These systems included a BMP4-driven differentiation of H9 hESCs and a tamoxifen-induced differentiation of CA1 Sox17/ER^{T2} hESCs towards definitive endoderm precursors. Secondly, SRM assays for proteins primarily from the NOTCH, Hedgehog, Wnt, and Activin/Nodal signaling pathways were developed. Finally, quantitative protein expression data was obtained through use of a consolidated scheduled SRM protocol for analysis of differentiated and undifferentiated stem cell lysates.

By obtaining quantitative data in order to characterize the stem cell signaling networks responsible for promoting pluripotency and the exit from pluripotency, this research will

help improve understanding of the signaling networks and, in turn, the development of defined media for optimal cell culture conditions, more effective conditions for cell-differentiation protocols, leading to more effective stem cell research.

2 Methods

2.1 SRM Assay Development

Thirty-three initial protein targets were selected through a literature search, including members of the canonical Wnt signaling pathway, the Activin/Nodal signaling pathway, Hedgehog signaling pathway, and Notch signaling pathway. Protein sequences were obtained from Uniprot and loaded into the SRM assay development software Skyline. Proteins were digested *in silico* with trypsin, cleaving at arginine and lysine. Human spectral libraries from GPMDB and NIST were loaded into Skyline. Peptides predicted to be proteotypic were selected through use of several online applications, and through use of criteria outlined by Lange *et al.*[60] Briefly, peptides selected had no missed cleavages, were 8-25 residues in length, were neither extremely hydrophilic or hydrophobic, and lacked residues susceptible to oxidation like tryptophan and methionine. When unavoidable, methionine oxidation was taken into account in transition mass. PeptideCutter was used to predict efficiency of tryptic digestion, while the GPMDB was used to identify whether target peptides were previously observed. Finally, target peptide sequences were submitted to Protein BLAST by NCBI to confirm specificity for the target protein.

2.2 Peptide Synthesis

Peptides were synthesized in-house on the MultiPepRS peptide synthesizer (Intavis) at the 5-µmol level using the FMOC protocol on WANG Resin. Offline, arginine or lysine residues were coupled to the resin before being used on the synthesizer.

Wang resin was suspended in a peptide synthesis vessel in dichloromethane (DCM), and washed three times with DCM. The amino acid to be coupled was dissolved in DCM with 2,6-dichlorobenzoyl chloride and pyridine base, and allowed to mix for five minutes. The activated amino acid solution was added to the peptide synthesis vessel and was allowed to react with the resin for 4-6 hours, or overnight. Following coupling, resin was washed six times with DCM. Resin coupling was quantitated using UV-Vis spectroscopy, if substitution was less than desired (<0.3mmol/g), amino acid coupling was repeated. Resin was capped with acetic anhydride/disisopropylethylamine solution in DCM to

deactivate hydroxyl groups on the resin. Resin was washed six times with DCM and stored in a vacuum desiccator until use. After synthesis was complete, peptides were dried and cleaved from resin with cleavage cocktail (95% trifluoroacetic acid, 2.5% ddH2O, 2.5% triisopropylsilane) and precipitated by dropwise addition to cold diethyl ether. Precipitated peptides were pelleted, solublized in 10% glacial acetic acid (GAA) in ddH_2O, and lyophilized. Lyophilized crude peptide was stored at -80°C. 1 nmol/mL stock solutions of each peptide were made. Serial dilution was performed to create working solutions of 100 fmol/µL. Peptide cocktails were injected into the 4000 QTRAP® to obtain MS/MS spectra. Briefly, an SRM-triggered DDA protocol was developed for each peptide, to obtain both SRM transition and MS/MS sequence data, confirming peptide identity. Y and b fragment ions were targeted for the doubly and triply charged precursors of each target peptide. The top five transitions for each peptide were pooled into a general SRM protocol for use on cell lysates to confirm endogenous detection.

2.3 Cell Culture

Unless otherwise stated, all cell culture reagents were obtained from Life Technologies. Human embryonic stem cell lines H9 (WiCell) and CA1 were obtained from Dr. Cheryle Seguin of The University of Western Ontario.[2, 43, 52] hESCs were cultured and propagated on gamma-irradiated MEFs (CF-1 (GlobalStem), 0.5 M per 6 well plate, or 4DR), and fed daily with hESC media (DMEM/F12, 20% KOSR, 1% NEAA, L-Glutamine, β-mercaptoethanol (Fisher), and 4 ng/mL bFGF). 0.5M MEFs were plated on 6-well culture plates coated with a 0.1% solution of gelatin. Cultures were incubated at 37°C and 5% CO_2. To prevent differentiation, at confluency, cells were passaged either mechanically or using trypsin. Mechanical passaging was performed using a Pasteur pipette that was heated and pulled into a picking tool. This pick was used to separate cell colonies into small clumps, which were later plated on a new cell culture plate. For enzymatic passaging, cells were washed twice with PBS, and treated with 0.5 mL 0.25% trypsin per well for 2-3 minutes. Colonies were broken up with vigorous pipetting, collected, and trypsin was deactivated with 1.5 mL hESC media. Colonies were passaged onto a fresh culture plate.

Excess cells were suspended in cryopreservation media (50% hESC media, 45% KOSR, 5% DMSO) and stored in liquid nitrogen for future use. Fresh cultures were started by thawing a vial of previously frozen hESCs obtained from liquid nitrogen storage. Vials were thawed in a 37°C water bath until a single ice crystal remained. Vials were disinfected with 70% ethanol. Thawed cells were diluted in 4 ml of hESC media and plated into one well of a 6-well plate containing a MEF feeder layer. Media was changed daily. Upon colony formation (up to two weeks), cells were passaged and expanded.

Before experiments, cells were passaged and cultured on the feeder-free basement membrane Geltrex®. 6-well plates were coated with 30 µL/mL Geltrex® solution, and stored at 37°C for at least 1 hour for polymerization to occur. Control cells were fed with MEF-conditioned hESC media. To create MEF-CM, hESC media was conditioned on MEFs for 48 hours, collected, filtered and aliquoted into 36 mL fractions and frozen at -20°C until needed for cell culture. Fresh hESC media was added to frozen aliquots to create a 70/30 hESC/MEF-CM media mixture which was used for feeder-free cell culture. Differentiation media was identical to hESC media, except lacking bFGF and instead containing either 0.1nM 4-OHT or 10 ng/mL rhBMP4 (R&D Systems). CA1 Sox17-ERT2 Clone K cell media was also supplemented with 0.6 ug/mL puromycin. Cells were differentiated for 96 hours.

2.4 Protein Extraction

Adherent cells were washed twice with 2 mL of cold PBS (Life Technologies). Cells were detached by incubating with 0.25% trypsin for 1-2 minutes, which was deactivated with hESC media. Cells were washed with DPBS. Cells were lysed in urea cell lysis buffer (8M urea, 50 mM ammonium bicarbonate, 1x HALT™ protease inhibitor cocktail (Thermo Scientific)) and incubated for 20 minutes on ice, with occasional vortex mixing. To shear genomic DNA, ensure membrane lysis, and lower sample viscosity, cell lysates were briefly sonicated. Samples were centrifuged at 10 000 × *g* for 10 minutes to remove debris, aliquoted and stored at -80°C for future analysis.

2.5 Bradford Assay

Protein samples were quantified by a modified Bradford assay. [104, 105] 10 µL of sample was diluted to 80 µL using ddH_2O. A 1 mg/mL solution of bovine serum albumin (BSA) was used as a standard. A serial dilution scheme was performed on a 96-well plate as illustrated in **Figure 5**. Varying amounts of sample was added to each well along with a diluent matching the make-up of the diluted sample. 200 µL of Coomassie Protein Assay Reagent (Thermo Scientific) was added to each well and allowed to react for five minutes. Absorbance at 595 nm was measured using a Victor^{3}V 1420 Multilabel Counter (Perkin Elmer). Protein concentration was determined from the equation generated from the BSA standard dilution curve.

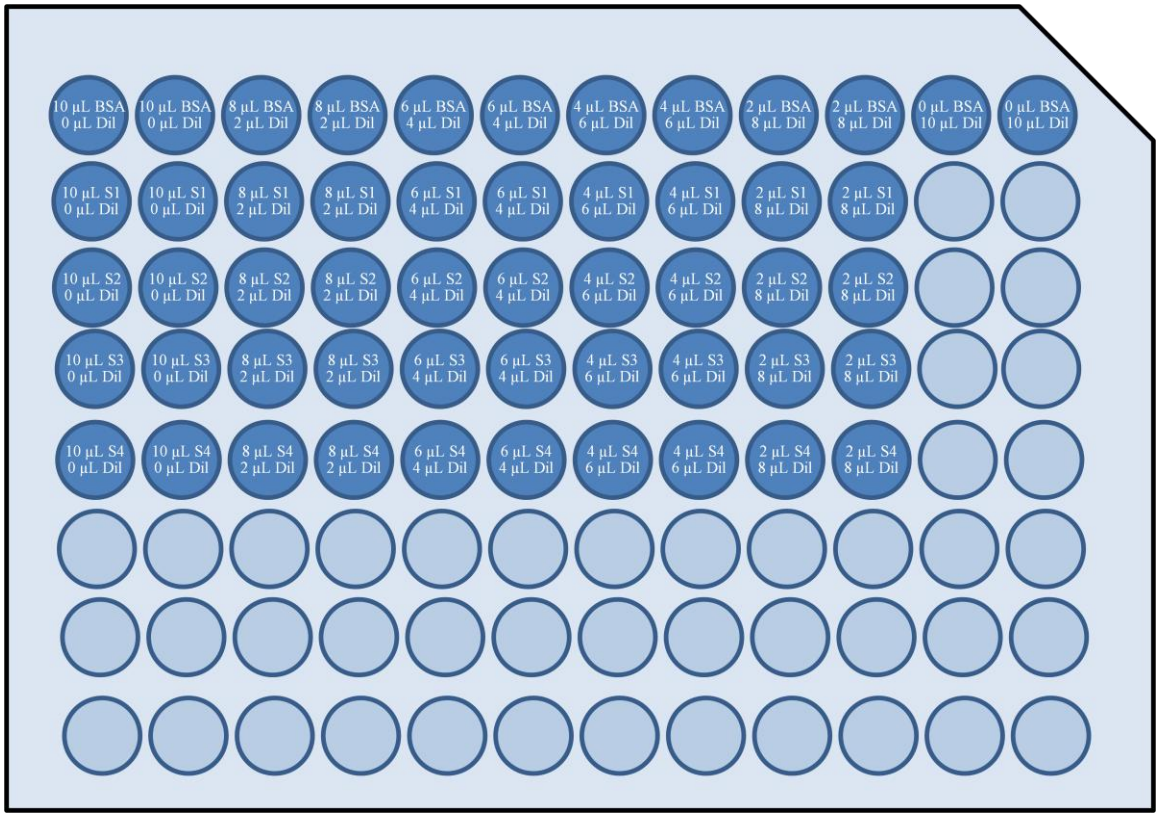

Figure 5. Bradford Assay setup. A serial dilution of BSA protein standard and samples were resuspended to a total of 10 µL per well with diluent bringing lysis buffer concentrations to acceptable levels for assay. 200 µL of Coomassie Protein Assay Reagent was added to each well and allowed to react for 5 minutes.

2.6 Flow Cytometry

Cells cultured on Geltrex® were dissociated to a single-cell state with 1 mL of 0.25% trypsin-EDTA solution. Trypsin was deactivated by adding it 1:1 to trypsin neutralizer (Life Technologies). Cells were passed through a cell strainer, washed, and pelleted. Cell count was determined by taking a 10 µL aliquot for use with a hemacytometer. Cells were resuspended in FACS Buffer (PBS, 10% FBS) and divided equally among FACS tubes. Cells were washed and pelleted. Cells were treated with aqua LIVE/DEAD® Fixable Dead Cell Stain (Invitrogen), incubated, washed and pelleted. Cells were treated with surface marker conjugated-antibodies for Alexa Fluor® 647-SSEA1 and PE-SSEA3 (eBioscience), incubated for 20 minutes, then washed and pelleted. SSEA1 is a surface marker of differentiation, while SSEA3 is a surface marker of pluripotency. Cells were fixed with 200 µL 4% paraformaldehyde (PFA) solution for 10 minutes, washed, then permeablized with 200 µL 0.1% Triton X-100 for 10 minutes and washed. Cells were treated with antibodies for intracellular pluripotency marker Alexa Fluor® 488-Oct4 (eBioscience), incubated for 20 minutes, and then washed. Cells were analyzed using an LSRII flow cytometer (BD Biosciences). For establishment of instrument parameters, compensation controls, and fluorescence intensities, singly-stained compensation beads (BD Biosciences) were used as well as unstained fixed and permeablized hESCs. Fluorescence Minus One (FMO) controls were also analyzed, to help discriminate between positive and negative signals. At least 20 000 events were acquired for fully stained samples. Differentiated and undifferentiated samples were paired and run on the same day. Flow cytometry data was analyzed in software FlowJo. All analysis was performed on the gated live cell population, designated as being negative for aqua LIVE/DEAD® fluorescence. Experiments were conducted in duplicate.

2.7 Immunofluorescence

Cells cultured on Geltrex were washed twice with PBS and incubated in fixing solution (4% paraformaldehyde, 10% sucrose in PBS) at room temperature for 20 minutes. Cells were washed with PBS. Cells being stained for intracellular markers were treated with permeablization solution (0.1% Triton X-100 in PBS) and incubated for 10 minutes at

room temperature. Cells were washed with PBS, and treated with DAKO Protein Block to eliminate nonspecific staining. Primary antibodies for Oct-4, SSEA4 and SSEA1 (Millipore) were added at a 2 µg/mL concentration in 0.1% BSA solution and rocked for 1 hour. Plates were sealed with Parafilm and incubated at 4°C overnight. Primary antibody solution was removed, secondary antibody solution was added at a 1 µg/mL concentration in 0.1% BSA solution, and rocked for 30 minutes to 1 hour. Secondary antibodies used were Alexa Fluor® 488 goat anti-mouse IgG and Alexa Fluor® 568 goat anti-mouse IgM (Invitrogen). Secondary antibody solution was collected, cells were rinsed with PBS. Cells were treated with 0.3 nM DAPI for nuclear staining, washed, and then imaged by fluorescent microscopy with the Leica STP6000 at 10X magnification.

2.8 Localization of SOX17

CA1 Sox17/ERT2 Clone K cells were manually passaged onto Geltrex-coated glass coverslips and allowed to attach for 24-hours. Cells were treated for 2 hours with 0.1 uM 4-OHT, washed, fixed, permeablized, treated with DAKO protein block and stained with SOX17 mouse anti-human Alexa Fluor® 488-conjugated antibody (BD Pharmigen) for one hour. Cells were treated with DAPI for nuclear staining. Immunofluorescence confocal microscopy was conducted on the LSM510 Meta Confocal Microscope (Zeiss).

2.9 RT-PCR

Total RNA was extracted from cells through use of 5-Prime PerfectPure RNA Extraction Kit. 400 µL of lysis solution was added per well of confluent cells, and plates were incubated and rocked for five minutes at room temperature. Lysis solution was pipetted vigorously, and added to the RNA purification column. Purification columns were centrifuged at 13 000 g for 1 minute and collection tubes were replaced after each step. RNA was washed once with 400 µL Wash 1 solution, twice with 200 µL Wash 2 solution, and eluted with 50 µL of Elution solution. Total RNA was quantified by using either a Nanodrop or plate reader. Absorbance ratios of 260 nm/280 nm and 260nm/230nm were monitored for sample quality. After quantification, RNA samples were stored at -80°C until further use.

cDNA was synthesized using the high capacity cDNA Reverse Transcription Kit

(Applied Biosystems). 2 µg of RNA sample was mixed with 10 µL of master mix (2.0 µL 10X RT buffer, 0.8 µL 25X dNTP, 2.0 µL 10X RT random primers, 1.0 µL reverse transcriptase, 4.2 µL nuclease-free H_2O) and brought up to 20 µL with ddH_2O. The mixed samples were placed in a thermocycler set at 25°C for 10 minutes, 37°C for 120 minutes, 85°C for 5 minutes and kept at 4°C. 1:100 dilutions of synthesized cDNA were used in RT-PCR reactions. SYBR Green Master Mix (Bio Rad) was used. Samples were incubated at 95°C for 3 minutes. Samples were then amplified at 95°C for ten seconds followed by annealing at 60°C for forty cycles. Melt curve data was obtained by increasing temperature from 65°C to 95°C in 0.5°C increments. Primers for targets can be seen in **Table 1**. Markers of endoderm Cerberus, CXCR4, DLX5, GATA4 and GATA6 were used to confirm endoderm formation in CA1K differentiation system. Sox17 was monitored to confirm constitutive expression of the transcript across differentiation. Pluripotency markers Oct4, Nanog and Nodal were used to monitor loss of pluripotency in both H9 and CA1K differentiation systems. All samples were normalized to GusB expression. Each biological replicate was run in triplicate for each target. RT-PCR data was analyzed using the ΔΔCT method.[106]

Table 1. List of Real-Time RT-PCR Primers.

Gene	Gene Accession No.	Forward Primer	Reverse Primer
TBP	NM_003194	TGTGCACAGGAGCCAAGAGT	ATTTTCTTGCTGCCAGTCTGG
CER1	NM_005454	ACAGTGCCCTTCAGCCAGACT	ACAACTACTTTTTCACAGCCTTCGT
CXCR4	NP_001008540	CACCGCATCTGGAGAACCA	GCCCATTTCCTCGGTGTAGTT
DLX5	NM_005221	CGCCTCGCTGGGATTG	CTTGATCTTGGATCTTTTGTTCTGAA
GATA4	NM_002052	TCCAAACCAGAAAACGGAAGC	GCCCGTAGTGAGATGACAGG
GATA6	NM_005257	GCGGGCTCTACAGCAAGATG	ACAGTTGGCACAGGACAATCC
NANOG	NM_024865	TGATTTGTGGGCCTGAAGAAA	GAGGCATCTCAGCAGAAGACA
OCT4	NM_002701	TGGGCTCGAGAAGGATGTG	GCATAGTCGCTGCTTGATCG
SOX17	NM_022454	GGCGCAGCAGAATCCAGA	CCACGACTTGCCCAGCAT
NODAL	NP_060525	TGACTTCTCCTTCCTGAGCC	GGGACAAAGTGACAGTGAATAG
GUSB	NP_000172	ACGCAGAAAATATGTGGTTGGA	GCACTCTCGTCGGTGACTGTT

2.10 Dimethyl Labeling

Subsequent to tryptic digestion, peptides were labeled by isotopic dimethyl labeling for quantification purposes.[107] Samples were treated with formaldehyde or deuterated-formaldehyde (Sigma), vortexed, and incubated for five minutes. Sodium cyanoborohydride was added to the samples, which were allowed to incubate for two hours. Undifferentiated samples were given the "light" label, and differentiated samples were given the "heavy". After labeling, reactions were quenched by the addition of 10% formic acid, and samples were mixed 1:1 and desalted as previously described. Combined samples were brought to dryness in a vacuum centrifuge and reconstituted in 10% formic acid for MS analysis.

2.11 Gel Electrophoresis

Samples were separated by 1D gel electrophoresis. 100 ug of protein lysate was diluted 1:2 with 2X loading buffer (4% SDS, 20% glycerol, 120 mM Tris-Cl pH 6.8, 200 mM DTT, 0.1% bromophenol blue) and loaded onto a 1.5 mm 12% SDS-PAGE gel. 2 µL of PrecisionPlus DualColour Protein Standard (Bio-Rad) was added to provide a molecular weight ladder. Gels were run at a constant voltage of 200V. Finished gels were fixed for one hour or overnight in fixing solution (50% methanol, 10% glacial acetic acid in water), stained in Coomassie stain solution (50% methanol, 10% glacial acetic acid, 0.1% Brilliant Blue R-250 in water) for 25-40 minutes, and destained in destain solution (45% methanol, 10% glacial acetic acid, in water) until background was clear. Gel was scanned, imaged, and stored in 5% glacial acetic acid at 4°C until use.

2.12 In-gel Tryptic Digestion

Gel lanes were cut into fractions, which were cut into ~2 mm cubes, put in microcentrifuge tubes and destained with alternating washes with destaining solution (1 M ammonium bicarbonate/20% acetonitrile in ddH_2O) and washing solution (50% methanol/5% acetic acid in ddH_2O). Once gel pieces were completely destained, they were dehydrated with acetonitrile. Gel pieces were then rehydrated with dithiothreitol (DTT) solution (10mM DTT in 100mM ammonium bicarbonate) and

allowed to reduce for 30 minutes. Excess DTT solution was removed, and iodoacetamide solution (100mM IAA in 100mM ammonium bicarbonate) was added, and gel pieces were allowed to reduce for 30 minutes. IAA solution was removed, and gel pieces were dehydrated with acetonitrile, allowed to rehydrate with 100 mM ammonium bicarbonate, then dehydrated once more with acetonitrile. Gel pieces were completely dried in a vacuum centrifuge. Gel pieces were fully rehydrated with trypsin (Fisher) solution (20 ug/mL trypsin in 50 mM ammonium bicarbonate), and allowed to incubate on ice for 10 minutes. Excess trypsin solution was removed, gel pieces were covered in 50 mM ammonium bicarbonate and allowed to digest overnight at 37°C, for at least 18 hours. Supernatants were collected, followed by two extractions with 10% formic acid, and a final extraction with acetonitrile. Supernatants were pooled and volume was reduced in a vacuum centrifuge. Prior to MS analysis, samples were reconstituted in 10% formic acid.

2.13 In-Solution Tryptic Digestion

100 ug of protein lysate was resuspended up to 100 µL in 50 mM ammonium bicarbonate. The sample was reduced with 5 µL of DTT solution (200 mM DTT in 100mM ammonium bicarbonate) at room temperature for 45 minutes, vortexing occasionally.. Samples were centrifuged at 5000xg for 30 seconds. Sample was alkylated with 20 µL IAA solution (200 mM iodoacetamide in 100 mM ammonium bicarbonate) at room temperature for 45 minutes, vortexing occasionally. Excess IAA was neutralized by adding 10 µL of DTT solution, and left to incubate for 45 minutes at room temperature. Sample was diluted with 50 mM ammonium bicarbonate to bring buffers to levels acceptable for a trypsin digest. Trypsin solution was added to sample (1:25 trypsin to protein) and sample was left to digest overnight for at least 18 hours at 37°C. Tryptic samples were acidified 1:2 with 10% formic acid and desalted using 1 mL C-18 SPE columns (Phenomenex). Columns were primed with 3×1 mL aliquots of Buffer B (acetonitrile + 0.1% formic acid), and washed with 3×1 mL aliquots of Buffer A (ddH_2O + 0.1% formic acid). Sample was loaded and washed with 3×1 mL aliquots of Buffer A. Sample was eluted with 400 µL Buffer C (50% Buffer A, 50% Buffer B). Eluent was brought to dryness using a vacuum centrifuge and reconstituted in 10% formic acid before mass spectrometry analysis.

2.14 Mass Spectrometry

SRM experiments were performed on the 4000 QTRAP® mass spectrometer (AB SCIEX) coupled to a nanoAcquity HPLC system, operating in nanospray mode. The HPLC system was equipped with a 2 mm X 180 um inner diameter trap column packed with C18 beads (5 um, SymmetryC18, Waters nanoAcquity) ahead of a 20 cm X 75 um inner diameter C18 analytical column (1.7 µm BEH130 C18, Waters) and a PicoTip silica tip emitter (New Objective). Samples were run on a 2-hour linear gradient at 0.3 µL/min from 95-40% solvent A (Solvent A: ddH2O + 0.1% formic acid, Solvent B: acetonitrile + 0.1% formic acid) followed by a column reequilibration step (10 minutes 40-5% solvent A, 15 minutes 5% solvent A, 25 minutes 95% solvent A). A scheduled SRM protocol pooling the optimized transitions was used, with a 2 second scan time, and 4 minute acquisition window.

The mass spectrometer was operated in positive ion mode, with IonSpray voltage of 2300V, interface heater temperature of 120°C, curtain gas of 20, ion source gas of 25, entrance potential of 10, collision cell exit potential of 10, and medium collision gas pressure. Initial transition collision energies were calculated using Skyline default settings for 4000 QTRAP®, using the formula $CE = 0.057(m/z) - 4.265$ for doubly charged precursor ions, and $CE = 0.031(m/z) + 7.082$ for triply charged precursors.

Collision energy was optimized for each precursor by using the Skyline CE optimization method. Synthetic peptide was injected into the instrument, while the voltage was altered stepwise by +/- 5 V. The optimum voltage was identified from the maximum peak area and used for all subsequent analyses.

2.15 MS Data Analysis

Instrument specific .wiff data files were converted to mzML through use of MSConvert, and SRM data was imported into Skyline software for visualization and further downstream analysis.[71] Savitzky-Golay smoothing was applied to chromatograms, and peaks were assessed to assure software's automatic peak picking was successful. Peaks were selected manually. A report was exported from Skyline containing information on

peak areas and retention times for further processing. Statistical analysis was performed as described by Bisson *et al.*, using formulae seen in **Figure 6**.[80] By using weighted averages and discriminatory values, outlier transitions can be disregarded in calculating overall fold change. The transition response I_t^s for each sample was calculated from a weighted average of technical replicates in triplicate as seen in equation 1. The weighted value w_i was based on the signal-to-noise (S/N) ratio, in which transitions with S/N < 5 were assigned a weight of 0, S/N > 20 were assigned a weight of 1, and intermediate values S/N values were assigned based on a sigmoidal curve. Transitional fold change F_t was determined using equation 2. The weight for transitional fold change w_t is determined with equations 3 and 4, favouring changes with low standard deviation and high absolute difference. Peptide fold change weight w_p is calculated by equation 5, while peptide fold change F_p is calculated by equation 6 for all transitions with the same behaviour (*i.e.* up or down) as the peptide. Protein fold change is calculated by equation 7 while the protein discriminating factor or average weight value w_{pr} was calculated by equation 8. Bisson *et al.* showed a weight value of 0.7 to be equivalent to a p-value of 0.05. This value was used for determination of significance in protein fold change for the purposes of this study.

(1) $$I_t^s = \frac{\sum_i^{nt} w_i I_i}{\sum_i^{nt} w_i}$$

(2) $$F_t = \frac{I_t^{s2}}{I_t^{s1}}$$

(3) $$x_t = \frac{\left|I_t^{s2} - I_t^{s1}\right|}{std(I_t^{s2}) + std(I_t^{s1})}$$

(4) $$w_t = f(x_t) * sign(I_t^{s2} - I_t^{s1})$$

(5) $$F_p = \frac{\sum^{np} |w_t| F_t}{\sum^{np} |w_t|}$$

(6) $$w_p = \frac{\sum^{np} w_t}{np}$$

(7) $$F_{pr}^{UP} = \frac{\sum^{npr} w_p F_p}{\sum^{npr} w_p}, (w_p > 0) \quad \text{and} \quad F_{pr}^{DW} = \frac{\sum^{npr} |w_p| F_p}{\sum^{npr} |w_p|}, (w_p < 0)$$

(8) $$w_{pr}^{UP} = \frac{\sum^{npr} w_p}{npr}, (w_p > 0) \quad \text{and} \quad w_{pr}^{DW} = \frac{\sum^{npr} |w_p|}{npr}, (w_p < 0)$$

Figure 6. Equations for statistical analysis of SRM transitions .[80] Based on the signal-to-noise ratio of the measurement, each transition is assigned a value from 0 to 1, with a S/N < 5 = 0, a S/N >20 = 1, and intermediate values determined by a sigmoidal curve. Transition fold changes are calculated and weighted, and combined into peptide and then protein fold changes. Using this method, outlier measurements are removed from the analysis.

3 Results

3.1 Cell Line Differentiation and Characterization

Two model systems were used to model protein expression changes that occur as human embryonic stem cells (hESC) differentiate. Specifically, two human embryonic stem cell lines were chosen, H9, derived by the Wisconsin stem cell group led by Jamie Thomson, and CA1, derived by Andras Nagy at the University of Toronto. [2, 43, 52] **Figure 7** illustrates the two differentiation schemes. By treating H9 cells with recombinant human Bone Morphogenic Protein-4 (rhBMP4) over the course of 96 hours, cells would be driven towards a more differentiated phenotype, that of trophoblast or mesoderm[108]. The CA1 line contains a transgene that constitutively expresses a Sox17/Estrogen Receptor (ERT2) fusion protein that is localized to the cytoplasm under non-induced conditions. Upon induction with 4-hydroxytamoxifen (4-OHT) the protein translocates to the nucleus and directs differentiation of the cells towards a definitive endoderm precursor state. Specifically, the line used was CA1 Sox17/ERT2 Puro Clone K (CA1K), obtained from Dr. Cheryle Seguin.[53]

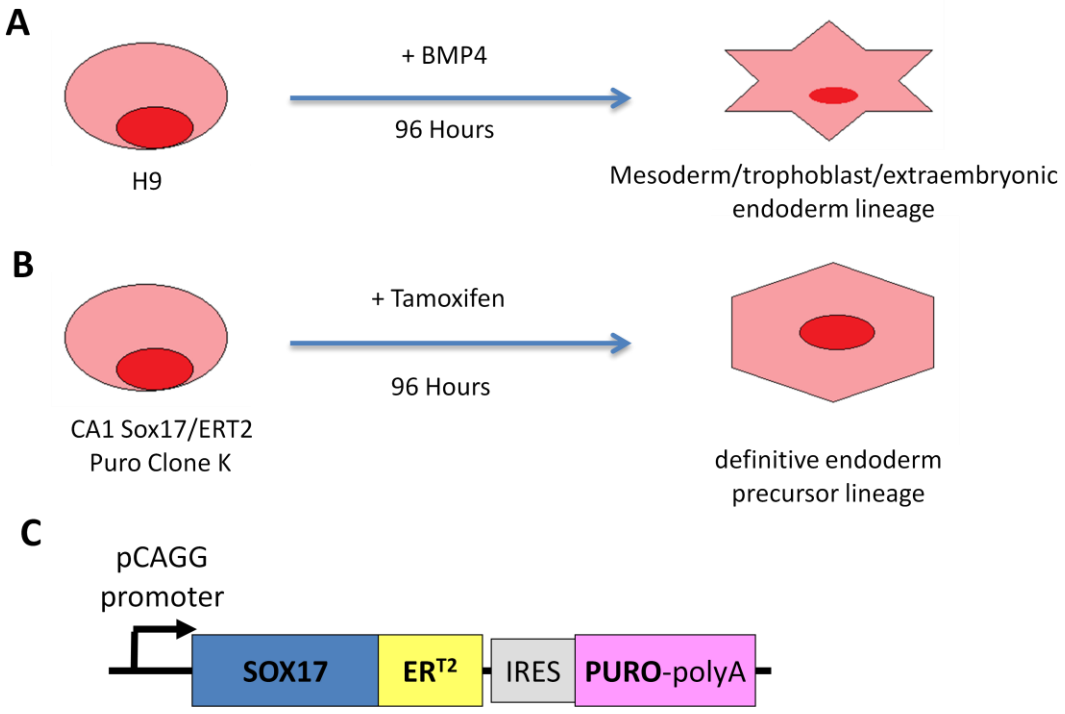

Figure 7. hESC differentiation models. A. H9 differentiation protocol. H9 cells are treated for 96 hours with hESC media containing rhBMP4. **B.** CA1K differentiation protocol. CA1K cells are treated for 96 hours with hESC media containing 4-OHT. **C.** Transgene responsible for constituitive Sox17/ERT2 protein expression, including expression of a puromycin resistance gene for selection. pCAGG – strong promoter. ER^{T2} - human estrogen receptor. IRES – Internal ribosome entry site.

These two hESC differentiation methods provide two distinct systems within which to monitor protein changes. The H9 differentiation is more apparent, providing a model expected to manifest large changes in protein expression. The CA1K differentiation offers a model expected to provide more subtle changes, as the differentiated cells still retain some aspects of pluripotency. In addition, the CA1K differentiation process is more directed, leading to a less heterogeneous cell population.

As seen by phase contrast microscopy in **Figure 8**, the phenotypic change can be confirmed visually. Prior to differentiation, cell colonies consist of round, tightly packed cells with defined borders. H9 BMP4 differentiation tends to result in fewer, smaller colonies containing cells with extended morphology, while CA1 differentiation results in cells with a more cobblestone-like appearance, while still maintaining dense colonies. To validate both of these approaches and confirm successful differentiation, several techniques were used, including immunofluorescence, RT-PCR, and flow cytometry.

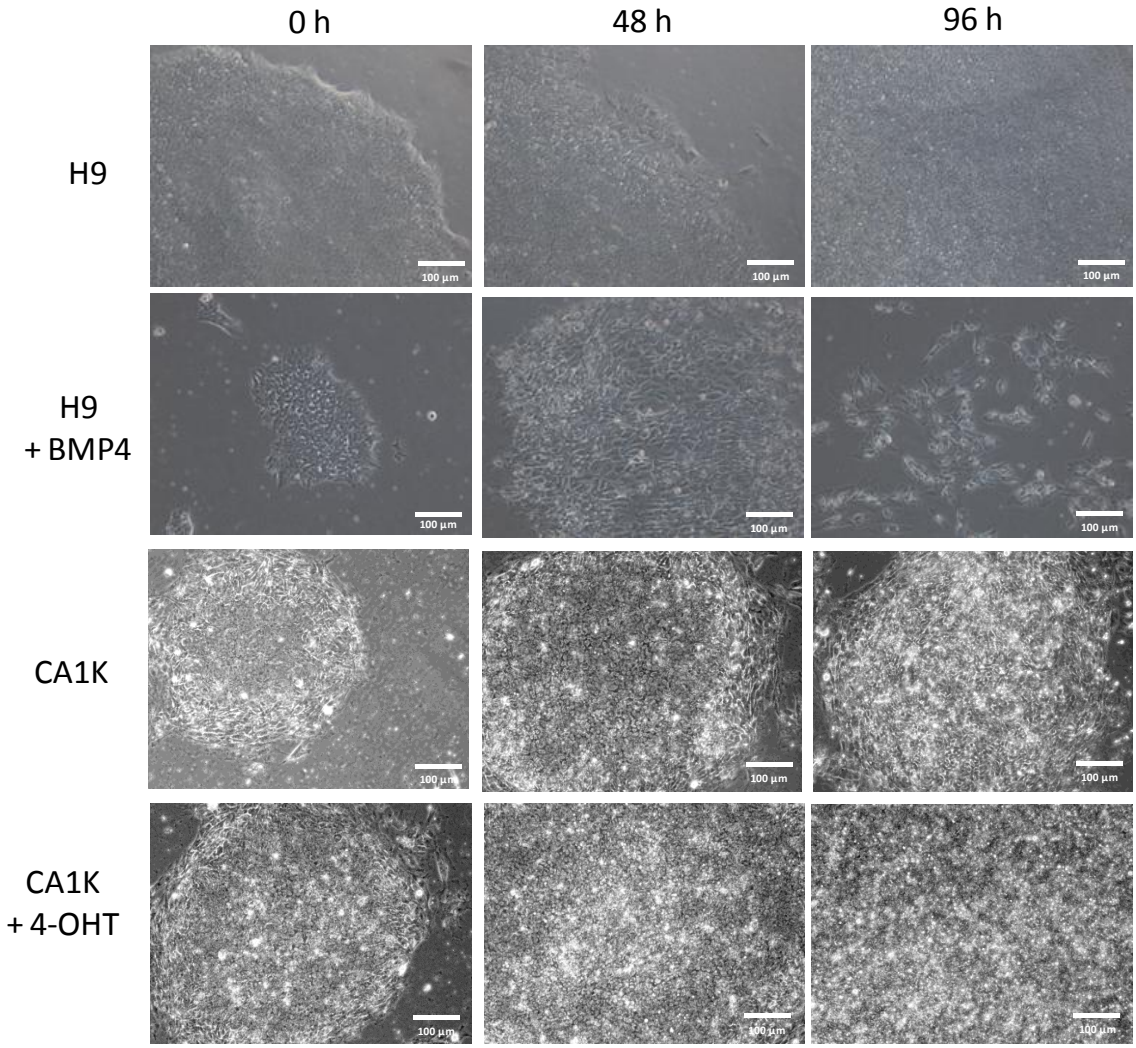

Figure 8. Changes in hESC morphology after exposure to differentiation factors. hESCs were passaged and plated on Geltrex basement membrane matrix. H9s were treated with differentiation media containing 10 ng/µL rhBMP4 to induce differentiation, or cultured in MEF-CM as a control. CA1K cells were treated with differentiation media containing 0.1 nM 4-OHT or cultured in MEF-CM. Media was changed daily, and phase contrast micrographs at 10X magnification were taken at 24 hour intervals to monitor changes in morphology. H9 differentiation led to colony disruption and elongated cells, CA1K differentiation kept colony structure, with slightly more cobblestone-like cells.

3.1.1 Immunofluorescence

To confirm the change in phenotype and a loss of pluripotency, immunofluorescence experiments were performed. hESC cells in feeder-free culture were treated with BMP4 or 4-OHT for 96 hours, fixed and stained for several factors of interest. These factors included Oct4, a nuclear transcription factor required for pluripotency, SSEA4, a cell surface marker of pluripotency, SSEA1, a cell surface marker of differentiation, and DAPI for nuclear staining. **Figure 9** illustrates the results of the immunofluorescence experiments. During H9 differentiation, bright green fluorescence localized at the nucleus and cell membrane is very pronounced in undifferentiated samples, indicating high Oct4 and SSEA4 expression. In differentiated samples, SSEA1 expression is more pronounced, as seen in red-yellow patches.

Undifferentiated CA1Ks show bright green fluorescence localized to the nucleus, indicative of high Oct4 expression. Upon differentiation, nuclear staining is reduced and red surface staining is increased, indicative of increased SSEA1 expression. Likewise, strong SSEA4 fluorescence is seen in the undifferentiated cells, while the red fluorescence of SSEA1 expression becomes more prominent in the differentiated cells.

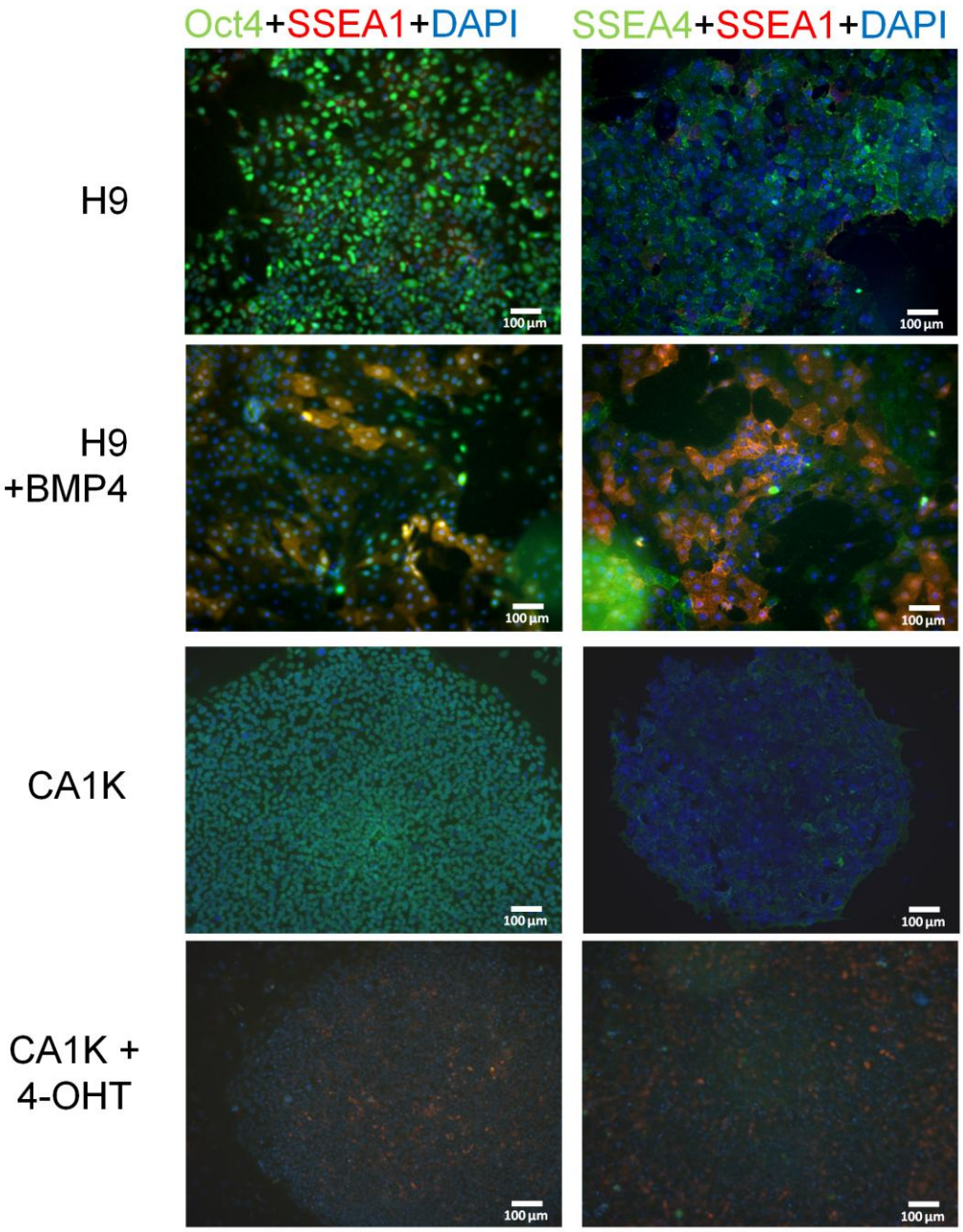

Figure 9. Immunofluorescence of Differentiated Cells. Immunofluorescence staining was performed on undifferentiated and differentiated cell lines. Cells were allowed to differentiate for 96 hours under treatment with 0.1 nM 4-hydroxytamoxifen (4-OHT) or 10ng/mL rhBMP4. Cells were stained for pluripotency markers Oct4 (intracellular) and SSEA4 (surface), and surface differentiation marker SSEA1. DAPI nuclear staining was also used. Three biological replicates were performed for each differentiation protocol.

3.1.2 Confocal Microscopy of Sox17/ERT2 Translocation

To ensure that the tamoxifen-inducible Sox17/ERT2 system successfully results in the fusion protein being translocated to the nucleus, immunofluorescence experiments combined with confocal microscopy were performed. CA1 Sox17/ERT2 clone K cells were cultured on Geltrex-coated coverslips for 24 hours, then treated with tamoxifen for two hours, then fixed and stained with a conjugated Alexa Fluor®488 Sox17 antibody. As shown by the green staining in **Figure 10**, in uninduced cells, the fusion protein is spread out across the cytoplasm and fluorescence is diffuse. Upon two hours of treatment, the green fluorescence becomes more concentrated and co-localizes with the blue DAPI nuclear stain, showing the fusion protein does translocate to the nucleus.

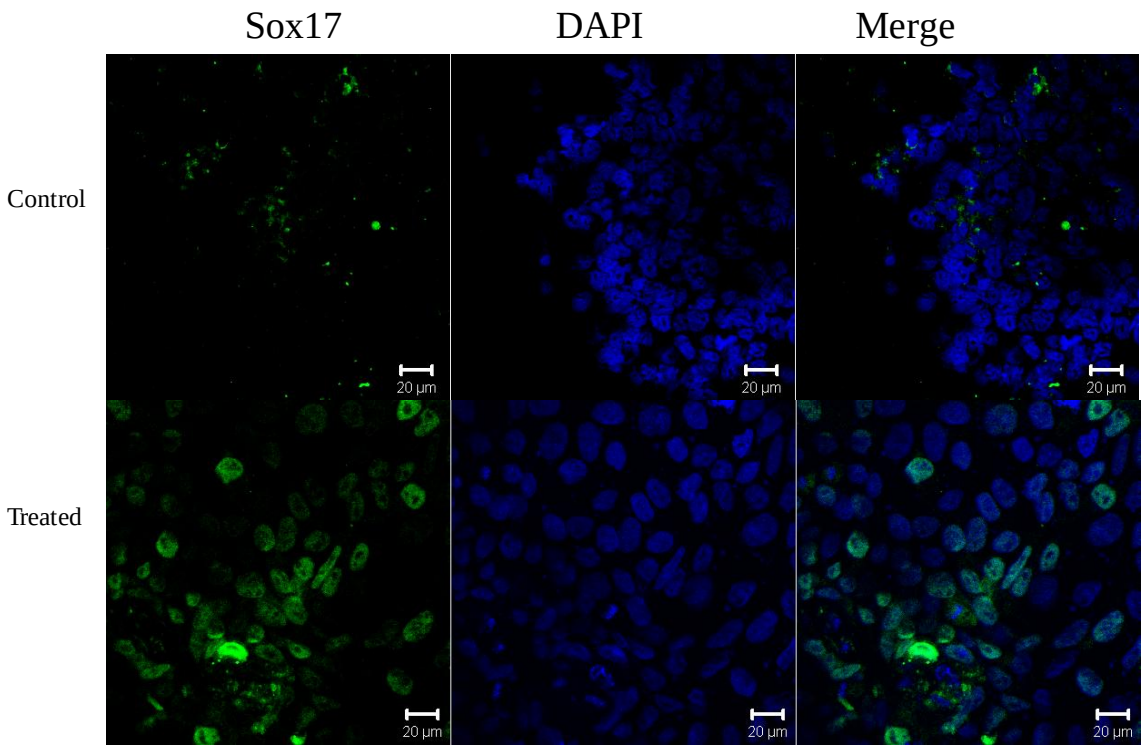

Figure 10. Confocal Microscopy of Sox17 Nuclear Localization. CA1 Sox17ERT2 Puro Clone K cells were grown on Geltrex coated coverslips for 24 hours. Cells were treated with 0.1 nM 4-OHT for 2 hours, then mounted, stained for Sox17 and DAPI, and imaged using a confocal microscope. A single biological replicate was performed.

3.1.3 Real-Time RT-PCR Analysis of hESC Differentiation

To confirm that cell differentiation was occurring at the transcription level, RT-PCR experiments were performed. H9 or CA1K cells were again seeded onto Geltrex, and treated with BMP4 or tamoxifen, or kept as a control for 96 hours. RNA was extracted, and cDNA was synthesized. As the CA1K line was being differentiated towards definitive endoderm, expression of endodermal markers including Cerberus, CXCR4, DLX5, GATA4, and GATA6 were analyzed, along with pluripotency markers Nodal, Oct4, and Nanog. Constitutively expressed proteins β-glucuronidase (GusB) and TATA-binding protein (TBP) were used as loading controls. The -ΔΔCt method was used for quantitation.[106] All expression levels were normalized to GusB expression, as it is a housekeeping gene expected to remain stable across differentiation. Fold change of mRNA expression was expressed relative to the undifferentiated sample. As H9 BMP4 differentiation was a less directed method of differentiation, only the pluripotency markers Oct4, Nanog, and Nodal were monitored.

Figure 11A illustrates expression changes in H9 BMP4 differentiation with an N = 6. Oct4 expression was decreased by 50%, while Nanog expression dropped by 75%. Previous RT-PCR analyses have shown that BMP4 treatment results in decreased expression of Oct4 and Nanog over a 96-hour time course. [50, 109]

Figure 11B illustrates expression changes in tamoxifen-induced differentiation of CA1K cells with N=9. Endoderm markers Cerberus, CXCR4, DLX5, GATA4 and GATA6 were all seen to be upregulated, while Oct4, Nanog and Nodal remained stable or slightly decreased in expression, consistent with the gene expression results for the stable SOX17 overexpressing cell line generated by Seguin *et al.*[53]

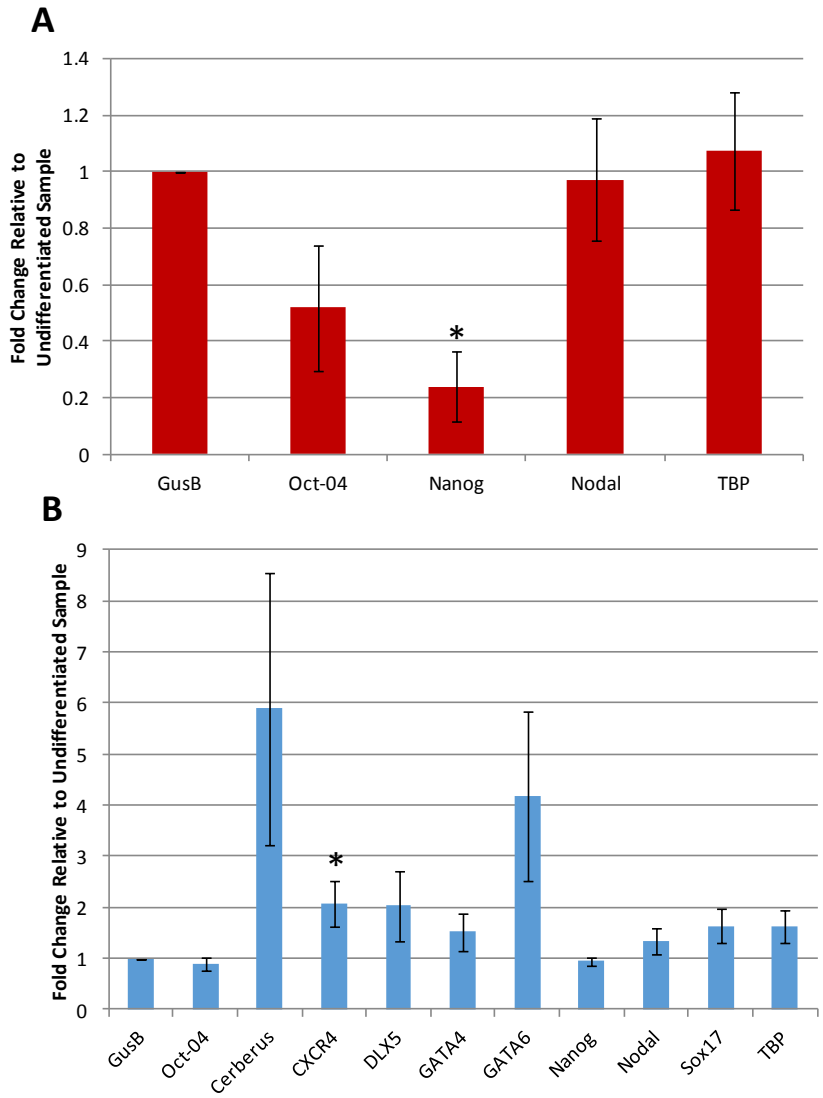

Figure 11. Real-Time RT-PCR Data for Cell Differentiation. Real-time RT-PCR experiments were performed on cDNA obtained from differentiated **A.** H9 and **B.** CA1 Sox17/Ert2 Puro Clone K cell lines, differentiated for 96 hours upon treatment with 0.1 nM 4-OHT or 10 ng/mL rhBMP4 respectively. Data was normalized to GusB expression. -ΔΔCt method was used for quantitation. Bars represent fold change of expression relative to undifferentiated sample, error bars represent standard error of the mean. Changes found to be significant according to a two-tailed t-test with $p < 0.05$ were marked with *. 9 biological replicates were performed for CA1K differentiation. 6 biological replicates were performed for H9 differentiation.

3.1.4 Flow Cytometry Analysis of Differentiated hESC Populations

To confirm that cell differentiation was occurring at the cellular protein level, flow cytometry experiments were performed. hESCs cultured on Geltrex™ were dissociated and labelled with conjugated antibodies for pluripotency markers Oct4 and SSEA3, and differentiation marker SSEA1. Fixation is required to analyze Oct4, which kills the entire cell population. To ensure analysis was performed on live cells, an Aqua viability dye was first used in order to gate on the live population. The viability dye binds to exposed membrane, hence dead cells will exhibit greater overall fluorescence. All analysis was performed on the live population, which exhibits lower fluorescence.

Each treatment was performed in biological duplicate, and a single representative replicate has been presented. hESCs survive poorly when dissociated to the single-cell state, becoming prone to apoptosis and differentiation.[110] Thus, only 20-50% live cells were available for analysis, as seen in **Figure 12B** and **12C**. Histograms showing the change in fluorescence for each marker can be seen in **Figure 12D-F**.

For Oct4 expression in H9s, cells exhibited a 2.3-fold decrease in median fluorescence upon differentiation, which is significantly lower for $p < 0.05$. For SSEA1 expression, exhibited a 37-fold increase in median fluorescence upon differentiation. For SSEA3 expression, exhibited a 2.2-fold decrease in median fluorescence upon differentiation. Dot plots comparing multiple proteins in **Figure12G-I** confirm that the differentiated and undifferentiated cells form two distinct populations.

Figure 13 illustrates flow cytometry data for CA1K differentiation. For Oct4 expression in CA1K cells exhibited a 1.3-fold increase in median fluorescence upon differentiation. As expected, the differentiated CA1K cells still express Oct4.[53] For SSEA1 expression exhibited a 1.5-fold increase in median fluorescence upon differentiation. For SSEA3 expression exhibited a 1.08-fold decrease in median fluorescence upon differentiation. The dot plots also signify that the populations of these differentiated and undifferentiated cells are far less distinct than the H9 cells in terms of these pluripotency markers. These cells cannot definitively be called differentiated taking only flow cytometry data into account.

Taking the immunofluorescence, RT-PCR, and flow cytometry experiments together, we can confirm that we have two distinct, but equally valid differentiation models with which to detect protein changes that occur during differentiation: the H9 differentiation model to illustrate drastic changes, and the more subtle CA1K differentiation model.

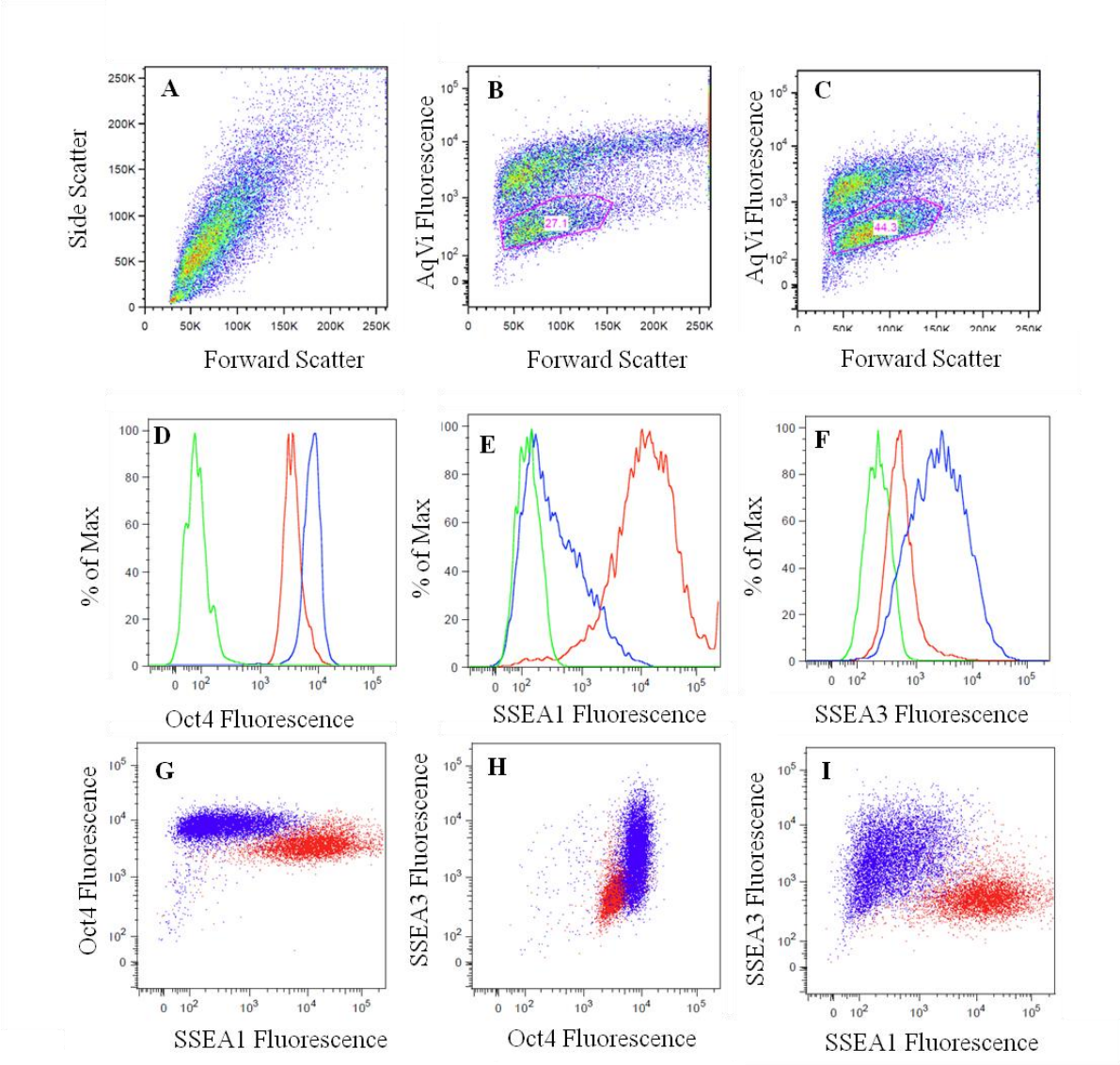

Figure 12. Flow cytometry of H9 Differentiation. H9 cells were differentiated for 96 hours in 10 ng/mL rhBMP4. Cells were dissociated to the single cell state, stained with AqVi LIVE/DEAD® dye, fixed, then stained with SSEA1, SSEA3, and Oct4 conjugated antibodies. All analysis was conducted on the gated live cell population. Fluorescence is on the log scale. Red = differentiated. Blue = undifferentiated. Green = Fluorescence minus One (FMO) **A**. Forward scatter vs. side scatter for fully stained H9 cells**. B-C**. Aqua viability dye fluorescence vs. Forward scatter for fully stained BMP4 treated and untreated cells. **D-F.** Histograms for Oct4, SSEA1 and SSEA3 expression. Fluorescence is on the log scale. **G-I.** Dot plots for undifferentiated and differentiated cell populations. Two biological replicates were performed.

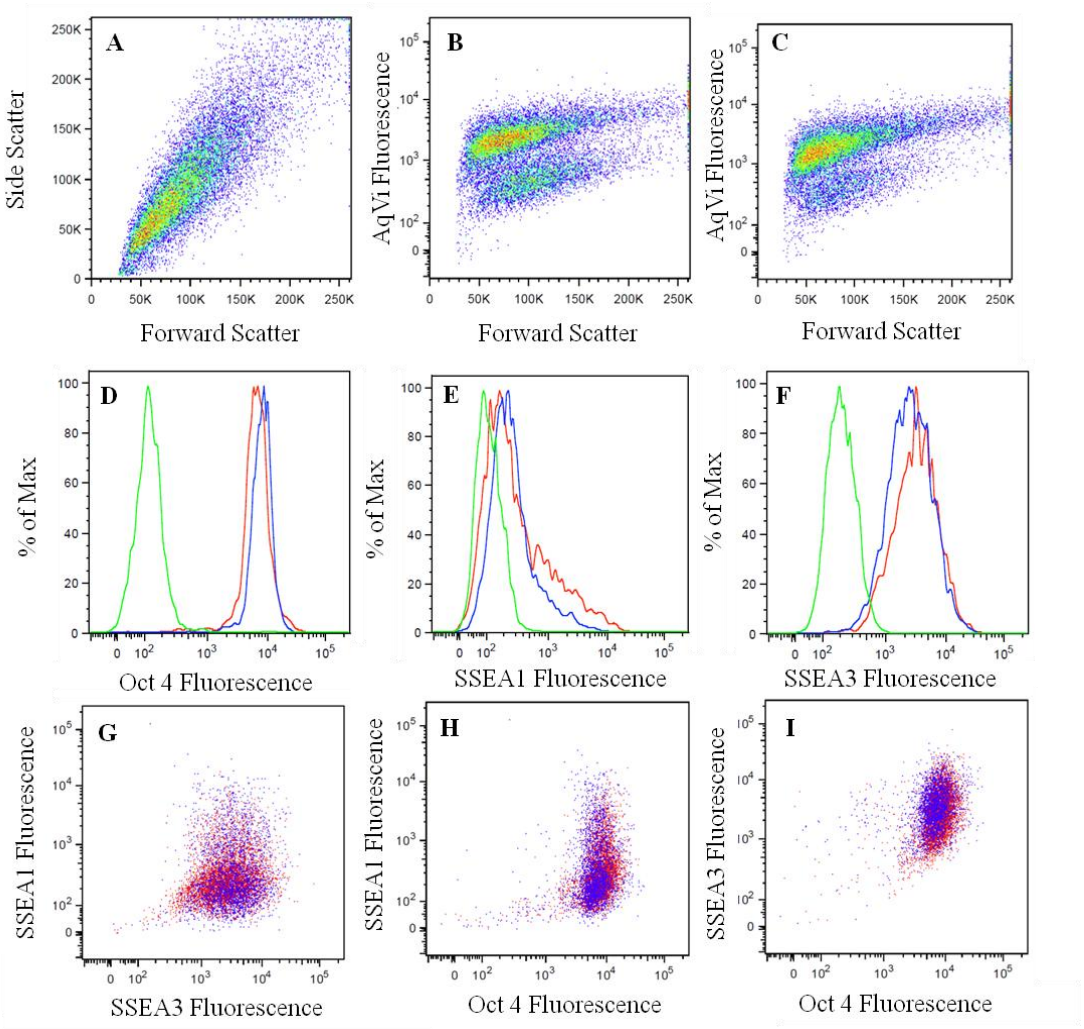

Figure 13. Flow cytometry of CA1K Differentiation. CA1K cells were differentiated for 96 hours in 0.1 nM 4-OHT. Cells were dissociated to the single cell state, stained with Aqua LIVE/DEAD® viability dye, fixed, then stained with SSEA1, SSEA3, and Oct4 conjugated antibodies. All analysis was conducted on the gated live cell population. Red = differentiated. Blue = undifferentiated. Green = Fluorescence minus One (FMO) negative control. **A.** Forward scatter vs. side scatter for fully stained CA1K cells**. B-C**. Aqua viability dye fluorescence vs. forward scatter for fully stained 4-OHT treated and untreated cells. **D-F**. Histograms for Oct4, SSEA1 and SSEA3 expression. Fluorescence is on the log scale. **G-I**. Dot plots for undifferentiated and differentiated cell populations. Two biological replicates were performed.

3.2 SRM Assay Development

Stem cell pluripotency is controlled by a complex network of signaling pathways and proteins. Potential SRM targets were selected through an extensive literature search for notable proteins responsible for pluripotency maintenance, with an emphasis on proteins from the Notch, Hedgehog, Wnt, and Activin/Nodal signaling pathways. Thirty-three initial protein targets were selected, and are listed with Uniprot accession numbers and corresponding peptides in **Table 2**. Thirty-three preliminary targets were initially chosen in order to fill a 96-well peptide synthesis plate, with the potential for more targets in future studies.

Two or three tryptic peptides corresponding to each target protein were chosen for synthesis. Protein sequences were obtained from the online database Uniprot and loaded into the SRM assay development software Skyline. The protein sequences were subjected to an *in silico* trypsin digest, preferentially cleaving at arginine and lysine residues, except for when followed by a proline residue. Human protein spectral libraries were downloaded from the Global Proteome Machine Database (GPMDB) and the National Institute of Standards and Technology and loaded into Skyline. Peptides that were previously observed experimentally were given preference in the selection process. However, many target proteins were not present in the library. Criteria set out by Lange *et al.* for SRM target selection were followed and input into the filter function in Skyline.[60] Peptides were limited to 8-25 residues in length, residues prone to oxidation such as methionine and tryptophan were excluded, and Skyline generated a list of peptides matching either the library or filter. Certain protein sequences were unable to provide peptides meeting these criteria due to a large amount of methionine in the sequence, Nodal, in particular. In these cases, methionine was accepted and oxidation was accounted for. Peptides were checked for protein specificity using protein BLAST.[111] PeptideCutter was used to assess probability of tryptic cleavage for the target peptides[112]. Target peptides were synthesized in-house at the 5 μmol level using the FMOC protocol on an Intavis multiple peptide synthesizer.

Table 2. List of target proteins and peptides.

Protein	Accession	Peptide	Protein	Accession	Peptide
Wnt1	P04628	QNPGILHSVSGGLQSAVR	SUFU	Q9UMX1	VHEFTGTDGPSGFGFELTFR
		ETAFIFAITSAGVTHSVAR			GIETDGSNLSGVSAK
		ACNSSSPALDGCELLCCGR			GLEINSKPVLPPINPQR
DVL-1	O14640	NVLSNRPVHAYK	Frizzled-1	Q9UP38	FPVHGAGELCVGQNTSDK
		LSSSTEQSTSSR			GGFPGGAGASER
		SQASATAPGLPPPHPTTK			VPSYLNYHFLGEK
AXIN-1	O15169	SDIYLEYTR	WIF-1	Q9Y5W5	VLIGFEEDILIVSEGK
		DAHEENPESILDEHVQR			ASVVQVGFPCLGK
					TCQQAECPGGCR
Lefty-1	O75610	LPPNSELVQAVLR	Nodal	Q96S42	VPSTCCAPVK
		QPLLLQVSVQR			TKPLSMLYVDNGR
		EHLGPLASGAHK			GQPSSPSPLAYMLSLYR
DKK1	O94907	NGICVSSDQNHFR	POUF51	Q01860	LEQNPEESQDIK
		SSDCASGLCCAR			FEALQLSFK
		DHHQASNSSR			WVEEADNNENLQEICK
Cerberus	O95813	TVPFSQTITHEGCEK	Patched	Q13635	TYVEVVHQSVAQNSTQK
		VVVQNNLCFGK			TEYDPHTHVYYTTAEPR
		TPASQGVILPIK			LPTPSPEPPPSVVR
P53	P04637	LGFLHSGTAK	Sonic Hedgehog	Q15465	ELTPNYNPDIIFK
		SVTCTYSPALNK			SGGCFPGSATVHLEQGGTK
		RPILTIITLEDSSGNLLGR			LAHALLAALAPAR
Wnt2	P09544	ESAFVYAISSAGVVFAITR	FRAT-1	Q92837	APGPLAAAVPADK
		CHGVSGSCTLR			LLQQLVLSGNLIK
		CQDCLEALDVHTCK			
GLI3	P10071	TSPNSLVTILNNSR	Smoothened	Q99835	GAASSGNATGPGPR
		IKPDEDLPSPGAR			FNSSGQCEVPLVR
		GQQEQPEGTTLVK			DYVLCQANVTIGLPTK
APC	P25054	NVSSLIATNEDHR	Wnt3a	P56704	IGIQECQHQFR
		SAEDPVSEVPAVSQHPR			ESAFVHAIASAGVAFAVTR
		NDSLSSLDFDDDDVDLSR			SCAEGTAAICGCSSR
Akt1	P31749	TFHVETPEER	Wnt5a	P41221	ETAFTYAVSAAGVVNAMSR
		FYGAEIVSALDYLHSEK			FNSPTTQDLVYIDPSPDYCVR
		TFCGTPEYLAPEVLEDNDYGR			NESTGSLGTQGR
Beta-Catenin	P35222	HAVVNLINYQDDAELATR	Activin-A (homodimer, beta A chain)	P08476	EGSDLSVVER
		LLNDEDQVVVNK			HPQGSLDTGEEAEEVGLK
		NEGVATYAAAVLFR			SELLLSEK
CDKI1 Aka p21	P38936	DCDALMAGCIQEAR	TDGF/Cripto-1	P13385	FSYSVIWIMAISK
		WNFDFVTETPLEGDFAWER			DDSIWPQEEPAIRPR
					TPELPPSAR
NOTCH1	P46531	NGGTCDLLTLTEYK	Hes1	Q14469	NSSSPVAATPASVNTTPDKPK
		GSIVYLEIDNR			FLSTCEGVNTEVR
		FEEPVVLPDLDDQTDHR			LGSQAGEAAK
GSK3-Beta	P49841	VIGNGSFGVVYQAK	Hey1	Q9Y5J3	YLSIIEGLDASDPLR
		DIKPQNLLLDPDTAVLK			LVSHLNNYASQR
		IQAAASTPTNATAASDANTGDR			LGSAHPEAPALR
SFRP-1	Q8N474	FYTKPPQCVDIPADLR	SRFP-2	Q96HF1	LPNLLGHETMK
		SEAIIEHLCASEFALR			EVLEQAGAWIPLVMK
		SQYLLTAIHK			DSLQCTCEEMNDINAPYLVMGQK
Nanog	Q9H9S0	TVFSSTQLCVLNDR			
		YLSLQQMQELSNILNLSYK			
		NSNGVTQK			

Upon synthesis, peptides were cleaved, precipitated, lyophilized and stored at -80°C until use. A small aliquot was taken and injected directly into a Quattro Micro triple quadrupole mass spectrometer (Waters) to confirm the theoretical peptide mass was present. In all cases, the most abundant ions corresponded to the theoretical peptide mass, with an estimated 80% purity, and thus crude peptide was used without further purification.[66] Synthetic peptides were serially diluted to a 100 fmol/µL working solution, and MS/MS data was obtained for each generated peptide on the 4000 QTRAP®. SRM-triggered DDA methods were generated for each peptide, looking specifically for y and b ions generated by doubly and triply charged precursors. The doubly charged precursor was selected in most cases, unless the target peptide contained a histidine residue or a lysine/arginine residue followed by proline, in which case the triply charged precursor was preferred. Five of the top transitions were collected and compiled in a general SRM protocol. Transitions were prioritized by having fragment m/z greater than the precursor m/z, overall intensity, and favouring y-ions. Retention times were noted and reacquired when the LC gradient was altered. SRM chromatograms showing the five transitions chosen along with corresponding MS/MS data for each target peptide can be seen in **Figures 14-46**. Multiple co-eluting transitions as seen in the chromatograms serve to identify the target peptide, while the area under the curve of each transition can be integrated to obtain quantitative information about peptide abundance. Though peptides can be identified solely by multiple transitions, MS/MS sequence data was also obtained in order to confirm the target sequence.

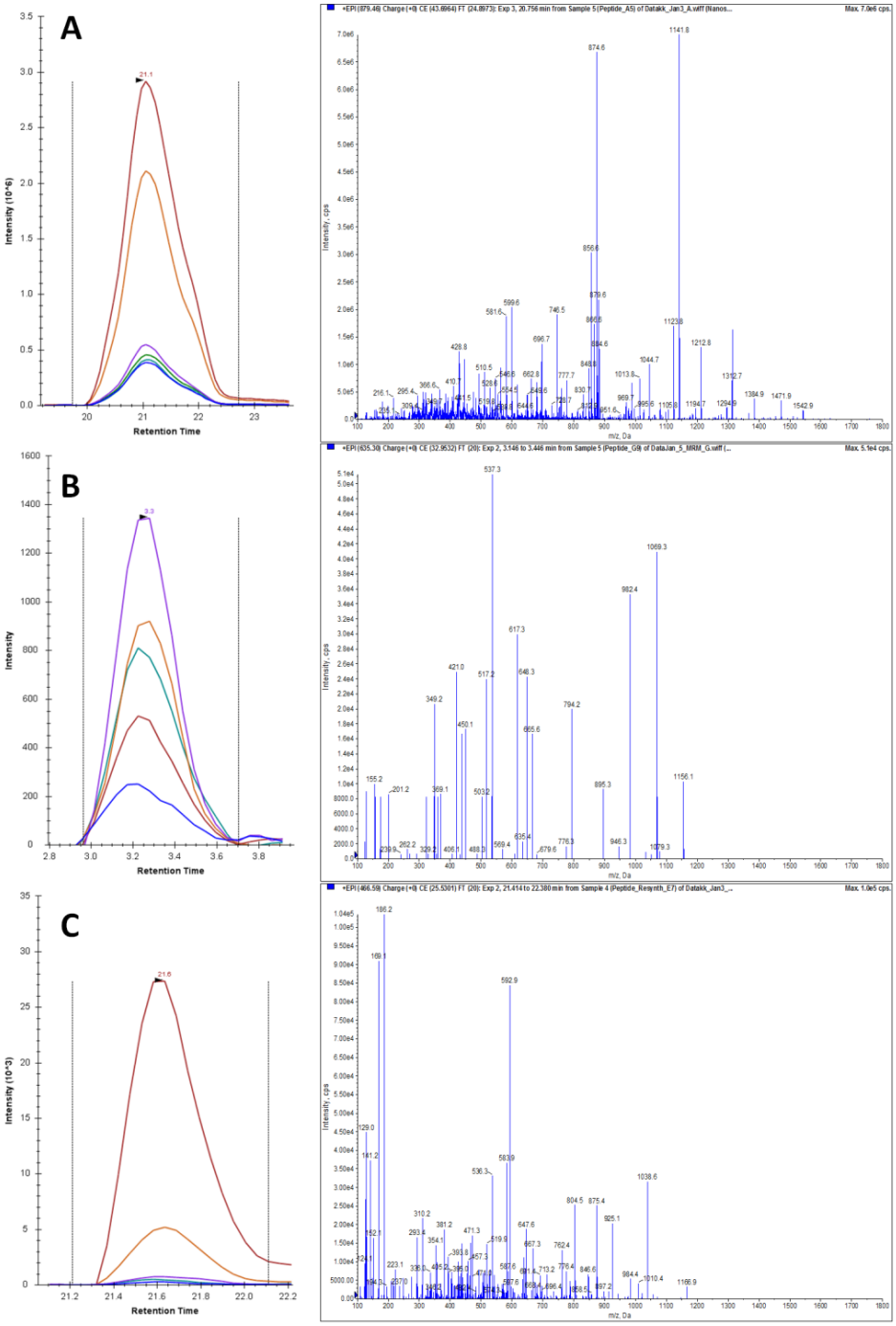

Figure 14. SRM and MS/MS data for protein Dishevelled. SRM-triggered MS/MS spectra were obtained for synthetic peptide targets. Top five SRM transitions are shown in a chromatogram (left). Sequence information can be confirmed with MS/MS spectra (right). **A.** SQASATAPGLPPPHPTTK (m/z=879.46^{++}) **B.** LSSSTEQSTSSR (m/z=635.30^{++}) **C.** NVLSNRPVHAYK (m/z=466.59^{+++})

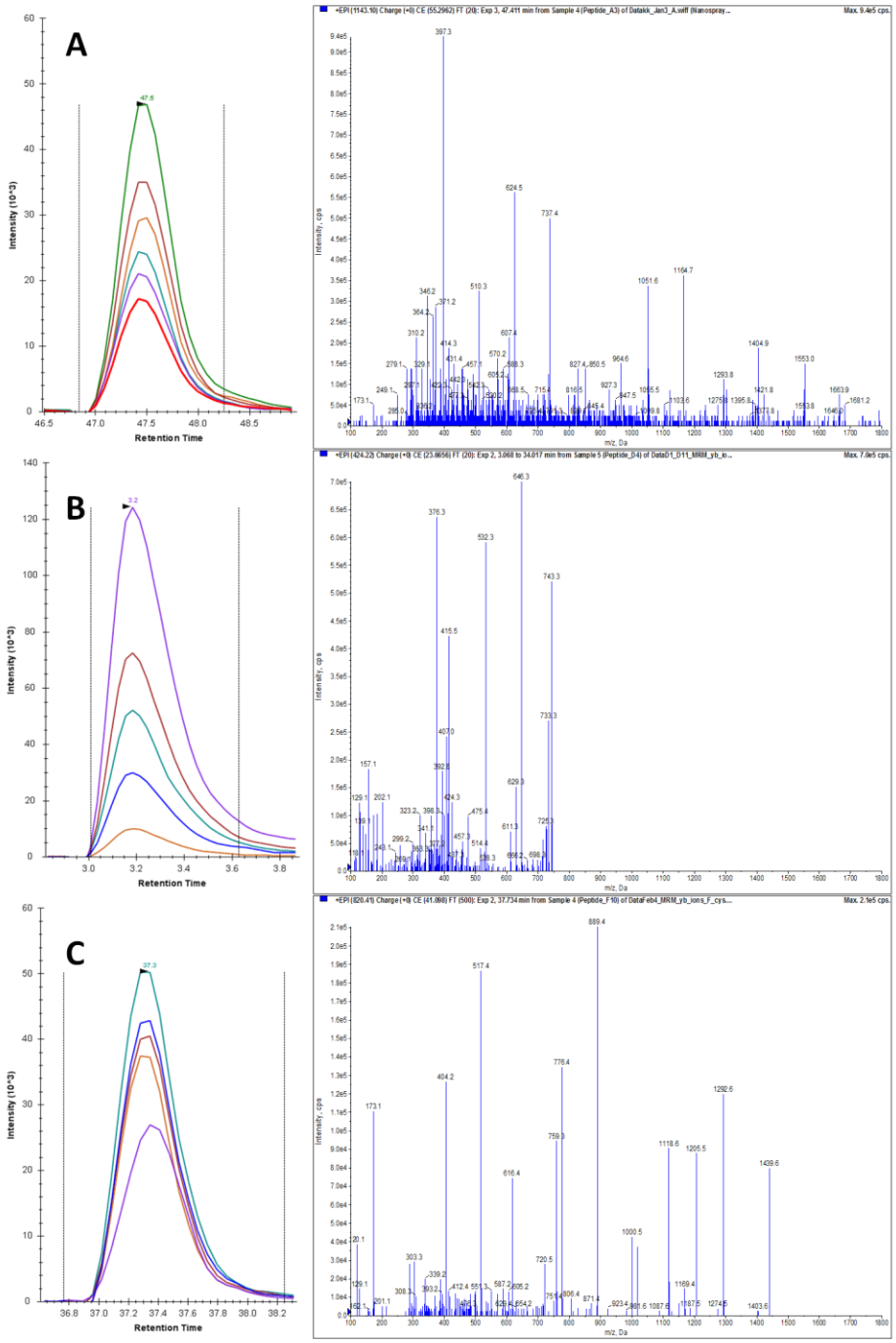

Figure 15. SRM and MS/MS data for protein Nanog. SRM-triggered MS/MS spectra were obtained for synthetic peptide targets. Top five SRM transitions are shown in a chromatogram (left). Sequence information can be confirmed with MS/MS spectra (right). **A.** YLSLQQMQELSNILNLSYK (m/z=1143.10^{++}) **B.** NSNGVTQK (m/z=424.22^{++}) **C.** TVFSSTQLCVLNDR(m/z=820.41^{++})

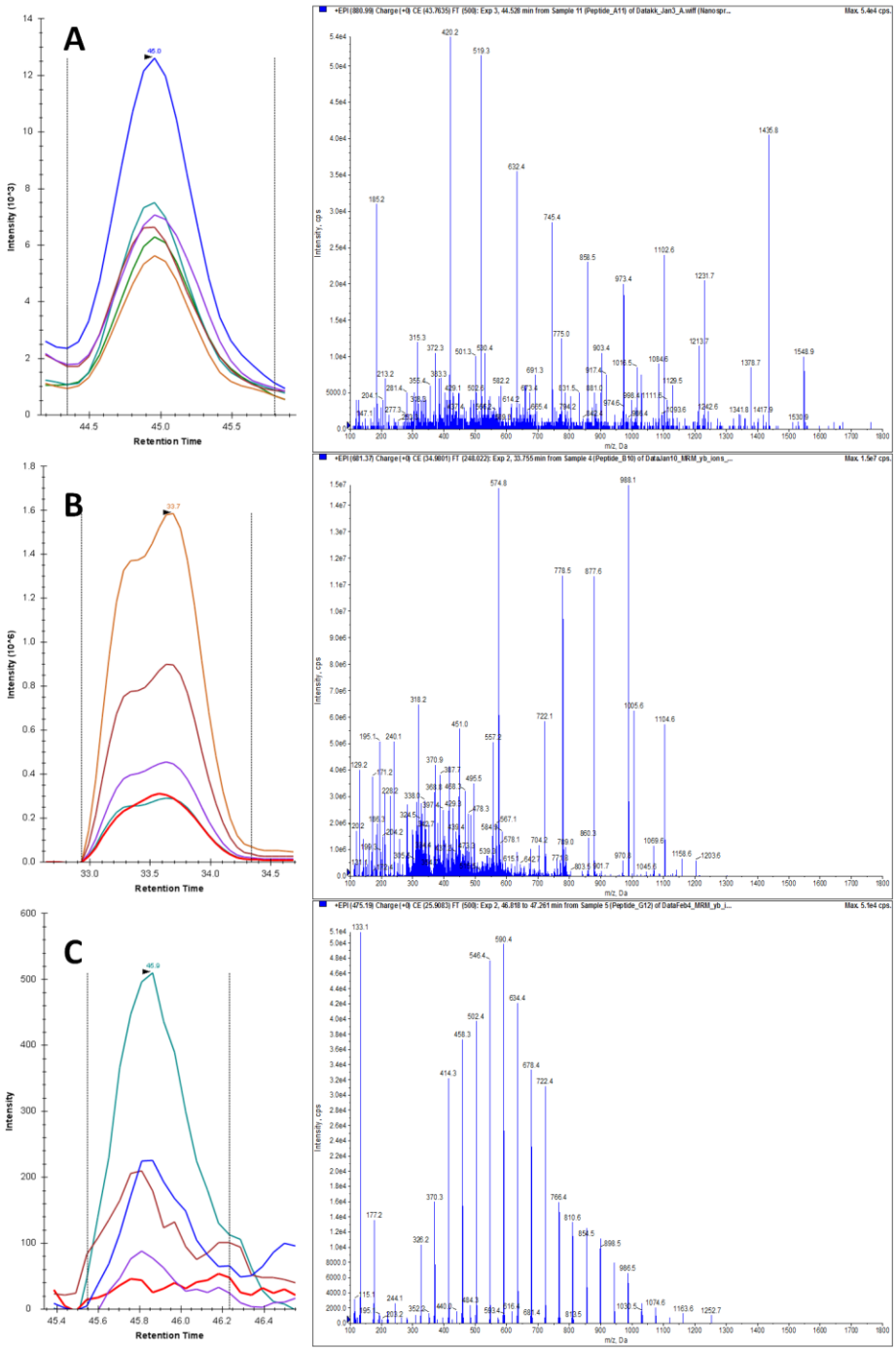

Figure 16. SRM and MS/MS data for protein WIF1. SRM-triggered MS/MS spectra were obtained for synthetic peptide targets. Top five SRM transitions are shown in a chromatogram (left). Sequence information can be confirmed with MS/MS spectra (right). **A.** VLIGFEEDILIVSEGK (m/z=880.99^{++}) **B.** ASVVQVGFPCLGK (m/z=681.37^{++}) **C.** TCQQAECPGGCR (m/z=712.28^{++})

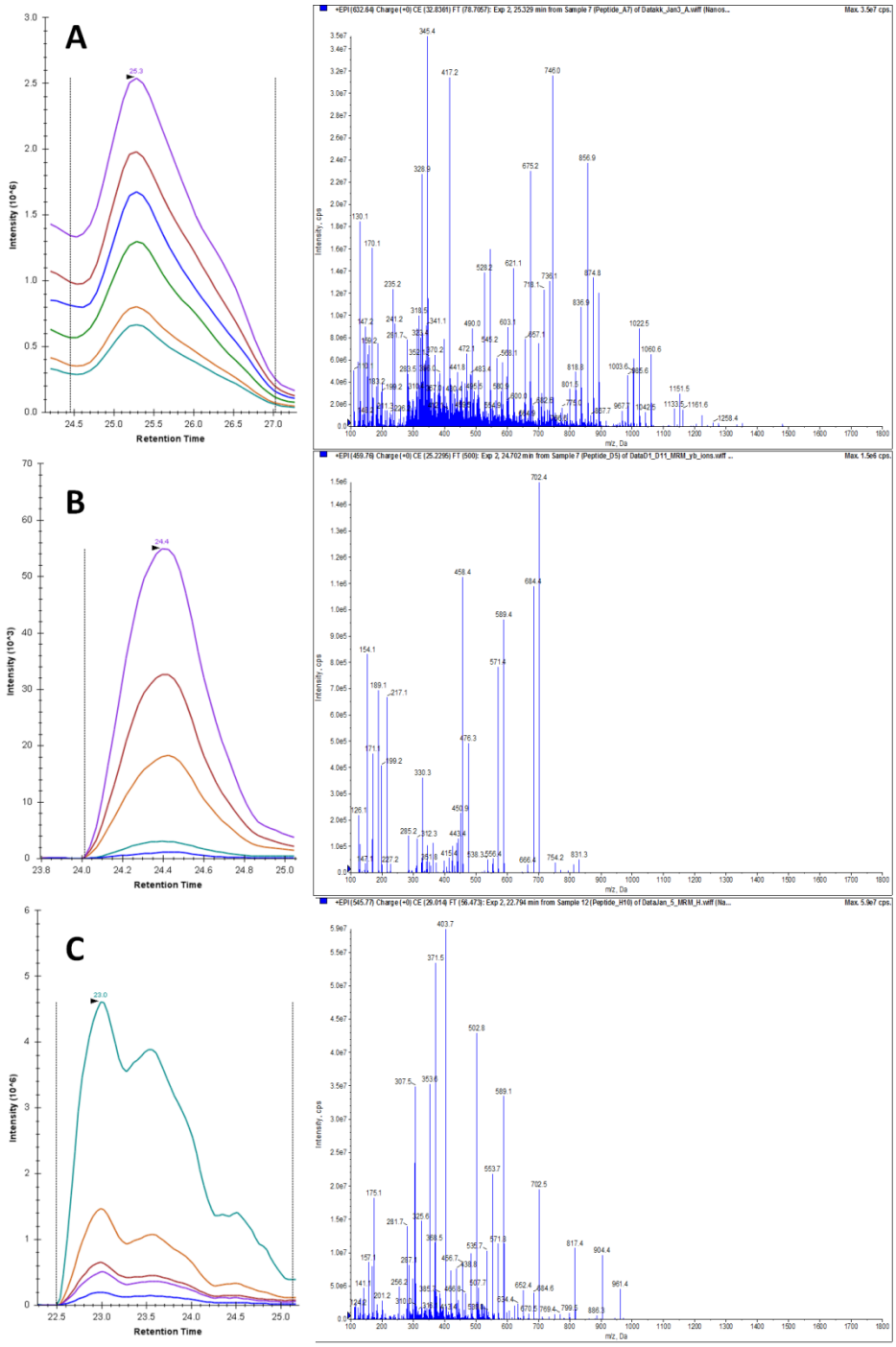

Figure 17. SRM and MS/MS data for protein Activin A. SRM-triggered MS/MS spectra were obtained for synthetic peptide targets. Top five SRM transitions are shown in a chromatogram (left). Sequence information can be confirmed with MS/MS spectra (right). **A.** HPQGSLDTGEEAEEVGLK (m/z=632.64^{+++}) **B.** SELLLSEK (m/z=459.46^{++}) **C.** EGSDLSVVER (m/z=545.77^{++})

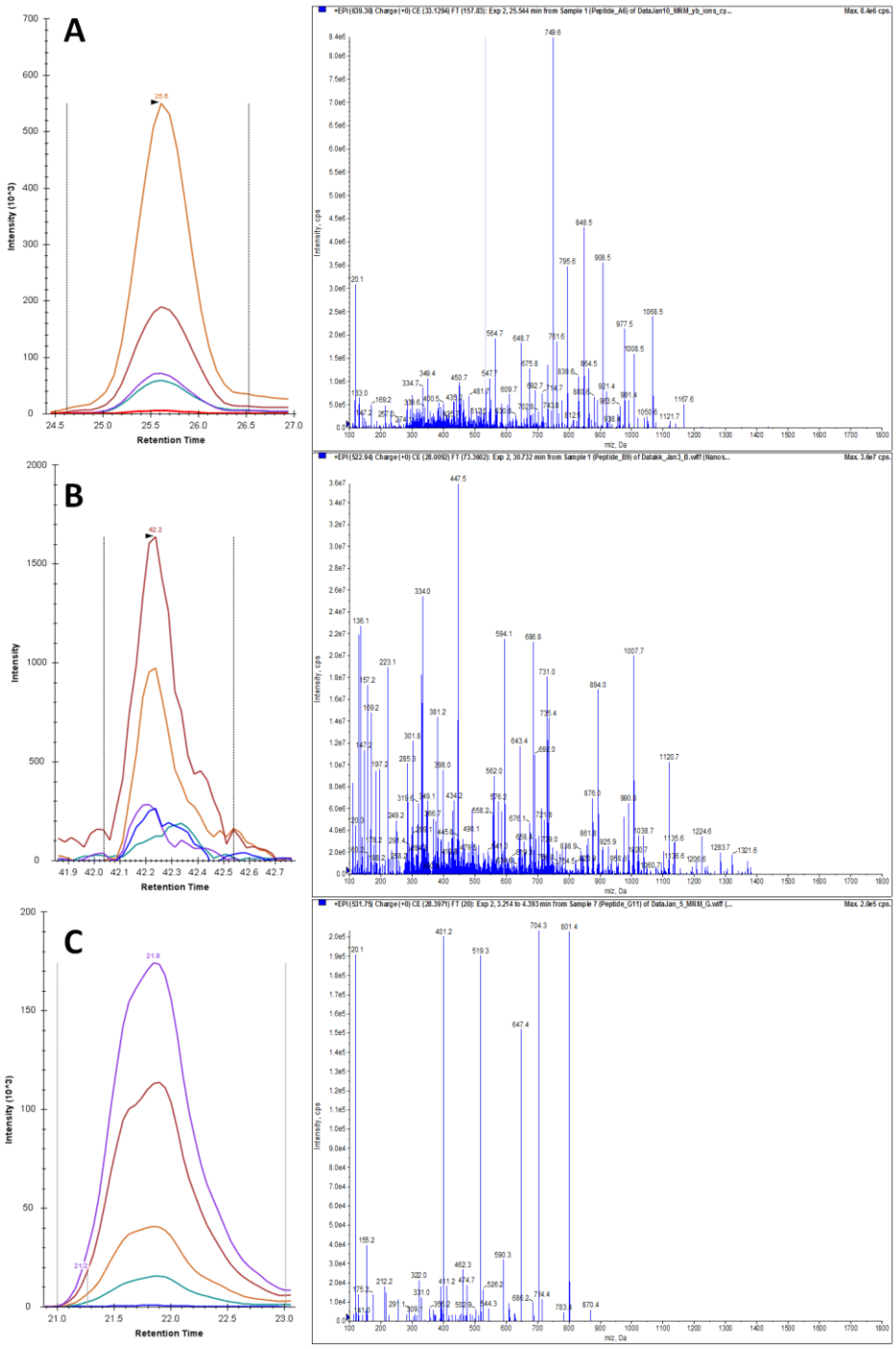

Figure 18. SRM and MS/MS data for protein Frizzled1. SRM-triggered MS/MS spectra were obtained for synthetic peptide targets. Top five SRM transitions are shown in a chromatogram (left). Sequence information can be confirmed with MS/MS spectra (right). **A.** FPVHGAGELCVGQNTSDK (m/z=639.30^{+++}) **B.** VPSYLNYHFLGEK (m/z=522.94^{++}) **C.** GGFPGGAGASER (m/z=531.75^{++})

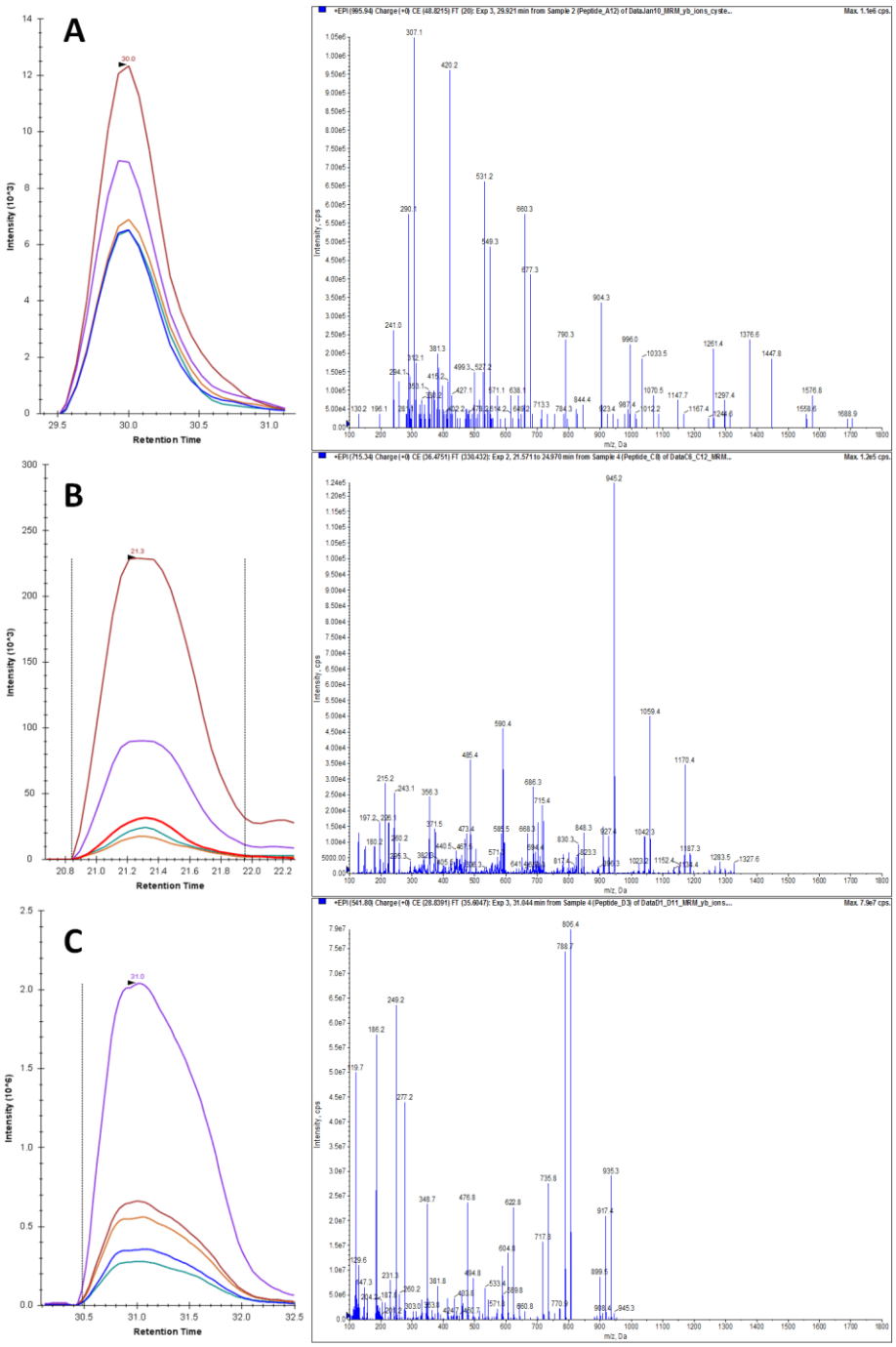

Figure 19. SRM and MS/MS data for protein Oct4. SRM-triggered MS/MS spectra were obtained for synthetic peptide targets. Top five SRM transitions are shown in a chromatogram (left). Sequence information can be confirmed with MS/MS spectra (right). **A.** WVEEADNNENLQEICK (m/z=995.94^{++}) **B.** LEQNPEESQDIK (m/z=715.34^{++}) **C.** FEALQLSFK (m/z=541.79^{++})

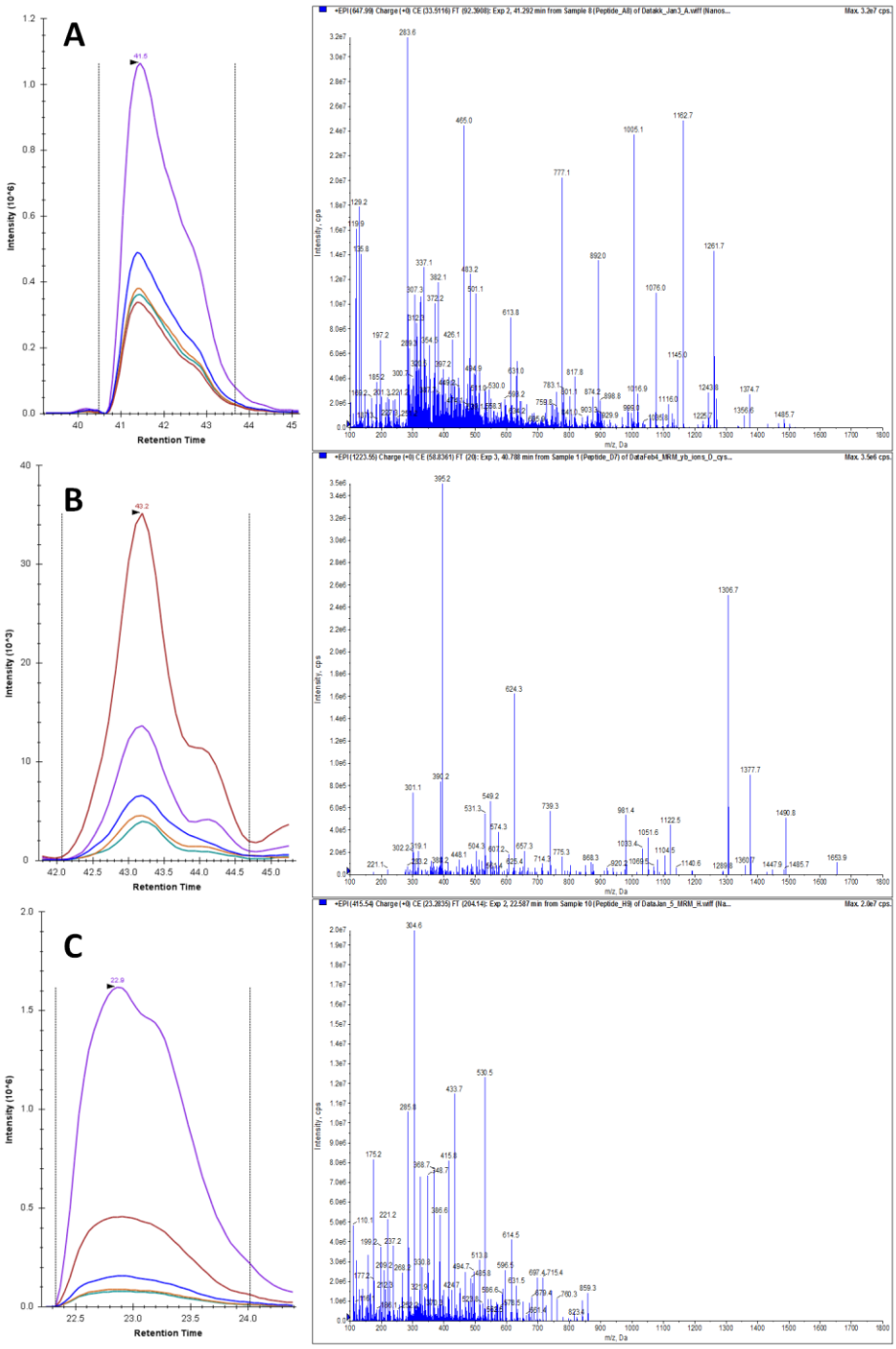

Figure 20. SRM and MS/MS data for protein Akt1. SRM-triggered MS/MS spectra were obtained for synthetic peptide targets. Top five SRM transitions are shown in a chromatogram (left). Sequence information can be confirmed with MS/MS spectra (right). **A.** FYGAEIVSALDYLHSEK (m/z=647.99^{+++}) **B.** TFCGTPEYLAPEVLEDNDYGR (m/z=1223.55^{++}) **C.** TFHVETPEER (m/z=415.54^{+++})

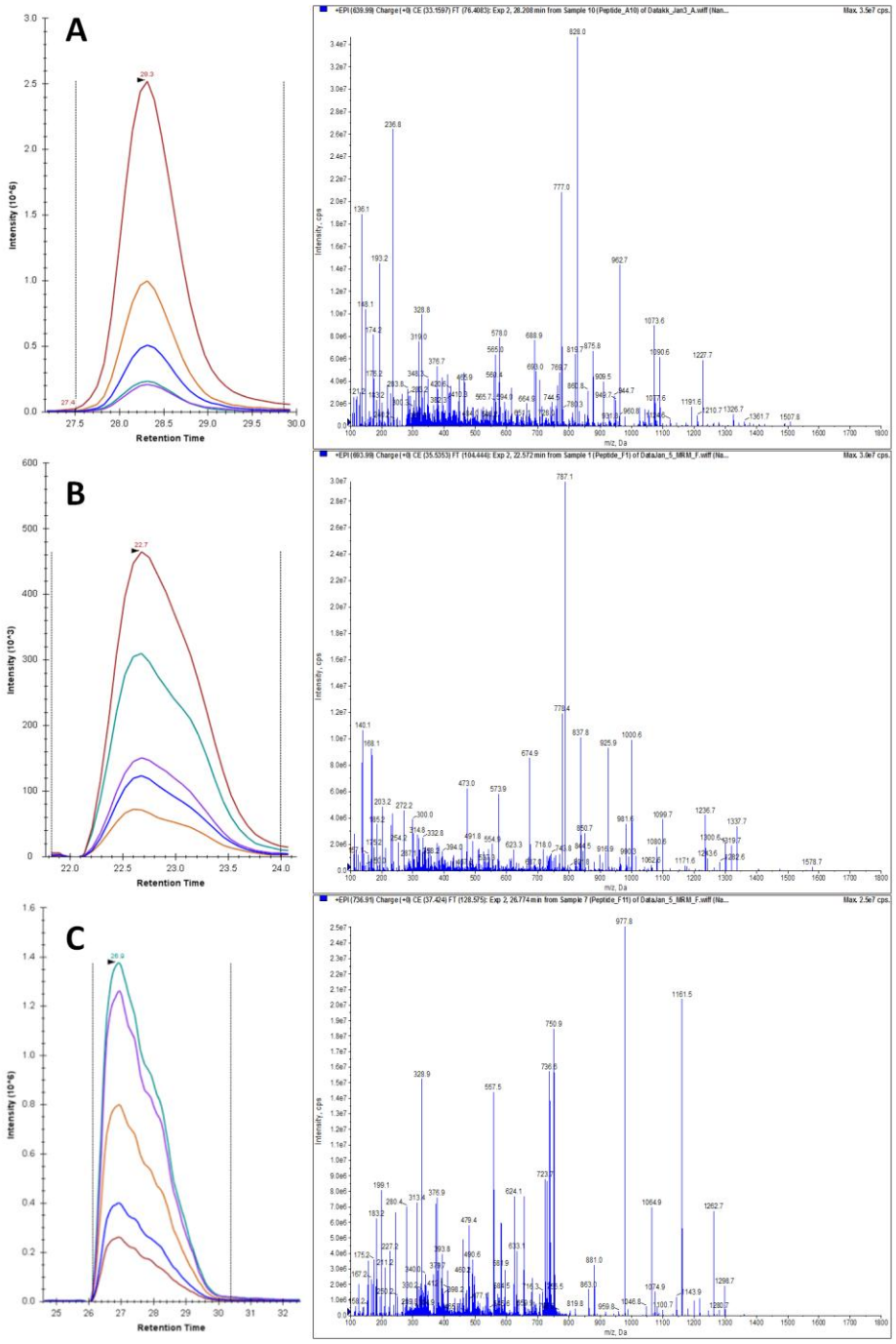

Figure 21. SRM and MS/MS data for protein Patched. SRM-triggered MS/MS spectra were obtained for synthetic peptide targets. Top five SRM transitions are shown in a chromatogram (left). Sequence information can be confirmed with MS/MS spectra (right). **A.** TYVEVVHQSVAQNSTQK (m/z=639.99^{+++}) **B.** TEYDPHTHVYYTTAEPR (m/z=693.99^{+++}) **C.** LPTPSPEPPPSVVR (m/z=736.91^{++})

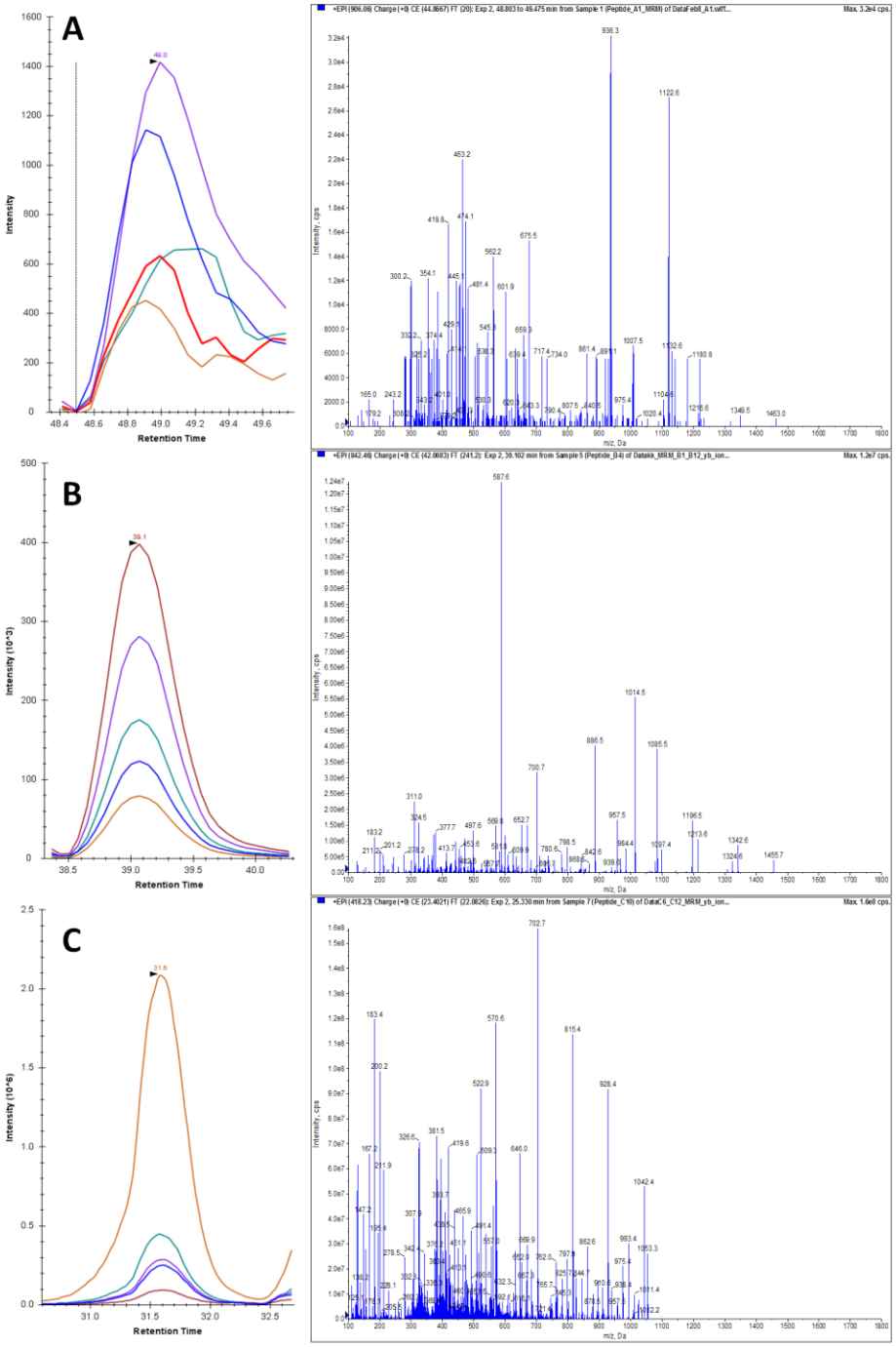

.

Figure 22. SRM and MS/MS data for protein SFRP2. SRM-triggered MS/MS spectra were obtained for synthetic peptide targets. Top five SRM transitions are shown in a chromatogram (left). Sequence information can be confirmed with MS/MS spectra (right). **A.** DSLQCTCEEMNDINAPYLVMGQK (m/z=906.06^{+++}) **B.** EVLEQAGAWIPLVMK (m/z=842.46^{++}) **C.** LPNLLGHETMK (m/z=418.23^{+++})

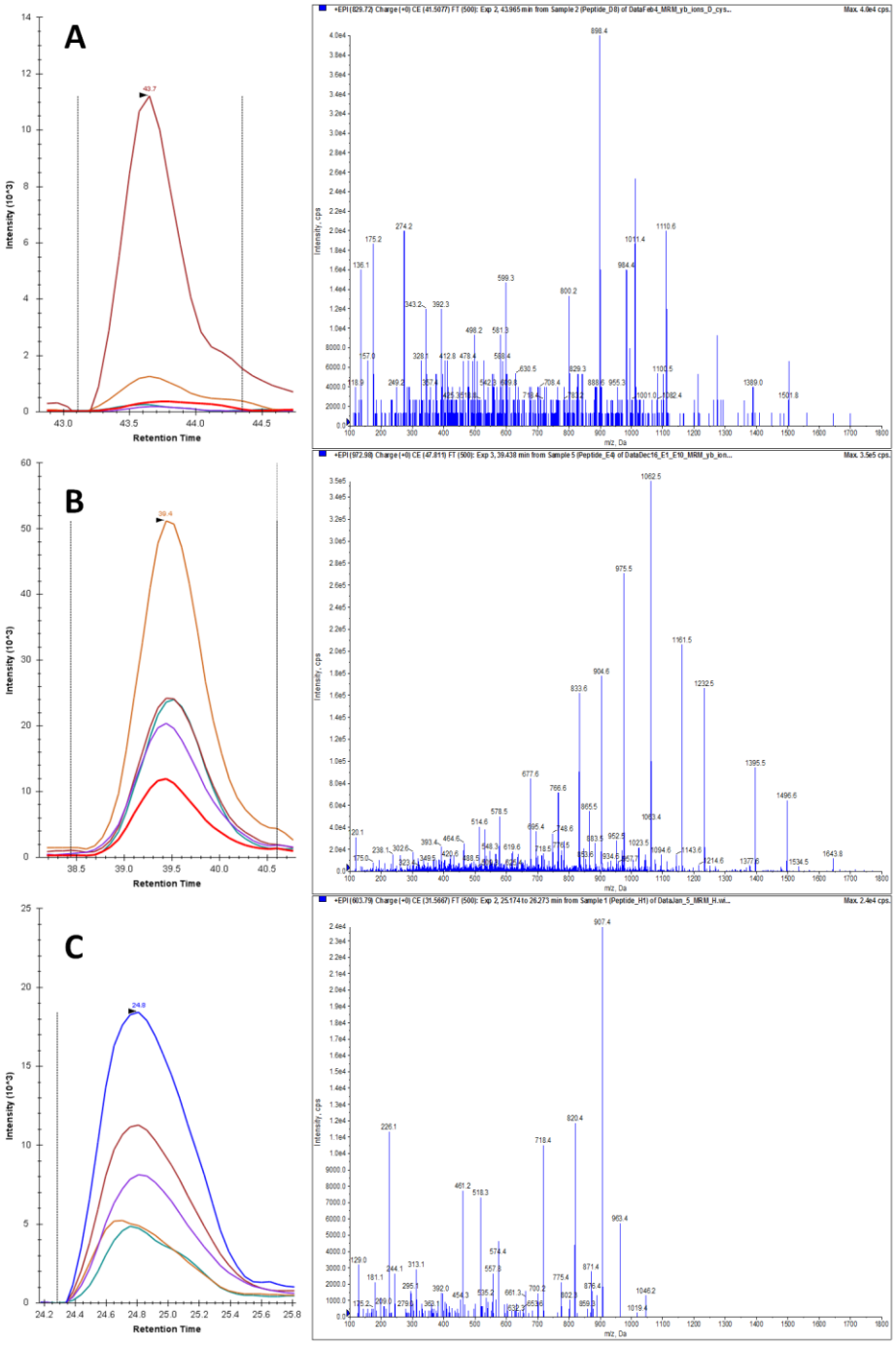

.

Figure 23. SRM and MS/MS data for protein Wnt5a. SRM-triggered MS/MS spectra were obtained for synthetic peptide targets. Top five SRM transitions are shown in a chromatogram (left). Sequence information can be confirmed with MS/MS spectra (right). **A.** FNSPTTQDLVYIDPSPDYCVR (m/z=829.72^{+++}) **B.** ETAFTYAVSAAGVVNAMSR (m/z=972.98^{++}) **C.** NESTGSLGTQGR (m/z=603.79^{++})

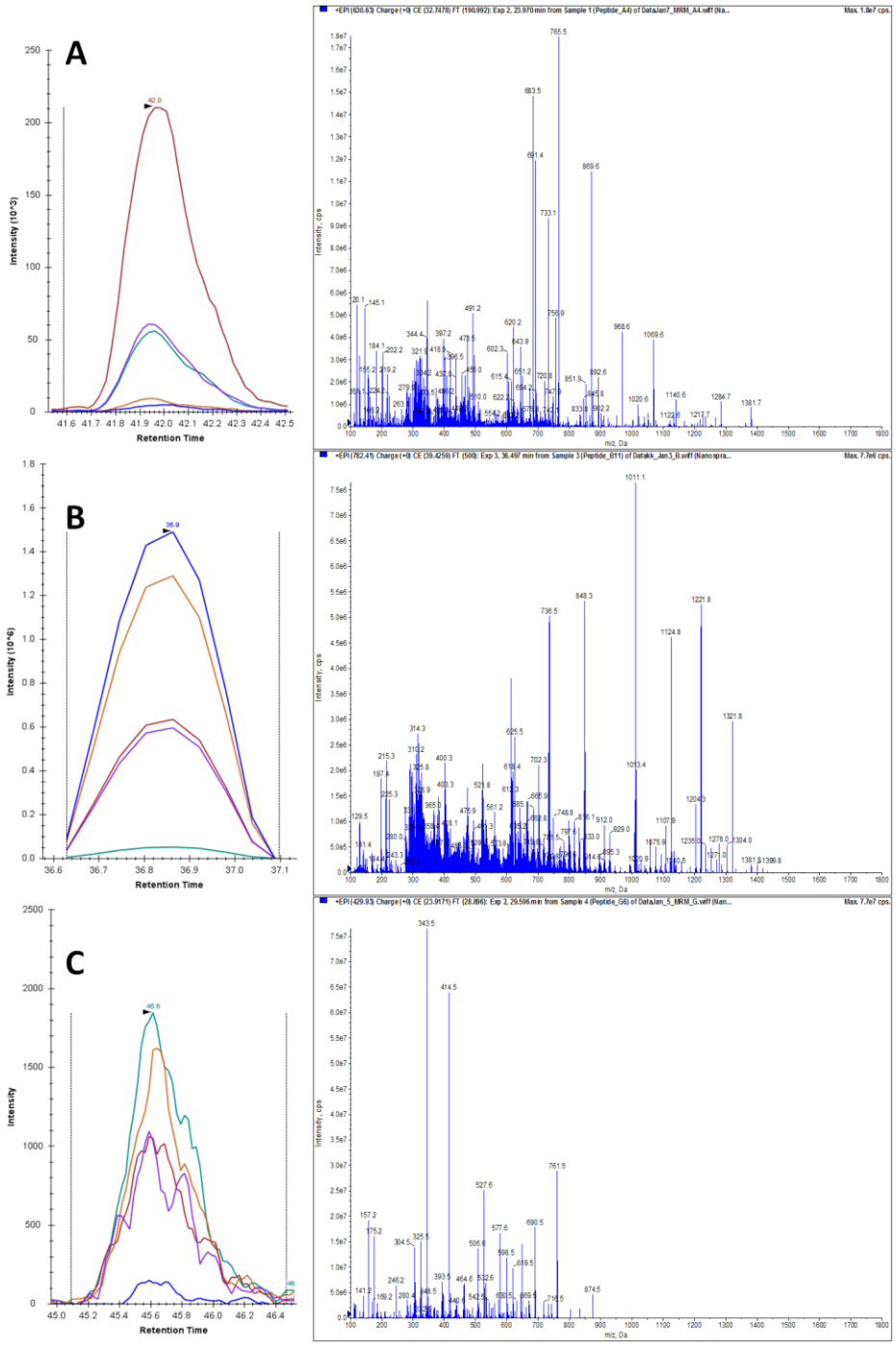

Figure 24. SRM and MS/MS data for protein Sonic hedgehog. SRM-triggered MS/MS spectra were obtained for synthetic peptide targets. Top five SRM transitions are shown in a chromatogram (left). Sequence information can be confirmed with MS/MS spectra (right). **A.** SGGCFPGSATVHLEQGGTK (m/z=630.63^{+++}) **B.** ELTPNYNPDIIFK (m/z=782.41^{++}) **C.** LAHALLAALAPAR (m/z=429.93^{+++})

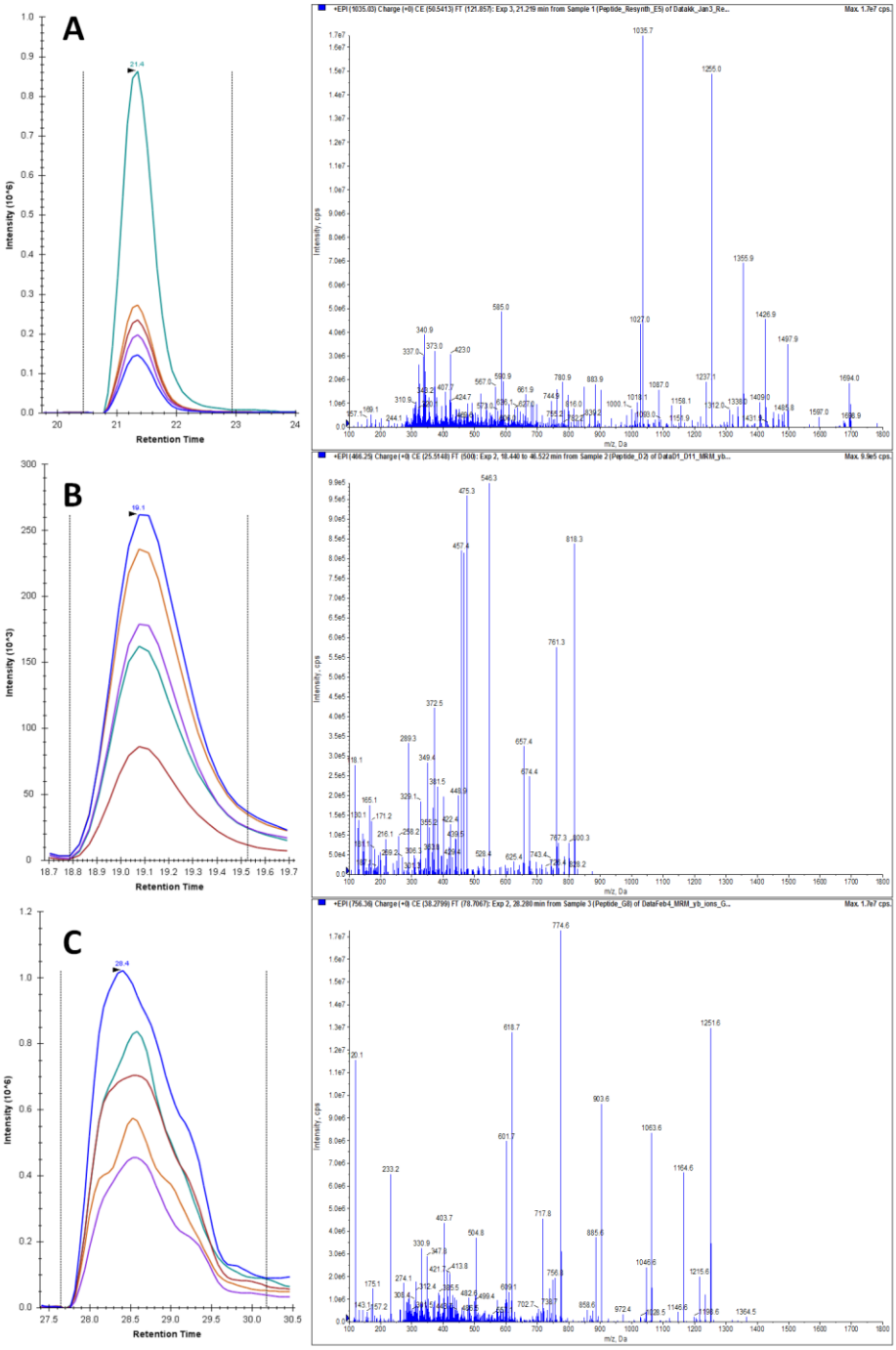

.

Figure 25. SRM and MS/MS data for protein HES1. SRM-triggered MS/MS spectra were obtained for synthetic peptide targets. Top five SRM transitions are shown in a chromatogram (left). Sequence information can be confirmed with MS/MS spectra (right). **A.** NSSSPVAATPASVNTTPDKPK (m/z=1035.03^{++}) **B.** LGSQAGEAAK (m/z=466.25^{++}) **C.** FLSTCEGVNTEVR (m/z=756.36^{++})

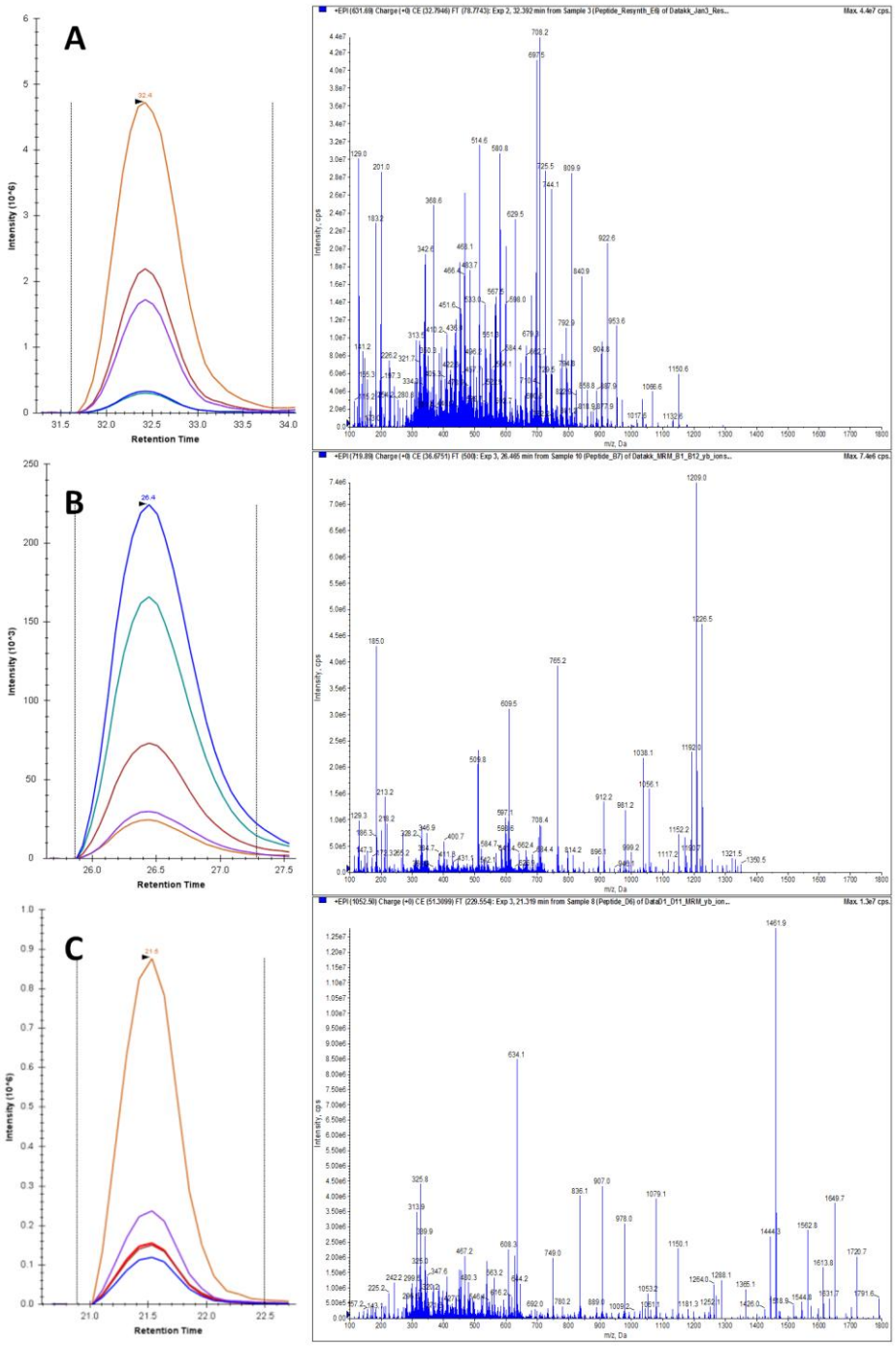

Figure 26. SRM and MS/MS data for protein GSK3β. SRM-triggered MS/MS spectra were obtained for synthetic peptide targets. Top five SRM transitions are shown in a chromatogram (left). Sequence information can be confirmed with MS/MS spectra (right). **A.** DIKPQNLLLDPDTAVLK (m/z=631.69^{+++}) **B.** VIGNGSFGVVYQAK (m/z=719.89^{++}) **C.** IQAAASTPTNATAASDANTGDR (m/z=1052.50^{++})

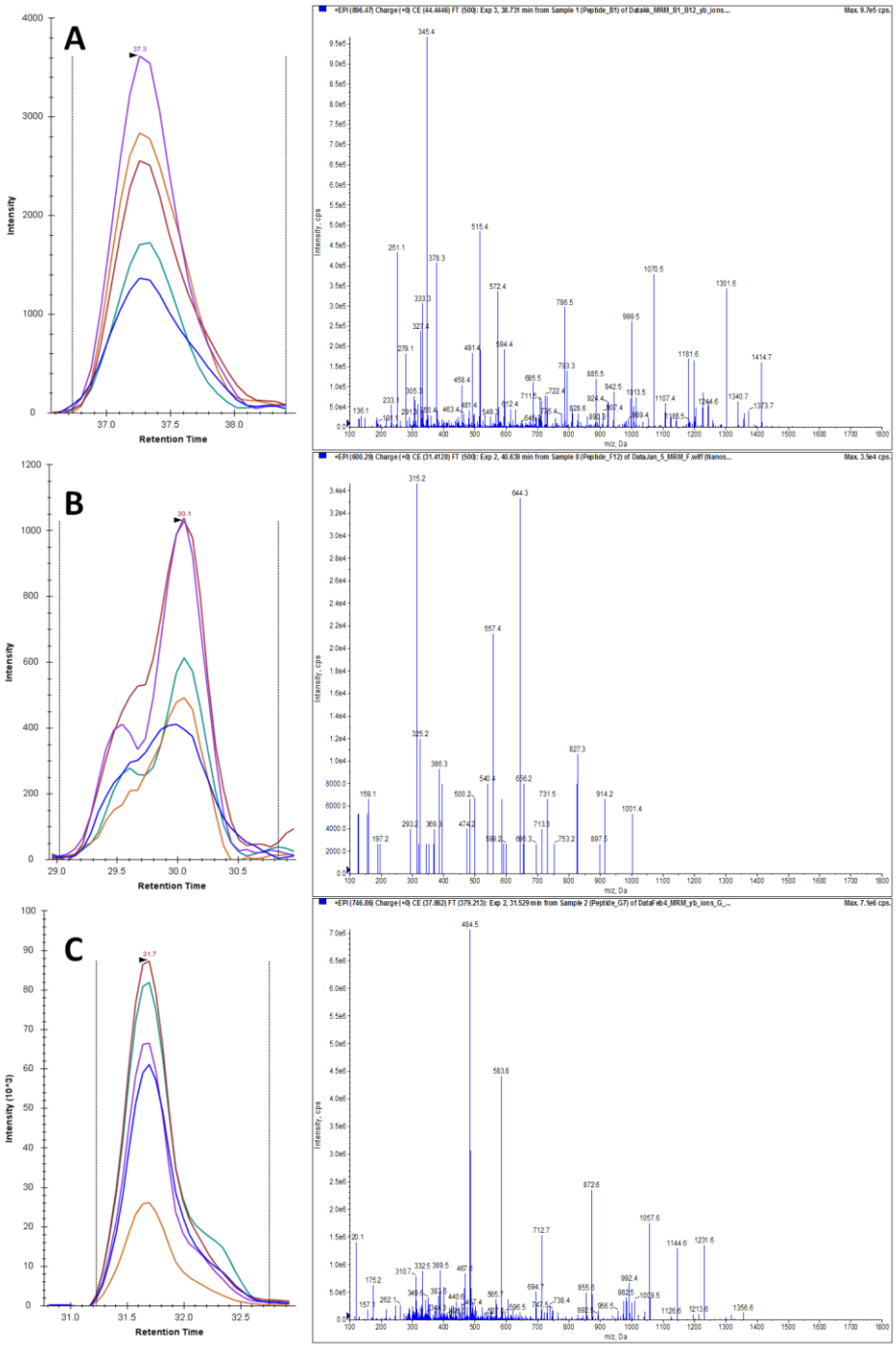

Figure 27. SRM and MS/MS data for protein Smoothened. SRM-triggered MS/MS spectra were obtained for synthetic peptide targets. Top five SRM transitions are shown in a chromatogram (left). Sequence information can be confirmed with MS/MS spectra (right). **A.** DYVLCQANVTIGLPTK (m/z=896.47^{++}) **B.** GAASSGNATGPGPR (m/z=600.29^{++}) **C.** FNSSGQCEVPLVR (m/z=746.86^{++})

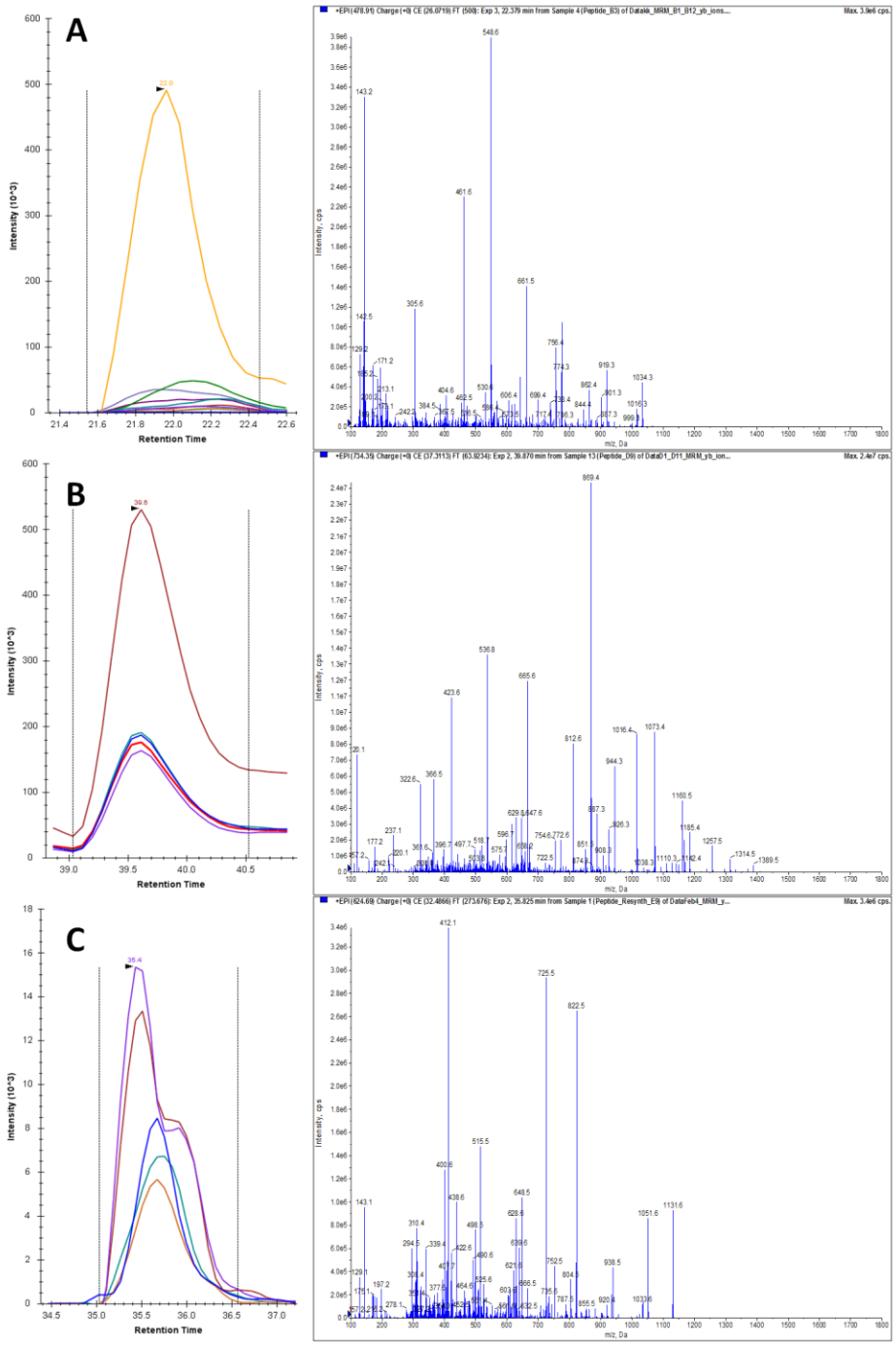

Figure 28. SRM and MS/MS data for protein SUFU. SRM-triggered MS/MS spectra were obtained for synthetic peptide targets. Top five SRM transitions are shown in a chromatogram (left). Sequence information can be confirmed with MS/MS spectra (right). **A.** GIETDGSNLSGVSAK (m/z=478.91^{+++}) **B.** VHEFTGTDGPSGFGFELTFR (m/z=734.35^{++}) **C.** GLEINSKPVLPPINPQR (m/z=624.69^{+++})

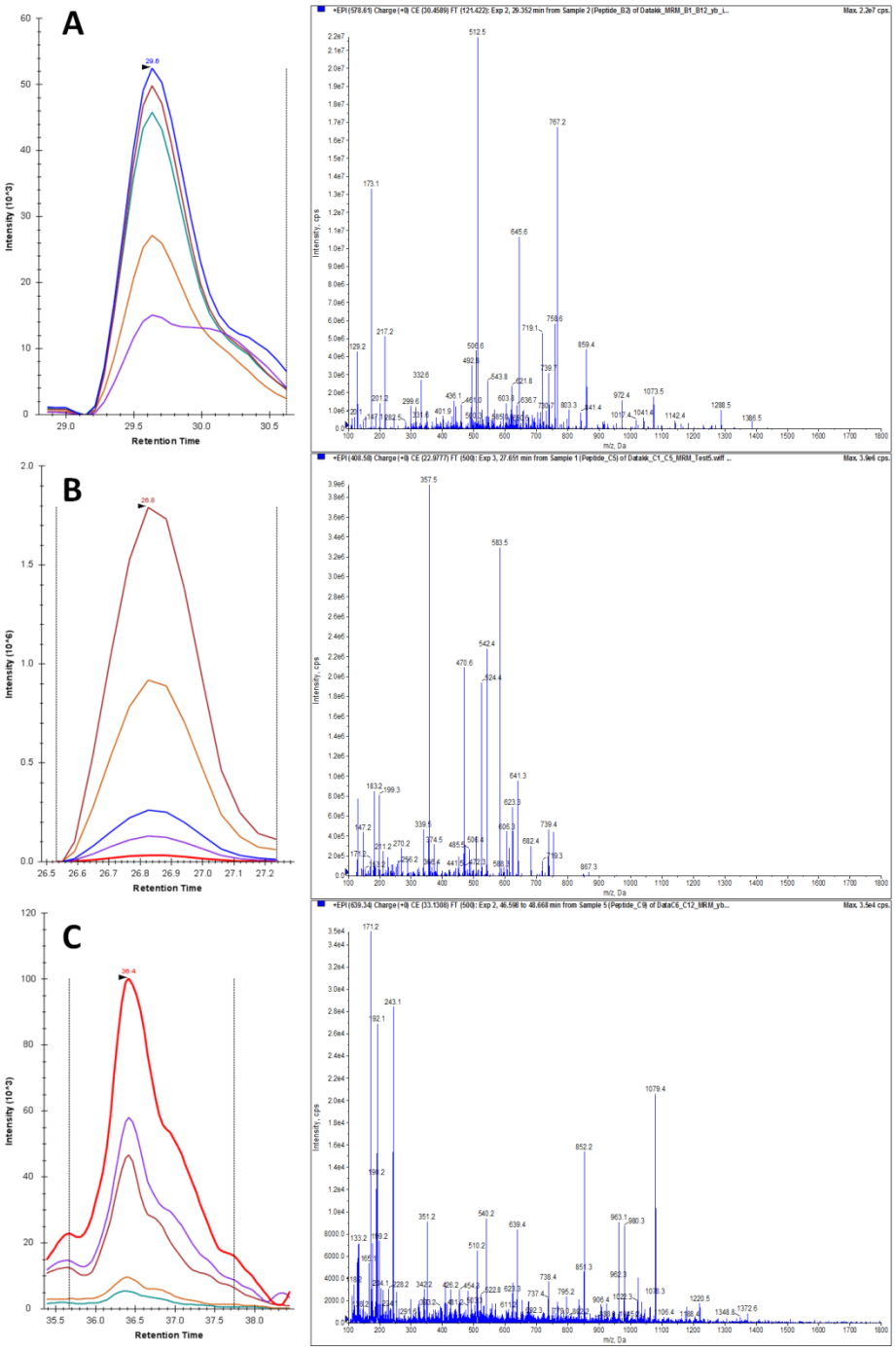

Figure 29. SRM and MS/MS data for protein Cerberus. SRM-triggered MS/MS spectra were obtained for synthetic peptide targets. Top five SRM transitions are shown in a chromatogram (left). Sequence information can be confirmed with MS/MS spectra (right). **A.** TVPFSQTITHEGCEK (m/z=578.61^{+++}) **B.** TPASQGVILPIK (m/z=408.58^{+++}) **C.** VVVQNNLCFGK (m/z=639.33^{++})

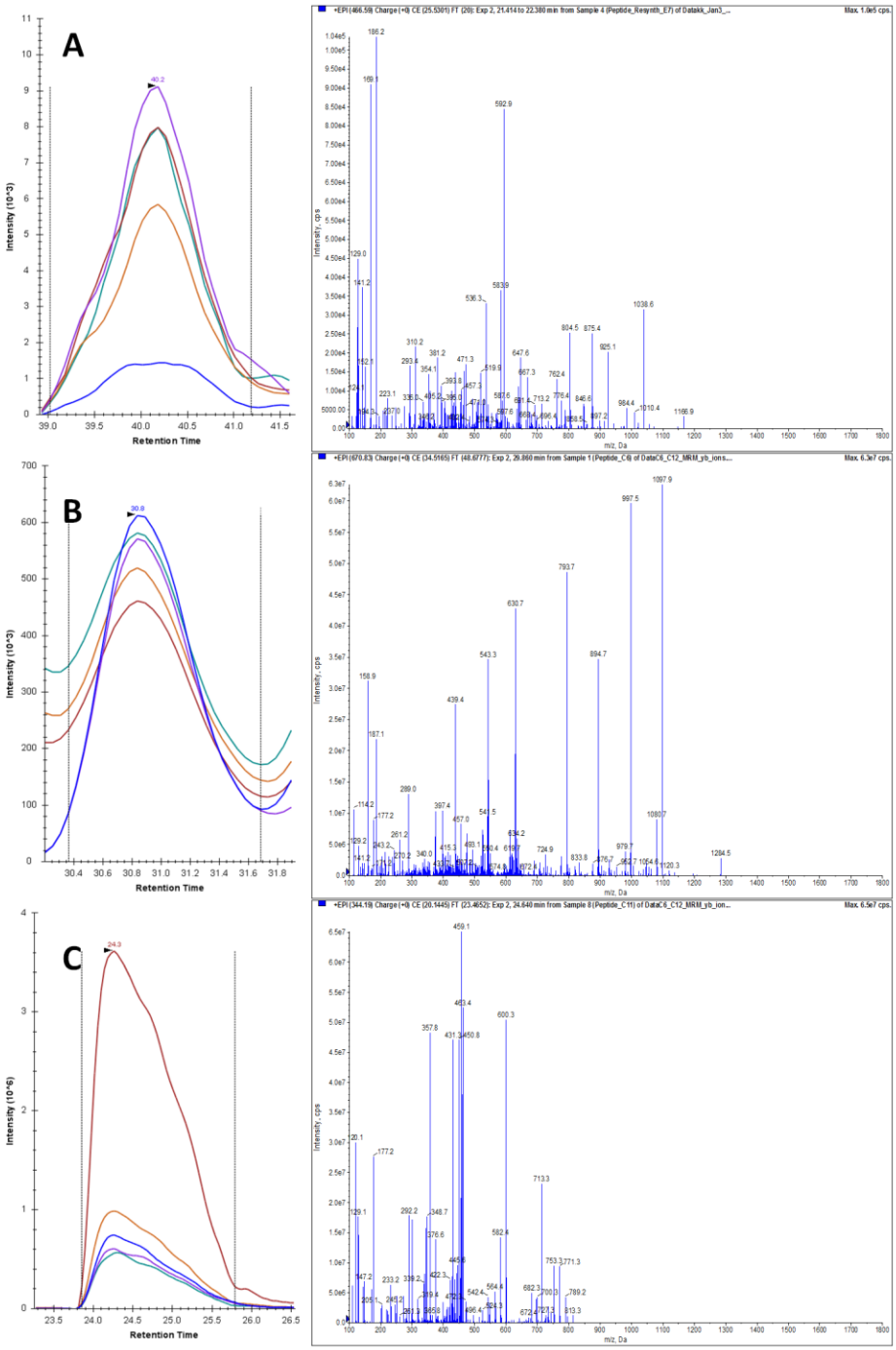

Figure 30. SRM and MS/MS data for protein p53. SRM-triggered MS/MS spectra were obtained for synthetic peptide targets. Top five SRM transitions are shown in a chromatogram (left). Sequence information can be confirmed with MS/MS spectra (right). **A.** RPILTIITLEDSSGNLLGR (m/z=690.06^{+++}) **B.** SVTCTYSPALNK (m/z=670.83^{++}) **C.** LGFLHSGTAK (m/z=344.19^{+++})

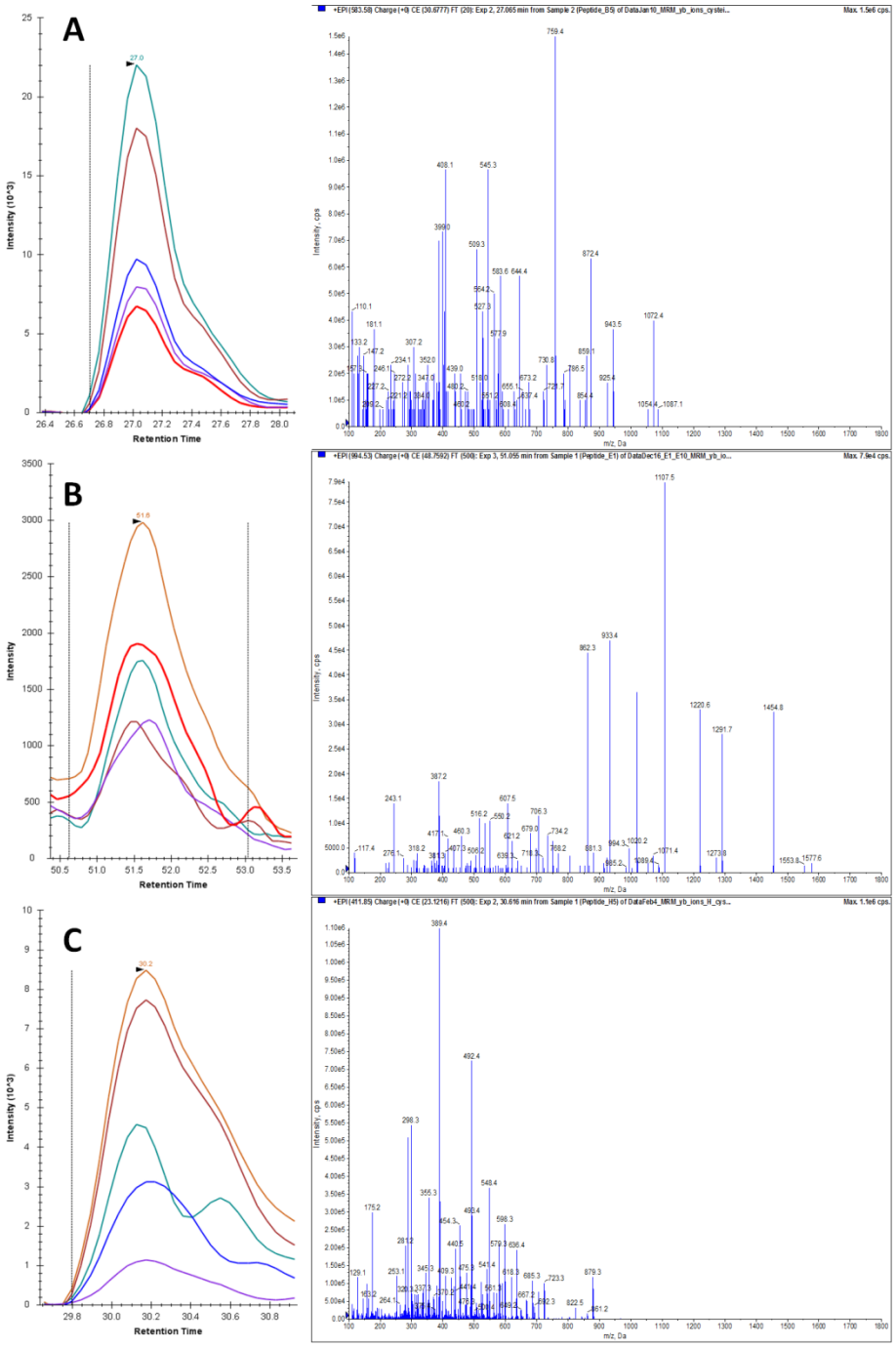

Figure 31. SRM and MS/MS data for protein Wnt2. SRM-triggered MS/MS spectra were obtained for synthetic peptide targets. Top five SRM transitions are shown in a chromatogram (left). Sequence information can be confirmed with MS/MS spectra (right). **A.** CQDCLEALDVHTCK (m/z=583.58^{+++}) **B.** ESAFVYAISSAGVVFAITR (m/z=994.53^{++}) **C.** CHGVSGSCTLR (m/z=411.85^{+++})

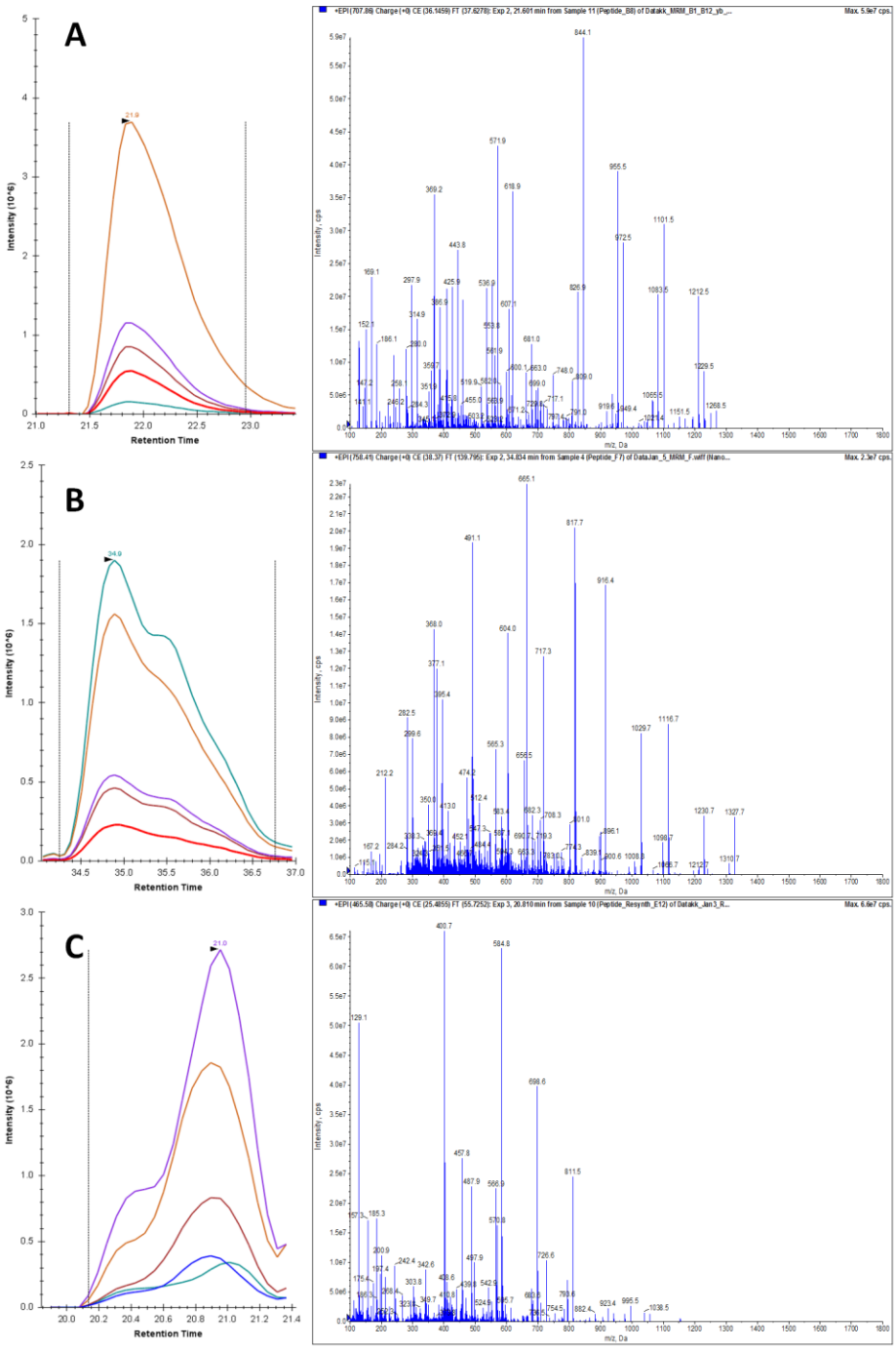

Figure 32. SRM and MS/MS data for protein Gli3. SRM-triggered MS/MS spectra were obtained for synthetic peptide targets. Top five SRM transitions are shown in a chromatogram (left). Sequence information can be confirmed with MS/MS spectra (right). **A.** GQQEQPEGTTLVK (m/z=707.86^{++}) **B.** TSPNSLVTILNNSR (m/z=758.41^{++}) **C.** IKPDEDLPSPGAR (m/z=465.58^{+++})

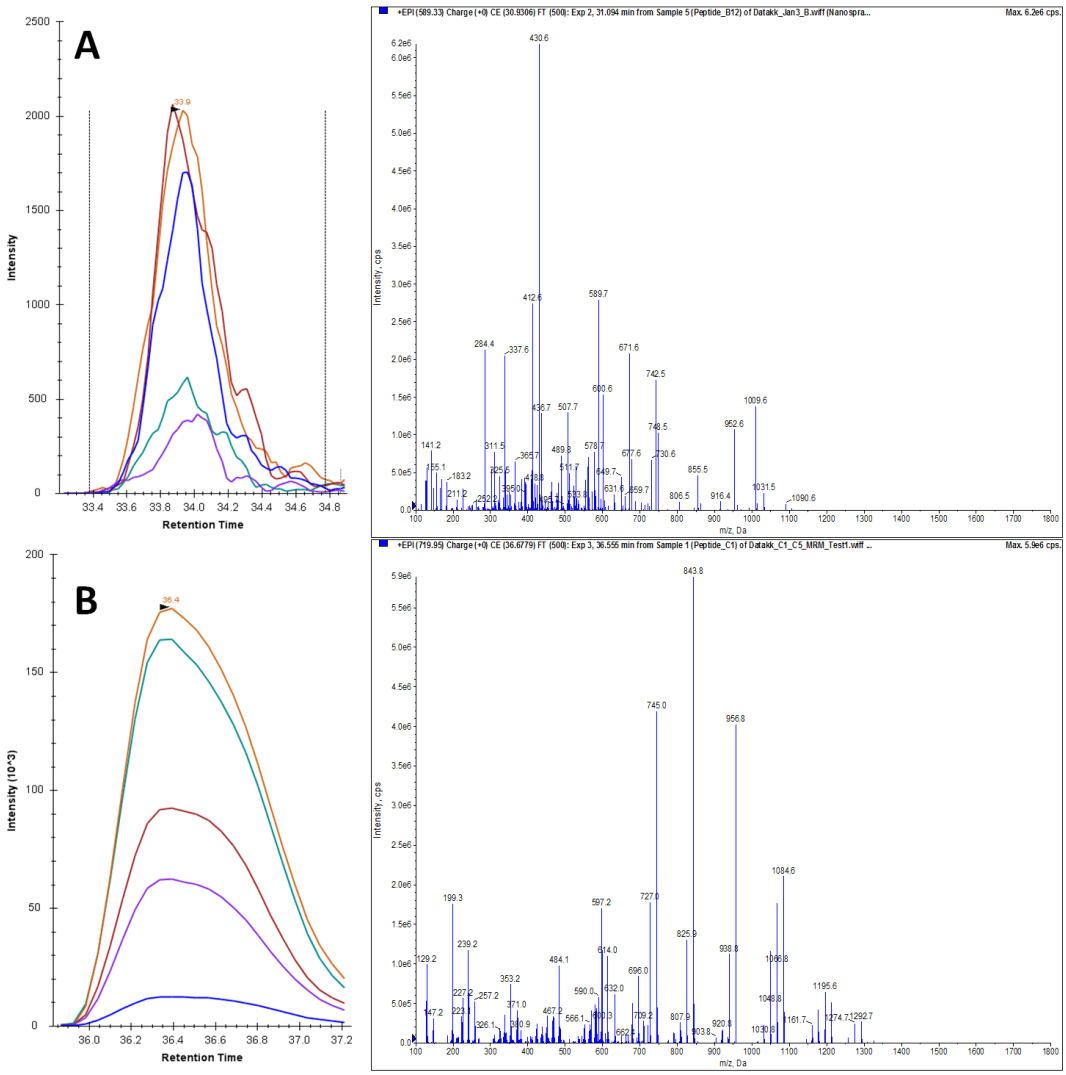

.

Figure 33. SRM and MS/MS data for protein FRAT1. SRM-triggered MS/MS spectra were obtained for synthetic peptide targets. Top five SRM transitions are shown in a chromatogram (left). Sequence information can be confirmed with MS/MS spectra (right). **A.** APGPLAAAVPADK (m/z=589.33^{++}) **B.** LLQQLVLSGNLIK (m/z=719.95^{++})

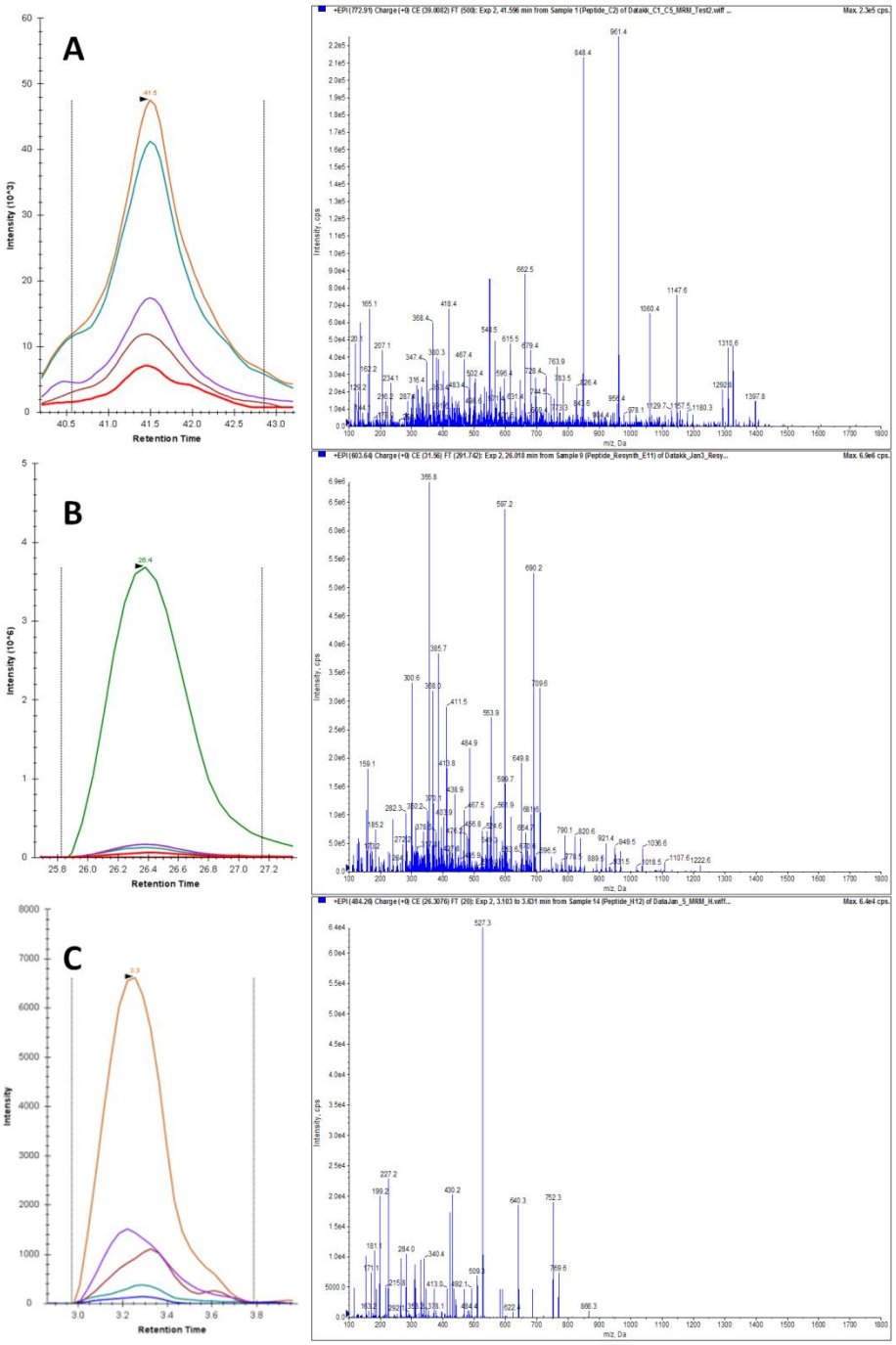

Figure 34. SRM and MS/MS data for protein Cripto-1. SRM-triggered MS/MS spectra were obtained for synthetic peptide targets. Top five SRM transitions are shown in a chromatogram (left). Sequence information can be confirmed with MS/MS spectra (right). **A.** FSYSVIWIMAISK (m/z=772.91^{++}) **B.** DDSIWPQEEPAIRPR (m/z=603.64^{+++}) **C.** TPELPPSAR (m/z=484.26^{++})

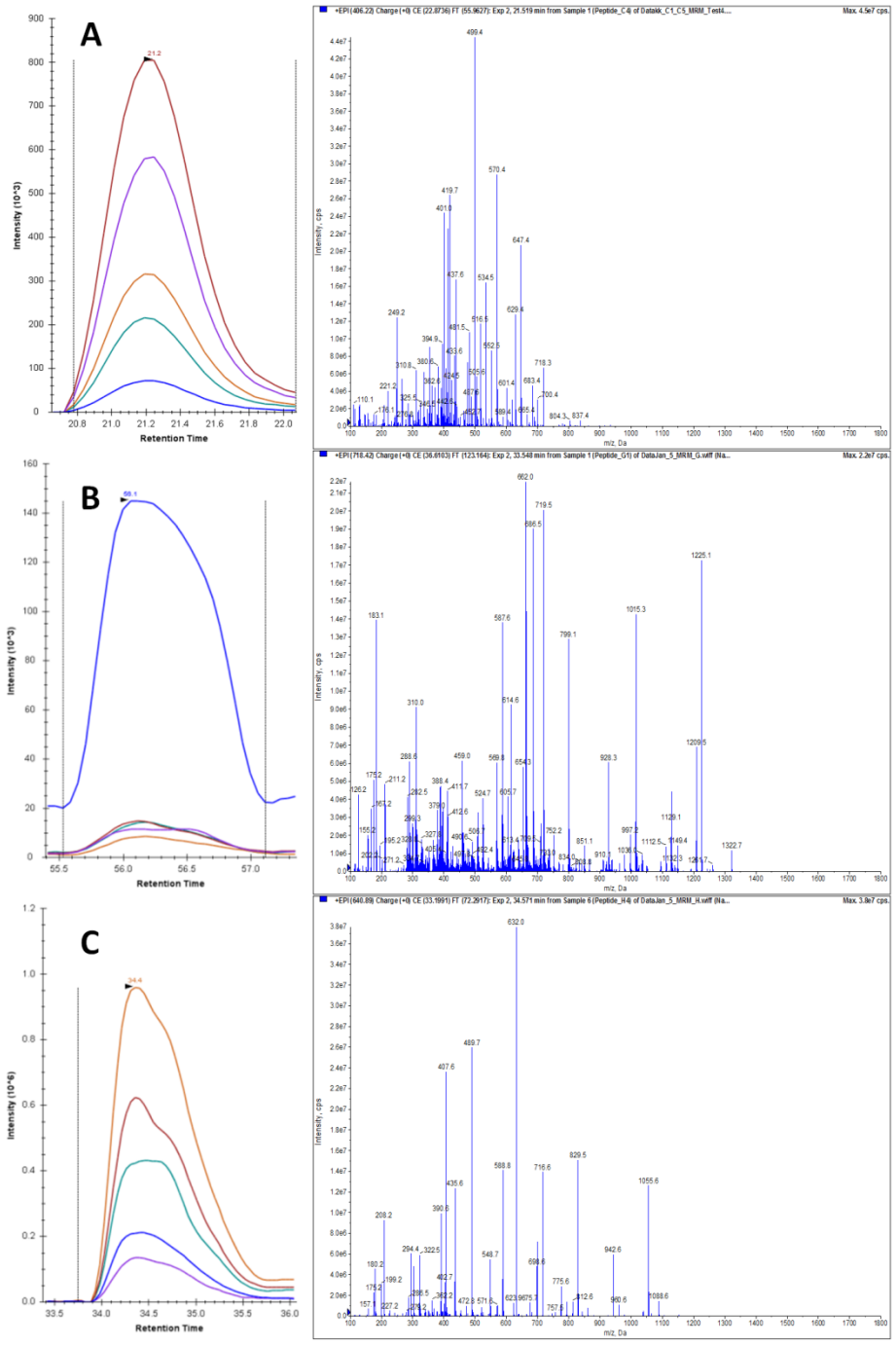

Figure 35. SRM and MS/MS data for protein Lefty1. SRM-triggered MS/MS spectra were obtained for synthetic peptide targets. Top five SRM transitions are shown in a chromatogram (left). Sequence information can be confirmed with MS/MS spectra (right). **A.** EHLGPLASGAHK (m/z=406.22^{+++}) **B.** LPPNSELVQAVLR (m/z=718.41^{++}) **C.** QPLLLQVSVQR (m/z=640.89^{++})

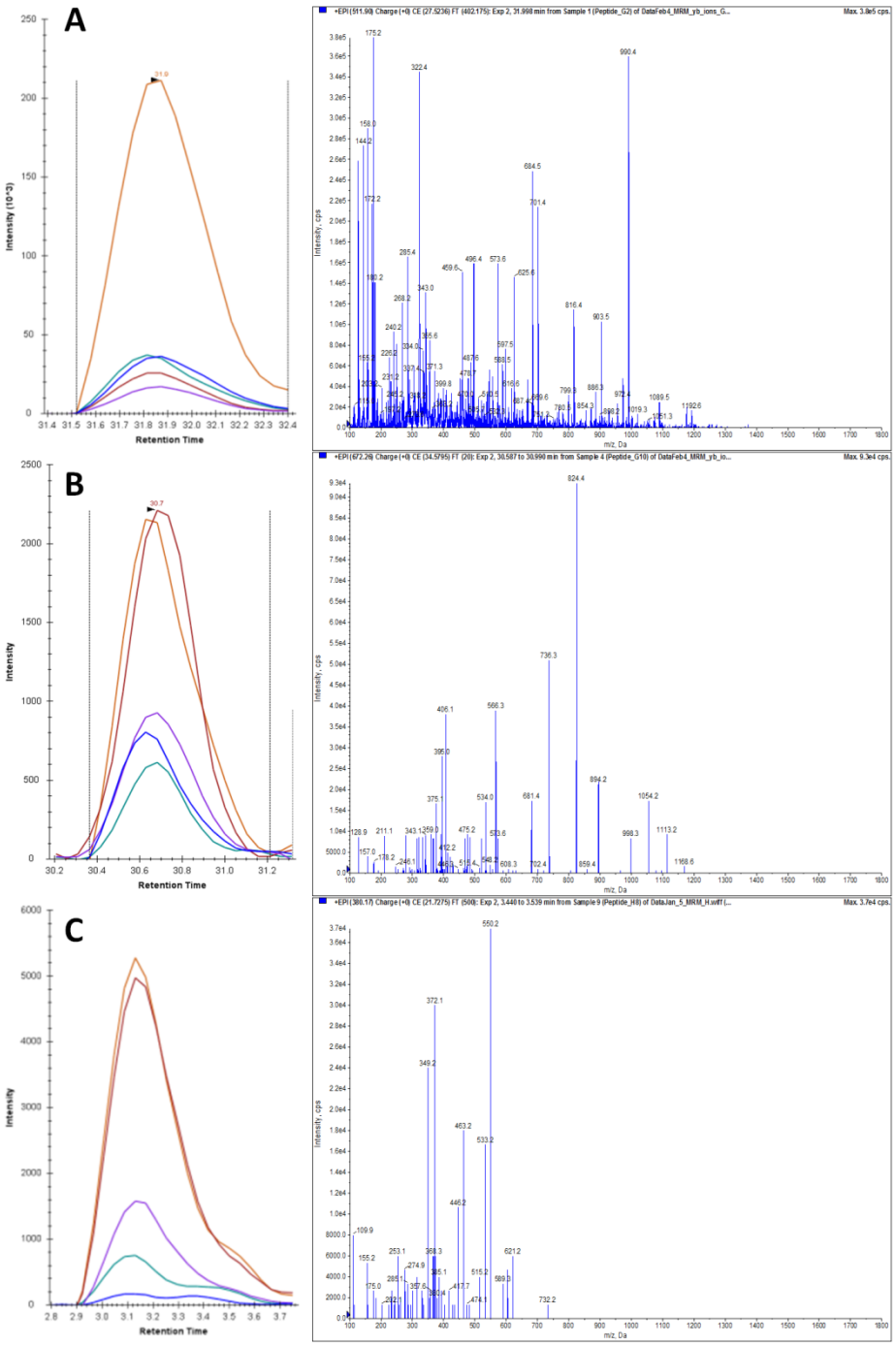

.

Figure 36. SRM and MS/MS data for protein DKK1. SRM-triggered MS/MS spectra were obtained for synthetic peptide targets. Top five SRM transitions are shown in a chromatogram (left). Sequence information can be confirmed with MS/MS spectra (right). **A.** NGICVSSDQNHFR (m/z=511.90^{+++}) **B.** SSDCASGLCCAR (m/z=672.26^{++}) **C.** DHHQASNSSR (m/z=380.17^{+++})

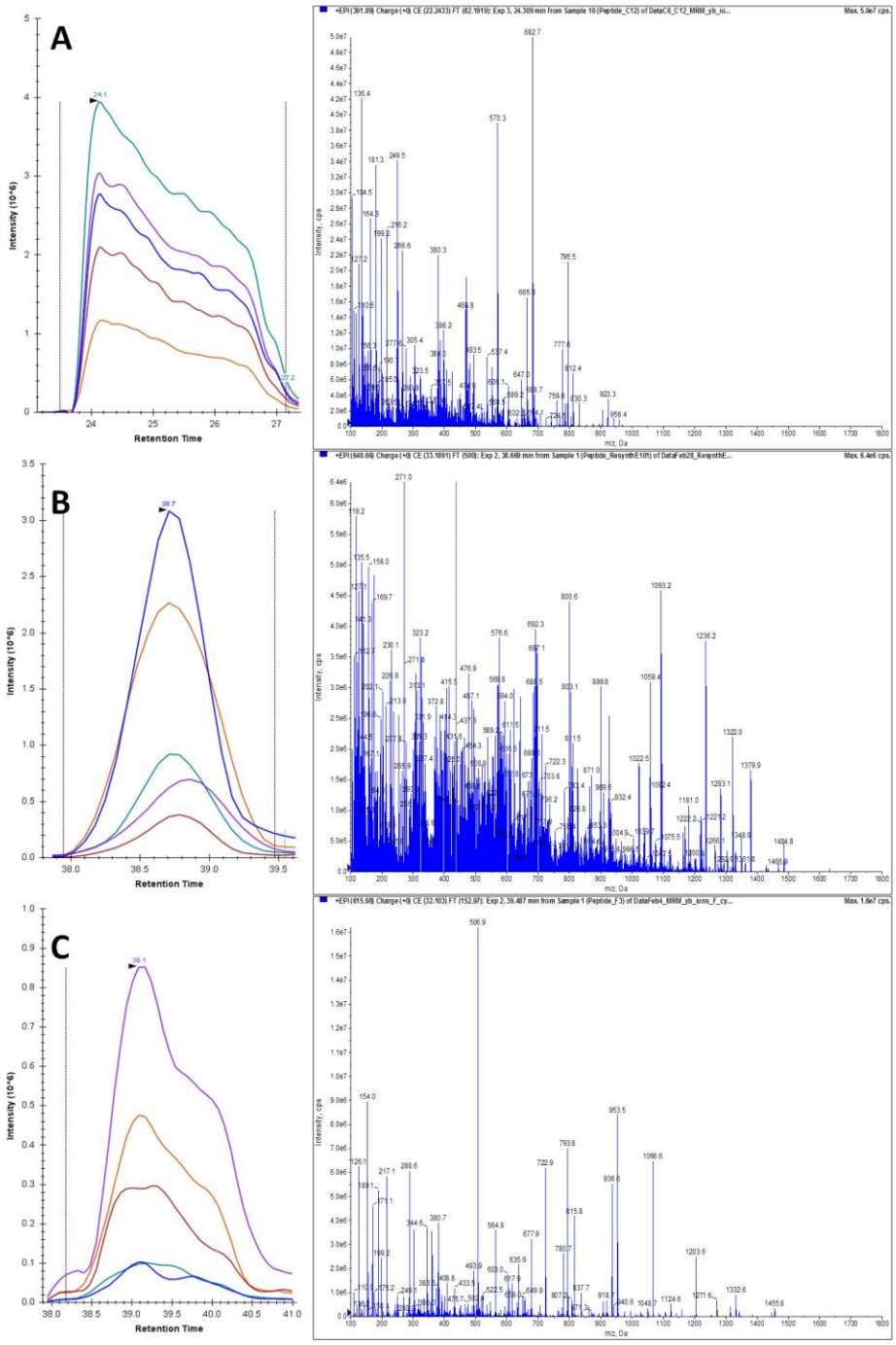

Figure 37. SRM and MS/MS data for protein SFRP1. SRM-triggered MS/MS spectra were obtained for synthetic peptide targets. Top five SRM transitions are shown in a chromatogram (left). Sequence information can be confirmed with MS/MS spectra (right). **A.** SQYLLTAIHK (m/z=391.89^{+++}) **B.** FYTKPPQCVDIPADLR (m/z=640.66^{+++}) **C.** SEAIIEHLCASEFALR (m/z=615.98^{+++})

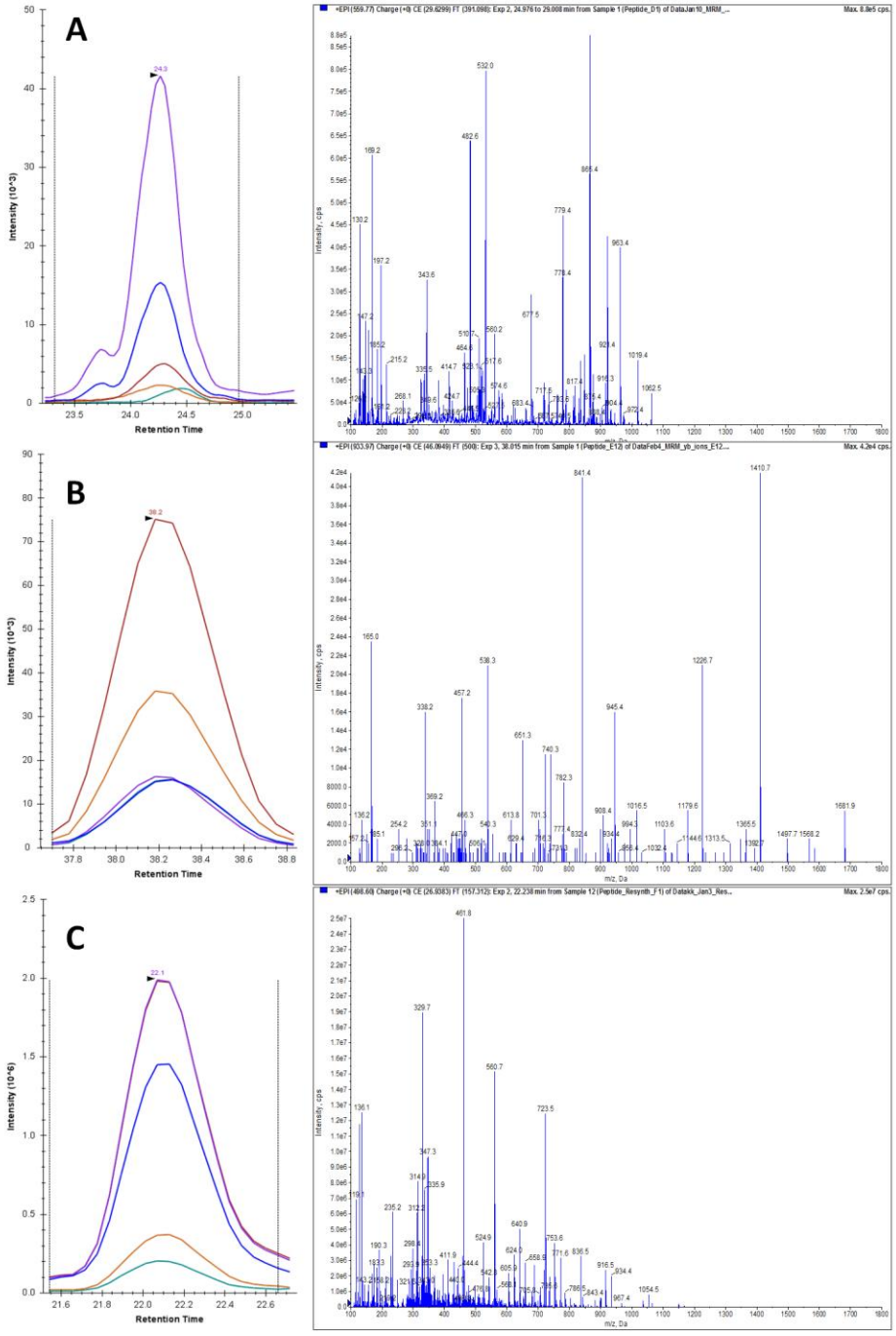

Figure 38. SRM and MS/MS data for protein Nodal. SRM-triggered MS/MS spectra were obtained for synthetic peptide targets. Top five SRM transitions are shown in a chromatogram (left). Sequence information can be confirmed with MS/MS spectra (right). **A.** VPSTCCAPVK (m/z=559.77^{++}) **B.** GQPSSPSPLAYMLSLYR (m/z=933.97^{++}) **C.** TKPLSMLYVDNGR (m/z=498.60^{+++})

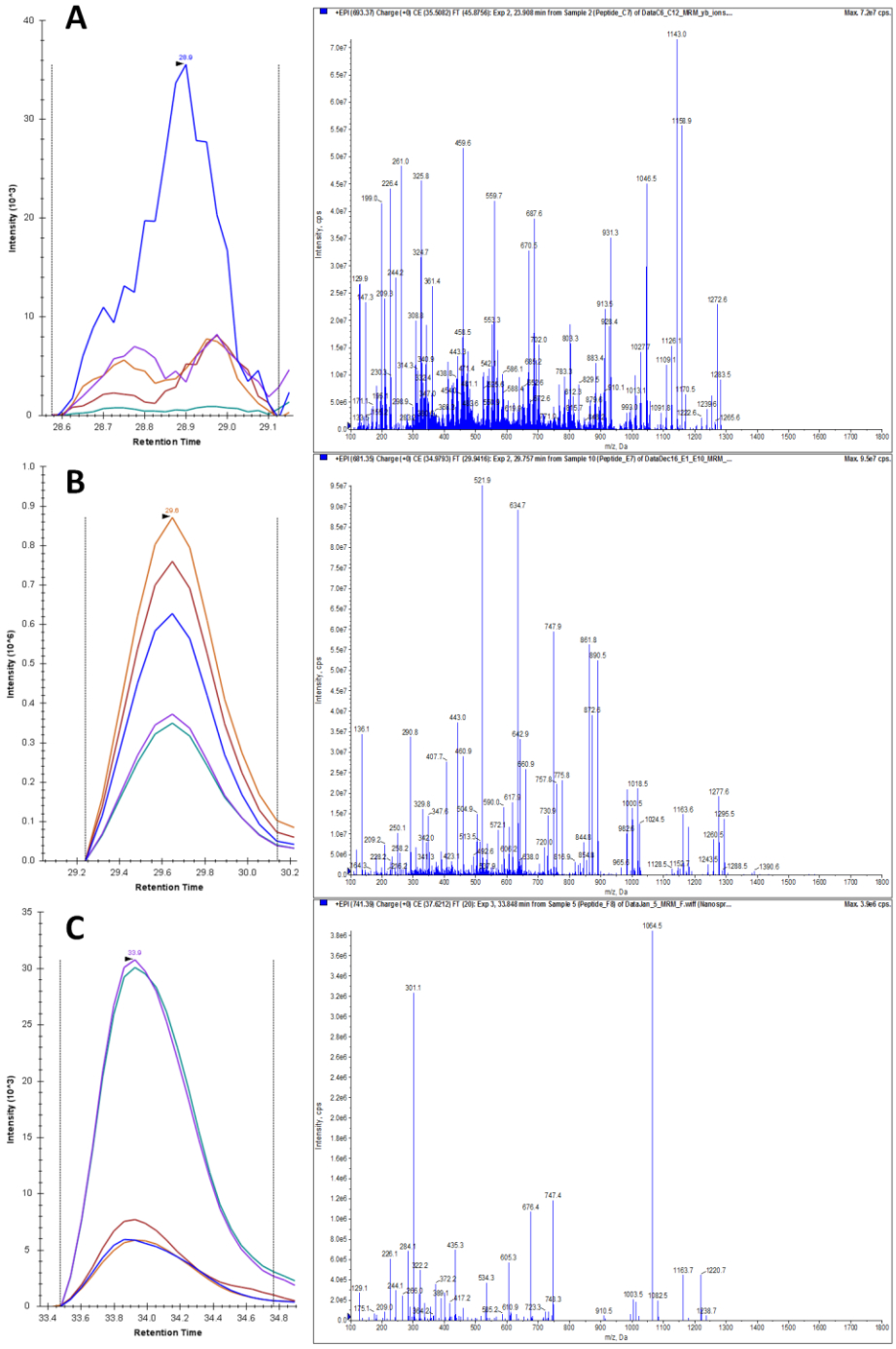

Figure 39. SRM and MS/MS data for protein β-Catenin. SRM-triggered MS/MS spectra were obtained for synthetic peptide targets. Top five SRM transitions are shown in a chromatogram (left). Sequence information can be confirmed with MS/MS spectra (right). **A.** LLNDEDQVVVNK (m/z=693.37^{++}) **B.** HAVVNLINYQDDAELATR (m/z=681.35^{+++}) **C.** NEGVATYAAAVLFR (m/z=741.39^{++})

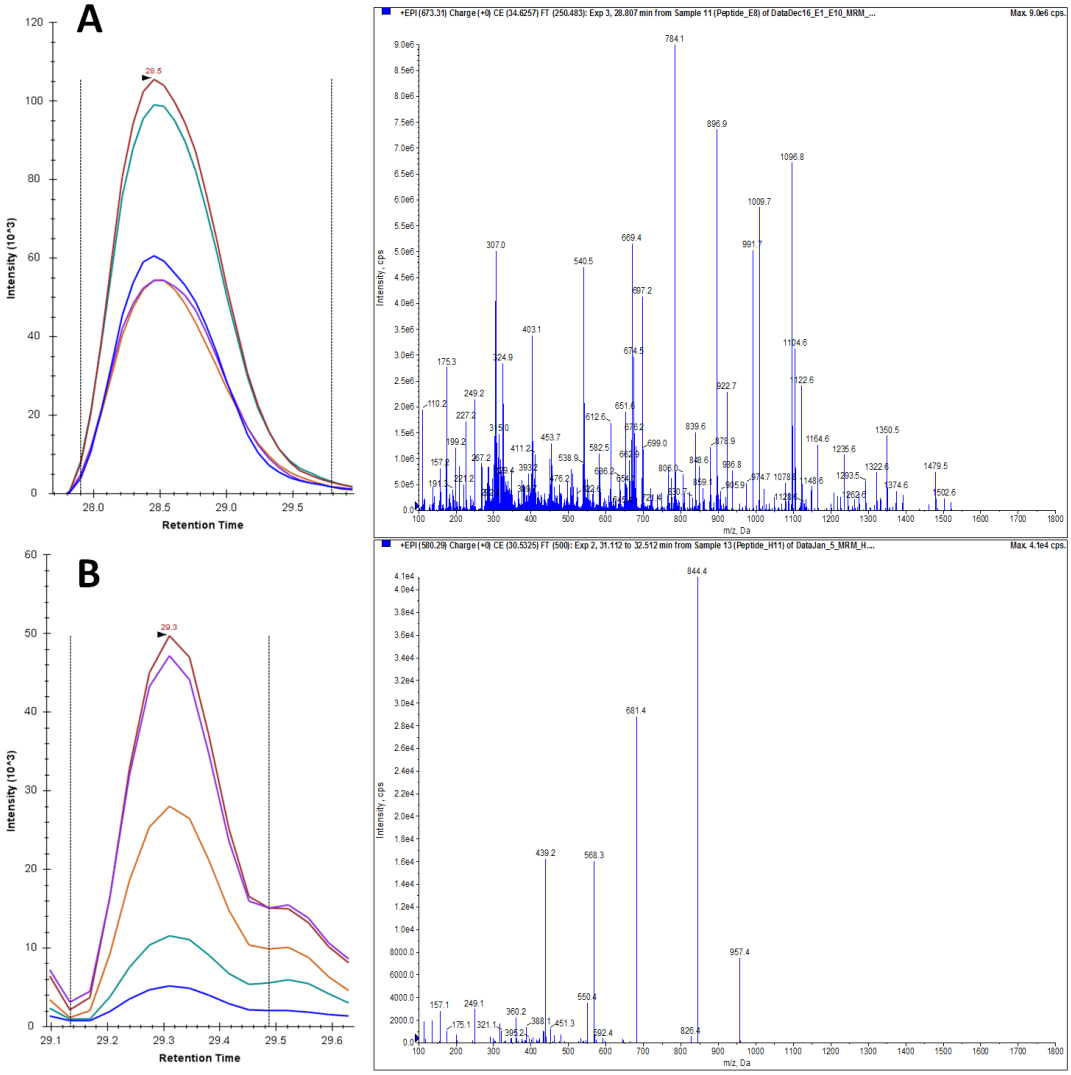

Figure 40. SRM and MS/MS data for protein Axin1. SRM-triggered MS/MS spectra were obtained for synthetic peptide targets. Top five SRM transitions are shown in a chromatogram (left). Sequence information can be confirmed with MS/MS spectra (right). **A.** DAHEENPESILDEHVQR (m/z=673.31^{++}) **B.** SDIYLEYTR (m/z=580.29^{++})

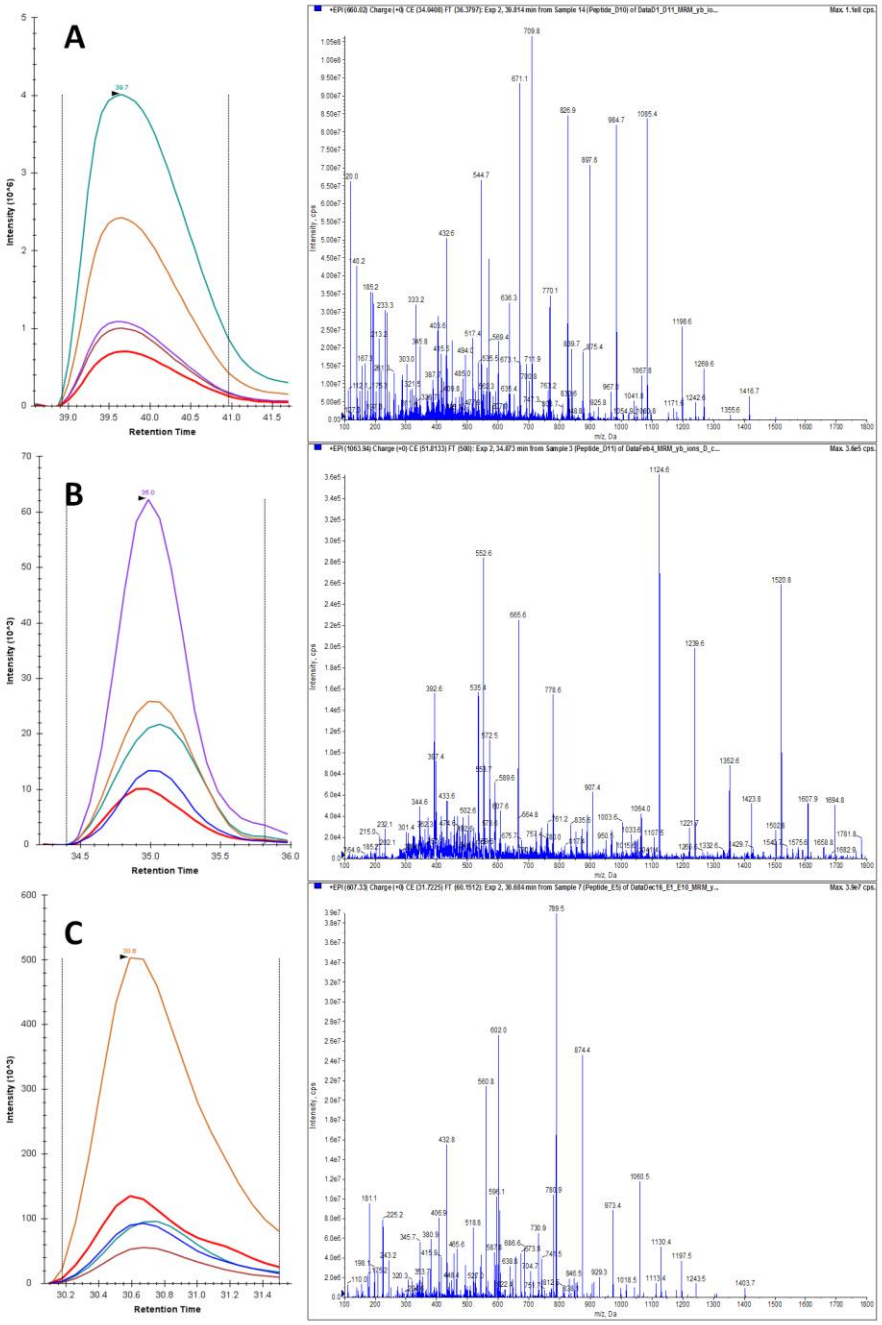

Figure 41. SRM and MS/MS data for protein Wnt1. SRM-triggered MS/MS spectra were obtained for synthetic peptide targets. Top five SRM transitions are shown in a chromatogram (left). Sequence information can be confirmed with MS/MS spectra (right). **A.** ETAFIFAITSAGVTHSVAR (m/z=660.18^{+++}) **B.** ACNSSSPALDGCELLCCGR (m/z=1063.94^{++}) **C.** QNPGILHSVSGGLQSAVR (m/z=607.33^{+++})

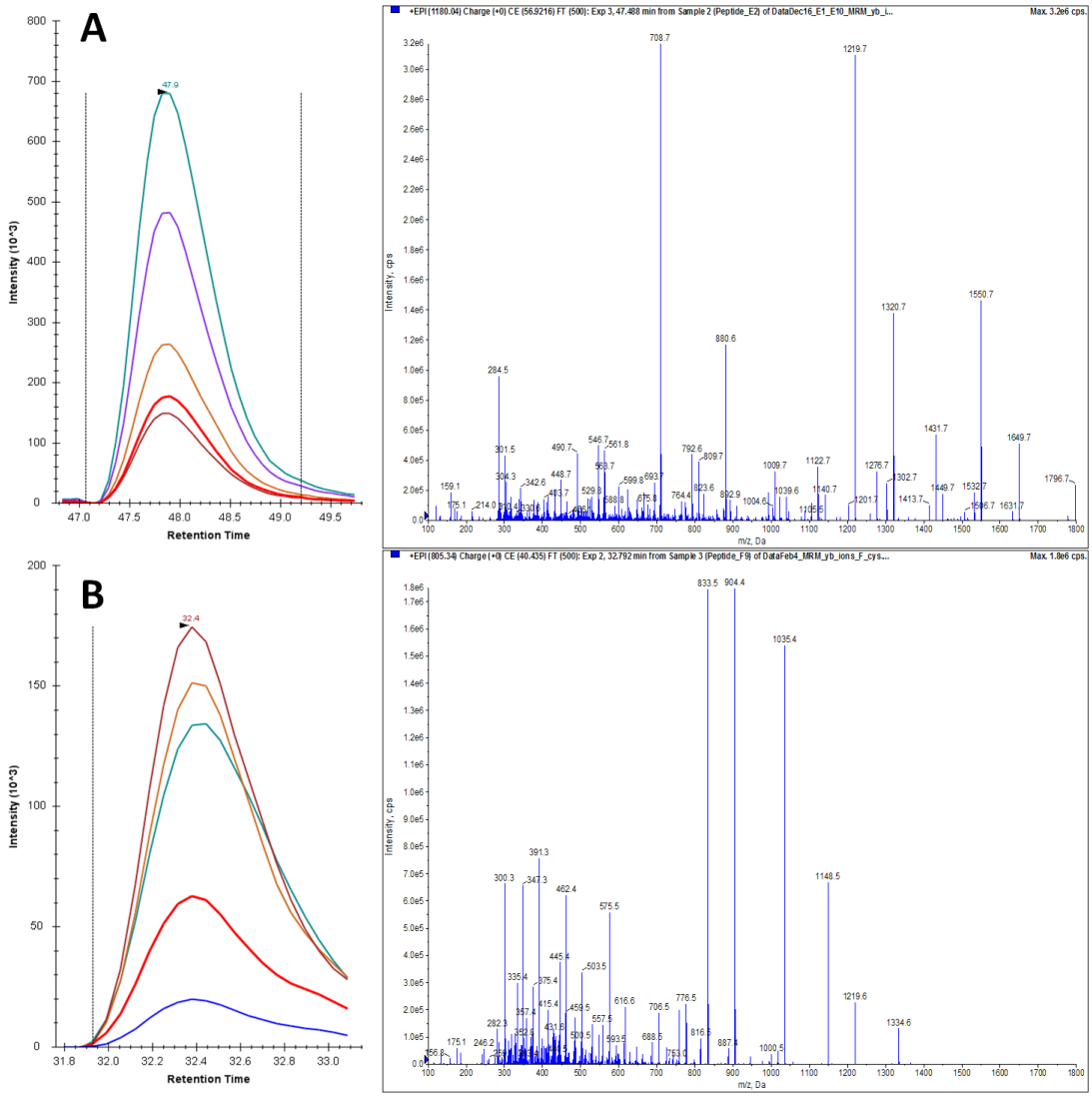

Figure 42. SRM and MS/MS data for protein CDKI1. SRM-triggered MS/MS spectra were obtained for synthetic peptide targets. Top five SRM transitions are shown in a chromatogram (left). Sequence information can be confirmed with MS/MS spectra (right). **A.** WNFDFVTETPLEGDFAWER (m/z=1180.04^{++}) **B.** DCDALMAGCIQEAR (m/z=805.34^{++})

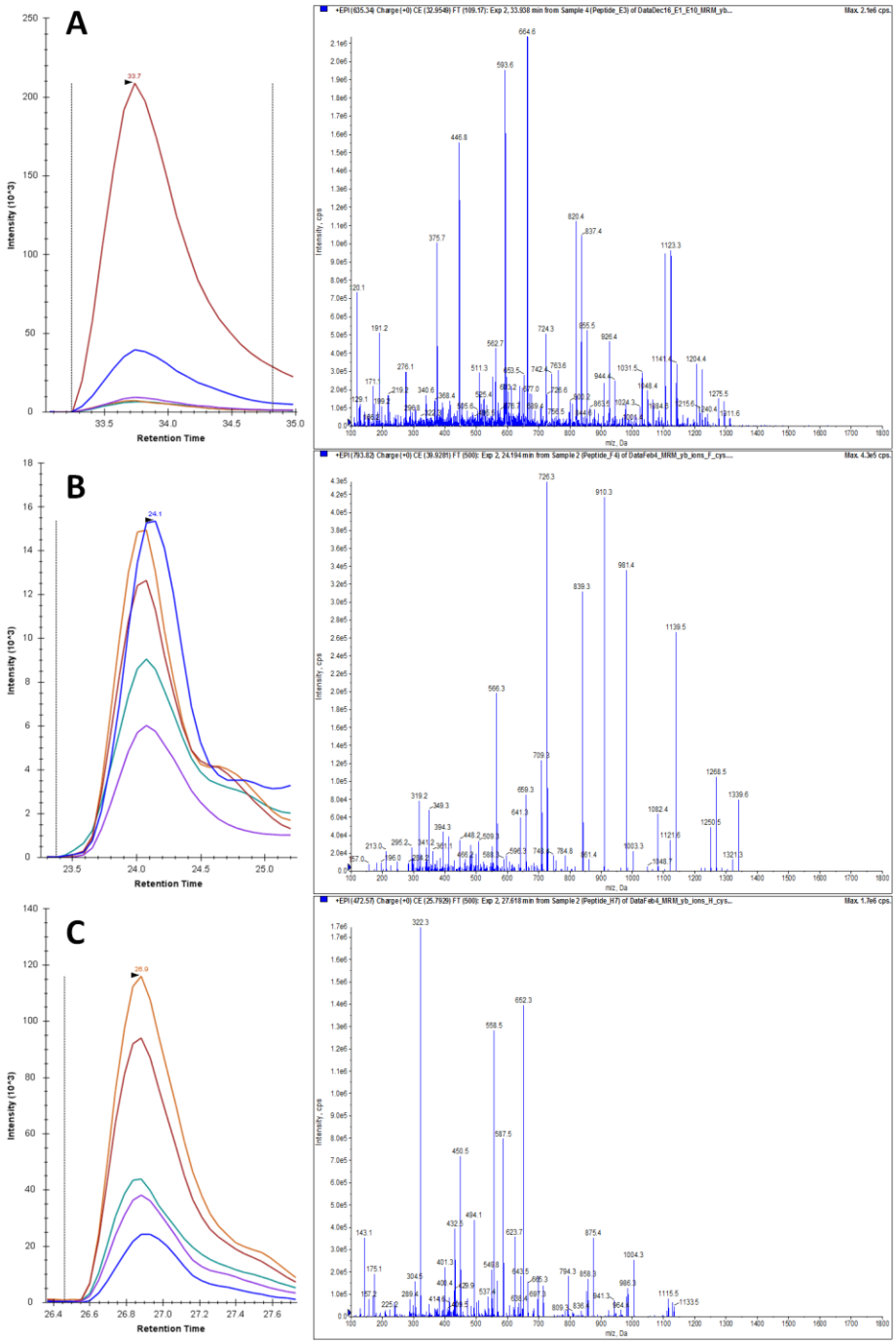

Figure 43. SRM and MS/MS data for protein Wnt3A. SRM-triggered MS/MS spectra were obtained for synthetic peptide targets. Top five SRM transitions are shown in a chromatogram (left). Sequence information can be confirmed with MS/MS spectra (right). **A.** ESAFVHAIASAGVAFAVTR ($m/z=635.34^{+++}$) **B.** SCAEGTAAICGCSSR ($m/z=793.82^{++}$) **C.** IGIQECQHQFR ($m/z=472.57^{+++}$)

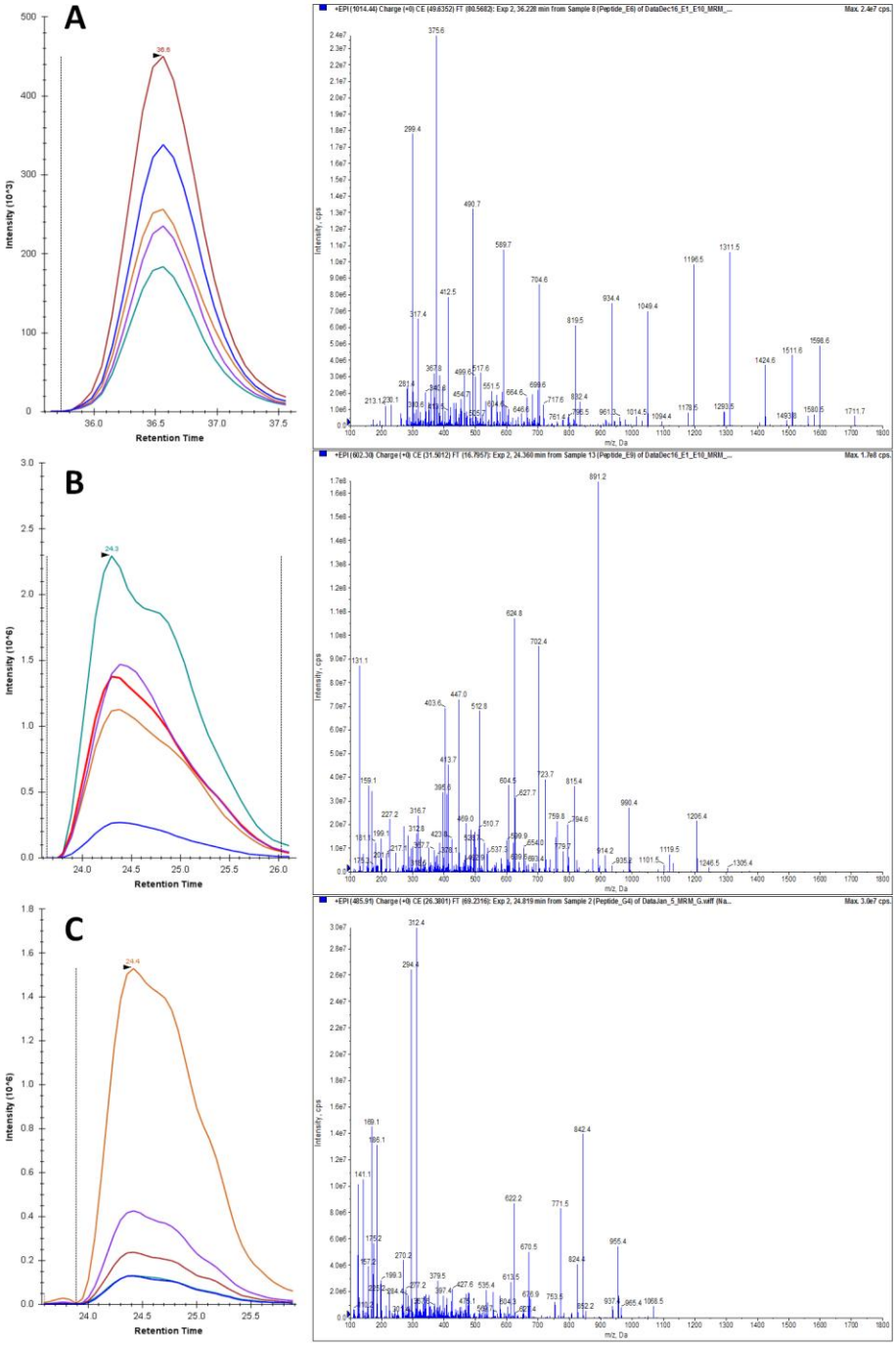

.

Figure 44. SRM and MS/MS data for protein APC. SRM-triggered MS/MS spectra were obtained for synthetic peptide targets. Top five SRM transitions are shown in a chromatogram (left). Sequence information can be confirmed with MS/MS spectra (right). **A.** NDSLSSLDFDDDDVDLSR (m/z=1014.44^{++}) **B.** SAEDPVSEVPAVSQHPR (m/z=762.30^{+++}) **C.** NVSSLIATNEDHR (m/z=485.91^{+++})

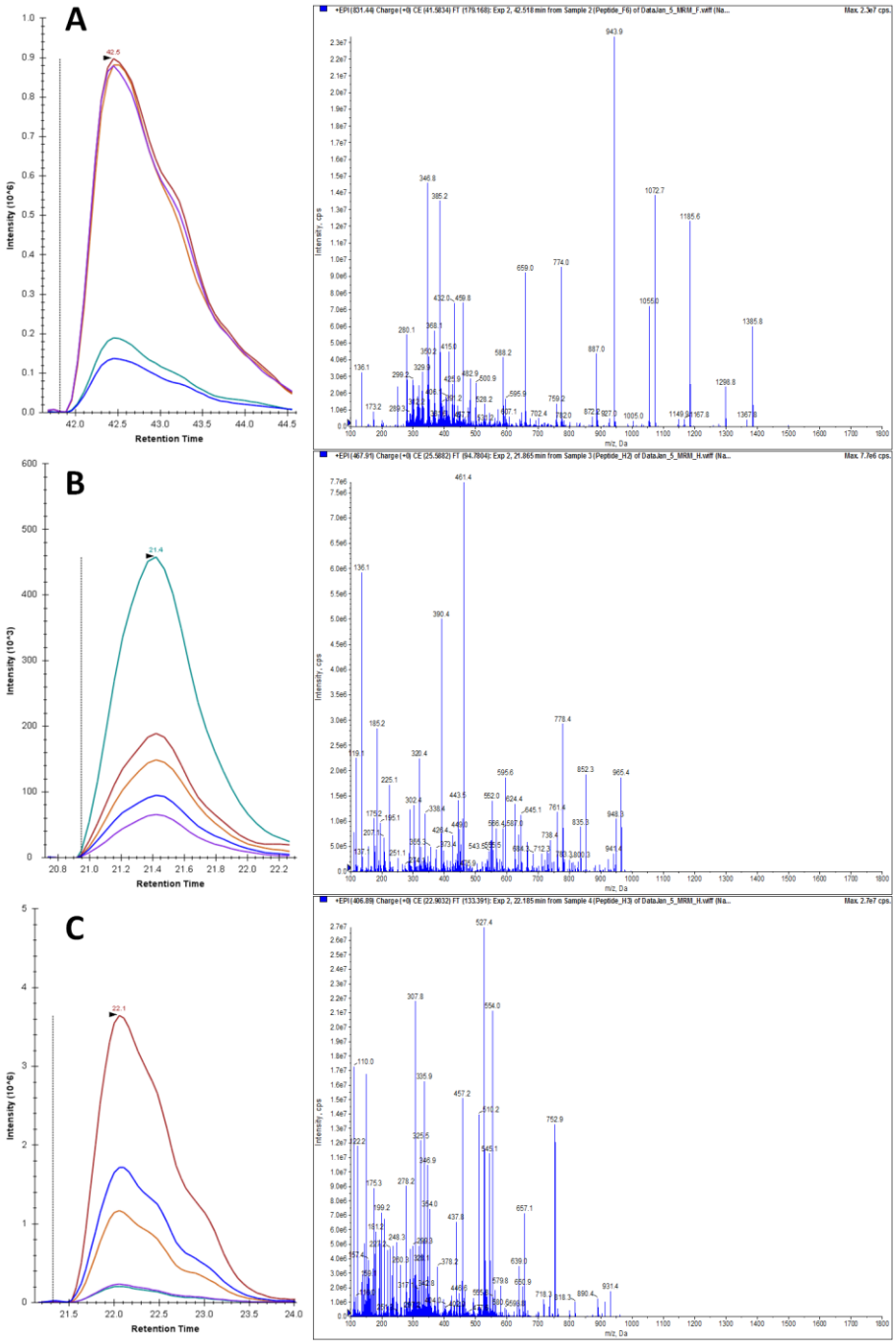

Figure 45. SRM and MS/MS data for protein Hey1. SRM-triggered MS/MS spectra were obtained for synthetic peptide targets. Top five SRM transitions are shown in a chromatogram (left). Sequence information can be confirmed with MS/MS spectra (right). **A.** YLSIIEGLDASDPLR (m/z=831.44^{++}) **B.** LVSHLNNYASQR (m/z=467.91^{+++}) **C.** LGSAHPEAPALR (m/z=406.89^{+++})

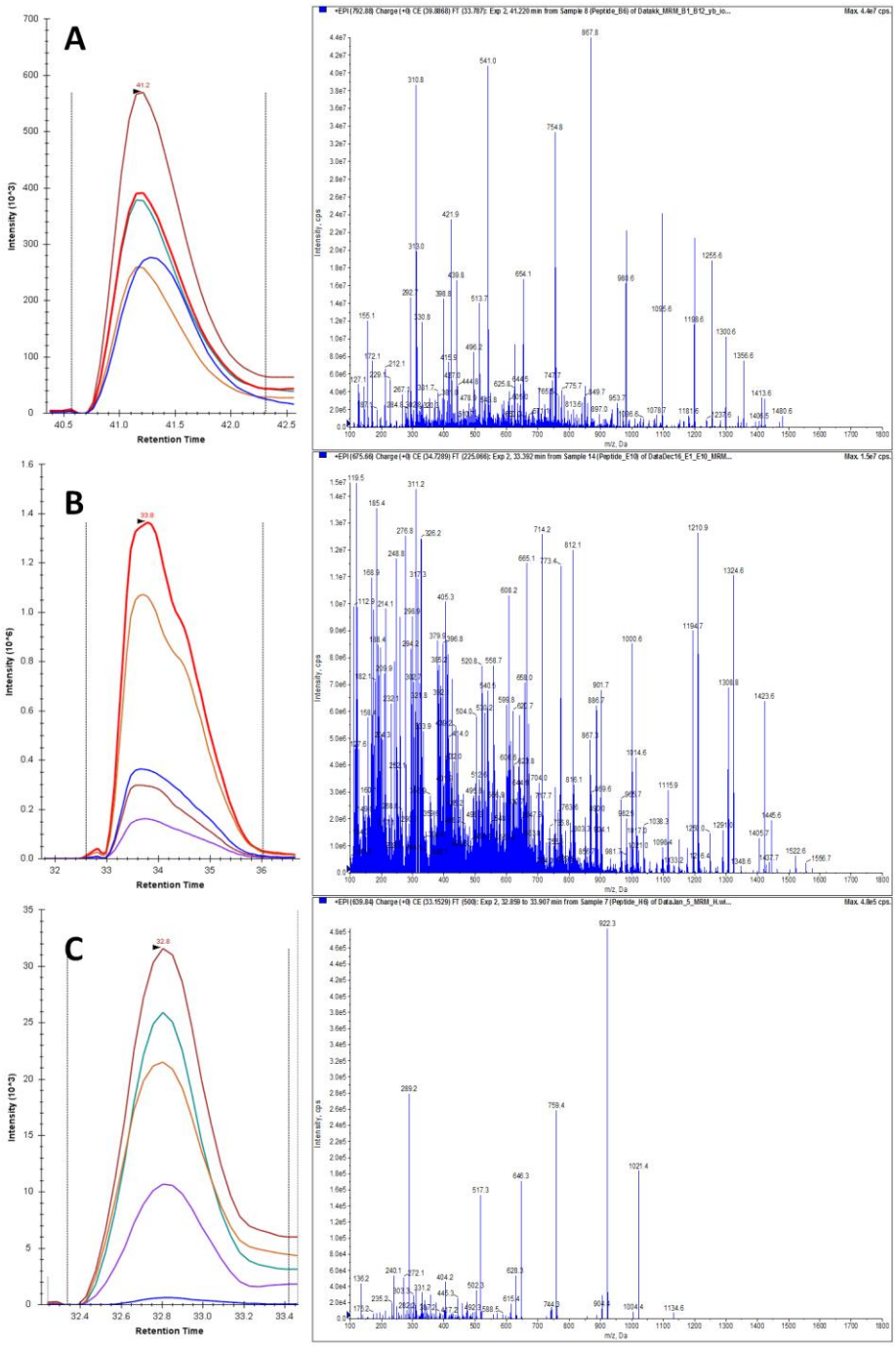

Figure 46. SRM and MS/MS data for protein Notch1. SRM-triggered MS/MS spectra were obtained for synthetic peptide targets. Top five SRM transitions are shown in a chromatogram(left). Sequence information can be confirmed with MS/MS spectra (right).**A.** NGGT**C**DLLTLTEYK (m/z=792.88^{++}) **B.** FEEPVVLPDLDDQTDHR (m/z=675.66^{+++}) **C.** GSIVYLEIDNR (m/z=639.84^{++})

To ensure optimal transition signal, each peptide was subjected to the collision energy optimization feature in Skyline. Collision energy voltage was changed stepwise by +/- 5 V. The voltage giving the maximum peak area was used for all subsequent analyses.

In order to confirm that target peptides could be detected endogenously, the SRM protocols were tested on tryptic digests of CA1K cell lysates. A great deal of optimization took place. Multiple HPLC gradients were used before finalizing a 170 minute gradient consisting of a 120 minute gradient of 5-40% acetonitrile, followed by a 50 minute re-equilibration step. Sample injection varied from 2-10 µL or 2-12.5 µg of peptides to determine optimal signal while retaining enough sample for multiple replicates. Dwell time was tested from 20-45 ms. Transitions were sorted into three protocols by protein mass range, with a high (311 kDa - 53 kDa) middle (49kDa - 39kDa) and low (38 kDa - 18kDa). The general SRM protocol was split into three methods containing 160 transitions each, with a dwell time of 20 ms. 5 µL injections of 10 µg of peptide sample were used. To improve cycle time, an SRM-triggered MS/MS scan was not included. Peptides were confirmed to be detected when 4 or more SRM transitions co-eluted. **Table 3** shows the target peptides identified in SRM analyses of tryptic digests of unfractionated CA1K cell lysates, 66% of targets were identified. Target peptides that were identified were eluting at a reproducible time point with similar chromatographic activity, as seen in sample chromatograms in **Figure 47**. Since peptides were being successfully detected, a quantitative labeling technique was introduced in order to monitor changes between differentiated and undifferentiated samples.

Table 3.Target Peptides Detected via SRM in Unlabeled Cell CA1K Lysates.

Protein	Peptide	CA1K	CA1K Diff	Protein	Peptide	CA1K	CA1K Diff
Wnt1	QNPGILHSVSGGLQSAVR	✓	✓	SUFU	VHEFTGTDGPSGFGFELTFR	✓	✓
	ETAFIFAITSAGVTHSVAR	✓	✓		GIETDGSNLSGVSAK	✓	✓
	ACNSSSPALDGCELLCCGR	✓	✓		GLEINSKPVLPPINPQR		
DVL-1	NVLSNRPVHAYK	✓		Frizzled-1	FPVHGAGELCVGQNTSDK	✓	✓
	LSSSTEQSTSSR	✓	✓		GGFPGGAGASER	✓	✓
	SQASATAPGLPPPHPTTK	✓	✓		VPSYLNYHFLGEK	✓	✓
AXIN-1	SDIYLEYTR	✓	✓	WIF-1	VLIGFEEDILIVSEGK		
	DAHEENPESILDEHVQR	✓	✓		ASVVQVGFPCLGK	✓	✓
					TCQQAECPGGCR	✓	✓
Lefty-1	LPPNSELVQAVLR	✓	✓	Nodal	VPSTCCAPVK	✓	
	QPLLLQVSVQR	✓	✓		TKPLSMLYVDNGR	✓	✓
	EHLGPLASGAHK	✓			GQPSSPSPLAYMLSLYR	✓	✓
DKK1	NGICVSSDQNHFR			POUF51	LEQNPEESQDIK		
	SSDCASGLCCAR				FEALQLSFK	✓	✓
	DHHQASNSSR	✓	✓		WVEEADNNENLQEICK	✓	✓
Cerberus	TVPFSQTITHEGCEK	✓	✓	Patched	TYVEVVHQSVAQNSTQK	✓	✓
	VVVQNNLCFGK				TEYDPHTHVYYTTAEPR		
	TPASQGVILPIK	✓	✓		LPTPSPEPPPSVVR		
P53	LGFLHSGTAK			Sonic Hedgehog	ELTPNYNPDIIFK	✓	✓
	SVTCTYSPALNK	✓			SGGCFPGSATVHLEQGGTK		✓
	RPILTIITLEDSSGNLLGR	✓	✓		LAHALLAALAPAR	✓	✓
Wnt2	ESAFVYAISSAGVVFAITR		✓	FRAT-1	APGPLAAAVPADK	✓	✓
	CHGVSGSCTLR	✓	✓		LLQQLVLSGNLIK	✓	✓
	CQDCLEALDVHTCK						
GLI3	TSPNSLVTILNNSR	✓	✓	Smoothened	GAASSGNATGPGPR	✓	✓
	IKPDEDLPSPGAR	✓			FNSSGQCEVPLVR	✓	
	GQQEQPEGTTLVK				DYVLCQANVTIGLPTK	✓	✓
APC	NVSSLIATNEDHR	✓	✓	Wnt3a	IGIQECQHQFR	✓	✓
	SAEDPVSEVPAVSQHPR	✓	✓		ESAFVHAIASAGVAFAVTR		
	NDSLSSLDFDDDDVDLSR				SCAEGTAAICGCSSR		
Akt1	TFHVETPEER			Wnt5a	ETAFTYAVSAAGVVNAMSR		
	FYGAEIVSALDYLHSEK	✓	✓		FNSPTTQDLVYIDPSPDYCVR		
	TFCGTPEYLAPEVLEDNDYGR	✓	✓		NESTGSLGTQGR	✓	✓
Beta-Catenin	HAVVNLINYQDDAELATR	✓	✓	Activin-A (homodimer, beta A chain)	EGSDLSVVER		✓
	LLNDEDQVVVNK	✓	✓		HPQGSLDTGEEAEEVGLK		
	NEGVATYAAAVLFR	✓	✓		SELLLSEK	✓	✓
CDKI1 Aka p21	DCDALMAGCIQEAR	✓	✓	TDGF/Cripto -1	FSYSVIWIMAISK		
	WNFDFVTETPLEGDFAWER		✓		DDSIWPQEEPAIRPR		
					TPELPPSAR		
NOTCH1	NGGTCDLLTLTEYK	✓	✓	Hes1	NSSSPVAATPASVNTTPDKPK		✓
	GSIVYLEIDNR				FLSTCEGVNTEVR	✓	
	FEEPVVLPDLDDQTDHR	✓	✓		LGSQAGEAAK		
GSK3-Beta	VIGNGSFGVVYQAK	✓	✓	Hey1	YLSIIEGLDASDPLR		✓
	DIKPQNLLLDPDTAVLK	✓	✓		LVSHLNNYASQR		
	IQAAASTPTNATAASDANTGDR	✓	✓		LGSAHPEAPALR		
SFRP-1	FYTKPPQCVDIPADLR	✓	✓	SRFP-2	LPNLLGHETMK		
	SEAIIEHLCASEFALR				EVLEQAGAWIPLVMK	✓	
	SQYLLTAIHK	✓			DSLQCTCEEMNDINAPYLVMGQK		
Nanog	TVFSSTQLCVLNDR	✓	✓	Beta-Actin	VAPEEHPVLLTEAPLNPK	✓	✓
	YLSLQQMQELSNILNLSYK	✓	✓		GYSFTTTAER	✓	✓
	NSNGVTQK	✓			SYELPDGQVITIGNER	✓	✓

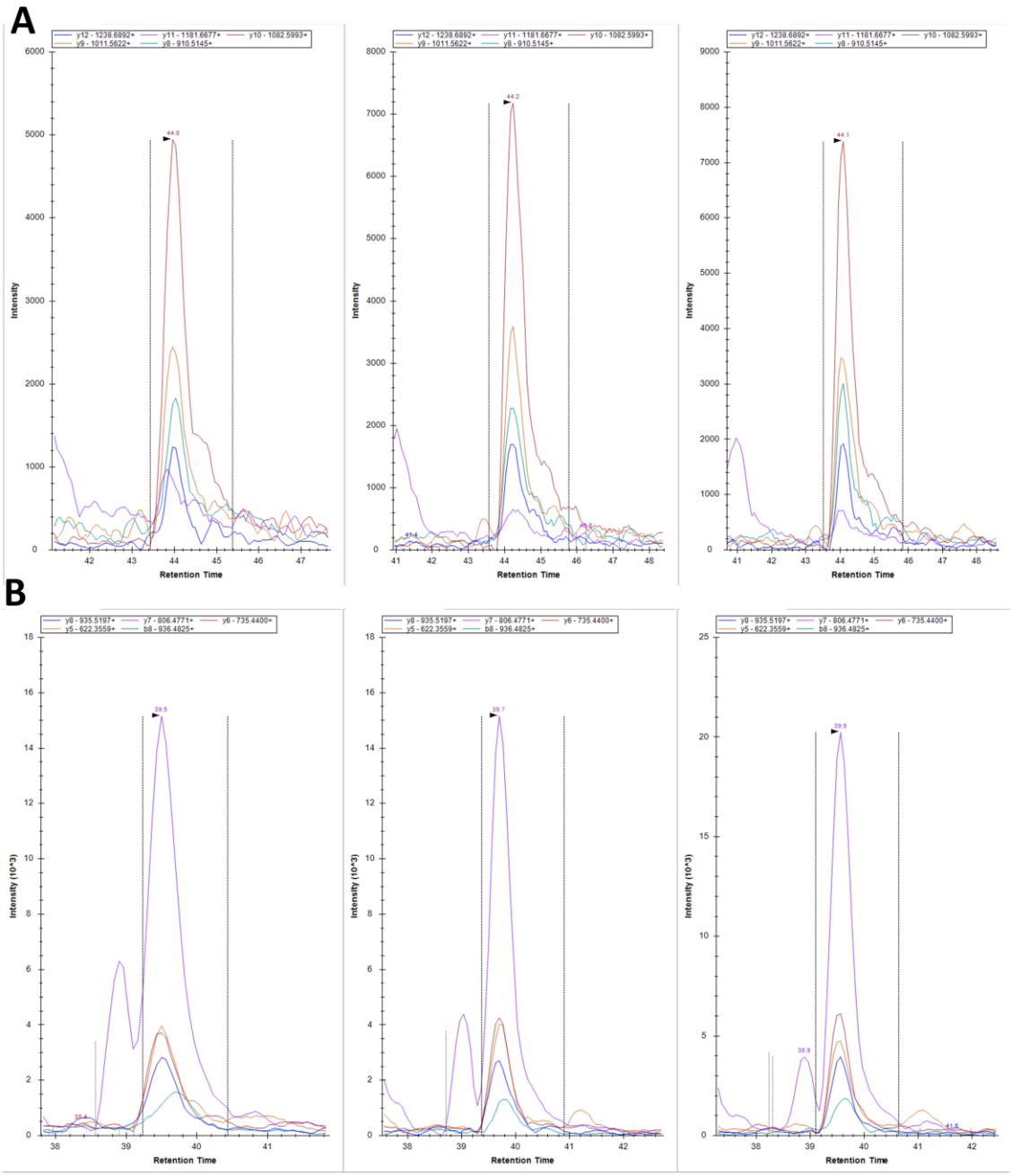

Figure 47. Target peptides were detected in tryptic digests of undifferentiated CA1K cell lysate. Sample SRM data for **A.** β-catenin peptide NEGVATYAAAVLFR. **B.** Oct4 peptide FEALQLSFK, imaged in Skyline software. Each graph represents an independent biological replicate with similar retention times and intensities upon repeated injections. Each peak represents a single transition for the respective peptide.

3.3 Dimethyl Label Incorporation

In order to quantify the protein changes between differentiated and undifferentiated cell populations, dimethyl labeling was chosen as a labeling technique. With the benefits of being added at the peptide level and being relatively inexpensive, if could be used with already harvested protein sample. To ensure the dimethyl labeling protocol was functioning properly, the target peptide HPQGSLDTGEEAEEVGLK was subjected to both the light and heavy labeling process, as seen in **Figure 4**. Dimethyl labeling occurred at primary amines, which include the N-terminus and the lysine side chain. SRM assays were generated for the light, heavy, and unlabeled versions of the peptide, and each treatment of the peptide was analyzed for the presence of each transition. As seen in **Figure 48**, in each treatment, the expected transitions are detected. The light labeled peptide is uniquely detected in the light dimethyl label treatment, and the heavy labeled peptide is uniquely detected in the heavy dimethyl label treatment. The light and heavy treatments retain some unlabeled peptide, however, this amounts to less than 0.1% of the total signal. The intensity of the labeled peptide is greater than 10^6 cps, suggesting nearly 100% incorporation. The labeled transitions are unique to their respective treatments. In addition, the retention times do not differ substantially between treatments. As the dimethyl label causes peptides to become slightly more hydrophobic, the retention time is expected to increase slightly. [91] As seen in **Figure 47**, for this sample peptide the retention time increases slightly from 19.9 minutes to 20.2 minutes. In addition, the MS/MS fragmentation and transition intensities are nearly identical between labeling techniques. To determine whether the labeling could accurately quantify samples in an SRM assay, a BSA tryptic digest was dimethyl-labeled and mixed in 1:2, 1:1, and 2:1 light-to-heavy ratios. Acquired SRM intensities matched those values.

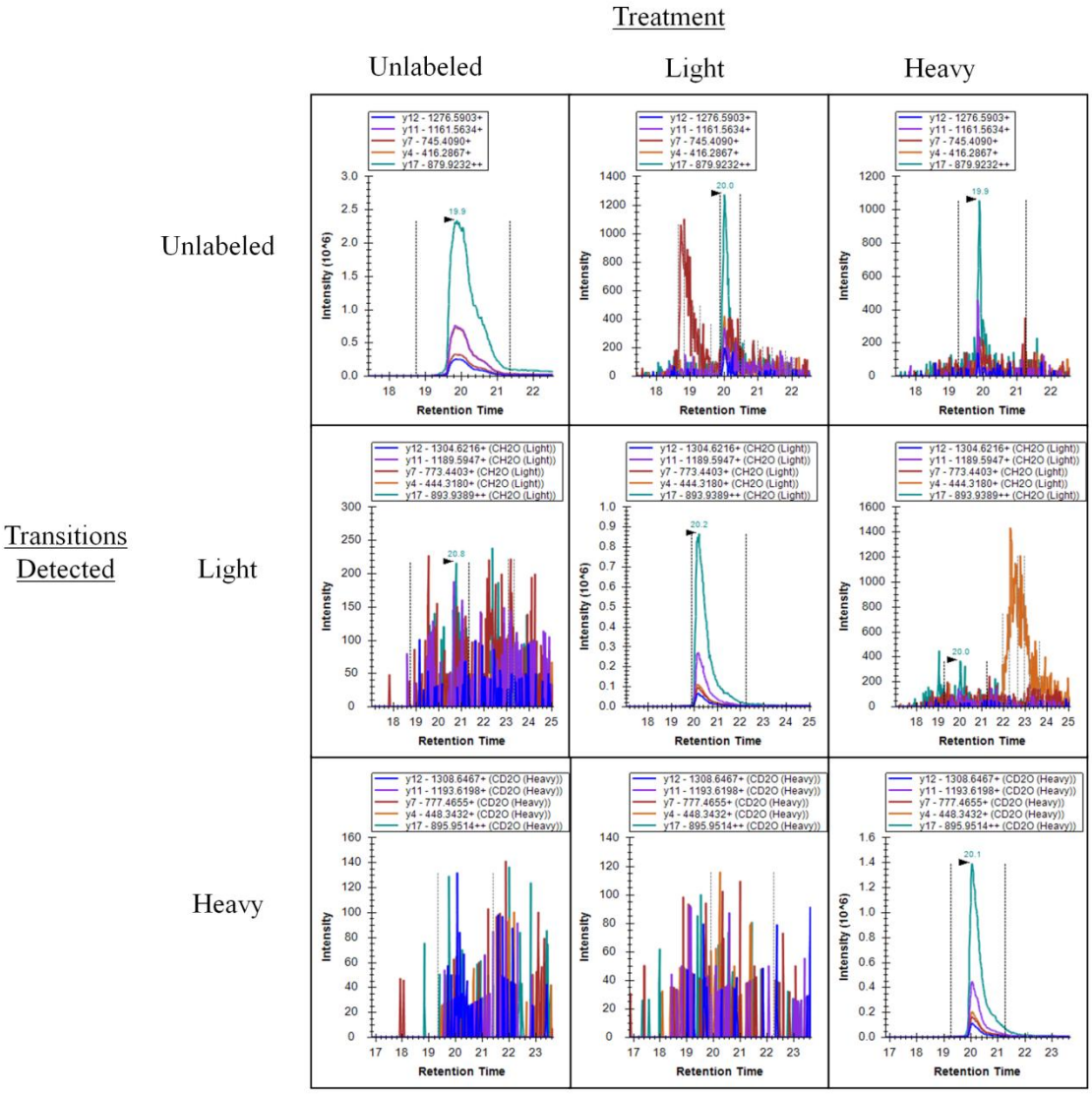

Figure 48. Efficiency of dimethyl labeling of peptides. Target peptide HPQGSLDTGEEAEEVGLK was treated with both the heavy and light dimethyl labels and left unlabeled. Peptide was subjected to LC-SRM analysis. Transitions for the unlabeled, light, and heavy labeled peptides were monitored for each treatment. The chromatograms depict the intensities and retention times of the detected transitions.

3.4 Quantitation and Scheduled Method

Because the protein expression changes were expected to be more drastic, the H9 differentiation line was used. H9 cell lysates treated with BMP4 were subjected to in-solution trypsin digests and subjected to dimethyl labeling. Undifferentiated cells were treated with the light label, while differentiated cells were treated with the heavy label. The samples were mixed in a 1:1 ratio, desalted, dried, and resuspended in 10% formic acid. However, by introducing the heavy and light label within one sample, the number of transitions requiring detection has doubled, requiring six unscheduled instrument runs of 160 transitions each. Because this consumed a great deal of sample, limiting the availability for technical replicates, as well as being an inefficient use of instrument time, a scheduled SRM method was developed. Within a scheduled SRM method, transitions are only scanned for within a given window of their retention times, allowing for more efficient instrument usage and more transitions to be detected in each run. Cycle time determines the amount of time it takes to cycle through concurrently measured transitions. Retention times were obtained for synthetic heavy and light dimethyl labeled peptides, and transitions were reconfirmed. Some b ions were enhanced in dimethyl labeled peptides and were added to the protocol if they exceeded y ion intensities. To ensure maximum sensitivity, retention time windows of 1 to 4 minutes were tested, along with cycle times of 1 to 3 seconds, as seen in **Figure 49**. Ideal chromatographic peaks were well defined by multiple data points over the course of elution and easily separated from the noise, and completely within the retention time window. It was determined that a cycle time of 2 seconds led to the best peak shapes and a 4 minute retention time window accounted for any variation in chromatography. A single protocol encompassing 990 transitions was created. A table summarizing the SRM method containing each transition targeted, including collision energy, declustering potential, and retention time can be seen in **Appendix A**.

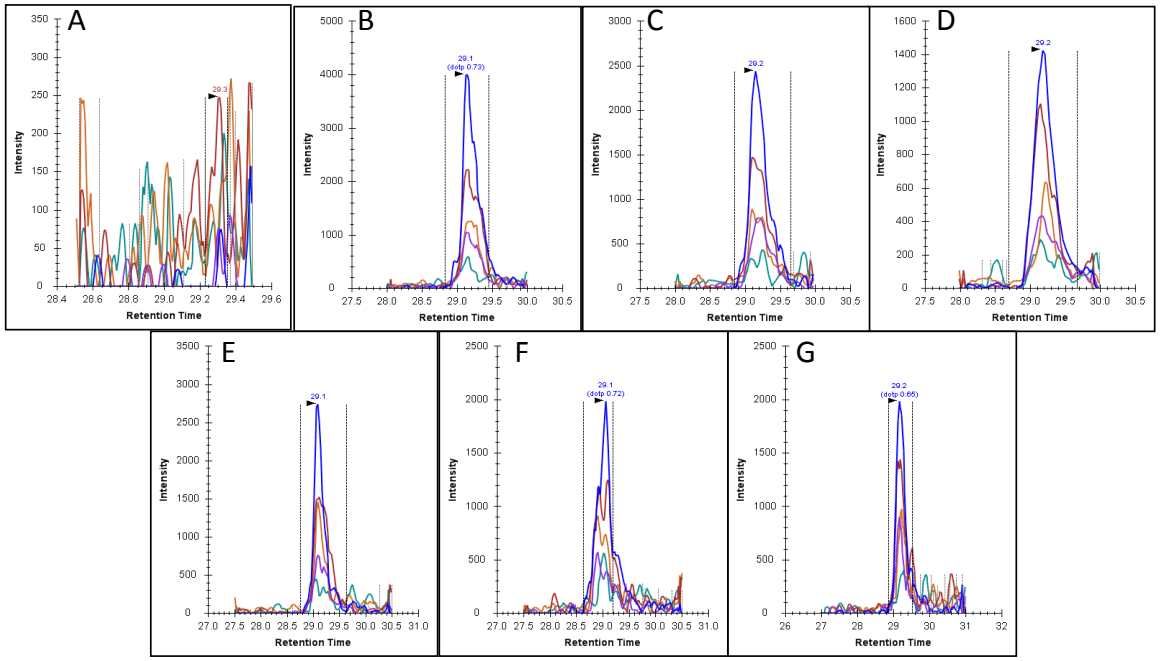

Figure 49. Optimization of scheduled SRM method settings. Scheduled SRM method settings for retention time windows and cycle times were tested on dimethyl-labeled H9 lysate. Depicted are SRM chromatograms for β-actin peptide GYSFTTTAER under varying acquisition conditions. **A.** 1 minute window, 1 second scan time **B.** 2 minute window, 1 second scan time **C.** 2 minute window, 2 second scan time **D.** 2 minute window, 3 second scan time **E.** 3 minute window, 1 second scan time **F.** 3 minute window, 2 second scan time **G.** 4 minute window, 1 second scan time.

H9 cells differentiated through treatment with BMP4 and undifferentiated controls were harvested, lysed, and subjected to an in-solution tryptic digest. Upon digestion, samples were dimethyl labeled and mixed 1:1 ahead of SRM analysis. Differentiated sample was heavy labeled, undifferentiated sample was light labeled. Four biological samples were injected in triplicate using the scheduled SRM protocol. Sample SRM chromatograms from the can be seen in **Figure 50**. Three proteins were found to be reproducibly detectable for all three peptides for each target within both differentiated and undifferentiated H9 cells and thus capable of quantitation: β-catenin, Wnt1, and β-actin. The peak areas for each peptide's transitions were used for quantitation. All three were subjected to statistical analysis as described by Bisson *et al.*[80] Briefly, transitions were scored based on their signal-to-noise ratio to limit the influence of outlier data, and transition, peptide, and protein fold changes were calculated from weighted transition peak areas. Fold change expression upon differentiation can be seen in **Figure 51**. β-catenin expression was shown to increase by 11-fold during H9 differentiation, while Wnt1 expression was shown to increase 3.4-fold. B-actin expression decreased by 1.5 fold. None of these changes were found to be statistically significant by the protein weight threshold cut-off described in the analysis, but under a less stringent quantification method of summing all transitions for each peptide of a protein, beta-catenin differential expression was found to be significant for $p < 0.05$. Other Wnt signalling pathway-related proteins seemed to be preferentially detected in the differentiated sample, however, under this analysis, no other proteins were found to be quantifiable, as peptides were either not present, or lost in the noise of a complex sample. **Table 4** outlines some of the targets that have and have not been detected. Lefty and Hey1 appeared to by preferentially detected in differentiated samples. Detection was defined by the presence of two or more coeluting transitions, quantification require more stringent criteria. For some that have been detected, SRM signal varied considerably between technical replicates, excluding them from statistical analysis. For others, such as the SFRP2 targets, intensities were too low to separate from the background. Other peptide targets experienced poor chromatography resulting in peaks eluting outside the set retention window. Other targets exhibited detection of one or two transitions, or a single peptide, not enough to confirm target identity. Interference from co-eluting

peptides may also be responsible for causing much of the noise preventing proper detection. Mean peak areas and standard deviation for each transition in the scheduled SRM protocol can be seen in **Appendix B.**

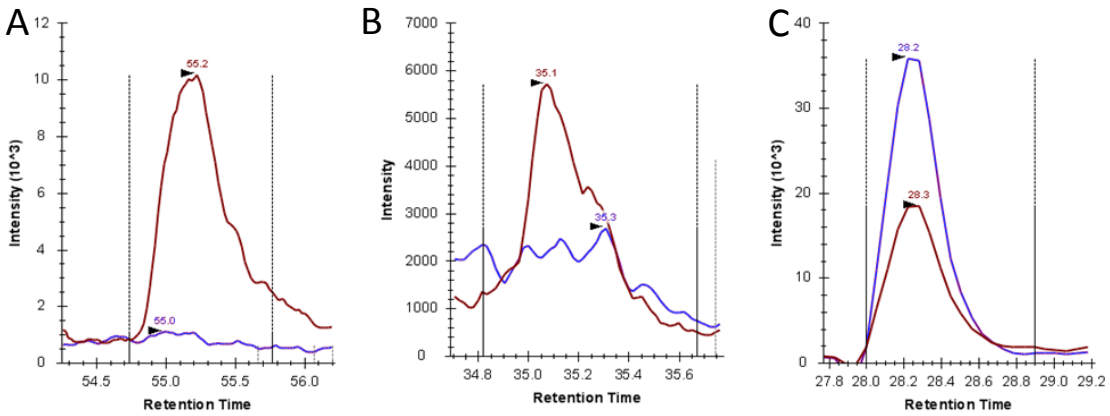

Figure 50. Scheduled SRM data for dimethyl labeled H9 lysate. Chromatograms represent the sum of all transitions for the given peptide. Blue represents undifferentiated sample, red represents differentiated sample. **A.** β-catenin. - NEGVATYAAAVLFR **B.** Wnt1 - QNPGILHSVSGGLQSAVR **C.** Actin - GYSFTTTAER

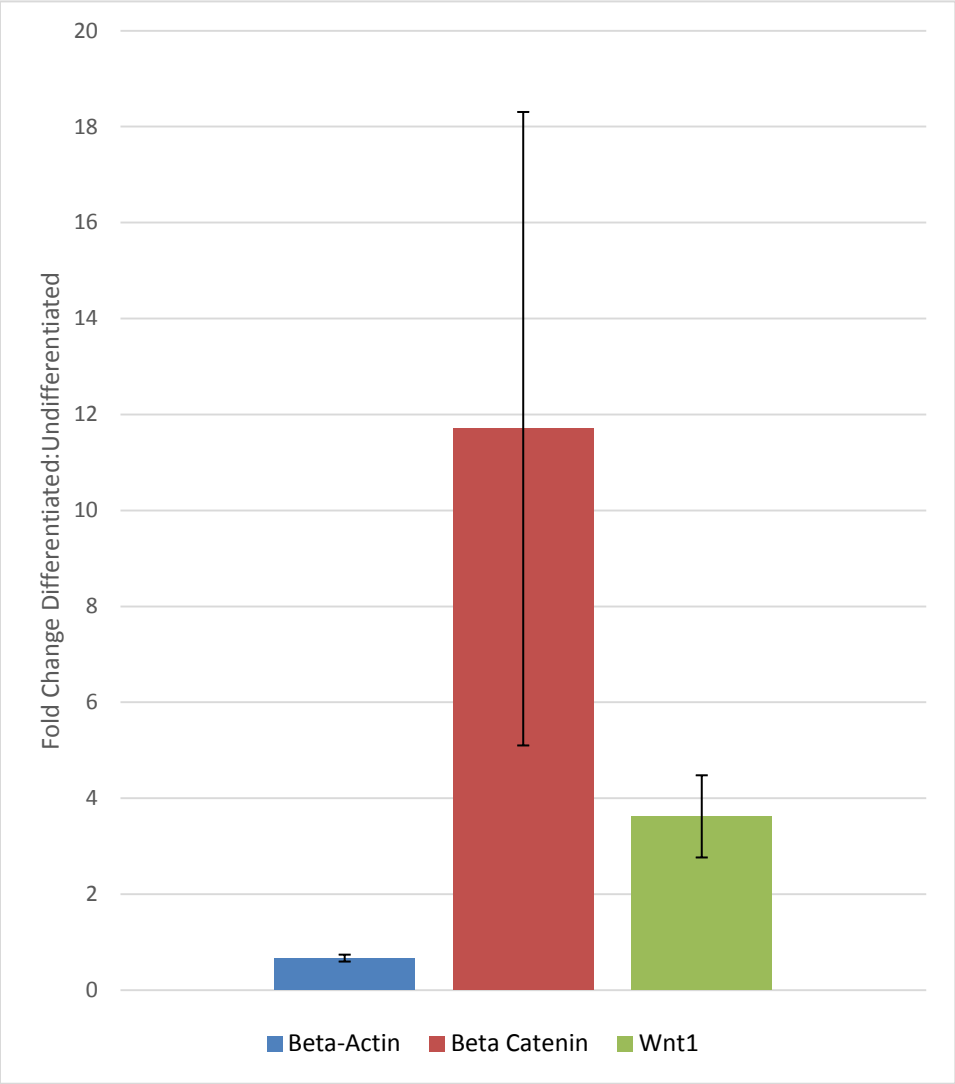

Figure 51. Protein fold change for H9 BMP4-driven differentiation. 100 µg of H9 and H9BMP4 cell lysates were tryptically digested, dimethyl labelled, and mixed 1:1. Samples were run on the scheduled SRM method. Peak areas for transitions were integrated and subjected to statistical analysis and expressed as protein fold change of differentiated cells relative to undifferentiated cells. Error bars are the weighted standard error of each protein's peptide fold change values. Four biological replicates were used.

Table 4. Peptide targets detected in dimethyl labelled H9 cell lysates.

		Sample 1		Sample 2		Sample 3		Sample 4	
Protein	Peptide	Light	Heavy	Light	Heavy	Light	Heavy	Light	Heavy
Wnt1	QNPGILHSVSGGLQSAVR	✓	✓	✓	✓	✓	✓	✓	✓
	ETAFIFAITSAGVTHSVAR	✓	✓	✓	✓	✓	✓	✓	✓
	ACNSSSPALDGCELLCCGR	✓	✓	✓	✓	✓	✓	✓	✓
Lefty-1	LPPNSELVQAVLR		✓		✓		✓		✓
	QPLLLQVSVQR		✓		✓		✓		✓
	EHLGPLASGAHK		✓		✓		✓		✓
DKK1	NGICVSSDQNHFR								
	SSDCASGLCCAR								
	DHHQASNSSR	✓		✓		✓		✓	
Cerberus	TVPFSQTITHEGCEK	✓	✓	✓	✓	✓	✓	✓	✓
	VVVQNNLCFGK		✓		✓		✓		✓
	TPASQGVILPIK	✓		✓		✓		✓	
GLI3	TSPNSLVTILNNSR	✓	✓	✓	✓	✓	✓	✓	✓
	IKPDEDLPSPGAR	✓		✓		✓		✓	
	GQQEQPEGTTLVK								
Akt1	TFHVETPEER		✓		✓		✓		✓
	FYGAEIVSALDYLHSEK	✓		✓		✓		✓	
	TFCGTPEYLAPEVLEDNDYGR	✓		✓		✓		✓	
Beta-Catenin	HAVVNLINYQDDAELATR	✓	✓	✓	✓	✓	✓	✓	✓
	LLNDEDQVVVNK	✓	✓	✓	✓	✓	✓	✓	✓
	NEGVATYAAAVLFR	✓	✓	✓	✓	✓	✓	✓	✓
GSK3-Beta	VIGNGSFGVVYQAK		✓		✓		✓		✓
	DIKPQNLLLDPDTAVLK		✓		✓		✓		✓
	IQAAASTPTNATAASDANTGDR	✓	✓	✓	✓	✓	✓	✓	✓
SFRP-1	FYTKPPQCVDIPADLR	✓		✓		✓		✓	
	SEAIIEHLCASEFALR		✓		✓		✓		✓
	SQYLLTAIHK	✓		✓		✓		✓	
Nanog	TVFSSTQLCVLNDR	✓		✓		✓		✓	
	YLSLQQMQELSNILNLSYK	✓	✓		✓		✓		✓
	NSNGVTQK	✓	✓	✓	✓	✓	✓	✓	✓
WIF-1	VLIGFEEDILIVSEGK	✓		✓					
	ASVVQVGFPCLGK		✓		✓		✓		✓
	TCQQAECPGGCR	✓		✓		✓		✓	
Nodal	VPSTCCAPVK		✓		✓		✓		✓
	TKPLSMLYVDNGR		✓		✓		✓		✓
	GQPSSPSPLAYMLSLYR								
POUF51	LEQNPEESQDIK								
	FEALQLSFK	✓		✓		✓		✓	
	WVEEADNNENLQEICK								
Sonic Hedgehog	ELTPNYNPDIIFK		✓		✓		✓		✓
	SGGCFPGSATVHLEQGGTK	✓		✓		✓		✓	
	LAHALLAALAPAR		✓		✓		✓		✓
FRAT-1	APGPLAAAVPADK	✓		✓		✓		✓	
	LLQQLVLSGNLIK								
TDGF/Cripto-1	FSYSVIWIMAISK						✓		
	DDSIWPQEEPAIRPR	✓	✓	✓	✓	✓	✓	✓	✓
	TPELPPSAR								
Hes1	NSSSPVAATPASVNTTPDKPK			✓	✓			✓	✓
	FLSTCEGVNTEVR								
	LGSQAGEAAK								
Hey1	YLSIIEGLDASDPLR		✓		✓		✓		✓
	LVSHLNNYASQR		✓		✓		✓		✓
	LGSAHPEAPALR		✓		✓		✓		✓
SRFP-2	LPNLLGHETMK	✓	✓	✓	✓	✓	✓	✓	✓
	EVLEQAGAWIPLVMK	✓	✓	✓	✓	✓	✓	✓	✓
	DSLQCTCEEMNDINAPYLVMGQK	✓	✓	✓	✓	✓	✓	✓	✓
Beta-Actin	VAPEEHPVLLTEAPLNPK	✓	✓	✓	✓	✓	✓	✓	✓
	GYSFTTTAER	✓	✓	✓	✓	✓	✓	✓	✓
	SYELPDGQVITIGNER	✓	✓	✓	✓	✓	✓	✓	✓

Due to the lack of reproducibility and inability to reliably detect many of the initial targets, several steps were taken in order to overcome the problem. The non-fractionated dimethyl-labelled cell lysate may have been too complex to identify many of the target proteins, the peptide targets may be being masked by more abundant species, the peptides may be below the limit of detection, or alternately, the predicted proteotypic peptides were not being generated by tryptic digests.

3.5 Single Protein Digests

To empirically confirm whether the peptides identified were in fact proteotypic and appearing in tryptic digests, single protein digests were performed on a set of four purified recombinant human proteins: Nodal, Activin-A, Lefty, and Cripto. 1 ug aliquots of each were run on a 12% SDS PAGE Gel, and subjected to in-gel tryptic digestion. SRM assays corresponding to all possible tryptic fragments for the specified protein were generated, including fragments with oxidized methionine. To observe exactly which peptides were being produced by the digest, the sample was also subjected to Top 12 MS/MS analysis on the Q Exactive™. MS data was uploaded to PEAKS for de novo sequencing and database searching. As seen in **Figure 52**, upwards of 90% protein coverage was observed for Nodal, with similar results for the other protein digests. 34 unique peptides were observed for Nodal, 48 unique peptides were observed for Activin A, 11 unique peptides were observed for Cripto, and 23 unique peptides were observed for Lefty. The peptides previously selected for the SRM protocol were also observed, with the exception of Activin-A. Activin-A is heavily processed before secretion, and the Uniprot sequence did not reflect that, leading to SRM target selection for peptides that should not be present in the mature protein. Those peptide targets were replaced for future analyses. SRM analysis of the single protein digests on the 4000 QTRAP® led to considerably less peptide identification. For Cripto, 3/12 potential peptides were identified via SRM. For Activin A, 2/3 peptides were identified via SRM. For Lefty, 8/18 potential peptides were identified. For Nodal, 1/11 potential peptides were identified. An equivalent amount of sample was injected on both instruments, with the Q Exactive™ identifying far more potential peptide targets than the 4000 QTRAP®.

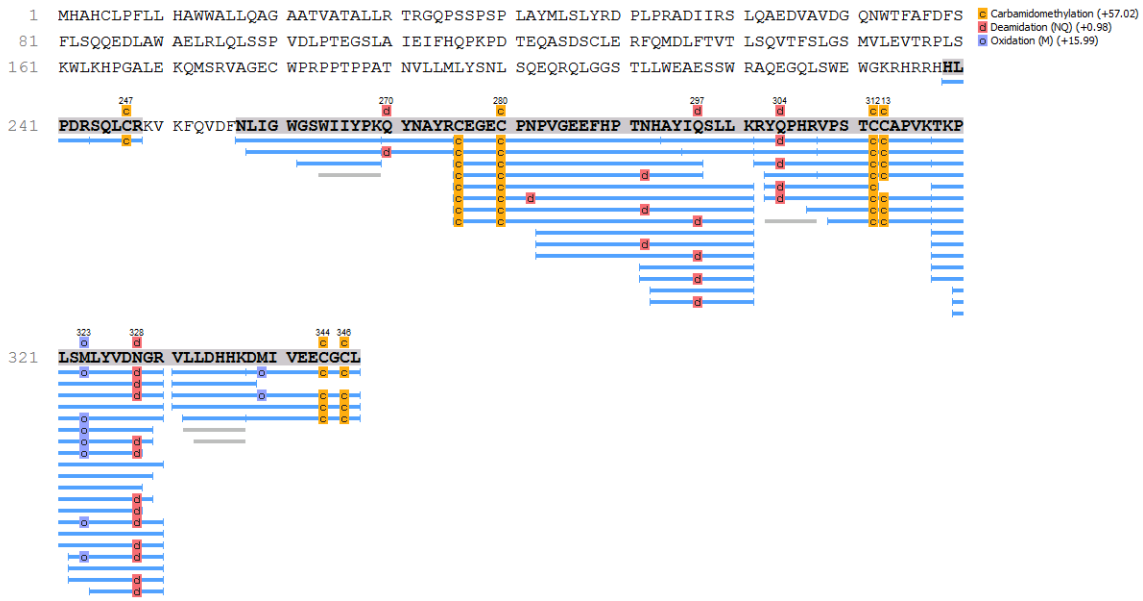

Figure 52. Sequence coverage for Nodal digest. A tryptic digest was performed on rHNodal, and was subjected to LC-MS/MS on the Q Exactive™. Blue lines represent identified peptide sequences, in order of PEAKS peptide score, while coloured squares represent post-translational modifications carbamidomethylation, deamidation, and oxidation. Mature nodal consists only of residues 238-347.

3.6 Fractionation Experiments

The dimethyl scheduled SRM protocol contained 990 transitions. The 4000 QTRAP® is limited to detecting a maximum of 1000 transitions in a single method, so the method may have been too close to the upper optimal limit.

To solve this issue, the scheduled method was divided in two, splitting the transitions by proteins in a high (>50 kDa) and a low (<50kDa) fraction. In order to simplify the sample complexity in the same manner, lysates were run on a 12% SDS-PAGE gel and fractionated into the high and low fractions as seen in **Figure 53A**. A sample SDS-PAGE gel can be seen in **Figure 54.** An in-gel tryptic digest was performed, and samples were subjected to LC-MS. Peptide targets found in the high fraction included those from Axin1, β-Catenin, β-Actin and Akt1, while those found in the low fraction included peptides from WIF1, Cerberus, DKK1, HES1 and FRAT1. Representative samples can be seen in **Figure 55**. A fair amount of noise still surrounds the peaks identified.

Another fractionation was performed by cutting an SDS-PAGE gel into five fractions, as seen in **Figure 53B.** However, few peptide identifications were made beyond the most abundant, such as β-catenin and β-actin. **Figure 56A** illustrates that background noise was cut substantially, as the β-catenin peptide peak is very distinct. In **Figure 56B-C**, a single target transition was observed in the absence of co-eluting peaks, suggesting the presence of the target, but not confirming the identity. Further studies into fractionation could improve target detection by simplifying sample complexity, reducing noise and co-eluting peptides or interferences.

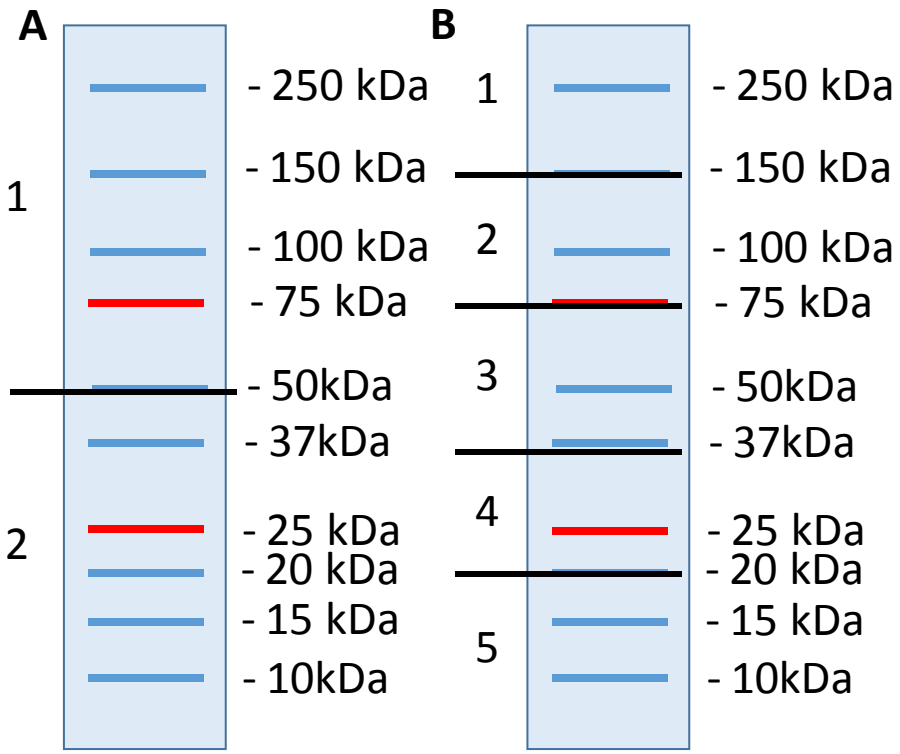

Figure 53. 1D SDS-PAGE fractionation schemes. To lower sample complexity, samples were loaded on 1D SDS-PAGE gels. Two fractionation schemes were used: A. Greater than 50 kDA and lower than 50 kDA. B. Five fractions of > 150 kDa, 150-75 kDA, 75 – 37 kDa, 37-20 kDa, <20 kDA.

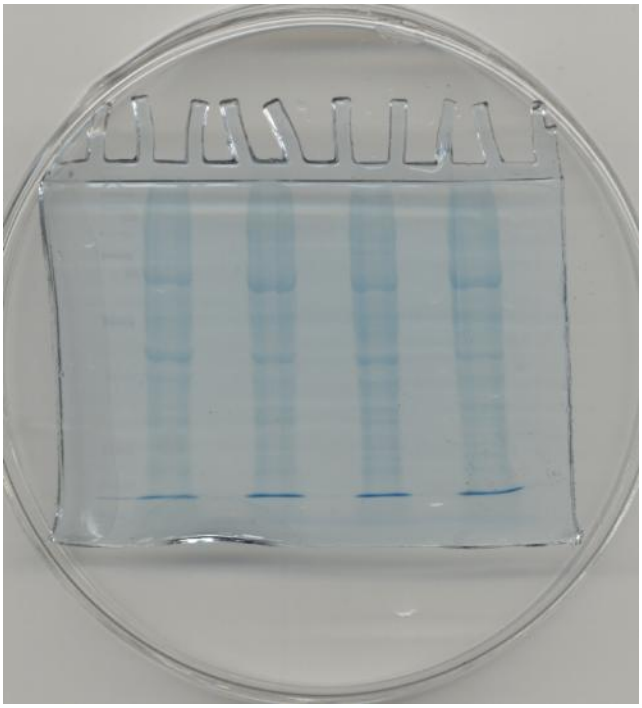

Figure 54. Sample SDS-PAGE Gel. 100 ug of hESC lysate was loaded in each lane. 2 uL of PrecisionPlus DualColour Protein Standard was loaded in leftmost lane as a molecular weight ladder. Gel was run at 200V until dye front was removed. Gel was fixed, stained with Coomassie Brilliant Blue R-250, destained, and imaged.

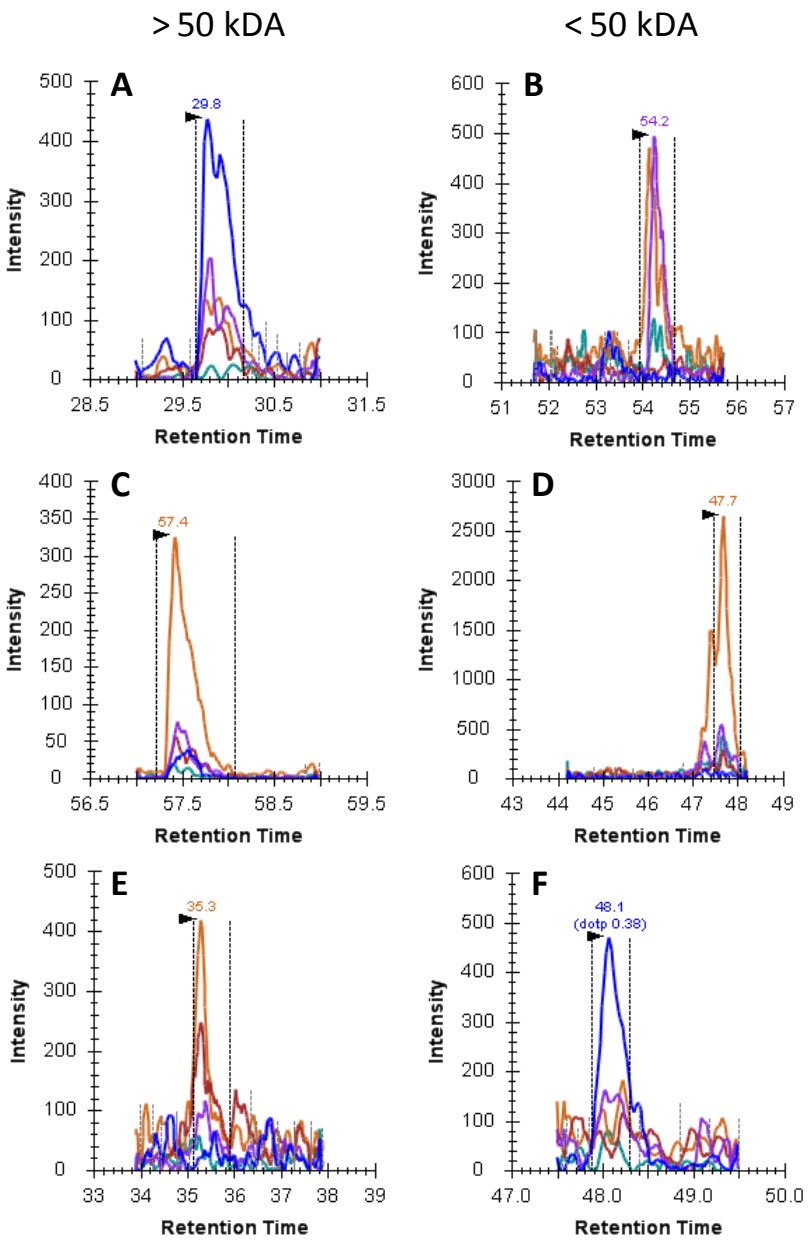

Figure 55. SRM chromatograms for peptide targets detected after SDS-PAGE fractionation. Unlabeled H9 cell lysate was loaded onto a 12% SDS-PAGE gel. The lane was cut into two fractions: > 50kDa and < 50kDa. Lowered sample complexity led to improved detection of certain peptide targets. **A.** β-catenin – LLNDEDQVVVNK **B.** Frat1 – LLQQLVLSGNLIK **C.** Akt1 - FYGAEIVSALDYLHSEK **D.** WIF1– ASVVQVGFPCLGK **E.** Axin1 - SDIYLEYTR **F.** Oct4 – FEALQLSFK.

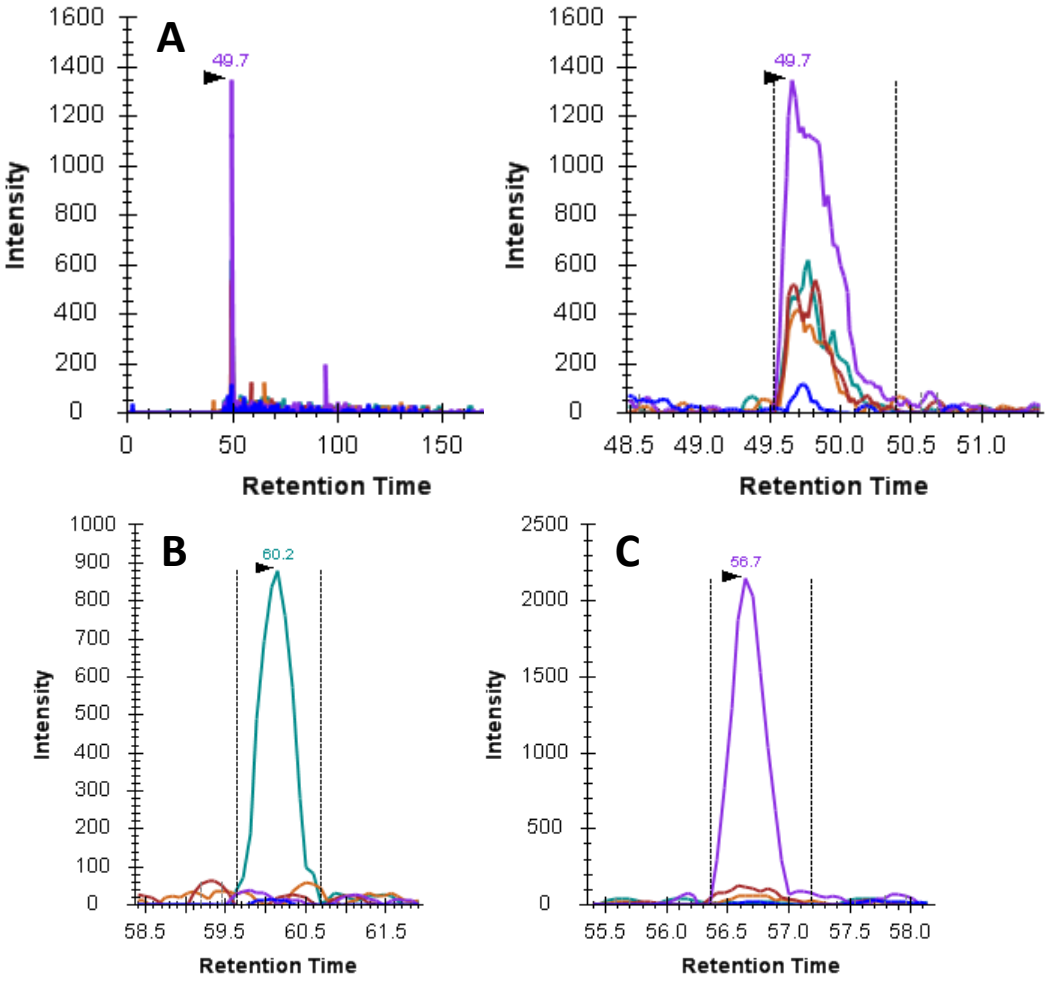

Figure 56. Five-piece SDS-PAGE fractionation of H9 lysate. To decrease sample complexity, H9 lysate underwent SDS-PAGE, and the gel lane was fractionated into five fractions. Following an in-gel tryptic digest, samples underwent SRM analysis. **A**. SRM chromatogram for β-catenin peptide LLNDEDQVVVNK, zoomed out to full gradient (left) and zoomed in on eluted peak (right). **B.** SRM chromatogram for Wnt2 peptide CQDCLEALDVHTCK. **C.** SRM chromatogram for DKK1 peptide DHHQASNSSR.

4 Discussion

Because of the complex network of signaling factors and proteins responsible for maintaining stem cell pluripotency, as well as SRM's ability to filter through complex samples to identify low abundance proteins, SRM was posited as a technique that could detect and quantify a defined set of proteins simultaneously, allowing the characterization of a cell line's "protein fingerprint," thereby providing another tool in stem cell characterization. In this study, two distinct models of differentiation were characterized for use as a model system to test SRM's capability to detect and quantify protein changes within hPSCs. Successful detection would serve as a proof of principle that SRM is a valid method of proteome characterization that could be further applied to more directed analyses of secreted, deposited, and membrane proteins.

4.1 Cell Line Differentiation and Characterization

Two distinct models of hESC differentiation were characterized in this study. The BMP4-directed differentiation of H9 cells served as a drastic differentiation method that resulted in visibly apparent differentiation. The Sox17/ERT2 tamoxifen inducible CA1 cell line served as a more nuanced model of differentiation. Cells in which Sox17 was active were expected to maintain some capacity for multipotency, as they have previously been shown to be capable of endoderm and mesoderm generation, but not ectoderm.[53] In addition, this directed differentiation method was expected to generate a more homogeneous culture of differentiated cells. Through phase contrast microscopy, the difference between the two systems was apparent. While tamoxifen-induced CA1K differentiation resulted in colonies with a slight cobblestone structure, BMP4-driven differentiation of H9s resulted in a breakdown of colony structure, as cells attained a flattened and elongated morphology. In order to validate these approaches and confirm differentiation was occurring, immunofluorescence, RT-PCR and flow cytometry experiments were conducted.

4.1.1 Immunofluorescence

Immunofluorescence staining for pluripotency and differentiation markers allowed for visualization of their presence in cell colonies in culture. Both the undifferentiated H9 and CA1K lines exhibited strong nuc Oct4 and SSEA4 expression. Some slight SSEA1 expression can be seen in the outer edges of the H9 colonies, likely caused by spontaneous differentiation. Oct4 expression is clearly intracellular and nuclear, as expected for a transcription factor, while SSEA4 expression is on the surface membrane. Upon differentiation, CA1Ks exhibit a decrease in overall Oct4 and SSEA4 expression, while SSEA1 expression becomes more prominent. For H9 differentiation, the red-yellow patches of fluorescence indicate increased levels of SSEA1 expression coinciding with expression of the pluripotency markers. Oct4 expression is expected to decrease upon BMP4 differentiation, as is SSEA4. Here, the staining is less prominent but still present. As the Oct4 staining appears more diffuse, it may be a cross-excitation between the two antibodies, as Alexa Fluor® 488 and Alexa Fluor® 568 share a slight overlap in excitiation wavelengths. The aforementioned flattened morphology is also present in the differentiated H9 cells. Thus, at the culture level, protein markers indicate differentiation is occurring.

Immunofluorescence and confocal microscopy confirmed that the Sox17/ERT2 fusion protein successfully translocated to the nucleus upon tamoxifen induction. Within two hours of tamoxifen treatment, Sox17 clearly colocalizes with nuclear staining and can promote the transcription of endoderm specific genes.

4.1.2 RT-PCR

Within the CA1K line, real-time RT-PCR analysis shows that endoderm markers Cerberus, CXCR4, DLX5, GATA4 and GATA6 are being upregulated and transcribed at the RNA level upon induction and translocation of the SOX17/ERT2 fusion protein. Oct4 and Nanog transcription were still maintained, as previously described by Seguin *et al.*[53] Of the markers analyzed, only the increase in CXCR4 expression was found to be significant with $p<0.05$. This may be due to the variation inherent in cell culture, as Cerberus expression in particular varied considerably between samples. Though the

changes are subtle and not immediately apparent by the protein immunofluorescence, the process is working as described and a definitive endoderm precursor was being produced, as the changes in transcript levels agreed with those in previously described SOX17 overexpressing CA1s.[53] The system is typically used for further downstream differentiation. Sox17 positive cells have been shown to express markers of liver, pancreas and intestinal epithelium upon further differentiation.[113] The purpose for this study was to provide a subtle systemic change in protein expression rather than a more terminal differentiation process.

Real-time RT-PCR analysis of H9 differentiation showed that the expression of the pluripotency factors Oct4 and Nanog were downregulated by approximately 50 and 75% respectively, which is to be expected as these cells should have far less differentiation potential. The decrease in expression of these factors has also been confirmed in literature.[109]

4.1.3 Flow Cytometry

Flow cytometry experiments showed the differentiated populations are distinct from the undifferentiated hESC populations. Prior to use of the viability dye, analyses were confounded by autofluorescence of the dead cells. Being able to gate on the live cell population ensured that the marker expression was valid. The negative control included on the histograms was Fluorescence Minus One (FMO). The FMO was fully stained for all markers except for the one it serves as a negative control for. Rather than simply using a fully unstained control, it can account for any cross-reaction between the other antibodies that might interfere with the target fluorescence. For the H9 differentiation protocol, both differentiated and undifferentiated cells were positive for Oct4 expression compared to the negative control, however, Oct4 expression is reduced 2.3-fold upon differentiation. The undifferentiated population stained primarily negative for SSEA1 expression. The 37-fold increase in median fluorescence upon differentiation indicates a large shift in the population of the cells toward the differentiated state. SSEA3 expression also decreases 2.2-fold upon differentiation. As seen in the histogram, the level SSEA3 expression is variable among the undifferentiated population, but upon differentiation it

greatly decreases. SSEA3 expression has been shown to decrease more rapidly than SSEA4 upon differentiation, perhaps the varied expression represents a subpopulation of cells ready to make the transition away from pluripotency.[114] SSEA3 is similar to SSEA4 in that they are both glycosphingolipids and cell surface markers of pluripotency. Neither SSEA3 nor SSEA4 is essential for hESC pluripotency, but loss of expression of either is usually an effect of differentiation.[115]

As expected, CA1K differentiation was far more subtle, and most pluripotency markers were maintained. Oct4 expression was slightly increased and SSEA3 expression was mostly maintained. Median SSEA1 expression is decreased, but the histogram shows that part of the population has increased expression. The dot plots in particular make it difficult to consider that the tamoxifen-induced cells are in fact differentiating. Taken alone, tamoxifen-induced differentiation showed no significant changes by flow cytometry.

Taking the three validation methods together, it has been established that the two model systems of differentiation have been well characterized using standard methods. Tamoxifen induction of the Sox17 was confirmed by the localization experiment, while definitive endoderm production was confirmed by the upregulation of the markers CXCR4, Cerberus, DLX5, GATA4 and GATA6 as shown by RT-PCR analysis. Hence, they could be used to determine if SRM-based techniques can be used to similarly detect alterations in hESC differentiation.

4.2 SRM Assay Development

A key benefit of SRM is the ability to identify and quantify protein expression without the use of antibodies. Antibodies may not be available for desired targets, development costs are large, and cross-reactivity can be an issue. With SRM, target design involves the analysis and synthesis of peptides, which can be produced inexpensively with modern synthesizers. Any protein can be enzymatically digested to generate peptide targets. Unlike some antibodies where the epitope is unknown, SRM is more specific in that the target is always a known peptide.[116]

Protein targets were identified through a literature search and the peptides corresponding to them were chosen primarily through use of various SRM tools available online. The actual peptides chosen were often limited by the protein sequence itself. Lange *et al.*'s guidelines such as not including methionine or tryptophan weren't feasible for certain proteins.[60] In the case of Nodal, there was a single peptide candidate in the tryptic digest that did not contain a methionine residue. As SRM is a targeted technique, post-translational modifications that are not included in the list of transitions will not be detected due to the change in *m/z*. Including these modifications greatly increases the amount of transitions required for an SRM method, so it is often best to avoid the residues if possible. Glutamine and asparagine residues are also prone to deamidation which could also cause problems with SRM detection. Protein sequences obtained from Uniprot were tryptically digested *in silico* in Skyline and target peptides were selected from the list. To ensure protein specificity, each sequence was submitted to a protein BLAST search, and tryptic efficiency for each peptide was calculated using PeptideCutter. The GPMDB and SRMAtlas served as potential sources of SRM targets; however, the majority of their SRM peptides were theoretical rather than based on empirical observation.[68, 117] Many of the target proteins did not have corresponding peptides in either of those databases. This indicates that they were never detected, possibly due to their low abundance. Because of this, synthetic peptides were generated in-house and optimal transitions were determined from acquired MS/MS data with the aid of Skyline.

Though all these tools exist to aid in selecting "proteotypic" peptides, basing target selection on theoretical peptides and *in silico* digestions rather than previous observations has its pitfalls. Some proteins are heavily modified and cleaved from their transcribed protein sequence. This led to some selected targets that should not be present in the mature protein, thus explaining difficulty in identification, particularly secreted proteins. For example, several of the peptides originally chosen for Activin A were not present in the active protein, necessitating the selection of new target peptides.

Transition selection was accomplished by subjecting synthetic peptides to LC-MS/MS. Specifically SRM-triggered data-dependent acquisition scans, in which detection of a

transition triggers the 4000 QTRAP® to acquire MS/MS data, were used in order to obtain both optimal transitions in terms of chromatography and intensity, as well as sequence information to validate the peptide's identity. The top five transitions for each given peptide and corresponding MS/MS data can be seen in **Figures 14-46**. Each coloured line in the chromatogram represents a fragment ion of the precursor mass, or one of the peaks in the MS/MS spectrum. Transition selection was primarily based on intensity, but also giving preference to fragment ions greater in *m/z* than the precursor. These transitions were selected and consolidated in a general protocol for cell lysates. The protocol was optimized for numerous instrument parameters, including collision energy, dwell time, sample injection amounts, and varying chromatographic gradients.

4.3 Detection in Cell Lysates

The general SRM protocol was tested on CA1K lysates to confirm endogenous detection, and roughly 65% of target peptides were identified in samples repeatedly. Proteins such as β-catenin and Oct4 were detected reproducibly, as seen in **Figure 47**. Dimethyl labeling was introduced as a method of relative quantitation so protein expression levels could be compared between differentiated and undifferentiated cells.[75] Dimethyl labeling has previously been shown to couple effectively with SRM on the 4000 QTRAP® by Aye *et al*.[118] The label was shown to be well incorporated when tested on a synthetic peptide, and tests proceeded on H9 lysates. To account for the doubling in transitions when including both heavy and light-labeled peptides in the same sample, a scheduled method was developed in order to maximize the amount of transitions in each method. The labeling didn't appear to drastically affect peptide fragmentation, however, transition selections were reconfirmed on labeled synthetic peptides. New transitions were incorporated where signal intensities improved upon original selections, as some peptides had enriched b ions after the labeling.

4.4 Wnt Signaling Pathway Upregulated in BMP4 Induced Differentiation

The canonical Wnt signaling pathway plays a key and controversial role in hPSC signaling. Sumi *et al.* claim Wnt signaling has a biphasic role in maintenance of self-

renewal and differentiation of hPSCs based on β-catenin expression.[119] Basal levels of β -catenin appear to maintain self-renewal, while inhibition of GSK3β promotes accumulation of β-catenin, which drives cells to a differentiated state.[36] A study by Davidson *et al.* refutes this by showing that Wnt and β-catenin signaling are actively repressed by Oct4 expression in the pluripotent state through siRNA knockdown of Oct4.[120] In either case, Wnt signaling appears to play a role in determining stem cell pluripotency. Two components of the Wnt signaling pathway, Wnt1 and β-catenin, were detected and found to be upregulated upon BMP4-driven H9 differentiation using the scheduled SRM method, which both agrees and disagrees with the literature. Activin A/BMP4 treatment of hESCs was shown to induce expression of canonical Wnt signaling, while BMP4 has also been shown to be an antagonist of the Wnt signaling pathway through inhibition of Akt signaling, further cementing the complexity of the network surrounding hPSCs.[121, 122] However, due to sensitivity and detection issues, quantitation information could not be determined for other targets. In particular, if the expression change in β-catenin was that drastic, members of the β-catenin destruction complex such as Axin, GSK3β, and APC would have been expected to be detected. Axin in particular has been shown to be the concentration-limiting factor in formation of the β-catenin destruction complex, so lowered expression would correspond to increased β-catenin levels. [123]

4.5 Detection and Sensitivity Issues

Detection and sensitivity issues were a factor in being unable to obtain quantitative data for many targets. While many protein targets were previously detected by antibody-based techniques such as Western blotting, many of these targets have been rarely detected by mass spectrometry, as signified by their absence in online spectral libraries. To maximize instrument efficiency and the number of proteins quantified per run, a scheduled SRM protocol was used. One limitation of using the scheduled method is the loss of control of dwell time. In a scheduled method, only cycle time is determined directly, therefore the dwell time will be a function of how many concurrent transitions are being detected.[75, 124] If many transitions are co-eluting or being scanned for during the same time period, low abundance peptides in particular may not experience a long enough dwell time, and

sensitivity could suffer. In addition, use of a scheduled method requires the use of retention times, and a recurring problem was the shifting of peptide retention times from run-to-run, necessitating the four minute acquisition window. Week-to-week and month-to-month variability in the instrument itself will affect measurements.[94] A smaller retention time window would lead to fewer transitions being detected at one time, but could miss the target altogether if it elutes outside of that narrow range. Using a different mass spectrometer and software platform, the Domon group developed a technique known as intelligent SRM (iSRM). [62] In this method, detection of a set of two primary transitions triggered the acquisition of six secondary transitions from which sequence data could be simulated. A dynamic range of 10 amol – 100 fmol was shown against a complex background, with a method exceeding 6000 transitions per 60 minutes. In contrast, the 4000 QTRAP® is limited to detecting 1000 scheduled transitions at a time, and exhibited a much higher limit of detection.

The dimethyl labeling protocol as a quantitation method may also be reconsidered. Though incorporation was strong and near-complete, it's still ultimately a relative quantitation method. Use of the AQUA method of spiking isotopically-labeled synthetic peptides of a known amount could have simplified matters on some levels.[90] Firstly, the labeled peptide would be assured of being present in the sample, thus the endogenous peptide could be confirmed as being either below the limit of detection or not present in the sample. With dimethyl labeling, if the target is not detected in either sample, that confirmation could not be made. Secondly, the labeled peptide would serve as an internal standard, allowing for the direct quantitation of how much endogenous peptide is present in the sample. This would enable one to clearly establish the limit of detection and provide a better idea of how abundant the target protein is in relation to the total amount of sample injected. However, the cost of this approach would be substantially more than dimethyl labeling.

Another concern with dimethyl labeling is the relatively small minimum mass difference of 4 Da, which may cause overlapping spectra to occur.[125] This may have caused issues with co-isolation of both the heavy and light species at Q1, leading to poor detection by the instrument. Both Q1 and Q3 are set to unit resolution, meaning they can only

distinguish between species with a difference of 1 *m/z*. This problem could be averted by preferentially selecting lysine containing peptides, selecting doubly charged precursors, or incorporating a heavier dimethyl label by using deuterated sodium cyanoborohydride in addition to deuterated formaldehyde. Stable isotope labeling in cell culture, or SILAC, incorporates a higher mass label as well, and by incorporating the label during cell culture growth, it could minimize the amount of downstream variation during sample preparation.[88] SILAC has been coupled with SRM in an analysis seeking to identify secreted biomarkers.[126]

Comparing the sequence coverage of recombinant human proteins obtained from the top 12 method on the Q Exactive™ and the SRM scans on the 4000 QTRAP®, it is clear there are confounding factors causing the difference in detection. Firstly, as observed in **Figure 52**, many of the observed peptides contain post-translational modifications such as oxidation or deamidation, as well as non-specific cleavages. As stated previously, SRM is a targeted method, and unless these PTMs are accounted for, they will not be detected.[60] However, by including these modified peptides in the analysis, experimental time is increased considerably. An alternate method would be to exclude the residues prone to deamidation, namely glutamine and asparagine, however, after already excluding methionine and tryptophan, excluding one-fifth of potential residues severely limits the amount of peptide candidates, and many proteins may not possess sequences compatible with those criteria. In either case, the presence of PTM peptides, particularly the oxidized or deamidated versions, will affect quantitation of the unmodified peptide. Hence changes in post-translational modifications that may occur during differentiation could confound results by appearing as alterations in expression. This may particularly affect secreted proteins, such as Wnts, which undergo extensive modifications.[127, 128] Much of the problem with methionine oxidation in proteomics is that it occurs incompletely. Partial oxidation complicates MS analysis by creating multiple species and spreading out the total signal among them. It occurs readily when methionine is exposed to air, as well as during storage. To work around this problem, Pesavento *et al.* selectively oxidized all methionine and cysteine residues through treatment with performic acid within their sample.[129] In doing so, they were able to analyze the true

abundance ratios of histones as well as identify novel PTMs. However, the caveat is that side reactions such as formylation of lysine and nonspecific cleavage of asparagine or tryptophan can occur upon treatment with performic acid, leading to a more complex sample.[130] Other PTMs that were not considered in this study but may play a factor in peptide detection include glycosylation, phosphorylation, and lipidation. Many targets in the study are secreted, including proteins such as Wnt1and Nodal, which are heavily modified and processed prior to secretion.[127, 128] Glycosylation of Nodal improves its stability.[131] Glycosylation and lipidation can interfere with proteolytic enzymes' ability to cleave the protein backbone. Glycosidase treatment can increase total peptide identification. [132] Delipidation can be performed by protein precipitation in acetone/methanol or chloroform/methanol, though this did not appear to aid in improving protein sequence coverage of plasma membrane associated proteins of hESCs.[133]

4.6 Sample Preparation

Unfractionated in-solution digests may have also been a poor choice in sample workup, considering the complexity of the sample, particularly after combining two lysates in the dimethyl labeling protocol. More than 100,000 detectable peptide species elute from a cell lysate sample during shotgun proteomic analysis, with sensitivity and sequencing speed being limitations in actual peptide identification.[134] Interference by the sheer amount of peptide species may be preventing low abundance peptides from being detected. Undersampling of data is an issue that results from the complexity of proteomes and protein digests.[97] Co-fragmentation of peptides is a concern in shotgun proteomics, however, the Q3 filter of SRM makes it less likely that peptides will co-fragment.[135] There has been a growing movement towards using unfractionated samples, for instance, making use of the filter-assisted sample preparation (FASP) method popularized by Matthias Mann.[136] In this method, cell lysates are reduced, alkylated and trypsinized on a membrane, even in the presence of high concentrations of detergent. Reagents and detergents are removed through repeated washes with an 8 M urea solution, which is in turn removed through washes with ammonium bicarbonate followed by centrifugation. The method allows for the benefits of detergent use without requiring protein precipitation, improving sample preparation and recovery. However, these were also

coupled with ultralong analytical HPLC columns, as well as long separation gradients.[98] Sample throughput suffers but identifications may increase. A two-hour gradient may not have been sufficient to properly separate the lysate sample within the SRM studies. Retention times for peptide targets were frequently overlapping, leading to a large amount of concurrently detected transitions and a lowered sensitivity due to the decreased dwell time. A longer or gradient could have more effectively separated the targets and potentially increased sensitivity. However, it could also have led to peak broadening and less defined signals.[99]

The lysis buffer used was urea-based, and commonly used in proteomic samples. However, urea-based buffers have been shown to cause carbamylation in proteins when heated for extended periods of time.[137] The effect is more drastic at higher concentrations, but as all in-solution digests of cell lysates were performed at urea concentrations of less than 2 M, the effects should be minimal. Still, an alternate lysis buffer was tested, M-PER Mammalian Protein Extraction Reagent (Thermo), composed of a proprietary detergent in 25 mM bicine buffer. In-solution digests using either M-PER or urea lysis buffer were performed and run on a Top 12 method on the Orbitrap Elite, with urea buffer resulting in a superior number of protein identifications. The M-PER buffer could solublize proteins that might be missed with the urea buffer, such as membrane proteins like Frizzled or Smoothened, potentially presenting itself as a complementary procedure.

The SDS-PAGE fractionation methods described slightly improved peptide detection; however, SRM intensities were still fairly low, and particularly noisy. This suggests that there are still unresolved issues taking place. These could have involved deficiencies with sample preparation or with the instrument. Depletion of abundant proteins or subcellular fractionation prior to sample workup could improve signal and detection of low abundance targets. The issues with reproducibility may also be a product of the differentiation process. The mixture of cells becomes markedly more complex going from the pluripotent to the differentiated state, introducing more variability in protein expression.

Issues with instrument sensitivity itself may also be a factor. In order to judge signal intensity and for tuning and calibration purposes, a commercially available peptide standard was used. Glu-1-Fibrinopeptide B (Glu-Fib, Sigma) has a sequence of EGVNDNEEGFFSAR and produces characteristic ions of *m/z* 1570.6^{+} and 785.8^{++}. A 1 pmol/uL solution was infused into the instrument for initial tuning, while 200 fmol was typically injected on a simple gradient to assess SRM signal. A 200 fmol injection typically resulted in a signal intensity of 10^4-10^5 counts per second (cps) under optimal conditions. At peak performance, the 4000 QTRAP® should be capable of detecting peptides at a sub-femtomole level, with 50 attomoles given as a lower limit of detection.[66] Upon serial dilution of Glu-Fib standard, the limit of detection was typically between 1-10 fmol of peptide. This presents an issue when the stated goal of the study is detecting proteins of low abundance. HPLC columns, both trapping and analytical, were replaced, as was the emitter tip, suggesting the issue may be with the 4000 QTRAP® instrument.

4.7 Future Experiments

Future studies should explore more extensive fractionation of protein samples to overcome issues of sensitivity. Methods such as strong cation exchange (SCX) may be able to simplify the complexity of the sample to improve detection of low abundance factors. Alternately, the amount of biological sample used could be scaled up in order to see more of the less abundant species. Many of the protein targets were secreted or membrane proteins. It would be worthwhile to enrich these fractions using subcellular fractionation techniques or by collecting conditioned media and performing fraction-specific SRM assays, rather than analyzing whole cell lysates, simplifying the complexity of the assay.

Further studies into parallel reaction monitoring are also suggested. With the Q Exactive™'s ability to monitor all potential transitions of a peptide at once, in addition to quicker assay development, each measurement could be validated with MS/MS spectra. Adding an Enhanced Product Ion (EPI) scan to an SRM method to acquire MS/MS data for sequencing on the 4000 QTRAP® increases cycle time substantially, potentially leading to a loss of sensitivity. The Q Exactive™'s ability to acquire MS/MS data

simultaneously eliminates that problem. The sequence information obtained would prevent falsely identifying a peptide in the case of multiple peaks with co-eluting transitions.

Once a method is optimized, analysis and characterization of multiple hESC as well as iPSC lines should be performed. Variations between cell lines affecting differentiation potentials have been previously documented, therefore, the more cell lines that are profiled, the better the understanding of stem cell signaling. In addition, monitoring the changes in protein expression during reprogramming of somatic cells to iPSCs could help us better understand the process by which pluripotency is regained from terminally differentiated cells. Currently, iPSC generation is a very inefficient process and better characterization of the pathways responsible could result in more effective derivation.[138]

A successful SRM protocol could also be applied to time-course differentiation assays. Again, many of the factors monitored are transient and dose-dependent in their action, so by monitoring the protein changes over various time-points as cells differentiate, a better understanding of the mechanisms responsible for altering cell fate could be elucidated.

4.8 Conclusion

SRM is a sensitive and selective technique; however, as with any other proteomic technique, it is highly dependent on sample preparation and instrument optimization. In this thesis, we validated two distinct hESC differentiation models within which protein expression changes could be monitored. While some protein and peptide targets responsible for hESC pluripotency have been identified and quantified, the network of proteins responsible for maintaining stem cell pluripotency must still be fully characterized quantitatively, which could be accomplished through improvements in the SRM method. A better understanding of these complex pathways would lead to better stem cell culture conditions, more effective differentiation protocols, and ultimately act as a contribution to hPSCs role in regenerative medicine.

5 References

1. Stewart, M.H., S.C. Bendall, and M. Bhatia, *Deconstructing human embryonic stem cell cultures: niche regulation of self-renewal and pluripotency.* J Mol Med (Berl), 2008. **86**(8): p. 875-86.

2. Thomson, J.A., et al., *Embryonic stem cell lines derived from human blastocysts.* Science, 1998. **282**(5391): p. 1145-7.

3. Huang, J., et al., *Association of telomere length with authentic pluripotency of ES/iPS cells.* Cell Res, 2011. **21**(5): p. 779-92.

4. Fraga, A.M., et al., *A survey of parameters involved in the establishment of new lines of human embryonic stem cells.* Stem Cell Rev, 2011. **7**(4): p. 775-81.

5. Buecker, C. and N. Geijsen, *Different flavors of pluripotency, molecular mechanisms, and practical implications.* Cell Stem Cell, 2010. **7**(5): p. 559-64.

6. Amit, M., et al., *Clonally derived human embryonic stem cell lines maintain pluripotency and proliferative potential for prolonged periods of culture.* Dev Biol, 2000. **227**(2): p. 271-8.

7. Daheron, L., et al., *LIF/STAT3 signaling fails to maintain self-renewal of human embryonic stem cells.* Stem Cells, 2004. **22**(5): p. 770-8.

8. Watanabe, K., et al., *A ROCK inhibitor permits survival of dissociated human embryonic stem cells.* Nat Biotechnol, 2007. **25**(6): p. 681-6.

9. Bendall, S.C., et al., *IGF and FGF cooperatively establish the regulatory stem cell niche of pluripotent human cells in vitro.* Nature, 2007. **448**(7157): p. 1015-21.

10. Levenstein, M.E., et al., *Basic fibroblast growth factor support of human embryonic stem cell self-renewal.* Stem Cells, 2006. **24**(3): p. 568-74.

11. Ludwig, T.E., et al., *Derivation of human embryonic stem cells in defined conditions.* Nat Biotechnol, 2006. **24**(2): p. 185-7.

12. Hughes, C.S., L.M. Postovit, and G.A. Lajoie, *Matrigel: a complex protein mixture required for optimal growth of cell culture.* Proteomics. **10**(9): p. 1886-90.

13. Ludwig, T. and A.T. J, *Defined, feeder-independent medium for human embryonic stem cell culture.* Curr Protoc Stem Cell Biol, 2007. **Chapter 1**: p. Unit 1C 2.

14. Boyer, L.A., et al., *Core transcriptional regulatory circuitry in human embryonic stem cells.* Cell, 2005. **122**(6): p. 947-56.

15. Walker, E., et al., *Prediction and testing of novel transcriptional networks regulating embryonic stem cell self-renewal and commitment.* Cell Stem Cell, 2007. **1**(1): p. 71-86.

16. Stefanovic, S., et al., *Interplay of Oct4 with Sox2 and Sox17: a molecular switch from stem cell pluripotency to specifying a cardiac fate.* J Cell Biol, 2009. **186**(5): p. 665-73.

17. Wang, Z., et al., *Distinct lineage specification roles for NANOG, OCT4, and SOX2 in human embryonic stem cells.* Cell Stem Cell, 2012. **10**(4): p. 440-54.

18. Van Hoof, D., et al., *Phosphorylation dynamics during early differentiation of human embryonic stem cells.* Cell Stem Cell, 2009. **5**(2): p. 214-26.

19. Prowse, A.B., et al., *Identification of potential pluripotency determinants for human embryonic stem cells following proteomic analysis of human and mouse fibroblast conditioned media.* J Proteome Res, 2007. **6**(9): p. 3796-807.

20. van Amerongen, R. and R. Nusse, *Towards an integrated view of Wnt signaling in development.* Development, 2009. **136**(19): p. 3205-14.

21. Hughes, C., et al., *Mass spectrometry-based proteomic analysis of the matrix microenvironment in pluripotent stem cell culture.* Mol Cell Proteomics. **11**(12): p. 1924-36.

22. Neveu, P., et al., *MicroRNA profiling reveals two distinct p53-related human pluripotent stem cell states.* Cell Stem Cell, 2010. **7**(6): p. 671-81.

23. Lee, D.F., et al., *Regulation of embryonic and induced pluripotency by aurora kinase-p53 signaling.* Cell Stem Cell, 2012. **11**(2): p. 179-94.

24. Liu, N., et al., *Molecular mechanisms involved in self-renewal and pluripotency of embryonic stem cells.* J Cell Physiol, 2007. **211**(2): p. 279-86.

25. Fox, V., et al., *Cell-cell signaling through NOTCH regulates human embryonic stem cell proliferation.* Stem Cells, 2008. **26**(3): p. 715-23.

26. Lee, J.B., et al., *Notch-HES1 signaling axis controls hemato-endothelial fate decisions of human embryonic and induced pluripotent stem cells.* Blood. **122**(7): p. 1162-73.

27. Vallier, L., M. Alexander, and R.A. Pedersen, *Activin/Nodal and FGF pathways cooperate to maintain pluripotency of human embryonic stem cells.* J Cell Sci, 2005. **118**(Pt 19): p. 4495-509.

28. Vallier, L., et al., *Activin/Nodal signalling maintains pluripotency by controlling Nanog expression.* Development, 2009. **136**(8): p. 1339-49.

29. Topczewska, J.M., et al., *Embryonic and tumorigenic pathways converge via Nodal signaling: role in melanoma aggressiveness.* Nat Med, 2006. **12**(8): p. 925-32.

30. Bianco, C., et al., *Role of Cripto-1 in stem cell maintenance and malignant progression.* Am J Pathol. **177**(2): p. 532-40.

31. Harkness, L., et al., *Identification of a membrane proteomic signature for human embryonic stem cells independent of culture conditions.* Stem Cell Res, 2008. **1**(3): p. 219-27.

32. Katoh, M., *CER1 is a common target of WNT and NODAL signaling pathways in human embryonic stem cells.* Int J Mol Med, 2006. **17**(5): p. 795-9.

33. Wu, S.M., et al., *Role of Sonic hedgehog signaling and the expression of its components in human embryonic stem cells.* Stem Cell Res. **4**(1): p. 38-49.

34. James, D., et al., *TGFbeta/activin/nodal signaling is necessary for the maintenance of pluripotency in human embryonic stem cells.* Development, 2005. **132**(6): p. 1273-82.

35. Kattman, S.J., et al., *Stage-specific optimization of activin/nodal and BMP signaling promotes cardiac differentiation of mouse and human pluripotent stem cell lines.* Cell Stem Cell, 2011. **8**(2): p. 228-40.

36. Singh, A.M., et al., *Signaling network crosstalk in human pluripotent cells: a Smad2/3-regulated switch that controls the balance between self-renewal and differentiation.* Cell Stem Cell, 2012. **10**(3): p. 312-26.

37. Kelly, K.F., et al., *beta-catenin enhances Oct-4 activity and reinforces pluripotency through a TCF-independent mechanism.* Cell Stem Cell, 2011. **8**(2): p. 214-27.

38. Takahashi, K. and S. Yamanaka, *Induction of pluripotent stem cells from mouse embryonic and adult fibroblast cultures by defined factors.* Cell, 2006. **126**(4): p. 663-76.

39. Takahashi, K., et al., *Induction of pluripotent stem cells from adult human fibroblasts by defined factors.* Cell, 2007. **131**(5): p. 861-72.

40. Yu, J., et al., *Induced pluripotent stem cell lines derived from human somatic cells.* Science, 2007. **318**(5858): p. 1917-20.

41. Maherali, N. and K. Hochedlinger, *Guidelines and techniques for the generation of induced pluripotent stem cells.* Cell Stem Cell, 2008. **3**(6): p. 595-605.

42. Ellis, J., et al., *Benefits of utilizing gene-modified iPSCs for clinical applications.* Cell Stem Cell, 2010. **7**(4): p. 429-30.

43. Adewumi, O., et al., *Characterization of human embryonic stem cell lines by the International Stem Cell Initiative.* Nat Biotechnol, 2007. **25**(7): p. 803-16.

44. Chaerkady, R., et al., *Comparative proteomics of human embryonic stem cells and embryonal carcinoma cells.* Proteomics, 2010. **10**(7): p. 1359-73.

45. Bock, C., et al., *Reference Maps of human ES and iPS cell variation enable high-throughput characterization of pluripotent cell lines.* Cell, 2011. **144**(3): p. 439-52.

46. Boulting, G.L., et al., *A functionally characterized test set of human induced pluripotent stem cells.* Nat Biotechnol, 2011. **29**(3): p. 279-86.

47. Munoz, J., et al., *The quantitative proteomes of human-induced pluripotent stem cells and embryonic stem cells.* Mol Syst Biol, 2011. **7**: p. 550.

48. Zhang, P., et al., *Short-term BMP-4 treatment initiates mesoderm induction in human embryonic stem cells.* Blood, 2008. **111**(4): p. 1933-41.

49. Goldman, O., et al., *A boost of BMP4 accelerates the commitment of human embryonic stem cells to the endothelial lineage.* Stem Cells, 2009. **27**(8): p. 1750-9.

50. Xu, R.H., et al., *BMP4 initiates human embryonic stem cell differentiation to trophoblast.* Nat Biotechnol, 2002. **20**(12): p. 1261-4.

51. Bernardo, A.S., et al., *BRACHYURY and CDX2 mediate BMP-induced differentiation of human and mouse pluripotent stem cells into embryonic and extraembryonic lineages.* Cell Stem Cell, 2011. **9**(2): p. 144-55.

52. Peerani, R., et al., *Niche-mediated control of human embryonic stem cell self-renewal and differentiation.* Embo Journal, 2007. **26**(22): p. 4744-4755.

53. Seguin, C.A., et al., *Establishment of endoderm progenitors by SOX transcription factor expression in human embryonic stem cells.* Cell Stem Cell, 2008. **3**(2): p. 182-95.

54. Perkins, D.N., et al., *Probability-based protein identification by searching sequence databases using mass spectrometry data.* Electrophoresis, 1999. **20**(18): p. 3551-3567.

55. Geer, L.Y., et al., *Open mass spectrometry search algorithm.* J Proteome Res, 2004. **3**(5): p. 958-64.

56. Zhang, J., et al., *PEAKS DB: de novo sequencing assisted database search for sensitive and accurate peptide identification.* Mol Cell Proteomics. **11**(4): p. M111 010587.

57. Deutsch, E.W., et al., *A guided tour of the Trans-Proteomic Pipeline.* Proteomics, 2010. **10**(6): p. 1150-9.

58. Martens, L., et al., *mzML--a community standard for mass spectrometry data.* Mol Cell Proteomics, 2010. **10**(1): p. R110 000133.

59. Hager, J.W. and J.C.Y. Le Blanc, *Product ion scanning using a Q-q-Q(linear ion trap) (Q TRAP (TM)) mass spectrometer.* Rapid Communications in Mass Spectrometry, 2003. **17**(10): p. 1056-1064.

60. Lange, V., et al., *Selected reaction monitoring for quantitative proteomics: a tutorial.* Mol Syst Biol, 2008. **4**: p. 222.

61. Picotti, P. and R. Aebersold, *Selected reaction monitoring-based proteomics: workflows, potential, pitfalls and future directions.* Nat Methods, 2012. **9**(6): p. 555-66.

62. Kiyonami, R., et al., *Increased selectivity, analytical precision, and throughput in targeted proteomics.* Mol Cell Proteomics. **10**(2): p. M110 002931.

63. de Graaf, E.L., et al., *Improving SRM assay development: a global comparison between triple quadrupole, ion trap, and higher energy CID peptide fragmentation spectra.* J Proteome Res, 2011. **10**(9): p. 4334-41.

64. Gstaiger, M. and R. Aebersold, *Applying mass spectrometry-based proteomics to genetics, genomics and network biology.* Nature Reviews Genetics, 2009. **10**(9): p. 617-627.

65. Gallien, S., et al., *Highly multiplexed targeted proteomics using precise control of peptide retention time.* Proteomics, 2012. **12**(8): p. 1122-33.

66. Picotti, P., et al., *High-throughput generation of selected reaction-monitoring assays for proteins and proteomes.* Nat Methods, 2009. **7**(1): p. 43-6.

67. Craig, R., J.P. Cortens, and R.C. Beavis, *Open source system for analyzing, validating, and storing protein identification data.* J Proteome Res, 2004. **3**(6): p. 1234-42.

68. Deutsch, E.W., H. Lam, and R. Aebersold, *PeptideAtlas: a resource for target selection for emerging targeted proteomics workflows.* EMBO Rep, 2008. **9**(5): p. 429-34.

69. Stergachis, A.B., et al., *Rapid empirical discovery of optimal peptides for targeted proteomics.* Nat Methods, 2011. **8**(12): p. 1041-3.

70. Cham Mead, J.A., L. Bianco, and C. Bessant, *Free computational resources for designing selected reaction monitoring transitions.* Proteomics, 2010. **10**(6): p. 1106-26.

71. MacLean, B., et al., *Skyline: an open source document editor for creating and analyzing targeted proteomics experiments.* Bioinformatics. **26**(7): p. 966-8.

72. Maclean, B., et al., *Effect of collision energy optimization on the measurement of peptides by selected reaction monitoring (SRM) mass spectrometry.* Anal Chem, 2010. **82**(24): p. 10116-24.

73. Anderson, L. and C.L. Hunter, *Quantitative mass spectrometric multiple reaction monitoring assays for major plasma proteins.* Mol Cell Proteomics, 2006. **5**(4): p. 573-88.

74. Picotti, P., et al., *Full dynamic range proteome analysis of S. cerevisiae by targeted proteomics.* Cell, 2009. **138**(4): p. 795-806.

75. Murphy, J.P. and D.M. Pinto, *Targeted proteomic analysis of glycolysis in cancer cells.* J Proteome Res, 2010. **10**(2): p. 604-13.

76. Lopez, M.F., et al., *Mass spectrometric discovery and selective reaction monitoring (SRM) of putative protein biomarker candidates in first trimester Trisomy 21 maternal serum.* J Proteome Res, 2010. **10**(1): p. 133-42.

77. Lange, V., et al., *Targeted quantitative analysis of Streptococcus pyogenes virulence factors by multiple reaction monitoring.* Mol Cell Proteomics, 2008. **7**(8): p. 1489-500.

78. Chen, Y., et al., *Quantification of beta-catenin signaling components in colon cancer cell lines, tissue sections, and microdissected tumor cells using reaction monitoring mass spectrometry.* J Proteome Res, 2010. **9**(8): p. 4215-27.

79. Ludwig, C., et al., *Estimation of absolute protein quantities of unlabeled samples by selected reaction monitoring mass spectrometry.* Mol Cell Proteomics, 2011. **11**(3): p. M111 013987.

80. Bisson, N., et al., *Selected reaction monitoring mass spectrometry reveals the dynamics of signaling through the GRB2 adaptor.* Nat Biotechnol, 2011. **29**(7): p. 653-8.

81. Wolf-Yadlin, A., et al., *Multiple reaction monitoring for robust quantitative proteomic analysis of cellular signaling networks.* Proc Natl Acad Sci U S A, 2007. **104**(14): p. 5860-5.

82. Zubarev, R.A. and A. Makarov, *Orbitrap mass spectrometry.* Anal Chem, 2013. **85**(11): p. 5288-96.

83. Gallien, S., et al., *Targeted proteomic quantification on quadrupole-orbitrap mass spectrometer.* Mol Cell Proteomics, 2012. **11**(12): p. 1709-23.

84. Peterson, A.C., et al., *Parallel reaction monitoring for high resolution and high mass accuracy quantitative, targeted proteomics.* Mol Cell Proteomics, 2012. **11**(11): p. 1475-88.

85. Gallien, S., et al., *Selectivity of LC-MS/MS analysis: implication for proteomics experiments.* J Proteomics, 2012. **81**: p. 148-58.

86. *Labeling Methods in Mass Spectrometry Based Quantitative Proteomics.*

87. Ong, S.E. and M. Mann, *Stable isotope labeling by amino acids in cell culture for quantitative proteomics.* Methods Mol Biol, 2007. **359**: p. 37-52.

88. Ong, S.E., et al., *Stable isotope labeling by amino acids in cell culture, SILAC, as a simple and accurate approach to expression proteomics.* Molecular & Cellular Proteomics, 2002. **1**(5): p. 376-386.

89. Wiese, S., et al., *Protein labeling by iTRAQ: a new tool for quantitative mass spectrometry in proteome research.* Proteomics, 2007. **7**(3): p. 340-50.

90. Kirkpatrick, D.S., S.A. Gerber, and S.P. Gygi, *The absolute quantification strategy: a general procedure for the quantification of proteins and post-translational modifications.* Methods, 2005. **35**(3): p. 265-73.

91. Boersema, P.J., et al., *Multiplex peptide stable isotope dimethyl labeling for quantitative proteomics.* Nat Protoc, 2009. **4**(4): p. 484-94.

92. Boersema, P.J., et al., *Triplex protein quantification based on stable isotope labeling by peptide dimethylation applied to cell and tissue lysates.* Proteomics, 2008. **8**(22): p. 4624-32.

93. Gabut, M., et al., *An alternative splicing switch regulates embryonic stem cell pluripotency and reprogramming.* Cell, 2011. **147**(1): p. 132-46.

94. Fang, Y., D.P. Robinson, and L.J. Foster, *Quantitative analysis of proteome coverage and recovery rates for upstream fractionation methods in proteomics.* J Proteome Res, 2010. **9**(4): p. 1902-12.

95. Wolters, D.A., M.P. Washburn, and J.R. Yates, 3rd, *An automated multidimensional protein identification technology for shotgun proteomics.* Anal Chem, 2001. **73**(23): p. 5683-90.

96. Lee, Y.H., H.T. Tan, and M.C. Chung, *Subcellular fractionation methods and strategies for proteomics.* Proteomics, 2010. **10**(22): p. 3935-56.

97. Wang, H., et al., *Comparison of extensive protein fractionation and repetitive LC-MS/MS analyses on depth of analysis for complex proteomes.* J Proteome Res, 2009. **9**(2): p. 1032-40.

98. Kocher, T., et al., *Analysis of protein mixtures from whole-cell extracts by single-run nanoLC-MS/MS using ultralong gradients.* Nat Protoc, 2012. **7**(5): p. 882-90.

99. Hsieh, E.J., et al., *Effects of column and gradient lengths on peak capacity and peptide identification in nanoflow LC-MS/MS of complex proteomic samples.* J Am Soc Mass Spectrom, 2012. **24**(1): p. 148-53.

100. Bendall, S.C., et al., *An enhanced mass spectrometry approach reveals human embryonic stem cell growth factors in culture.* Mol Cell Proteomics, 2009. **8**(3): p. 421-32.

101. Brill, L.M., et al., *Phosphoproteomic analysis of human embryonic stem cells.* Cell Stem Cell, 2009. **5**(2): p. 204-13.

102. Rigbolt, K.T., et al., *System-wide temporal characterization of the proteome and phosphoproteome of human embryonic stem cell differentiation.* Sci Signal, 2011. **4**(164): p. rs3.

103. Yocum, A.K., et al., *Coupled global and targeted proteomics of human embryonic stem cells during induced differentiation.* Mol Cell Proteomics, 2008. **7**(4): p. 750-67.

104. Bradford, M.M., *A rapid and sensitive method for the quantitation of microgram quantities of protein utilizing the principle of protein-dye binding.* Anal Biochem, 1976. **72**: p. 248-54.

105. Bendall, S.C., A.T. Booy, and G. Lajoie, *Proteomic analysis of pluripotent stem cells.* Curr Protoc Stem Cell Biol, 2007. **Chapter 1**: p. Unit 1B 1.

106. Livak, K.J. and T.D. Schmittgen, *Analysis of relative gene expression data using real-time quantitative PCR and the 2(T)(-Delta Delta C) method.* Methods, 2001. **25**(4): p. 402-408.

107. Melanson, J.E., K.A. Chisholm, and D.M. Pinto, *Targeted comparative proteomics by liquid chromatography/matrix-assisted laser desorption/ionization triple-quadrupole mass spectrometry.* Rapid Communications in Mass Spectrometry, 2006. **20**(5): p. 904-910.

108. Das, P., et al., *Effects of fgf2 and oxygen in the bmp4-driven differentiation of trophoblast from human embryonic stem cells.* Stem Cell Res, 2007. **1**(1): p. 61-74.

109. Yu, P., et al., *FGF2 sustains NANOG and switches the outcome of BMP4-induced human embryonic stem cell differentiation.* Cell Stem Cell. **8**(3): p. 326-34.

110. Fong, C.Y., et al., *Nine-day-old human embryo cultured in vitro: a clue to the origins of embryonic stem cells.* Reprod Biomed Online, 2004. **9**(3): p. 321-5.

111. Madden, T.L., R.L. Tatusov, and J.H. Zhang, *Applications of network BLAST server.* Computer Methods for Macromolecular Sequence Analysis, 1996. **266**: p. 131-141.

112. Gasteiger E., H.C., Gattiker A., Duvaud S., Wilkins M.R., Appel R.D., Bairoch A., *Protein Identification and Analysis Tools on the ExPASy Server*, in *The Proteomics Protocols Handbook,* J.M. Walker, Editor. 2005, Humana Press.

113. Wang, P., et al., *Targeting SOX17 in human embryonic stem cells creates unique strategies for isolating and analyzing developing endoderm.* Cell Stem Cell, 2011. **8**(3): p. 335-46.

114. Draper, J.S., et al., *Surface antigens of human embryonic stem cells: changes upon differentiation in culture.* J Anat, 2002. **200**(Pt 3): p. 249-58.

115. Brimble, S.N., et al., *The cell surface glycosphingolipids SSEA-3 and SSEA-4 are not essential for human ESC pluripotency.* Stem Cells, 2007. **25**(1): p. 54-62.

116. Glukhova, V.A., et al., *Rapid assessment of RNAi-mediated protein depletion by selected reaction monitoring mass spectrometry.* J Proteome Res, 2013. **12**(7): p. 3246-54.

117. Walsh, G.M., et al., *Implementation of a data repository-driven approach for targeted proteomics experiments by multiple reaction monitoring.* J Proteomics, 2009. **72**(5): p. 838-52.

118. Aye, T.T., et al., *Use of Stable Isotope Dimethyl Labeling Coupled to Selected Reaction Monitoring to Enhance Throughput by Multiplexing Relative Quantitation of Targeted Proteins.* Analytical Chemistry, 2012. **84**(11): p. 4999-5006.

119. Sumi, T., et al., *Defining early lineage specification of human embryonic stem cells by the orchestrated balance of canonical Wnt/beta-catenin, Activin/Nodal and BMP signaling.* Development, 2008. **135**(17): p. 2969-79.

120. Davidson, K.C., et al., *Wnt/beta-catenin signaling promotes differentiation, not self-renewal, of human embryonic stem cells and is repressed by Oct4.* Proc Natl Acad Sci U S A. **109**(12): p. 4485-90.

121. Sumi, T., et al., *Defining early lineage specification of human embryonic stem cells by the orchestrated balance of canonical Wnt/beta-catenin, Activin/Nodal and BMP signaling.* Development, 2008. **135**(17): p. 2969-2979.

122. Paige, S.L., et al., *Endogenous Wnt/beta-Catenin Signaling Is Required for Cardiac Differentiation in Human Embryonic Stem Cells.* PLoS One, 2010. **5**(6).

123. Lee, E., et al., *The roles of APC and Axin derived from experimental and theoretical analysis of the Wnt pathway.* PLoS Biol, 2003. **1**(1): p. E10.

124. Maiolica, A., et al., *Targeted proteome investigation via selected reaction monitoring mass spectrometry.* J Proteomics, 2012. **75**(12): p. 3495-513.

125. Cappadona, S., et al., *Deconvolution of overlapping isotopic clusters improves quantification of stable isotope-labeled peptides.* J Proteomics. **74**(10): p. 2204-9.

126. Rangiah, K., et al., *Differential secreted proteome approach in murine model for candidate biomarker discovery in colon cancer.* J Proteome Res, 2009. **8**(11): p. 5153-64.

127. Takada, R., et al., *Monounsaturated fatty acid modification of Wnt protein: Its role in Wnt secretion.* Developmental Cell, 2006. **11**(6): p. 791-801.

128. Willert, K., et al., *Wnt proteins are lipid-modified and can act as stem cell growth factors.* Nature, 2003. **423**(6938): p. 448-452.

129. Pesavento, J.J., et al., *Mild performic acid oxidation enhances chromatographic and top down mass spectrometric analyses of histones.* Mol Cell Proteomics, 2007. **6**(9): p. 1510-26.

130. Dai, J.Q., et al., *Identification of degradation products formed during performic oxidation of peptides and proteins by high-performance liquid chromatography with matrix-assisted laser desorption/ionization and tandem mass spectrometry.* Rapid Communications in Mass Spectrometry, 2005. **19**(9): p. 1130-1138.

131. Le Good, J.A., et al., *Nodal stability determines signaling range.* Curr Biol, 2005. **15**(1): p. 31-6.

132. Dormeyer, W., et al., *A practical guide for the identification of membrane and plasma membrane proteins in human embryonic stem cells and human embryonal carcinoma cells.* Proteomics, 2008. **8**(19): p. 4036-53.

133. Dormeyer, W., et al., *Plasma membrane proteomics of human embryonic stem cells and human embryonal carcinoma cells.* J Proteome Res, 2008. **7**(7): p. 2936-51.

134. Michalski, A., J. Cox, and M. Mann, *More than 100,000 detectable peptide species elute in single shotgun proteomics runs but the majority is inaccessible to data-dependent LC-MS/MS.* J Proteome Res, 2011. **10**(4): p. 1785-93.

135. Malmstrom, L., et al., *Automated workflow for large-scale selected reaction monitoring experiments.* J Proteome Res, 2012. **11**(3): p. 1644-53.

136. Wisniewski, J.R., et al., *Universal sample preparation method for proteome analysis.* Nat Methods, 2009. **6**(5): p. 359-62.

137. Kollipara, L. and R.P. Zahedi, *Protein carbamylation: in vivo modification or in vitro artefact?* Proteomics, 2013. **13**(6): p. 941-4.

138. Hussein, S.M., et al., *Copy number variation and selection during reprogramming to pluripotency.* Nature, 2011. **471**(7336): p. 58-62.

Appendices

Appendix A: List of SRM transitions.

Precursor m/z	Fragment m/z	RT (min)	Target Protein, Peptide, Fragment Ion, Label	DP (V)	CE (V)
582.795	476.246	29.1	ACTB.GYSFTTTAER.+2y4. (Heavy)	72.4	28
580.783	476.246	29.1	ACTB.GYSFTTTAER.+2y4. (Light)	72.4	28
582.795	577.294	29.1	ACTB.GYSFTTTAER.+2y5. (Heavy)	72.4	28
580.783	577.294	29.1	ACTB.GYSFTTTAER.+2y5. (Light)	72.4	28
582.795	678.342	29.1	ACTB.GYSFTTTAER.+2y6. (Heavy)	72.4	28
580.783	678.342	29.1	ACTB.GYSFTTTAER.+2y6. (Light)	72.4	28
582.795	825.41	29.1	ACTB.GYSFTTTAER.+2y7. (Heavy)	72.4	28
580.783	825.41	29.1	ACTB.GYSFTTTAER.+2y7. (Light)	72.4	28
582.795	912.442	29.1	ACTB.GYSFTTTAER.+2y8. (Heavy)	72.4	28
580.783	912.442	29.1	ACTB.GYSFTTTAER.+2y8. (Light)	72.4	28
911.978	1298.67	47.1	ACTB.SYELPDGQVITIGNER.+2y12. (Heavy)	96.4	46.8
909.965	1298.67	47.1	ACTB.SYELPDGQVITIGNER.+2y12. (Light)	96.4	46.8
911.978	649.839	47.1	ACTB.SYELPDGQVITIGNER.+2y12+2. (Heavy)	96.4	46.8
909.965	649.839	47.1	ACTB.SYELPDGQVITIGNER.+2y12+2. (Light)	96.4	46.8
911.978	706.381	47.1	ACTB.SYELPDGQVITIGNER.+2y13+2. (Heavy)	96.4	46.8
909.965	706.381	47.1	ACTB.SYELPDGQVITIGNER.+2y13+2. (Light)	96.4	46.8
911.978	475.226	47.1	ACTB.SYELPDGQVITIGNER.+2y4. (Heavy)	96.4	46.8
909.965	475.226	47.1	ACTB.SYELPDGQVITIGNER.+2y4. (Light)	96.4	46.8
911.978	689.358	47.1	ACTB.SYELPDGQVITIGNER.+2y6. (Heavy)	96.4	46.8
909.965	689.358	47.1	ACTB.SYELPDGQVITIGNER.+2y6. (Light)	96.4	46.8
1009.592	1323.818	38.1	ACTB.VAPEEHPVLLTEAPLNPK.+2y12. (Heavy)	102.4	51.5
1005.567	1319.793	38.1	ACTB.VAPEEHPVLLTEAPLNPK.+2y12. (Light)	102.4	51.5
1009.592	908.511	38.1	ACTB.VAPEEHPVLLTEAPLNPK.+2y16+2. (Heavy)	102.4	51.5
1005.567	906.499	38.1	ACTB.VAPEEHPVLLTEAPLNPK.+2y16+2. (Light)	102.4	51.5
1009.592	600.402	38.1	ACTB.VAPEEHPVLLTEAPLNPK.+2y5. (Heavy)	102.4	51.5
1005.567	596.377	38.1	ACTB.VAPEEHPVLLTEAPLNPK.+2y5. (Light)	102.4	51.5
1009.592	671.439	38.1	ACTB.VAPEEHPVLLTEAPLNPK.+2y6. (Heavy)	102.4	51.5
1005.567	667.414	38.1	ACTB.VAPEEHPVLLTEAPLNPK.+2y6. (Light)	102.4	51.5
1009.592	901.529	38.1	ACTB.VAPEEHPVLLTEAPLNPK.+2y8. (Heavy)	102.4	51.5
1005.567	897.504	38.1	ACTB.VAPEEHPVLLTEAPLNPK.+2y8. (Light)	102.4	51.5
669.362	914.459	53.2	AKT1.FYGAEIVSALDYLHSEK.+3b16+2. (Heavy)	78.4	26.2
666.679	912.446	53.2	AKT1.FYGAEIVSALDYLHSEK.+3b16+2. (Light)	78.4	26.2
669.362	1194.63	53.2	AKT1.FYGAEIVSALDYLHSEK.+3y10. (Heavy)	78.4	31.2
666.679	1190.605	53.2	AKT1.FYGAEIVSALDYLHSEK.+3y10. (Light)	78.4	31.2
669.362	1293.699	53.2	AKT1.FYGAEIVSALDYLHSEK.+3y11. (Heavy)	78.4	31.2
666.679	1289.674	53.2	AKT1.FYGAEIVSALDYLHSEK.+3y11. (Light)	78.4	31.2

669.362	832.446	53.2	AKT1.FYGAEIVSALDYLHSEK.+3y15+2. (Heavy)	78.4	25.2
666.679	830.433	53.2	AKT1.FYGAEIVSALDYLHSEK.+3y15+2. (Light)	78.4	25.2
669.362	913.977	53.2	AKT1.FYGAEIVSALDYLHSEK.+3y16+2. (Heavy)	78.4	26.2
666.679	911.965	53.2	AKT1.FYGAEIVSALDYLHSEK.+3y16+2. (Light)	78.4	26.2
1239.575	1209.538	50.3	AKT1.TFCGTPEYLAPEVLEDNDYGR.+2y10. (Heavy)	120.3	60.5
1237.563	1209.538	50.3	AKT1.TFCGTPEYLAPEVLEDNDYGR.+2y10. (Light)	120.3	60.5
1239.575	1306.591	50.3	AKT1.TFCGTPEYLAPEVLEDNDYGR.+2y11. (Heavy)	120.3	60.5
1237.563	1306.591	50.3	AKT1.TFCGTPEYLAPEVLEDNDYGR.+2y11. (Light)	120.3	60.5
1239.575	1377.628	50.3	AKT1.TFCGTPEYLAPEVLEDNDYGR.+2y12. (Heavy)	120.3	60.5
1237.563	1377.628	50.3	AKT1.TFCGTPEYLAPEVLEDNDYGR.+2y12. (Light)	120.3	60.5
1239.575	1490.712	50.3	AKT1.TFCGTPEYLAPEVLEDNDYGR.+2y13. (Heavy)	120.3	60.5
1237.563	1490.712	50.3	AKT1.TFCGTPEYLAPEVLEDNDYGR.+2y13. (Light)	120.3	60.5
1239.575	1080.496	50.3	AKT1.TFCGTPEYLAPEVLEDNDYGR.+2y9. (Heavy)	120.3	60.5
1237.563	1080.496	50.3	AKT1.TFCGTPEYLAPEVLEDNDYGR.+2y9. (Light)	120.3	60.5
426.221	646.35	27.6	AKT1.TFHVETPEER.+3b5. (Heavy)	61.4	21
424.879	642.325	27.6	AKT1.TFHVETPEER.+3b5. (Light)	61.4	21
426.221	747.397	27.6	AKT1.TFHVETPEER.+3b6. (Heavy)	61.4	18
424.879	743.372	27.6	AKT1.TFHVETPEER.+3b6. (Light)	61.4	18
426.221	433.204	27.6	AKT1.TFHVETPEER.+3y3. (Heavy)	61.4	24
424.879	433.204	27.6	AKT1.TFHVETPEER.+3y3. (Light)	61.4	24
426.221	530.257	27.6	AKT1.TFHVETPEER.+3y4. (Heavy)	61.4	21
424.879	530.257	27.6	AKT1.TFHVETPEER.+3y4. (Light)	61.4	21
426.221	631.305	27.6	AKT1.TFHVETPEER.+3y5. (Heavy)	61.4	20
424.879	631.305	27.6	AKT1.TFHVETPEER.+3y5. (Light)	61.4	20
1030.466	1196.507	46.8	APC.NDSLSSLDFDDDDVDLSR.+2y10. (Heavy)	105.1	48.6
1028.453	1196.507	46.8	APC.NDSLSSLDFDDDDVDLSR.+2y10. (Light)	105.1	48.6
1030.466	1311.534	46.8	APC.NDSLSSLDFDDDDVDLSR.+2y11. (Heavy)	105.1	48.6
1028.453	1311.534	46.8	APC.NDSLSSLDFDDDDVDLSR.+2y11. (Light)	105.1	48.6
1030.466	1424.618	46.8	APC.NDSLSSLDFDDDDVDLSR.+2y12. (Heavy)	105.1	48.6
1028.453	1424.618	46.8	APC.NDSLSSLDFDDDDVDLSR.+2y12. (Light)	105.1	48.6
1030.466	934.411	46.8	APC.NDSLSSLDFDDDDVDLSR.+2y8. (Heavy)	105.1	48.6
1028.453	934.411	46.8	APC.NDSLSSLDFDDDDVDLSR.+2y8. (Light)	105.1	48.6
1030.466	1049.438	46.8	APC.NDSLSSLDFDDDDVDLSR.+2y9. (Heavy)	105.1	48.6
1028.453	1049.438	46.8	APC.NDSLSSLDFDDDDVDLSR.+2y9. (Light)	105.1	48.6
496.597	578.291	31.5	APC.NVSSLIATNEDHR.+3y10+2. (Heavy)	66.5	19.1
495.255	578.291	31.5	APC.NVSSLIATNEDHR.+3y10+2. (Light)	66.5	19.1
496.597	621.807	31.5	APC.NVSSLIATNEDHR.+3y11+2. (Heavy)	66.5	18.1
495.255	621.807	31.5	APC.NVSSLIATNEDHR.+3y11+2. (Light)	66.5	18.1
496.597	771.338	31.5	APC.NVSSLIATNEDHR.+3y6. (Heavy)	66.5	25.1
495.255	771.338	31.5	APC.NVSSLIATNEDHR.+3y6. (Light)	66.5	25.1
496.597	842.375	31.5	APC.NVSSLIATNEDHR.+3y7. (Heavy)	66.5	26.1

495.255	842.375	31.5	APC.NVSSLIATNEDHR.+3y7. (Light)	66.5	26.1
496.597	955.459	31.5	APC.NVSSLIATNEDHR.+3y8. (Heavy)	66.5	25.1
495.255	955.459	31.5	APC.NVSSLIATNEDHR.+3y8. (Light)	66.5	25.1
612.984	1206.623	28.7	APC.SAEDPVSEVPAVSQHPR.+3y11. (Heavy)	75	30.8
611.643	1206.623	28.7	APC.SAEDPVSEVPAVSQHPR.+3y11. (Light)	75	30.8
612.984	701.875	28.7	APC.SAEDPVSEVPAVSQHPR.+3y13+2. (Heavy)	75	24.8
611.643	701.875	28.7	APC.SAEDPVSEVPAVSQHPR.+3y13+2. (Light)	75	24.8
612.984	759.389	28.7	APC.SAEDPVSEVPAVSQHPR.+3y14+2. (Heavy)	75	23.8
611.643	759.389	28.7	APC.SAEDPVSEVPAVSQHPR.+3y14+2. (Light)	75	23.8
612.984	823.91	28.7	APC.SAEDPVSEVPAVSQHPR.+3y15+2. (Heavy)	75	23.8
611.643	823.91	28.7	APC.SAEDPVSEVPAVSQHPR.+3y15+2. (Light)	75	23.8
612.984	891.48	28.7	APC.SAEDPVSEVPAVSQHPR.+3y8. (Heavy)	75	30.8
611.643	891.48	28.7	APC.SAEDPVSEVPAVSQHPR.+3y8. (Light)	75	30.8
683.997	783.381	33.1	AXN1.DAHEENPESILDEHVQR.+3y13+2. (Heavy)	80.2	33
682.656	783.381	33.1	AXN1.DAHEENPESILDEHVQR.+3y13+2. (Light)	80.2	33
683.997	783.374	33.1	AXN1.DAHEENPESILDEHVQR.+3y6. (Heavy)	80.2	32
682.656	783.374	33.1	AXN1.DAHEENPESILDEHVQR.+3y6. (Light)	80.2	32
683.997	896.458	33.1	AXN1.DAHEENPESILDEHVQR.+3y7. (Heavy)	80.2	33
682.656	896.458	33.1	AXN1.DAHEENPESILDEHVQR.+3y7. (Light)	80.2	33
683.997	1009.543	33.1	AXN1.DAHEENPESILDEHVQR.+3y8. (Heavy)	80.2	33
682.656	1009.543	33.1	AXN1.DAHEENPESILDEHVQR.+3y8. (Light)	80.2	33
683.997	1096.575	33.1	AXN1.DAHEENPESILDEHVQR.+3y9. (Heavy)	80.2	33
682.656	1096.575	33.1	AXN1.DAHEENPESILDEHVQR.+3y9. (Light)	80.2	33
596.313	624.354	33.6	AXN1.SDIYLEYTR.+2b5. (Heavy)	73.4	23.8
594.301	620.329	33.6	AXN1.SDIYLEYTR.+2b5. (Light)	73.4	23.8
596.313	568.273	33.6	AXN1.SDIYLEYTR.+2y4. (Heavy)	73.4	23.8
594.301	568.273	33.6	AXN1.SDIYLEYTR.+2y4. (Light)	73.4	23.8
596.313	681.357	33.6	AXN1.SDIYLEYTR.+2y5. (Heavy)	73.4	29.8
594.301	681.357	33.6	AXN1.SDIYLEYTR.+2y5. (Light)	73.4	29.8
596.313	844.42	33.6	AXN1.SDIYLEYTR.+2y6. (Heavy)	73.4	24.8
594.301	844.42	33.6	AXN1.SDIYLEYTR.+2y6. (Light)	73.4	24.8
596.313	957.504	33.6	AXN1.SDIYLEYTR.+2y7. (Heavy)	73.4	24.8
594.301	957.504	33.6	AXN1.SDIYLEYTR.+2y7. (Light)	73.4	24.8
829.368	1164.55	29.4	CDN1A.DCDALMAGCIQEAR.+2y10. (Heavy)	90.4	39.6
827.355	1164.55	29.4	CDN1A.DCDALMAGCIQEAR.+2y10. (Light)	90.4	39.6
829.368	1235.587	29.4	CDN1A.DCDALMAGCIQEAR.+2y11. (Heavy)	90.4	41.6
827.355	1235.587	29.4	CDN1A.DCDALMAGCIQEAR.+2y11. (Light)	90.4	41.6
829.368	833.393	29.4	CDN1A.DCDALMAGCIQEAR.+2y7. (Heavy)	90.4	36.6
827.355	833.393	29.4	CDN1A.DCDALMAGCIQEAR.+2y7. (Light)	90.4	36.6
829.368	904.431	29.4	CDN1A.DCDALMAGCIQEAR.+2y8. (Heavy)	90.4	36.6
827.355	904.431	29.4	CDN1A.DCDALMAGCIQEAR.+2y8. (Light)	90.4	36.6

829.368	1051.466	29.4	CDN1A.DCDALMAGCIQEAR.+2y9. (Heavy)	90.4	36.6
827.355	1051.466	29.4	CDN1A.DCDALMAGCIQEAR.+2y9. (Light)	90.4	36.6
1196.065	1219.574	67.9	CDN1A.WNFDFVTETPLEGDFAWER.+2y10. (Heavy)	117.1	58
1194.053	1219.574	67.9	CDN1A.WNFDFVTETPLEGDFAWER.+2y10. (Light)	117.1	58
1196.065	1320.622	67.9	CDN1A.WNFDFVTETPLEGDFAWER.+2y11. (Heavy)	117.1	59
1194.053	1320.622	67.9	CDN1A.WNFDFVTETPLEGDFAWER.+2y11. (Light)	117.1	59
1196.065	1449.664	67.9	CDN1A.WNFDFVTETPLEGDFAWER.+2y12. (Heavy)	117.1	58
1194.053	1449.664	67.9	CDN1A.WNFDFVTETPLEGDFAWER.+2y12. (Light)	117.1	58
1196.065	1009.437	67.9	CDN1A.WNFDFVTETPLEGDFAWER.+2y8. (Heavy)	117.1	60
1194.053	1009.437	67.9	CDN1A.WNFDFVTETPLEGDFAWER.+2y8. (Light)	117.1	60
1196.065	1122.521	67.9	CDN1A.WNFDFVTETPLEGDFAWER.+2y9. (Heavy)	117.1	58
1194.053	1122.521	67.9	CDN1A.WNFDFVTETPLEGDFAWER.+2y9. (Light)	117.1	58
644.428	1057.692	30	CER1.TPASQGVILPIK.+2y10. (Heavy)	75.8	32.6
640.403	1053.667	30	CER1.TPASQGVILPIK.+2y10. (Light)	75.8	32.6
644.428	714.543	30	CER1.TPASQGVILPIK.+2y6. (Heavy)	75.8	32.6
640.403	710.517	30	CER1.TPASQGVILPIK.+2y6. (Light)	75.8	32.6
644.428	771.564	30	CER1.TPASQGVILPIK.+2y7. (Heavy)	75.8	32.6
640.403	767.539	30	CER1.TPASQGVILPIK.+2y7. (Light)	75.8	32.6
644.428	899.623	30	CER1.TPASQGVILPIK.+2y8. (Heavy)	75.8	29.6
640.403	895.598	30	CER1.TPASQGVILPIK.+2y8. (Light)	75.8	29.6
644.428	986.655	30	CER1.TPASQGVILPIK.+2y9. (Heavy)	75.8	32.6
640.403	982.63	30	CER1.TPASQGVILPIK.+2y9. (Light)	75.8	32.6
599.981	661.321	31	CER1.TVPFSQTITHEGCEK.+3y11+2. (Heavy)	73.3	30
597.298	659.309	31	CER1.TVPFSQTITHEGCEK.+3y11+2. (Light)	73.3	30
599.981	734.856	31	CER1.TVPFSQTITHEGCEK.+3y12+2. (Heavy)	73.3	25
597.298	732.843	31	CER1.TVPFSQTITHEGCEK.+3y12+2. (Light)	73.3	25
599.981	783.382	31	CER1.TVPFSQTITHEGCEK.+3y13+2. (Heavy)	73.3	22
597.298	781.369	31	CER1.TVPFSQTITHEGCEK.+3y13+2. (Light)	73.3	22
599.981	892.413	31	CER1.TVPFSQTITHEGCEK.+3y7. (Heavy)	73.3	30
597.298	888.388	31	CER1.TVPFSQTITHEGCEK.+3y7. (Light)	73.3	30
599.981	1106.545	31	CER1.TVPFSQTITHEGCEK.+3y9. (Heavy)	73.3	30
597.298	1102.52	31	CER1.TVPFSQTITHEGCEK.+3y9. (Light)	73.3	30
671.394	1210.655	33.1	CER1.VVVQNNLCFGK.+2y10. (Heavy)	77.7	30.2
667.368	1206.63	33.1	CER1.VVVQNNLCFGK.+2y10. (Light)	77.7	30.2
671.394	770.417	33.1	CER1.VVVQNNLCFGK.+2y6. (Heavy)	77.7	30.2
667.368	766.392	33.1	CER1.VVVQNNLCFGK.+2y6. (Light)	77.7	30.2
671.394	884.46	33.1	CER1.VVVQNNLCFGK.+2y7. (Heavy)	77.7	31.2
667.368	880.435	33.1	CER1.VVVQNNLCFGK.+2y7. (Light)	77.7	31.2
671.394	1012.518	33.1	CER1.VVVQNNLCFGK.+2y8. (Heavy)	77.7	29.2
667.368	1008.493	33.1	CER1.VVVQNNLCFGK.+2y8. (Light)	77.7	29.2
671.394	1111.587	33.1	CER1.VVVQNNLCFGK.+2y9. (Heavy)	77.7	30.2

667.368	1107.562	33.1	CER1.VVVQNNLCFGK.+2y9. (Light)	77.7	30.2
692.034	779.508	39.8	CTNB1.HAVVNLINYQDDAELATR.+3b7. (Heavy)	80.8	26.2
690.692	775.482	39.8	CTNB1.HAVVNLINYQDDAELATR.+3b7. (Light)	80.8	26.2
692.034	893.551	39.8	CTNB1.HAVVNLINYQDDAELATR.+3b8. (Heavy)	80.8	27.2
690.692	889.525	39.8	CTNB1.HAVVNLINYQDDAELATR.+3b8. (Light)	80.8	27.2
692.034	1295.586	39.8	CTNB1.HAVVNLINYQDDAELATR.+3y11. (Heavy)	80.8	25.2
690.692	1295.586	39.8	CTNB1.HAVVNLINYQDDAELATR.+3y11. (Light)	80.8	25.2
692.034	890.421	39.8	CTNB1.HAVVNLINYQDDAELATR.+3y8. (Heavy)	80.8	30.2
690.692	890.421	39.8	CTNB1.HAVVNLINYQDDAELATR.+3y8. (Light)	80.8	30.2
692.034	1018.48	39.8	CTNB1.HAVVNLINYQDDAELATR.+3y9. (Heavy)	80.8	29.2
690.692	1018.48	39.8	CTNB1.HAVVNLINYQDDAELATR.+3y9. (Light)	80.8	29.2
725.424	1058.567	27.8	CTNB1.LLNDEDQVVVNK.+2b9. (Heavy)	81.7	35.3
721.398	1054.542	27.8	CTNB1.LLNDEDQVVVNK.+2b9. (Light)	81.7	35.3
725.424	1191.615	27.8	CTNB1.LLNDEDQVVVNK.+2y10. (Heavy)	81.7	33.3
721.398	1187.59	27.8	CTNB1.LLNDEDQVVVNK.+2y10. (Light)	81.7	33.3
725.424	833.503	27.8	CTNB1.LLNDEDQVVVNK.+2y7. (Heavy)	81.7	35.3
721.398	829.478	27.8	CTNB1.LLNDEDQVVVNK.+2y7. (Light)	81.7	35.3
725.424	962.545	27.8	CTNB1.LLNDEDQVVVNK.+2y8. (Heavy)	81.7	35.3
721.398	958.52	27.8	CTNB1.LLNDEDQVVVNK.+2y8. (Light)	81.7	35.3
725.424	1077.572	27.8	CTNB1.LLNDEDQVVVNK.+2y9. (Heavy)	81.7	34.3
721.398	1073.547	27.8	CTNB1.LLNDEDQVVVNK.+2y9. (Light)	81.7	34.3
757.419	1082.599	55	CTNB1.NEGVATYAAAVLFR.+2y10. (Heavy)	85.2	35
755.407	1082.599	55	CTNB1.NEGVATYAAAVLFR.+2y10. (Light)	85.2	35
757.419	1181.668	55	CTNB1.NEGVATYAAAVLFR.+2y11. (Heavy)	85.2	38
755.407	1181.668	55	CTNB1.NEGVATYAAAVLFR.+2y11. (Light)	85.2	38
757.419	1238.689	55	CTNB1.NEGVATYAAAVLFR.+2y12. (Heavy)	85.2	38
755.407	1238.689	55	CTNB1.NEGVATYAAAVLFR.+2y12. (Light)	85.2	38
757.419	910.515	55	CTNB1.NEGVATYAAAVLFR.+2y8. (Heavy)	85.2	37
755.407	910.515	55	CTNB1.NEGVATYAAAVLFR.+2y8. (Light)	85.2	37
757.419	1011.562	55	CTNB1.NEGVATYAAAVLFR.+2y9. (Heavy)	85.2	39
755.407	1011.562	55	CTNB1.NEGVATYAAAVLFR.+2y9. (Light)	85.2	39
390.856	550.267	27.6	DKK1.DHHQASNSSR.+3b4. (Heavy)	58.8	22.9
389.515	546.242	27.6	DKK1.DHHQASNSSR.+3b4. (Light)	58.8	22.9
390.856	463.226	27.6	DKK1.DHHQASNSSR.+3y4. (Heavy)	58.8	20.9
389.515	463.226	27.6	DKK1.DHHQASNSSR.+3y4. (Light)	58.8	20.9
390.856	550.258	27.6	DKK1.DHHQASNSSR.+3y5. (Heavy)	58.8	20.9
389.515	550.258	27.6	DKK1.DHHQASNSSR.+3y5. (Light)	58.8	20.9
390.856	621.295	27.6	DKK1.DHHQASNSSR.+3y6. (Heavy)	58.8	20.9
389.515	621.295	27.6	DKK1.DHHQASNSSR.+3y6. (Light)	58.8	20.9
390.856	443.71	27.6	DKK1.DHHQASNSSR.+3y8+2. (Heavy)	58.8	19.9
389.515	443.71	27.6	DKK1.DHHQASNSSR.+3y8+2. (Light)	58.8	19.9

522.586	625.273	27	DKK1.NGICVSSDQNHFR.+3y10+2. (Heavy)	68.4	21
521.244	625.273	27	DKK1.NGICVSSDQNHFR.+3y10+2. (Light)	68.4	21
522.586	681.815	27	DKK1.NGICVSSDQNHFR.+3y11+2. (Heavy)	68.4	21
521.244	681.815	27	DKK1.NGICVSSDQNHFR.+3y11+2. (Light)	68.4	21
522.586	903.407	27	DKK1.NGICVSSDQNHFR.+3y7. (Heavy)	68.4	28
521.244	903.407	27	DKK1.NGICVSSDQNHFR.+3y7. (Light)	68.4	28
522.586	990.439	27	DKK1.NGICVSSDQNHFR.+3y8. (Heavy)	68.4	28
521.244	990.439	27	DKK1.NGICVSSDQNHFR.+3y8. (Light)	68.4	28
522.586	545.257	27	DKK1.NGICVSSDQNHFR.+3y9+2. (Heavy)	68.4	23
521.244	545.257	27	DKK1.NGICVSSDQNHFR.+3y9+2. (Light)	68.4	23
688.289	1169.45	20.9	DKK1.SSDCASGLCCAR.+2y10. (Heavy)	80.1	31.1
686.276	1169.45	20.9	DKK1.SSDCASGLCCAR.+2y10. (Light)	80.1	31.1
688.289	736.323	20.9	DKK1.SSDCASGLCCAR.+2y6. (Heavy)	80.1	33.1
686.276	736.323	20.9	DKK1.SSDCASGLCCAR.+2y6. (Light)	80.1	33.1
688.289	823.355	20.9	DKK1.SSDCASGLCCAR.+2y7. (Heavy)	80.1	33.1
686.276	823.355	20.9	DKK1.SSDCASGLCCAR.+2y7. (Light)	80.1	33.1
688.289	894.392	20.9	DKK1.SSDCASGLCCAR.+2y8. (Heavy)	80.1	36.1
686.276	894.392	20.9	DKK1.SSDCASGLCCAR.+2y8. (Light)	80.1	36.1
688.289	1054.423	20.9	DKK1.SSDCASGLCCAR.+2y9. (Heavy)	80.1	33.1
686.276	1054.423	20.9	DKK1.SSDCASGLCCAR.+2y9. (Light)	80.1	33.1
651.328	1069.476	17	DVL1.LSSSTEQSTSSR.+2y10. (Heavy)	77.4	33.9
649.315	1069.476	17	DVL1.LSSSTEQSTSSR.+2y10. (Light)	77.4	33.9
651.328	665.321	17	DVL1.LSSSTEQSTSSR.+2y6. (Heavy)	77.4	34.9
649.315	665.321	17	DVL1.LSSSTEQSTSSR.+2y6. (Light)	77.4	34.9
651.328	794.364	17	DVL1.LSSSTEQSTSSR.+2y7. (Heavy)	77.4	35.9
649.315	794.364	17	DVL1.LSSSTEQSTSSR.+2y7. (Light)	77.4	35.9
651.328	895.412	17	DVL1.LSSSTEQSTSSR.+2y8. (Heavy)	77.4	33.9
649.315	895.412	17	DVL1.LSSSTEQSTSSR.+2y8. (Light)	77.4	33.9
651.328	982.444	17	DVL1.LSSSTEQSTSSR.+2y9. (Heavy)	77.4	34.9
649.315	982.444	17	DVL1.LSSSTEQSTSSR.+2y9. (Light)	77.4	34.9
487.964	608.859	26.2	DVL1.NVLSNRPVHAYK.+3y10+2. (Heavy)	65.1	21.5
485.281	606.846	26.2	DVL1.NVLSNRPVHAYK.+3y10+2. (Light)	65.1	21.5
487.964	658.393	26.2	DVL1.NVLSNRPVHAYK.+3y11+2. (Heavy)	65.1	23.5
485.281	656.38	26.2	DVL1.NVLSNRPVHAYK.+3y11+2. (Light)	65.1	23.5
487.964	746.45	26.2	DVL1.NVLSNRPVHAYK.+3y6. (Heavy)	65.1	21.5
485.281	742.425	26.2	DVL1.NVLSNRPVHAYK.+3y6. (Light)	65.1	21.5
487.964	508.801	26.2	DVL1.NVLSNRPVHAYK.+3y8+2. (Heavy)	65.1	25.5
485.281	506.788	26.2	DVL1.NVLSNRPVHAYK.+3y8+2. (Light)	65.1	25.5
487.964	552.317	26.2	DVL1.NVLSNRPVHAYK.+3y9+2. (Heavy)	65.1	23.5
485.281	550.304	26.2	DVL1.NVLSNRPVHAYK.+3y9+2. (Light)	65.1	23.5
608.015	1173.693	26	DVL1.SQASATAPGLPPPHPTTK.+3y11. (Heavy)	73.9	29.3

605.332	1169.668	26	DVL1.SQASATAPGLPPPHPTTK.+3y11. (Light)	73.9	29.3
608.015	752.427	26	DVL1.SQASATAPGLPPPHPTTK.+3y15+2. (Heavy)	73.9	23.3
605.332	750.414	26	DVL1.SQASATAPGLPPPHPTTK.+3y15+2. (Light)	73.9	23.3
608.015	787.946	26	DVL1.SQASATAPGLPPPHPTTK.+3y16+2. (Heavy)	73.9	22.3
605.332	785.933	26	DVL1.SQASATAPGLPPPHPTTK.+3y16+2. (Light)	73.9	22.3
608.015	809.482	26	DVL1.SQASATAPGLPPPHPTTK.+3y7. (Heavy)	73.9	30.3
605.332	805.457	26	DVL1.SQASATAPGLPPPHPTTK.+3y7. (Light)	73.9	30.3
608.015	906.535	26	DVL1.SQASATAPGLPPPHPTTK.+3y8. (Heavy)	73.9	28.3
605.332	902.509	26	DVL1.SQASATAPGLPPPHPTTK.+3y8. (Light)	73.9	28.3
621.389	984.603	29.5	FRAT1.APGPLAAAVPADK.+2y10. (Heavy)	74.1	30.3
617.364	980.578	29.5	FRAT1.APGPLAAAVPADK.+2y10. (Light)	74.1	30.3
621.389	1041.624	29.5	FRAT1.APGPLAAAVPADK.+2y11. (Heavy)	74.1	30.3
617.364	1037.599	29.5	FRAT1.APGPLAAAVPADK.+2y11. (Light)	74.1	30.3
621.389	632.392	29.5	FRAT1.APGPLAAAVPADK.+2y6. (Heavy)	74.1	33.3
617.364	628.366	29.5	FRAT1.APGPLAAAVPADK.+2y6. (Light)	74.1	33.3
621.389	703.429	29.5	FRAT1.APGPLAAAVPADK.+2y7. (Heavy)	74.1	33.3
617.364	699.404	29.5	FRAT1.APGPLAAAVPADK.+2y7. (Light)	74.1	33.3
621.389	774.466	29.5	FRAT1.APGPLAAAVPADK.+2y8. (Heavy)	74.1	34.3
617.364	770.441	29.5	FRAT1.APGPLAAAVPADK.+2y8. (Light)	74.1	34.3
752.01	1116.729	50.3	FRAT1.LLQQLVLSGNLIK.+2y10. (Heavy)	83.6	35.8
747.984	1112.704	50.3	FRAT1.LLQQLVLSGNLIK.+2y10. (Light)	83.6	35.8
752.01	1244.787	50.3	FRAT1.LLQQLVLSGNLIK.+2y11. (Heavy)	83.6	36.8
747.984	1240.762	50.3	FRAT1.LLQQLVLSGNLIK.+2y11. (Light)	83.6	36.8
752.01	776.518	50.3	FRAT1.LLQQLVLSGNLIK.+2y7. (Heavy)	83.6	32.8
747.984	772.493	50.3	FRAT1.LLQQLVLSGNLIK.+2y7. (Light)	83.6	32.8
752.01	875.586	50.3	FRAT1.LLQQLVLSGNLIK.+2y8. (Heavy)	83.6	37.8
747.984	871.561	50.3	FRAT1.LLQQLVLSGNLIK.+2y8. (Light)	83.6	37.8
752.01	988.67	50.3	FRAT1.LLQQLVLSGNLIK.+2y9. (Heavy)	83.6	38.8
747.984	984.645	50.3	FRAT1.LLQQLVLSGNLIK.+2y9. (Light)	83.6	38.8
660.675	1100.55	30.4	FZD1.FPVHGAGELCVGQNTSDK.+3b10. (Heavy)	77.7	27.9
657.991	1096.524	30.4	FZD1.FPVHGAGELCVGQNTSDK.+3b10. (Light)	77.7	27.9
660.675	940.519	30.4	FZD1.FPVHGAGELCVGQNTSDK.+3b9. (Heavy)	77.7	30.9
657.991	936.494	30.4	FZD1.FPVHGAGELCVGQNTSDK.+3b9. (Light)	77.7	30.9
660.675	781.399	30.4	FZD1.FPVHGAGELCVGQNTSDK.+3y7. (Heavy)	77.7	27.9
657.991	777.374	30.4	FZD1.FPVHGAGELCVGQNTSDK.+3y7. (Light)	77.7	27.9
660.675	880.467	30.4	FZD1.FPVHGAGELCVGQNTSDK.+3y8. (Heavy)	77.7	27.9
657.991	876.442	30.4	FZD1.FPVHGAGELCVGQNTSDK.+3y8. (Light)	77.7	27.9
660.675	1040.498	30.4	FZD1.FPVHGAGELCVGQNTSDK.+3y9. (Heavy)	77.7	27.9
657.991	1036.473	30.4	FZD1.FPVHGAGELCVGQNTSDK.+3y9. (Light)	77.7	27.9
547.78	576.308	22.7	FZD1.GGFPGGAGASER.+2b7. (Heavy)	69.9	22
545.767	572.283	22.7	FZD1.GGFPGGAGASER.+2b7. (Light)	69.9	22

547.78	590.289	22.7	FZD1.GGFPGGAGASER.+2y6. (Heavy)	69.9	31
545.767	590.289	22.7	FZD1.GGFPGGAGASER.+2y6. (Light)	69.9	31
547.78	647.311	22.7	FZD1.GGFPGGAGASER.+2y7. (Heavy)	69.9	31
545.767	647.311	22.7	FZD1.GGFPGGAGASER.+2y7. (Light)	69.9	31
547.78	704.332	22.7	FZD1.GGFPGGAGASER.+2y8. (Heavy)	69.9	31
545.767	704.332	22.7	FZD1.GGFPGGAGASER.+2y8. (Light)	69.9	31
547.78	801.385	22.7	FZD1.GGFPGGAGASER.+2y9. (Heavy)	69.9	25
545.767	801.385	22.7	FZD1.GGFPGGAGASER.+2y9. (Light)	69.9	25
544.307	658.353	42.2	FZD1.VPSYLNYHFLGEK.+3y10+2. (Heavy)	69.2	26.3
541.624	656.34	42.2	FZD1.VPSYLNYHFLGEK.+3y10+2. (Light)	69.2	26.3
544.307	701.869	42.2	FZD1.VPSYLNYHFLGEK.+3y11+2. (Heavy)	69.2	23.3
541.624	699.856	42.2	FZD1.VPSYLNYHFLGEK.+3y11+2. (Light)	69.2	23.3
544.307	750.395	42.2	FZD1.VPSYLNYHFLGEK.+3y12+2. (Heavy)	69.2	23.3
541.624	748.383	42.2	FZD1.VPSYLNYHFLGEK.+3y12+2. (Light)	69.2	23.3
544.307	625.386	42.2	FZD1.VPSYLNYHFLGEK.+3y5. (Heavy)	69.2	28.3
541.624	621.361	42.2	FZD1.VPSYLNYHFLGEK.+3y5. (Light)	69.2	28.3
544.307	1039.551	42.2	FZD1.VPSYLNYHFLGEK.+3y8. (Heavy)	69.2	27.3
541.624	1035.526	42.2	FZD1.VPSYLNYHFLGEK.+3y8. (Light)	69.2	27.3
739.919	1133.635	24.5	GLI3.GQQEQPEGTTLVK.+2y10. (Heavy)	82.7	33.1
735.894	1129.61	24.5	GLI3.GQQEQPEGTTLVK.+2y10. (Light)	82.7	33.1
739.919	1261.694	24.5	GLI3.GQQEQPEGTTLVK.+2y11. (Heavy)	82.7	32.1
735.894	1257.668	24.5	GLI3.GQQEQPEGTTLVK.+2y11. (Light)	82.7	32.1
739.919	779.481	24.5	GLI3.GQQEQPEGTTLVK.+2y7. (Heavy)	82.7	40.1
735.894	775.456	24.5	GLI3.GQQEQPEGTTLVK.+2y7. (Light)	82.7	40.1
739.919	876.534	24.5	GLI3.GQQEQPEGTTLVK.+2y8. (Heavy)	82.7	34.1
735.894	872.509	24.5	GLI3.GQQEQPEGTTLVK.+2y8. (Light)	82.7	34.1
739.919	1004.592	24.5	GLI3.GQQEQPEGTTLVK.+2y9. (Heavy)	82.7	32.1
735.894	1000.567	24.5	GLI3.GQQEQPEGTTLVK.+2y9. (Light)	82.7	32.1
486.952	762.448	28	GLI3.IKPDEDLPSPGAR.+3b6. (Heavy)	65.1	21.5
484.268	754.398	28	GLI3.IKPDEDLPSPGAR.+3b6. (Light)	65.1	21.5
486.952	875.532	28	GLI3.IKPDEDLPSPGAR.+3b7. (Heavy)	65.1	17.5
484.268	867.482	28	GLI3.IKPDEDLPSPGAR.+3b7. (Light)	65.1	17.5
486.952	577.278	28	GLI3.IKPDEDLPSPGAR.+3y11+2. (Heavy)	65.1	17.5
484.268	577.278	28	GLI3.IKPDEDLPSPGAR.+3y11+2. (Light)	65.1	17.5
486.952	584.315	28	GLI3.IKPDEDLPSPGAR.+3y6. (Heavy)	65.1	21.5
484.268	584.315	28	GLI3.IKPDEDLPSPGAR.+3y6. (Light)	65.1	21.5
486.952	812.426	28	GLI3.IKPDEDLPSPGAR.+3y8. (Heavy)	65.1	18.5
484.268	812.426	28	GLI3.IKPDEDLPSPGAR.+3y8. (Light)	65.1	18.5
774.438	1116.637	44.3	GLI3.TSPNSLVTILNNSR.+2y10. (Heavy)	86.4	43
772.426	1116.637	44.3	GLI3.TSPNSLVTILNNSR.+2y10. (Light)	86.4	43
774.438	1230.68	44.3	GLI3.TSPNSLVTILNNSR.+2y11. (Heavy)	86.4	43

772.426	1230.68	44.3	GLI3.TSPNSLVTILNNSR.+2y11. (Light)	86.4	43
774.438	817.453	44.3	GLI3.TSPNSLVTILNNSR.+2y7. (Heavy)	86.4	42
772.426	817.453	44.3	GLI3.TSPNSLVTILNNSR.+2y7. (Light)	86.4	42
774.438	916.521	44.3	GLI3.TSPNSLVTILNNSR.+2y8. (Heavy)	86.4	41
772.426	916.521	44.3	GLI3.TSPNSLVTILNNSR.+2y8. (Light)	86.4	41
774.438	1029.605	44.3	GLI3.TSPNSLVTILNNSR.+2y9. (Heavy)	86.4	43
772.426	1029.605	44.3	GLI3.TSPNSLVTILNNSR.+2y9. (Light)	86.4	43
663.751	1116.681	50.6	GSK3B.DIKPQNLLLDPDTAVLK.+3y10. (Heavy)	77.2	24.7
659.726	1112.656	50.6	GSK3B.DIKPQNLLLDPDTAVLK.+3y10. (Light)	77.2	24.7
663.751	865.039	50.6	GSK3B.DIKPQNLLLDPDTAVLK.+3y15+2. (Heavy)	77.2	23.7
659.726	861.014	50.6	GSK3B.DIKPQNLLLDPDTAVLK.+3y15+2. (Light)	77.2	23.7
663.751	775.486	50.6	GSK3B.DIKPQNLLLDPDTAVLK.+3y7. (Heavy)	77.2	24.7
659.726	771.461	50.6	GSK3B.DIKPQNLLLDPDTAVLK.+3y7. (Light)	77.2	24.7
663.751	890.513	50.6	GSK3B.DIKPQNLLLDPDTAVLK.+3y8. (Heavy)	77.2	22.7
659.726	886.488	50.6	GSK3B.DIKPQNLLLDPDTAVLK.+3y8. (Light)	77.2	22.7
663.751	1003.597	50.6	GSK3B.DIKPQNLLLDPDTAVLK.+3y9. (Heavy)	77.2	22.7
659.726	999.572	50.6	GSK3B.DIKPQNLLLDPDTAVLK.+3y9. (Light)	77.2	22.7
712.687	977.428	23	GSK3B.IQAAASTPTNATAASDANTGDR.+3y10. (Heavy)	82.3	33.8
711.345	977.428	23	GSK3B.IQAAASTPTNATAASDANTGDR.+3y10. (Light)	82.3	33.8
712.687	1078.476	23	GSK3B.IQAAASTPTNATAASDANTGDR.+3y11. (Heavy)	82.3	30.8
711.345	1078.476	23	GSK3B.IQAAASTPTNATAASDANTGDR.+3y11. (Light)	82.3	30.8
712.687	748.322	23	GSK3B.IQAAASTPTNATAASDANTGDR.+3y7. (Heavy)	82.3	26.8
711.345	748.322	23	GSK3B.IQAAASTPTNATAASDANTGDR.+3y7. (Light)	82.3	26.8
712.687	835.354	23	GSK3B.IQAAASTPTNATAASDANTGDR.+3y8. (Heavy)	82.3	26.8
711.345	835.354	23	GSK3B.IQAAASTPTNATAASDANTGDR.+3y8. (Light)	82.3	26.8
712.687	906.391	23	GSK3B.IQAAASTPTNATAASDANTGDR.+3y9. (Heavy)	82.3	29.8
711.345	906.391	23	GSK3B.IQAAASTPTNATAASDANTGDR.+3y9. (Light)	82.3	29.8
751.945	1087.608	37.1	GSK3B.VIGNGSFGVVYQAK.+2y10. (Heavy)	83.6	33.8
747.919	1083.583	37.1	GSK3B.VIGNGSFGVVYQAK.+2y10. (Light)	83.6	33.8
751.945	1258.673	37.1	GSK3B.VIGNGSFGVVYQAK.+2y12. (Heavy)	83.6	33.8
747.919	1254.648	37.1	GSK3B.VIGNGSFGVVYQAK.+2y12. (Light)	83.6	33.8
751.945	796.487	37.1	GSK3B.VIGNGSFGVVYQAK.+2y7. (Heavy)	83.6	35.8
747.919	792.461	37.1	GSK3B.VIGNGSFGVVYQAK.+2y7. (Light)	83.6	35.8
751.945	943.555	37.1	GSK3B.VIGNGSFGVVYQAK.+2y8. (Heavy)	83.6	33.8
747.919	939.53	37.1	GSK3B.VIGNGSFGVVYQAK.+2y8. (Light)	83.6	33.8
751.945	1030.587	37.1	GSK3B.VIGNGSFGVVYQAK.+2y9. (Heavy)	83.6	33.8
747.919	1026.562	37.1	GSK3B.VIGNGSFGVVYQAK.+2y9. (Light)	83.6	33.8
772.39	1164.531	30	HES1.FLSTCEGVNTEVR.+2y10. (Heavy)	86.3	36.8
770.377	1164.531	30	HES1.FLSTCEGVNTEVR.+2y10. (Light)	86.3	36.8
772.39	1251.563	30	HES1.FLSTCEGVNTEVR.+2y11. (Heavy)	86.3	36.8
770.377	1251.563	30	HES1.FLSTCEGVNTEVR.+2y11. (Light)	86.3	36.8

772.39	774.41	30	HES1.FLSTCEGVNTEVR.+2y7. (Heavy)	86.3	41.8
770.377	774.41	30	HES1.FLSTCEGVNTEVR.+2y7. (Light)	86.3	41.8
772.39	903.453	30	HES1.FLSTCEGVNTEVR.+2y8. (Heavy)	86.3	40.8
770.377	903.453	30	HES1.FLSTCEGVNTEVR.+2y8. (Light)	86.3	40.8
772.39	1063.484	30	HES1.FLSTCEGVNTEVR.+2y9. (Heavy)	86.3	39.8
770.377	1063.484	30	HES1.FLSTCEGVNTEVR.+2y9. (Light)	86.3	39.8
498.302	507.307	8	HES1.LGSQAGEAAK.+2y5. (Heavy)	65.1	27.3
494.277	503.282	8	HES1.LGSQAGEAAK.+2y5. (Light)	65.1	27.3
498.302	578.345	8	HES1.LGSQAGEAAK.+2y6. (Heavy)	65.1	25.3
494.277	574.32	8	HES1.LGSQAGEAAK.+2y6. (Light)	65.1	25.3
498.302	706.403	8	HES1.LGSQAGEAAK.+2y7. (Heavy)	65.1	23.3
494.277	702.378	8	HES1.LGSQAGEAAK.+2y7. (Light)	65.1	23.3
498.302	793.435	8	HES1.LGSQAGEAAK.+2y8. (Heavy)	65.1	23.3
494.277	789.41	8	HES1.LGSQAGEAAK.+2y8. (Light)	65.1	23.3
498.302	850.457	8	HES1.LGSQAGEAAK.+2y9. (Heavy)	65.1	25.3
494.277	846.432	8	HES1.LGSQAGEAAK.+2y9. (Light)	65.1	25.3
722.412	1318.782	27.1	HES1.NSSSPVAATPASVNTTPDKPK.+3y12. (Heavy)	81.4	33.5
718.386	1310.731	27.1	HES1.NSSSPVAATPASVNTTPDKPK.+3y12. (Light)	81.4	33.5
722.412	781.455	27.1	HES1.NSSSPVAATPASVNTTPDKPK.+3y15+2. (Heavy)	81.4	32.5
718.386	777.43	27.1	HES1.NSSSPVAATPASVNTTPDKPK.+3y15+2. (Light)	81.4	32.5
722.412	879.516	27.1	HES1.NSSSPVAATPASVNTTPDKPK.+3y17+2. (Heavy)	81.4	27.5
718.386	875.491	27.1	HES1.NSSSPVAATPASVNTTPDKPK.+3y17+2. (Light)	81.4	27.5
722.412	923.032	27.1	HES1.NSSSPVAATPASVNTTPDKPK.+3y18+2. (Heavy)	81.4	27.5
718.386	919.007	27.1	HES1.NSSSPVAATPASVNTTPDKPK.+3y18+2. (Light)	81.4	27.5
722.412	966.548	27.1	HES1.NSSSPVAATPASVNTTPDKPK.+3y19+2. (Heavy)	81.4	27.5
718.386	962.523	27.1	HES1.NSSSPVAATPASVNTTPDKPK.+3y19+2. (Light)	81.4	27.5
417.577	524.78	26.2	HEY1.LGSAHPEAPALR.+3y10+2. (Heavy)	60.8	18.7
416.235	524.78	26.2	HEY1.LGSAHPEAPALR.+3y10+2. (Light)	60.8	18.7
417.577	553.291	26.2	HEY1.LGSAHPEAPALR.+3y11+2. (Heavy)	60.8	19.7
416.235	553.291	26.2	HEY1.LGSAHPEAPALR.+3y11+2. (Light)	60.8	19.7
417.577	527.33	26.2	HEY1.LGSAHPEAPALR.+3y5. (Heavy)	60.8	24.7
416.235	527.33	26.2	HEY1.LGSAHPEAPALR.+3y5. (Light)	60.8	24.7
417.577	753.425	26.2	HEY1.LGSAHPEAPALR.+3y7. (Heavy)	60.8	24.7
416.235	753.425	26.2	HEY1.LGSAHPEAPALR.+3y7. (Light)	60.8	24.7
417.577	445.746	26.2	HEY1.LGSAHPEAPALR.+3y8+2. (Heavy)	60.8	22.7
416.235	445.746	26.2	HEY1.LGSAHPEAPALR.+3y8+2. (Light)	60.8	22.7
478.598	810.477	24.2	HEY1.LVSHLNNYASQR.+3b7. (Heavy)	65.2	21.6
477.256	806.452	24.2	HEY1.LVSHLNNYASQR.+3b7. (Light)	65.2	21.6
478.598	595.289	24.2	HEY1.LVSHLNNYASQR.+3y10+2. (Heavy)	65.2	18.6
477.256	595.289	24.2	HEY1.LVSHLNNYASQR.+3y10+2. (Light)	65.2	18.6
478.598	644.823	24.2	HEY1.LVSHLNNYASQR.+3y11+2. (Heavy)	65.2	21.6

477.256	644.823	24.2	HEY1.LVSHLNNYASQR.+3y11+2. (Light)	65.2	21.6
478.598	624.31	24.2	HEY1.LVSHLNNYASQR.+3y5. (Heavy)	65.2	22.6
477.256	624.31	24.2	HEY1.LVSHLNNYASQR.+3y5. (Light)	65.2	22.6
478.598	965.48	24.2	HEY1.LVSHLNNYASQR.+3y8. (Heavy)	65.2	25.6
477.256	965.48	24.2	HEY1.LVSHLNNYASQR.+3y8. (Light)	65.2	25.6
847.469	1072.527	58	HEY1.YLSIIEGLDASDPLR.+2y10. (Heavy)	91.7	40.1
845.457	1072.527	58	HEY1.YLSIIEGLDASDPLR.+2y10. (Light)	91.7	40.1
847.469	1185.611	58	HEY1.YLSIIEGLDASDPLR.+2y11. (Heavy)	91.7	38.1
845.457	1185.611	58	HEY1.YLSIIEGLDASDPLR.+2y11. (Light)	91.7	38.1
847.469	1385.727	58	HEY1.YLSIIEGLDASDPLR.+2y13. (Heavy)	91.7	39.1
845.457	1385.727	58	HEY1.YLSIIEGLDASDPLR.+2y13. (Light)	91.7	39.1
847.469	886.463	58	HEY1.YLSIIEGLDASDPLR.+2y8. (Heavy)	91.7	39.1
845.457	886.463	58	HEY1.YLSIIEGLDASDPLR.+2y8. (Light)	91.7	39.1
847.469	943.484	58	HEY1.YLSIIEGLDASDPLR.+2y9. (Heavy)	91.7	39.1
845.457	943.484	58	HEY1.YLSIIEGLDASDPLR.+2y9. (Light)	91.7	39.1
561.801	589.33	27.8	INHBA.EGSDLSVVER.+2y5. (Heavy)	70.9	28.8
559.788	589.33	27.8	INHBA.EGSDLSVVER.+2y5. (Light)	70.9	28.8
561.801	702.414	27.8	INHBA.EGSDLSVVER.+2y6. (Heavy)	70.9	30.8
559.788	702.414	27.8	INHBA.EGSDLSVVER.+2y6. (Light)	70.9	30.8
561.801	817.441	27.8	INHBA.EGSDLSVVER.+2y7. (Heavy)	70.9	27.8
559.788	817.441	27.8	INHBA.EGSDLSVVER.+2y7. (Light)	70.9	27.8
561.801	904.473	27.8	INHBA.EGSDLSVVER.+2y8. (Heavy)	70.9	28.8
559.788	904.473	27.8	INHBA.EGSDLSVVER.+2y8. (Light)	70.9	28.8
561.801	961.495	27.8	INHBA.EGSDLSVVER.+2y9. (Heavy)	70.9	30.8
559.788	961.495	27.8	INHBA.EGSDLSVVER.+2y9. (Light)	70.9	30.8
654.008	767.398	29.2	INHBA.HPQGSLDTGEEAEEVGLK.+3b7. (Heavy)	77.2	29.7
651.325	763.373	29.2	INHBA.HPQGSLDTGEEAEEVGLK.+3b7. (Light)	77.2	29.7
654.008	925.468	29.2	INHBA.HPQGSLDTGEEAEEVGLK.+3b9. (Heavy)	77.2	27.7
651.325	921.442	29.2	INHBA.HPQGSLDTGEEAEEVGLK.+3b9. (Light)	77.2	27.7
654.008	706.428	29.2	INHBA.HPQGSLDTGEEAEEVGLK.+3y6. (Heavy)	77.2	24.7
651.325	702.403	29.2	INHBA.HPQGSLDTGEEAEEVGLK.+3y6. (Light)	77.2	24.7
654.008	777.465	29.2	INHBA.HPQGSLDTGEEAEEVGLK.+3y7. (Heavy)	77.2	26.7
651.325	773.44	29.2	INHBA.HPQGSLDTGEEAEEVGLK.+3y7. (Light)	77.2	26.7
654.008	906.508	29.2	INHBA.HPQGSLDTGEEAEEVGLK.+3y8. (Heavy)	77.2	26.7
651.325	902.483	29.2	INHBA.HPQGSLDTGEEAEEVGLK.+3y8. (Light)	77.2	26.7
491.817	588.391	30	INHBA.SELLLSEK.+2b5. (Heavy)	64.6	21.9
487.792	584.365	30	INHBA.SELLLSEK.+2b5. (Light)	64.6	21.9
491.817	508.328	30	INHBA.SELLLSEK.+2y4. (Heavy)	64.6	24.9
487.792	504.303	30	INHBA.SELLLSEK.+2y4. (Light)	64.6	24.9
491.817	621.412	30	INHBA.SELLLSEK.+2y5. (Heavy)	64.6	25.9
487.792	617.387	30	INHBA.SELLLSEK.+2y5. (Light)	64.6	25.9

491.817	734.496	30	INHBA.SELLLSEK.+2y6. (Heavy)	64.6	22.9
487.792	730.471	30	INHBA.SELLLSEK.+2y6. (Light)	64.6	22.9
491.817	863.539	30	INHBA.SELLLSEK.+2y7. (Heavy)	64.6	21.9
487.792	859.513	30	INHBA.SELLLSEK.+2y7. (Light)	64.6	21.9
640.882	679.408	30	LFTY1.EHLGPLASGAHK.+2b6. (Heavy)	75.5	22.7
636.857	675.382	30	LFTY1.EHLGPLASGAHK.+2b6. (Light)	75.5	22.7
640.882	444.287	30	LFTY1.EHLGPLASGAHK.+2y4. (Heavy)	75.5	22.7
636.857	440.262	30	LFTY1.EHLGPLASGAHK.+2y4. (Light)	75.5	22.7
640.882	531.319	30	LFTY1.EHLGPLASGAHK.+2y5. (Heavy)	75.5	22.7
636.857	527.294	30	LFTY1.EHLGPLASGAHK.+2y5. (Light)	75.5	22.7
640.882	602.356	30	LFTY1.EHLGPLASGAHK.+2y6. (Heavy)	75.5	22.7
636.857	598.331	30	LFTY1.EHLGPLASGAHK.+2y6. (Light)	75.5	22.7
640.882	435.261	30	LFTY1.EHLGPLASGAHK.+2y9+2. (Heavy)	75.5	24.7
636.857	433.248	30	LFTY1.EHLGPLASGAHK.+2y9+2. (Light)	75.5	24.7
734.445	783.455	44	LFTY1.LPPNSELVQAVLR.+2b7. (Heavy)	83.5	33.7
732.433	779.43	44	LFTY1.LPPNSELVQAVLR.+2b7. (Light)	83.5	33.7
734.445	1128.637	44	LFTY1.LPPNSELVQAVLR.+2y10. (Heavy)	83.5	41.7
732.433	1128.637	44	LFTY1.LPPNSELVQAVLR.+2y10. (Light)	83.5	41.7
734.445	798.52	44	LFTY1.LPPNSELVQAVLR.+2y7. (Heavy)	83.5	41.7
732.433	798.52	44	LFTY1.LPPNSELVQAVLR.+2y7. (Light)	83.5	41.7
734.445	927.562	44	LFTY1.LPPNSELVQAVLR.+2y8. (Heavy)	83.5	41.7
732.433	927.562	44	LFTY1.LPPNSELVQAVLR.+2y8. (Light)	83.5	41.7
734.445	1014.594	44	LFTY1.LPPNSELVQAVLR.+2y9. (Heavy)	83.5	41.7
732.433	1014.594	44	LFTY1.LPPNSELVQAVLR.+2y9. (Light)	83.5	41.7
656.916	1152.71	40.5	LFTY1.QPLLLQVSVQR.+2y10. (Heavy)	77.8	37.3
654.904	1152.71	40.5	LFTY1.QPLLLQVSVQR.+2y10. (Light)	77.8	37.3
656.916	716.405	40.5	LFTY1.QPLLLQVSVQR.+2y6. (Heavy)	77.8	30.3
654.904	716.405	40.5	LFTY1.QPLLLQVSVQR.+2y6. (Light)	77.8	30.3
656.916	829.489	40.5	LFTY1.QPLLLQVSVQR.+2y7. (Heavy)	77.8	33.3
654.904	829.489	40.5	LFTY1.QPLLLQVSVQR.+2y7. (Light)	77.8	33.3
656.916	942.573	40.5	LFTY1.QPLLLQVSVQR.+2y8. (Heavy)	77.8	37.3
654.904	942.573	40.5	LFTY1.QPLLLQVSVQR.+2y8. (Light)	77.8	37.3
656.916	1055.657	40.5	LFTY1.QPLLLQVSVQR.+2y9. (Heavy)	77.8	37.3
654.904	1055.657	40.5	LFTY1.QPLLLQVSVQR.+2y9. (Light)	77.8	37.3
456.273	504.271	3.3	NANOG.NSNGVTQK.+2b5. (Heavy)	62	19.9
452.248	500.246	3.3	NANOG.NSNGVTQK.+2b5. (Light)	62	19.9
456.273	507.344	3.3	NANOG.NSNGVTQK.+2y4. (Heavy)	62	19.9
452.248	503.319	3.3	NANOG.NSNGVTQK.+2y4. (Light)	62	19.9
456.273	564.365	3.3	NANOG.NSNGVTQK.+2y5. (Heavy)	62	19.9
452.248	560.34	3.3	NANOG.NSNGVTQK.+2y5. (Light)	62	19.9
456.273	678.408	3.3	NANOG.NSNGVTQK.+2y6. (Heavy)	62	19.9

452.248	674.383	3.3	NANOG.NSNGVTQK.+2y6. (Light)	62	19.9
456.273	765.44	3.3	NANOG.NSNGVTQK.+2y7. (Heavy)	62	19.9
452.248	761.415	3.3	NANOG.NSNGVTQK.+2y7. (Light)	62	19.9
836.437	1205.594	41.8	NANOG.TVFSSTQLCVLNDR.+2y10. (Heavy)	90.9	41.5
834.425	1205.594	41.8	NANOG.TVFSSTQLCVLNDR.+2y10. (Light)	90.9	41.5
836.437	1292.626	41.8	NANOG.TVFSSTQLCVLNDR.+2y11. (Heavy)	90.9	39.5
834.425	1292.626	41.8	NANOG.TVFSSTQLCVLNDR.+2y11. (Light)	90.9	39.5
836.437	889.456	41.8	NANOG.TVFSSTQLCVLNDR.+2y7. (Heavy)	90.9	37.5
834.425	889.456	41.8	NANOG.TVFSSTQLCVLNDR.+2y7. (Light)	90.9	37.5
836.437	1017.515	41.8	NANOG.TVFSSTQLCVLNDR.+2y8. (Heavy)	90.9	39.5
834.425	1017.515	41.8	NANOG.TVFSSTQLCVLNDR.+2y8. (Light)	90.9	39.5
836.437	1118.562	41.8	NANOG.TVFSSTQLCVLNDR.+2y9. (Heavy)	90.9	39.5
834.425	1118.562	41.8	NANOG.TVFSSTQLCVLNDR.+2y9. (Light)	90.9	39.5
789.102	1196.719	58.7	NANOG.YLSLQQMQELSNILNLSYK.+3y10. (Heavy)	87.1	33.7
786.419	1192.694	58.7	NANOG.YLSLQQMQELSNILNLSYK.+3y10. (Light)	87.1	33.7
789.102	1325.761	58.7	NANOG.YLSLQQMQELSNILNLSYK.+3y11. (Heavy)	87.1	32.7
786.419	1321.736	58.7	NANOG.YLSLQQMQELSNILNLSYK.+3y11. (Light)	87.1	32.7
789.102	928.99	58.7	NANOG.YLSLQQMQELSNILNLSYK.+3y15+2. (Heavy)	87.1	25.7
786.419	926.977	58.7	NANOG.YLSLQQMQELSNILNLSYK.+3y15+2. (Light)	87.1	25.7
789.102	1029.048	58.7	NANOG.YLSLQQMQELSNILNLSYK.+3y17+2. (Heavy)	87.1	25.7
786.419	1027.035	58.7	NANOG.YLSLQQMQELSNILNLSYK.+3y17+2. (Light)	87.1	25.7
789.102	1083.635	58.7	NANOG.YLSLQQMQELSNILNLSYK.+3y9. (Heavy)	87.1	32.7
786.419	1079.609	58.7	NANOG.YLSLQQMQELSNILNLSYK.+3y9. (Light)	87.1	32.7
958	1242.655	46	NODAL.GQPSSPSPLAYMLSLYR.+2y10. (Heavy)	99.8	52
955.988	1242.655	46	NODAL.GQPSSPSPLAYMLSLYR.+2y10. (Light)	99.8	52
958	1329.687	46	NODAL.GQPSSPSPLAYMLSLYR.+2y11. (Heavy)	99.8	45
955.988	1329.687	46	NODAL.GQPSSPSPLAYMLSLYR.+2y11. (Light)	99.8	45
958	1426.74	46	NODAL.GQPSSPSPLAYMLSLYR.+2y12. (Heavy)	99.8	46
955.988	1426.74	46	NODAL.GQPSSPSPLAYMLSLYR.+2y12. (Light)	99.8	46
958	1513.772	46	NODAL.GQPSSPSPLAYMLSLYR.+2y13. (Heavy)	99.8	46
955.988	1513.772	46	NODAL.GQPSSPSPLAYMLSLYR.+2y13. (Light)	99.8	46
958	1032.518	46	NODAL.GQPSSPSPLAYMLSLYR.+2y8. (Heavy)	99.8	54
955.988	1032.518	46	NODAL.GQPSSPSPLAYMLSLYR.+2y8. (Light)	99.8	54
787.447	1183.578	30	NODAL.TKPLSMLYVDNGR.+2y10. (Heavy)	86.2	42.3
783.421	1183.578	30	NODAL.TKPLSMLYVDNGR.+2y10. (Light)	86.2	42.3
787.447	1280.63	30	NODAL.TKPLSMLYVDNGR.+2y11. (Heavy)	86.2	37.3
783.421	1280.63	30	NODAL.TKPLSMLYVDNGR.+2y11. (Light)	86.2	37.3
787.447	836.426	30	NODAL.TKPLSMLYVDNGR.+2y7. (Heavy)	86.2	42.3
783.421	836.426	30	NODAL.TKPLSMLYVDNGR.+2y7. (Light)	86.2	42.3
787.447	983.461	30	NODAL.TKPLSMLYVDNGR.+2y8. (Heavy)	86.2	41.3
783.421	983.461	30	NODAL.TKPLSMLYVDNGR.+2y8. (Light)	86.2	41.3

787.447	1070.494	30	NODAL.TKPLSMLYVDNGR.+2y9. (Heavy)	86.2	42.3
783.421	1070.494	30	NODAL.TKPLSMLYVDNGR.+2y9. (Light)	86.2	42.3
591.827	606.358	31	NODAL.VPSTCCAPVK.+2y5. (Heavy)	71.9	32.6
587.802	602.333	31	NODAL.VPSTCCAPVK.+2y5. (Light)	71.9	32.6
591.827	766.389	31	NODAL.VPSTCCAPVK.+2y6. (Heavy)	71.9	30.6
587.802	762.364	31	NODAL.VPSTCCAPVK.+2y6. (Light)	71.9	30.6
591.827	867.436	31	NODAL.VPSTCCAPVK.+2y7. (Heavy)	71.9	31.6
587.802	863.411	31	NODAL.VPSTCCAPVK.+2y7. (Light)	71.9	31.6
591.827	954.469	31	NODAL.VPSTCCAPVK.+2y8. (Heavy)	71.9	29.6
587.802	950.443	31	NODAL.VPSTCCAPVK.+2y8. (Light)	71.9	29.6
591.827	1051.521	31	NODAL.VPSTCCAPVK.+2y9. (Heavy)	71.9	29.6
587.802	1047.496	31	NODAL.VPSTCCAPVK.+2y9. (Light)	71.9	29.6
686.342	1211.529	43.6	NOTC1.FEEPVVLPDLDDQTDHR.+3y10. (Heavy)	80.4	33
685.001	1211.529	43.6	NOTC1.FEEPVVLPDLDDQTDHR.+3y10. (Light)	80.4	33
686.342	712.344	43.6	NOTC1.FEEPVVLPDLDDQTDHR.+3y12+2. (Heavy)	80.4	30
685.001	712.344	43.6	NOTC1.FEEPVVLPDLDDQTDHR.+3y12+2. (Light)	80.4	30
686.342	761.878	43.6	NOTC1.FEEPVVLPDLDDQTDHR.+3y13+2. (Heavy)	80.4	29
685.001	761.878	43.6	NOTC1.FEEPVVLPDLDDQTDHR.+3y13+2. (Light)	80.4	29
686.342	810.405	43.6	NOTC1.FEEPVVLPDLDDQTDHR.+3y14+2. (Heavy)	80.4	27
685.001	810.405	43.6	NOTC1.FEEPVVLPDLDDQTDHR.+3y14+2. (Light)	80.4	27
686.342	874.926	43.6	NOTC1.FEEPVVLPDLDDQTDHR.+3y15+2. (Heavy)	80.4	25
685.001	874.926	43.6	NOTC1.FEEPVVLPDLDDQTDHR.+3y15+2. (Light)	80.4	25
655.866	646.315	42.3	NOTC1.GSIVYLEIDNR.+2y5. (Heavy)	77.8	27.2
653.854	646.315	42.3	NOTC1.GSIVYLEIDNR.+2y5. (Light)	77.8	27.2
655.866	759.4	42.3	NOTC1.GSIVYLEIDNR.+2y6. (Heavy)	77.8	28.2
653.854	759.4	42.3	NOTC1.GSIVYLEIDNR.+2y6. (Light)	77.8	28.2
655.866	922.463	42.3	NOTC1.GSIVYLEIDNR.+2y7. (Heavy)	77.8	30.2
653.854	922.463	42.3	NOTC1.GSIVYLEIDNR.+2y7. (Light)	77.8	30.2
655.866	1021.531	42.3	NOTC1.GSIVYLEIDNR.+2y8. (Heavy)	77.8	29.2
653.854	1021.531	42.3	NOTC1.GSIVYLEIDNR.+2y8. (Light)	77.8	29.2
655.866	1134.615	42.3	NOTC1.GSIVYLEIDNR.+2y9. (Heavy)	77.8	32.2
653.854	1134.615	42.3	NOTC1.GSIVYLEIDNR.+2y9. (Light)	77.8	32.2
824.939	1287.68	45	NOTC1.NGGTCDLLTLTEYK.+2y10. (Heavy)	88.9	35.9
820.914	1283.655	45	NOTC1.NGGTCDLLTLTEYK.+2y10. (Light)	88.9	35.9
824.939	1388.728	45	NOTC1.NGGTCDLLTLTEYK.+2y11. (Heavy)	88.9	36.9
820.914	1384.703	45	NOTC1.NGGTCDLLTLTEYK.+2y11. (Light)	88.9	36.9
824.939	899.539	45	NOTC1.NGGTCDLLTLTEYK.+2y7. (Heavy)	88.9	36.9
820.914	895.513	45	NOTC1.NGGTCDLLTLTEYK.+2y7. (Light)	88.9	36.9
824.939	1012.623	45	NOTC1.NGGTCDLLTLTEYK.+2y8. (Heavy)	88.9	38.9
820.914	1008.598	45	NOTC1.NGGTCDLLTLTEYK.+2y8. (Light)	88.9	38.9
824.939	1127.65	45	NOTC1.NGGTCDLLTLTEYK.+2y9. (Heavy)	88.9	38.9

820.914	1123.625	45	NOTC1.NGGTCDLLTLTEYK.+2y9. (Light)	88.9	38.9
365.565	463.322	26.2	P53.LGFLHSGTAK.+3b4. (Heavy)	56.2	15.8
362.882	459.297	26.2	P53.LGFLHSGTAK.+3b4. (Light)	56.2	15.8
365.565	495.307	26.2	P53.LGFLHSGTAK.+3y5. (Heavy)	56.2	17.8
362.882	491.282	26.2	P53.LGFLHSGTAK.+3y5. (Light)	56.2	17.8
365.565	632.366	26.2	P53.LGFLHSGTAK.+3y6. (Heavy)	56.2	19.8
362.882	628.341	26.2	P53.LGFLHSGTAK.+3y6. (Light)	56.2	19.8
365.565	446.763	26.2	P53.LGFLHSGTAK.+3y8+2. (Heavy)	56.2	16.8
362.882	444.751	26.2	P53.LGFLHSGTAK.+3y8+2. (Light)	56.2	16.8
365.565	475.274	26.2	P53.LGFLHSGTAK.+3y9+2. (Heavy)	56.2	16.8
362.882	473.261	26.2	P53.LGFLHSGTAK.+3y9+2. (Light)	56.2	16.8
700.749	839.602	54.4	P53.RPILTIITLEDSSGNLLGR.+3b7. (Heavy)	81.4	32.5
699.407	835.576	54.4	P53.RPILTIITLEDSSGNLLGR.+3b7. (Light)	81.4	32.5
700.749	1047.506	54.4	P53.RPILTIITLEDSSGNLLGR.+3y10. (Heavy)	81.4	30.5
699.407	1047.506	54.4	P53.RPILTIITLEDSSGNLLGR.+3y10. (Light)	81.4	30.5
700.749	716.405	54.4	P53.RPILTIITLEDSSGNLLGR.+3y7. (Heavy)	81.4	28.5
699.407	716.405	54.4	P53.RPILTIITLEDSSGNLLGR.+3y7. (Light)	81.4	28.5
700.749	803.437	54.4	P53.RPILTIITLEDSSGNLLGR.+3y8. (Heavy)	81.4	30.5
699.407	803.437	54.4	P53.RPILTIITLEDSSGNLLGR.+3y8. (Light)	81.4	30.5
700.749	918.464	54.4	P53.RPILTIITLEDSSGNLLGR.+3y9. (Heavy)	81.4	30.5
699.407	918.464	54.4	P53.RPILTIITLEDSSGNLLGR.+3y9. (Light)	81.4	30.5
702.886	831.385	28.5	P53.SVTCTYSPALNK.+2b7. (Heavy)	80	29
698.861	827.36	28.5	P53.SVTCTYSPALNK.+2b7. (Light)	80	29
702.886	1186.607	28.5	P53.SVTCTYSPALNK.+2y10. (Heavy)	80	31
698.861	1182.582	28.5	P53.SVTCTYSPALNK.+2y10. (Light)	80	31
702.886	824.481	28.5	P53.SVTCTYSPALNK.+2y7. (Heavy)	80	29
698.861	820.456	28.5	P53.SVTCTYSPALNK.+2y7. (Light)	80	29
702.886	925.529	28.5	P53.SVTCTYSPALNK.+2y8. (Heavy)	80	31
698.861	921.504	28.5	P53.SVTCTYSPALNK.+2y8. (Light)	80	31
702.886	1085.56	28.5	P53.SVTCTYSPALNK.+2y9. (Heavy)	80	31
698.861	1081.535	28.5	P53.SVTCTYSPALNK.+2y9. (Light)	80	31
573.854	968.539	44	PO5F1.FEALQLSFK.+2b8. (Heavy)	70.6	25.6
569.829	964.514	44	PO5F1.FEALQLSFK.+2b8. (Light)	70.6	25.6
573.854	654.412	44	PO5F1.FEALQLSFK.+2y5. (Heavy)	70.6	24.6
569.829	650.387	44	PO5F1.FEALQLSFK.+2y5. (Light)	70.6	24.6
573.854	767.496	44	PO5F1.FEALQLSFK.+2y6. (Heavy)	70.6	25.6
569.829	763.471	44	PO5F1.FEALQLSFK.+2y6. (Light)	70.6	25.6
573.854	838.533	44	PO5F1.FEALQLSFK.+2y7. (Heavy)	70.6	24.6
569.829	834.508	44	PO5F1.FEALQLSFK.+2y7. (Light)	70.6	24.6
573.854	967.576	44	PO5F1.FEALQLSFK.+2y8. (Heavy)	70.6	27.6
569.829	963.551	44	PO5F1.FEALQLSFK.+2y8. (Light)	70.6	27.6

747.4	1219.61	23	PO5F1.LEQNPEESQDIK.+2y10. (Heavy)	83.3	33.5
743.375	1215.585	23	PO5F1.LEQNPEESQDIK.+2y10. (Light)	83.3	33.5
747.4	751.413	23	PO5F1.LEQNPEESQDIK.+2y6. (Heavy)	83.3	39.5
743.375	747.388	23	PO5F1.LEQNPEESQDIK.+2y6. (Light)	83.3	39.5
747.4	880.456	23	PO5F1.LEQNPEESQDIK.+2y7. (Heavy)	83.3	39.5
743.375	876.431	23	PO5F1.LEQNPEESQDIK.+2y7. (Light)	83.3	39.5
747.4	977.509	23	PO5F1.LEQNPEESQDIK.+2y8. (Heavy)	83.3	35.5
743.375	973.484	23	PO5F1.LEQNPEESQDIK.+2y8. (Light)	83.3	35.5
747.4	1091.552	23	PO5F1.LEQNPEESQDIK.+2y9. (Heavy)	83.3	35.5
743.375	1087.527	23	PO5F1.LEQNPEESQDIK.+2y9. (Light)	83.3	35.5
1028.001	1293.641	34.1	PO5F1.WVEEADNNENLQEICK.+2y10. (Heavy)	103.7	48.5
1023.975	1289.615	34.1	PO5F1.WVEEADNNENLQEICK.+2y10. (Light)	103.7	48.5
1028.001	1408.667	34.1	PO5F1.WVEEADNNENLQEICK.+2y11. (Heavy)	103.7	47.5
1023.975	1404.642	34.1	PO5F1.WVEEADNNENLQEICK.+2y11. (Light)	103.7	47.5
1028.001	1479.705	34.1	PO5F1.WVEEADNNENLQEICK.+2y12. (Heavy)	103.7	47.5
1023.975	1475.679	34.1	PO5F1.WVEEADNNENLQEICK.+2y12. (Light)	103.7	47.5
1028.001	1065.555	34.1	PO5F1.WVEEADNNENLQEICK.+2y8. (Heavy)	103.7	47.5
1023.975	1061.53	34.1	PO5F1.WVEEADNNENLQEICK.+2y8. (Light)	103.7	47.5
1028.001	1179.598	34.1	PO5F1.WVEEADNNENLQEICK.+2y9. (Heavy)	103.7	48.5
1023.975	1175.573	34.1	PO5F1.WVEEADNNENLQEICK.+2y9. (Light)	103.7	48.5
752.937	1064.573	31.7	PTC1.LPTPSPEPPPSVVR.+2y10. (Heavy)	84.8	42.7
750.925	1064.573	31.7	PTC1.LPTPSPEPPPSVVR.+2y10. (Light)	84.8	42.7
752.937	1161.626	31.7	PTC1.LPTPSPEPPPSVVR.+2y11. (Heavy)	84.8	40.7
750.925	1161.626	31.7	PTC1.LPTPSPEPPPSVVR.+2y11. (Light)	84.8	40.7
752.937	1262.674	31.7	PTC1.LPTPSPEPPPSVVR.+2y12. (Heavy)	84.8	40.7
750.925	1262.674	31.7	PTC1.LPTPSPEPPPSVVR.+2y12. (Light)	84.8	40.7
752.937	880.489	31.7	PTC1.LPTPSPEPPPSVVR.+2y8. (Heavy)	84.8	42.7
750.925	880.489	31.7	PTC1.LPTPSPEPPPSVVR.+2y8. (Light)	84.8	42.7
752.937	977.541	31.7	PTC1.LPTPSPEPPPSVVR.+2y9. (Heavy)	84.8	42.7
750.925	977.541	31.7	PTC1.LPTPSPEPPPSVVR.+2y9. (Light)	84.8	42.7
704.671	786.384	28.2	PTC1.TEYDPHTHVYYTTAEPR.+3y13+2. (Heavy)	81.7	32.6
703.329	786.384	28.2	PTC1.TEYDPHTHVYYTTAEPR.+3y13+2. (Light)	81.7	32.6
704.671	843.897	28.2	PTC1.TEYDPHTHVYYTTAEPR.+3y14+2. (Heavy)	81.7	29.6
703.329	843.897	28.2	PTC1.TEYDPHTHVYYTTAEPR.+3y14+2. (Light)	81.7	29.6
704.671	925.429	28.2	PTC1.TEYDPHTHVYYTTAEPR.+3y15+2. (Heavy)	81.7	29.6
703.329	925.429	28.2	PTC1.TEYDPHTHVYYTTAEPR.+3y15+2. (Light)	81.7	29.6
704.671	837.41	28.2	PTC1.TEYDPHTHVYYTTAEPR.+3y7. (Heavy)	81.7	33.6
703.329	837.41	28.2	PTC1.TEYDPHTHVYYTTAEPR.+3y7. (Light)	81.7	33.6
704.671	1000.473	28.2	PTC1.TEYDPHTHVYYTTAEPR.+3y8. (Heavy)	81.7	33.6
703.329	1000.473	28.2	PTC1.TEYDPHTHVYYTTAEPR.+3y8. (Light)	81.7	33.6
661.365	679.87	27.7	PTC1.TYVEVVHQSVAQNSTQK.+3y12+2. (Heavy)	77.8	26.9

658.681	677.857	27.7	PTC1.TYVEVVHQSVAQNSTQK.+3y12+2. (Light)	77.8	26.9
661.365	729.404	27.7	PTC1.TYVEVVHQSVAQNSTQK.+3y13+2. (Heavy)	77.8	27.9
658.681	727.392	27.7	PTC1.TYVEVVHQSVAQNSTQK.+3y13+2. (Light)	77.8	27.9
661.365	793.925	27.7	PTC1.TYVEVVHQSVAQNSTQK.+3y14+2. (Heavy)	77.8	26.9
658.681	791.913	27.7	PTC1.TYVEVVHQSVAQNSTQK.+3y14+2. (Light)	77.8	26.9
661.365	843.46	27.7	PTC1.TYVEVVHQSVAQNSTQK.+3y15+2. (Heavy)	77.8	26.9
658.681	841.447	27.7	PTC1.TYVEVVHQSVAQNSTQK.+3y15+2. (Light)	77.8	26.9
661.365	808.446	27.7	PTC1.TYVEVVHQSVAQNSTQK.+3y7. (Heavy)	77.8	23.9
658.681	804.421	27.7	PTC1.TYVEVVHQSVAQNSTQK.+3y7. (Light)	77.8	23.9
662.032	690.851	38.1	SFRP1.FYTKPPQCVDIPADLR.+3y12+2. (Heavy)	77.8	31.9
659.349	690.851	38.1	SFRP1.FYTKPPQCVDIPADLR.+3y12+2. (Light)	77.8	31.9
662.032	770.926	38.1	SFRP1.FYTKPPQCVDIPADLR.+3y13+2. (Heavy)	77.8	26.9
659.349	768.914	38.1	SFRP1.FYTKPPQCVDIPADLR.+3y13+2. (Light)	77.8	26.9
662.032	821.45	38.1	SFRP1.FYTKPPQCVDIPADLR.+3y14+2. (Heavy)	77.8	24.9
659.349	819.438	38.1	SFRP1.FYTKPPQCVDIPADLR.+3y14+2. (Light)	77.8	24.9
662.032	902.982	38.1	SFRP1.FYTKPPQCVDIPADLR.+3y15+2. (Heavy)	77.8	27.9
659.349	900.969	38.1	SFRP1.FYTKPPQCVDIPADLR.+3y15+2. (Light)	77.8	27.9
662.032	799.431	38.1	SFRP1.FYTKPPQCVDIPADLR.+3y7. (Heavy)	77.8	28.9
659.349	799.431	38.1	SFRP1.FYTKPPQCVDIPADLR.+3y7. (Light)	77.8	28.9
626.662	795.892	45.3	SFRP1.SEAIIEHLCASEFALR.+3b14+2. (Heavy)	76	26.2
625.321	793.88	45.3	SFRP1.SEAIIEHLCASEFALR.+3b14+2. (Light)	76	26.2
626.662	666.822	45.3	SFRP1.SEAIIEHLCASEFALR.+3y11+2. (Heavy)	76	26.2
625.321	666.822	45.3	SFRP1.SEAIIEHLCASEFALR.+3y11+2. (Light)	76	26.2
626.662	723.364	45.3	SFRP1.SEAIIEHLCASEFALR.+3y12+2. (Heavy)	76	25.2
625.321	723.364	45.3	SFRP1.SEAIIEHLCASEFALR.+3y12+2. (Light)	76	25.2
626.662	953.451	45.3	SFRP1.SEAIIEHLCASEFALR.+3y8. (Heavy)	76	31.2
625.321	953.451	45.3	SFRP1.SEAIIEHLCASEFALR.+3y8. (Light)	76	31.2
626.662	1066.535	45.3	SFRP1.SEAIIEHLCASEFALR.+3y9. (Heavy)	76	30.2
625.321	1066.535	45.3	SFRP1.SEAIIEHLCASEFALR.+3y9. (Light)	76	30.2
413.263	429.312	31.2	SFRP1.SQYLLTAIHK.+3y3. (Heavy)	59.7	22.2
410.58	425.287	31.2	SFRP1.SQYLLTAIHK.+3y3. (Light)	59.7	22.2
413.263	500.349	31.2	SFRP1.SQYLLTAIHK.+3y4. (Heavy)	59.7	20.2
410.58	496.324	31.2	SFRP1.SQYLLTAIHK.+3y4. (Light)	59.7	20.2
413.263	601.397	31.2	SFRP1.SQYLLTAIHK.+3y5. (Heavy)	59.7	19.2
410.58	597.372	31.2	SFRP1.SQYLLTAIHK.+3y5. (Light)	59.7	19.2
413.263	714.481	31.2	SFRP1.SQYLLTAIHK.+3y6. (Heavy)	59.7	19.2
410.58	710.456	31.2	SFRP1.SQYLLTAIHK.+3y6. (Light)	59.7	19.2
413.263	495.818	31.2	SFRP1.SQYLLTAIHK.+3y8+2. (Heavy)	59.7	16.2
410.58	493.805	31.2	SFRP1.SQYLLTAIHK.+3y8+2. (Light)	59.7	16.2
938.096	1168.633	41.5	SFRP2.DSLQCTCEEMNDINAPYLVMGQK.+3y10. (Heavy)	97.9	30.2
935.413	1164.608	41.5	SFRP2.DSLQCTCEEMNDINAPYLVMGQK.+3y10. (Light)	97.9	30.2

938.096	1281.717	41.5	SFRP2.DSLQCTCEEMNDINAPYLVMGQK.+3y11. (Heavy)	97.9	36.2
935.413	1277.692	41.5	SFRP2.DSLQCTCEEMNDINAPYLVMGQK.+3y11. (Light)	97.9	36.2
938.096	1038.473	41.5	SFRP2.DSLQCTCEEMNDINAPYLVMGQK.+3y17+2. (Heavy)	97.9	34.2
935.413	1036.46	41.5	SFRP2.DSLQCTCEEMNDINAPYLVMGQK.+3y17+2. (Light)	97.9	34.2
938.096	983.553	41.5	SFRP2.DSLQCTCEEMNDINAPYLVMGQK.+3y8. (Heavy)	97.9	33.2
935.413	979.528	41.5	SFRP2.DSLQCTCEEMNDINAPYLVMGQK.+3y8. (Light)	97.9	33.2
938.096	1054.59	41.5	SFRP2.DSLQCTCEEMNDINAPYLVMGQK.+3y9. (Heavy)	97.9	30.2
935.413	1050.565	41.5	SFRP2.DSLQCTCEEMNDINAPYLVMGQK.+3y9. (Light)	97.9	30.2
882.514	1133.669	53.6	SFRP2.EVLEQAGAWIPLVMK.+2y10. (Heavy)	93.1	40.8
878.489	1129.644	53.6	SFRP2.EVLEQAGAWIPLVMK.+2y10. (Light)	93.1	40.8
882.514	1261.728	53.6	SFRP2.EVLEQAGAWIPLVMK.+2y11. (Heavy)	93.1	39.8
878.489	1257.702	53.6	SFRP2.EVLEQAGAWIPLVMK.+2y11. (Light)	93.1	39.8
882.514	934.573	53.6	SFRP2.EVLEQAGAWIPLVMK.+2y7. (Heavy)	93.1	38.8
878.489	930.548	53.6	SFRP2.EVLEQAGAWIPLVMK.+2y7. (Light)	93.1	38.8
882.514	1005.61	53.6	SFRP2.EVLEQAGAWIPLVMK.+2y8. (Heavy)	93.1	39.8
878.489	1001.585	53.6	SFRP2.EVLEQAGAWIPLVMK.+2y8. (Light)	93.1	39.8
882.514	1062.632	53.6	SFRP2.EVLEQAGAWIPLVMK.+2y9. (Heavy)	93.1	41.8
878.489	1058.607	53.6	SFRP2.EVLEQAGAWIPLVMK.+2y9. (Light)	93.1	41.8
444.931	594.323	30.1	SFRP2.LPNLLGHETMK.+3y10+2. (Heavy)	62	20
442.248	592.311	30.1	SFRP2.LPNLLGHETMK.+3y10+2. (Light)	62	20
444.931	556.295	30.1	SFRP2.LPNLLGHETMK.+3y4. (Heavy)	62	25
442.248	552.27	30.1	SFRP2.LPNLLGHETMK.+3y4. (Light)	62	25
444.931	750.375	30.1	SFRP2.LPNLLGHETMK.+3y6. (Heavy)	62	24
442.248	746.35	30.1	SFRP2.LPNLLGHETMK.+3y6. (Light)	62	24
444.931	863.459	30.1	SFRP2.LPNLLGHETMK.+3y7. (Heavy)	62	23
442.248	859.434	30.1	SFRP2.LPNLLGHETMK.+3y7. (Light)	62	23
444.931	545.797	30.1	SFRP2.LPNLLGHETMK.+3y9+2. (Heavy)	62	20
442.248	543.784	30.1	SFRP2.LPNLLGHETMK.+3y9+2. (Light)	62	20
814.463	1252.687	47.5	SHH.ELTPNYNPDIIFK.+2y10. (Heavy)	88.2	35.3
810.438	1248.662	47.5	SHH.ELTPNYNPDIIFK.+2y10. (Light)	88.2	35.3
814.463	1353.735	47.5	SHH.ELTPNYNPDIIFK.+2y11. (Heavy)	88.2	36.3
810.438	1349.71	47.5	SHH.ELTPNYNPDIIFK.+2y11. (Light)	88.2	36.3
814.463	878.528	47.5	SHH.ELTPNYNPDIIFK.+2y7. (Heavy)	88.2	35.3
810.438	874.503	47.5	SHH.ELTPNYNPDIIFK.+2y7. (Light)	88.2	35.3
814.463	1041.592	47.5	SHH.ELTPNYNPDIIFK.+2y8. (Heavy)	88.2	40.3
810.438	1037.567	47.5	SHH.ELTPNYNPDIIFK.+2y8. (Light)	88.2	40.3
814.463	1155.635	47.5	SHH.ELTPNYNPDIIFK.+2y9. (Heavy)	88.2	41.3
810.438	1151.609	47.5	SHH.ELTPNYNPDIIFK.+2y9. (Light)	88.2	41.3
660.427	966.609	33.5	SHH.LAHALLAALAPAR.+2y10. (Heavy)	78.1	36.5
658.414	966.609	33.5	SHH.LAHALLAALAPAR.+2y10. (Light)	78.1	36.5
660.427	1103.668	33.5	SHH.LAHALLAALAPAR.+2y11. (Heavy)	78.1	35.5

658.414	1103.668	33.5	SHH.LAHALLAALAPAR.+2y11. (Light)	78.1	35.5
660.427	669.404	33.5	SHH.LAHALLAALAPAR.+2y7. (Heavy)	78.1	35.5
658.414	669.404	33.5	SHH.LAHALLAALAPAR.+2y7. (Light)	78.1	35.5
660.427	782.488	33.5	SHH.LAHALLAALAPAR.+2y8. (Heavy)	78.1	35.5
658.414	782.488	33.5	SHH.LAHALLAALAPAR.+2y8. (Light)	78.1	35.5
660.427	895.572	33.5	SHH.LAHALLAALAPAR.+2y9. (Heavy)	78.1	35.5
658.414	895.572	33.5	SHH.LAHALLAALAPAR.+2y9. (Light)	78.1	35.5
652.003	780.874	29.4	SHH.SGGCFPGSATVHLEQGGTK.+3b15+2. (Heavy)	77.1	30.6
649.319	778.862	29.4	SHH.SGGCFPGSATVHLEQGGTK.+3b15+2. (Light)	77.1	30.6
652.003	658.859	29.4	SHH.SGGCFPGSATVHLEQGGTK.+3y13+2. (Heavy)	77.1	30.6
649.319	656.846	29.4	SHH.SGGCFPGSATVHLEQGGTK.+3y13+2. (Light)	77.1	30.6
652.003	707.385	29.4	SHH.SGGCFPGSATVHLEQGGTK.+3y14+2. (Heavy)	77.1	28.6
649.319	705.373	29.4	SHH.SGGCFPGSATVHLEQGGTK.+3y14+2. (Light)	77.1	28.6
652.003	780.92	29.4	SHH.SGGCFPGSATVHLEQGGTK.+3y15+2. (Heavy)	77.1	30.6
649.319	778.907	29.4	SHH.SGGCFPGSATVHLEQGGTK.+3y15+2. (Light)	77.1	30.6
652.003	901.504	29.4	SHH.SGGCFPGSATVHLEQGGTK.+3y8. (Heavy)	77.1	31.6
649.319	897.479	29.4	SHH.SGGCFPGSATVHLEQGGTK.+3y8. (Light)	77.1	31.6
928.526	1045.655	49	SMO.DYVLCQANVTIGLPTK.+2y10. (Heavy)	96.5	41.8
924.5	1041.63	49	SMO.DYVLCQANVTIGLPTK.+2y10. (Light)	96.5	41.8
928.526	1173.714	49	SMO.DYVLCQANVTIGLPTK.+2y11. (Heavy)	96.5	41.8
924.5	1169.689	49	SMO.DYVLCQANVTIGLPTK.+2y11. (Light)	96.5	41.8
928.526	1333.745	49	SMO.DYVLCQANVTIGLPTK.+2y12. (Heavy)	96.5	41.8
924.5	1329.719	49	SMO.DYVLCQANVTIGLPTK.+2y12. (Light)	96.5	41.8
928.526	1446.829	49	SMO.DYVLCQANVTIGLPTK.+2y13. (Heavy)	96.5	41.8
924.5	1442.804	49	SMO.DYVLCQANVTIGLPTK.+2y13. (Light)	96.5	41.8
928.526	974.618	49	SMO.DYVLCQANVTIGLPTK.+2y9. (Heavy)	96.5	41.8
924.5	970.593	49	SMO.DYVLCQANVTIGLPTK.+2y9. (Light)	96.5	41.8
762.892	1144.578	31	SMO.FNSSGQCEVPLVR.+2y10. (Heavy)	85.6	39.3
760.88	1144.578	31	SMO.FNSSGQCEVPLVR.+2y10. (Light)	85.6	39.3
762.892	1231.61	31	SMO.FNSSGQCEVPLVR.+2y11. (Heavy)	85.6	36.3
760.88	1231.61	31	SMO.FNSSGQCEVPLVR.+2y11. (Light)	85.6	36.3
762.892	872.466	31	SMO.FNSSGQCEVPLVR.+2y7. (Heavy)	85.6	39.3
760.88	872.466	31	SMO.FNSSGQCEVPLVR.+2y7. (Light)	85.6	39.3
762.892	1000.524	31	SMO.FNSSGQCEVPLVR.+2y8. (Heavy)	85.6	38.3
760.88	1000.524	31	SMO.FNSSGQCEVPLVR.+2y8. (Light)	85.6	38.3
762.892	1057.546	31	SMO.FNSSGQCEVPLVR.+2y9. (Heavy)	85.6	41.3
760.88	1057.546	31	SMO.FNSSGQCEVPLVR.+2y9. (Light)	85.6	41.3
616.32	913.449	16.9	SMO.GAASSGNATGPGPR.+2y10. (Heavy)	74.9	30
614.307	913.449	16.9	SMO.GAASSGNATGPGPR.+2y10. (Light)	74.9	30
616.32	1000.481	16.9	SMO.GAASSGNATGPGPR.+2y11. (Heavy)	74.9	31
614.307	1000.481	16.9	SMO.GAASSGNATGPGPR.+2y11. (Light)	74.9	31

616.32	1071.518	16.9	SMO.GAASSGNATGPGPR.+2y12. (Heavy)	74.9	32
614.307	1071.518	16.9	SMO.GAASSGNATGPGPR.+2y12. (Light)	74.9	32
616.32	769.395	16.9	SMO.GAASSGNATGPGPR.+2y8. (Heavy)	74.9	31
614.307	769.395	16.9	SMO.GAASSGNATGPGPR.+2y8. (Light)	74.9	31
616.32	826.417	16.9	SMO.GAASSGNATGPGPR.+2y9. (Heavy)	74.9	31
614.307	826.417	16.9	SMO.GAASSGNATGPGPR.+2y9. (Light)	74.9	31
749.914	951.541	28	SUFU.GIETDGSNLSGVSAK.+2y10. (Heavy)	83.4	33.7
745.888	947.516	28	SUFU.GIETDGSNLSGVSAK.+2y10. (Light)	83.4	33.7
749.914	1066.568	28	SUFU.GIETDGSNLSGVSAK.+2y11. (Heavy)	83.4	33.7
745.888	1062.543	28	SUFU.GIETDGSNLSGVSAK.+2y11. (Light)	83.4	33.7
749.914	1167.615	28	SUFU.GIETDGSNLSGVSAK.+2y12. (Heavy)	83.4	33.7
745.888	1163.59	28	SUFU.GIETDGSNLSGVSAK.+2y12. (Light)	83.4	33.7
749.914	1296.658	28	SUFU.GIETDGSNLSGVSAK.+2y13. (Heavy)	83.4	33.7
745.888	1292.633	28	SUFU.GIETDGSNLSGVSAK.+2y13. (Light)	83.4	33.7
749.914	807.487	28	SUFU.GIETDGSNLSGVSAK.+2y8. (Heavy)	83.4	33.7
745.888	803.462	28	SUFU.GIETDGSNLSGVSAK.+2y8. (Light)	83.4	33.7
646.066	1115.727	38.8	SUFU.GLEINSKPVLPPINPQR.+3b10. (Heavy)	76.7	23.4
643.382	1107.677	38.8	SUFU.GLEINSKPVLPPINPQR.+3b10. (Light)	76.7	23.4
646.066	746.451	38.8	SUFU.GLEINSKPVLPPINPQR.+3y13+2. (Heavy)	76.7	23.4
643.382	744.438	38.8	SUFU.GLEINSKPVLPPINPQR.+3y13+2. (Light)	76.7	23.4
646.066	802.993	38.8	SUFU.GLEINSKPVLPPINPQR.+3y14+2. (Heavy)	76.7	24.4
643.382	800.98	38.8	SUFU.GLEINSKPVLPPINPQR.+3y14+2. (Light)	76.7	24.4
646.066	724.41	38.8	SUFU.GLEINSKPVLPPINPQR.+3y6. (Heavy)	76.7	30.4
643.382	724.41	38.8	SUFU.GLEINSKPVLPPINPQR.+3y6. (Light)	76.7	30.4
646.066	821.463	38.8	SUFU.GLEINSKPVLPPINPQR.+3y7. (Heavy)	76.7	24.4
643.382	821.463	38.8	SUFU.GLEINSKPVLPPINPQR.+3y7. (Light)	76.7	24.4
745.034	976.467	50.9	SUFU.VHEFTGTDGPSGFGFELTFR.+3b9. (Heavy)	84.7	30.8
743.692	972.442	50.9	SUFU.VHEFTGTDGPSGFGFELTFR.+3b9. (Light)	84.7	30.8
745.034	812.43	50.9	SUFU.VHEFTGTDGPSGFGFELTFR.+3y6. (Heavy)	84.7	28.8
743.692	812.43	50.9	SUFU.VHEFTGTDGPSGFGFELTFR.+3y6. (Light)	84.7	28.8
745.034	869.452	50.9	SUFU.VHEFTGTDGPSGFGFELTFR.+3y7. (Heavy)	84.7	30.8
743.692	869.452	50.9	SUFU.VHEFTGTDGPSGFGFELTFR.+3y7. (Light)	84.7	30.8
745.034	1016.52	50.9	SUFU.VHEFTGTDGPSGFGFELTFR.+3y8. (Heavy)	84.7	30.8
743.692	1016.52	50.9	SUFU.VHEFTGTDGPSGFGFELTFR.+3y8. (Light)	84.7	30.8
745.034	1073.542	50.9	SUFU.VHEFTGTDGPSGFGFELTFR.+3y9. (Heavy)	84.7	33.8
743.692	1073.542	50.9	SUFU.VHEFTGTDGPSGFGFELTFR.+3y9. (Light)	84.7	33.8
614.321	746.407	37.6	TDGF1.DDSIWPQEEPAIRPR.+3y12+2. (Heavy)	75.1	23.8
612.979	746.407	37.6	TDGF1.DDSIWPQEEPAIRPR.+3y12+2. (Light)	75.1	23.8
614.321	789.923	37.6	TDGF1.DDSIWPQEEPAIRPR.+3y13+2. (Heavy)	75.1	21.8
612.979	789.923	37.6	TDGF1.DDSIWPQEEPAIRPR.+3y13+2. (Light)	75.1	21.8
614.321	847.436	37.6	TDGF1.DDSIWPQEEPAIRPR.+3y14+2. (Heavy)	75.1	26.8

612.979	847.436	37.6	TDGF1.DDSIWPQEEPAIRPR.+3y14+2. (Light)	75.1	26.8
614.321	838.489	37.6	TDGF1.DDSIWPQEEPAIRPR.+3y7. (Heavy)	75.1	30.8
612.979	838.489	37.6	TDGF1.DDSIWPQEEPAIRPR.+3y7. (Light)	75.1	30.8
614.321	1095.591	37.6	TDGF1.DDSIWPQEEPAIRPR.+3y9. (Heavy)	75.1	30.8
612.979	1095.591	37.6	TDGF1.DDSIWPQEEPAIRPR.+3y9. (Light)	75.1	30.8
812.967	1195.706	69	TDGF1.FSYSVIWIMAISK.+2y10. (Heavy)	88	40.2
808.941	1191.681	69	TDGF1.FSYSVIWIMAISK.+2y10. (Light)	88	40.2
812.967	1358.769	69	TDGF1.FSYSVIWIMAISK.+2y11. (Heavy)	88	40.2
808.941	1354.744	69	TDGF1.FSYSVIWIMAISK.+2y11. (Light)	88	40.2
812.967	896.521	69	TDGF1.FSYSVIWIMAISK.+2y7. (Heavy)	88	39.8
808.941	892.496	69	TDGF1.FSYSVIWIMAISK.+2y7. (Light)	88	39.8
812.967	1009.605	69	TDGF1.FSYSVIWIMAISK.+2y8. (Heavy)	88	40.2
808.941	1005.58	69	TDGF1.FSYSVIWIMAISK.+2y8. (Light)	88	40.2
812.967	1108.674	69	TDGF1.FSYSVIWIMAISK.+2y9. (Heavy)	88	37.8
808.941	1104.649	69	TDGF1.FSYSVIWIMAISK.+2y9. (Light)	88	37.8
500.292	570.344	23.5	TDGF1.TPELPPSAR.+2b5. (Heavy)	66.4	23.3
498.28	566.318	23.5	TDGF1.TPELPPSAR.+2b5. (Light)	66.4	23.3
500.292	527.294	23.5	TDGF1.TPELPPSAR.+2y5. (Heavy)	66.4	27.3
498.28	527.294	23.5	TDGF1.TPELPPSAR.+2y5. (Light)	66.4	27.3
500.292	640.378	23.5	TDGF1.TPELPPSAR.+2y6. (Heavy)	66.4	27.3
498.28	640.378	23.5	TDGF1.TPELPPSAR.+2y6. (Light)	66.4	27.3
500.292	769.42	23.5	TDGF1.TPELPPSAR.+2y7. (Heavy)	66.4	27.3
498.28	769.42	23.5	TDGF1.TPELPPSAR.+2y7. (Light)	66.4	27.3
500.292	866.473	23.5	TDGF1.TPELPPSAR.+2y8. (Heavy)	66.4	28.3
498.28	866.473	23.5	TDGF1.TPELPPSAR.+2y8. (Light)	66.4	28.3
713.422	1136.643	44.4	WIF1.ASVVQVGFPCLGK.+2y10. (Heavy)	80.8	32.6
709.397	1132.618	44.4	WIF1.ASVVQVGFPCLGK.+2y10. (Light)	80.8	32.6
713.422	753.427	44.4	WIF1.ASVVQVGFPCLGK.+2y6. (Heavy)	80.8	29.6
709.397	749.401	44.4	WIF1.ASVVQVGFPCLGK.+2y6. (Light)	80.8	29.6
713.422	810.448	44.4	WIF1.ASVVQVGFPCLGK.+2y7. (Heavy)	80.8	29.6
709.397	806.423	44.4	WIF1.ASVVQVGFPCLGK.+2y7. (Light)	80.8	29.6
713.422	909.516	44.4	WIF1.ASVVQVGFPCLGK.+2y8. (Heavy)	80.8	30.6
709.397	905.491	44.4	WIF1.ASVVQVGFPCLGK.+2y8. (Light)	80.8	30.6
713.422	1037.575	44.4	WIF1.ASVVQVGFPCLGK.+2y9. (Heavy)	80.8	29.6
709.397	1033.55	44.4	WIF1.ASVVQVGFPCLGK.+2y9. (Light)	80.8	29.6
728.307	910.37	29.5	WIF1.TCQQAECPGGCR.+2b7. (Heavy)	83	36.3
726.295	906.344	29.5	WIF1.TCQQAECPGGCR.+2b7. (Light)	83	36.3
728.307	1162.473	29.5	WIF1.TCQQAECPGGCR.+2y10. (Heavy)	83	37.3
726.295	1162.473	29.5	WIF1.TCQQAECPGGCR.+2y10. (Light)	83	37.3
728.307	835.319	29.5	WIF1.TCQQAECPGGCR.+2y7. (Heavy)	83	38.3
726.295	835.319	29.5	WIF1.TCQQAECPGGCR.+2y7. (Light)	83	38.3

728.307	906.356	29.5	WIF1.TCQQAECPGGCR.+2y8. (Heavy)	83	36.3
726.295	906.356	29.5	WIF1.TCQQAECPGGCR.+2y8. (Light)	83	36.3
728.307	1034.414	29.5	WIF1.TCQQAECPGGCR.+2y9. (Heavy)	83	38.3
726.295	1034.414	29.5	WIF1.TCQQAECPGGCR.+2y9. (Light)	83	38.3
913.044	1134.655	73	WIF1.VLIGFEEDILIVSEGK.+2y10. (Heavy)	95.3	43
909.019	1130.63	73	WIF1.VLIGFEEDILIVSEGK.+2y10. (Light)	95.3	43
913.044	1263.698	73	WIF1.VLIGFEEDILIVSEGK.+2y11. (Heavy)	95.3	46
909.019	1259.673	73	WIF1.VLIGFEEDILIVSEGK.+2y11. (Light)	95.3	46
913.044	1410.766	73	WIF1.VLIGFEEDILIVSEGK.+2y12. (Heavy)	95.3	46
909.019	1406.741	73	WIF1.VLIGFEEDILIVSEGK.+2y12. (Light)	95.3	46
913.044	1467.788	73	WIF1.VLIGFEEDILIVSEGK.+2y13. (Heavy)	95.3	43
909.019	1463.763	73	WIF1.VLIGFEEDILIVSEGK.+2y13. (Light)	95.3	43
913.044	1005.613	73	WIF1.VLIGFEEDILIVSEGK.+2y9. (Heavy)	95.3	47
909.019	1001.588	73	WIF1.VLIGFEEDILIVSEGK.+2y9. (Light)	95.3	47
1079.968	1239.491	38.7	WNT1.ACNSSSPALDGCELLCCGR.+2y10. (Heavy)	108.7	53.4
1077.955	1239.491	38.7	WNT1.ACNSSSPALDGCELLCCGR.+2y10. (Light)	108.7	53.4
1079.968	1352.576	38.7	WNT1.ACNSSSPALDGCELLCCGR.+2y11. (Heavy)	108.7	52.4
1077.955	1352.576	38.7	WNT1.ACNSSSPALDGCELLCCGR.+2y11. (Light)	108.7	52.4
1079.968	1423.613	38.7	WNT1.ACNSSSPALDGCELLCCGR.+2y12. (Heavy)	108.7	51.4
1077.955	1423.613	38.7	WNT1.ACNSSSPALDGCELLCCGR.+2y12. (Light)	108.7	51.4
1079.968	1067.443	38.7	WNT1.ACNSSSPALDGCELLCCGR.+2y8. (Heavy)	108.7	53.4
1077.955	1067.443	38.7	WNT1.ACNSSSPALDGCELLCCGR.+2y8. (Light)	108.7	53.4
1079.968	1124.465	38.7	WNT1.ACNSSSPALDGCELLCCGR.+2y9. (Heavy)	108.7	60.4
1077.955	1124.465	38.7	WNT1.ACNSSSPALDGCELLCCGR.+2y9. (Light)	108.7	60.4
670.703	1085.57	53.4	WNT1.ETAFIFAITSAGVTHSVAR.+3y11. (Heavy)	79.2	32.5
669.362	1085.57	53.4	WNT1.ETAFIFAITSAGVTHSVAR.+3y11. (Light)	79.2	32.5
670.703	708.883	53.4	WNT1.ETAFIFAITSAGVTHSVAR.+3y14+2. (Heavy)	79.2	24.5
669.362	708.883	53.4	WNT1.ETAFIFAITSAGVTHSVAR.+3y14+2. (Light)	79.2	24.5
670.703	765.425	53.4	WNT1.ETAFIFAITSAGVTHSVAR.+3y15+2. (Heavy)	79.2	24.5
669.362	765.425	53.4	WNT1.ETAFIFAITSAGVTHSVAR.+3y15+2. (Light)	79.2	24.5
670.703	838.96	53.4	WNT1.ETAFIFAITSAGVTHSVAR.+3y16+2. (Heavy)	79.2	27.5
669.362	838.96	53.4	WNT1.ETAFIFAITSAGVTHSVAR.+3y16+2. (Light)	79.2	27.5
670.703	874.478	53.4	WNT1.ETAFIFAITSAGVTHSVAR.+3y17+2. (Heavy)	79.2	24.5
669.362	874.478	53.4	WNT1.ETAFIFAITSAGVTHSVAR.+3y17+2. (Light)	79.2	24.5
618.016	1060.575	36	WNT1.QNPGILHSVSGGLQSAVR.+3y11. (Heavy)	75.4	25.9
616.674	1060.575	36	WNT1.QNPGILHSVSGGLQSAVR.+3y11. (Light)	75.4	25.9
618.016	655.862	36	WNT1.QNPGILHSVSGGLQSAVR.+3y13+2. (Heavy)	75.4	25.9
616.674	655.862	36	WNT1.QNPGILHSVSGGLQSAVR.+3y13+2. (Light)	75.4	25.9
618.016	789.442	36	WNT1.QNPGILHSVSGGLQSAVR.+3y16+2. (Heavy)	75.4	25.9
616.674	789.442	36	WNT1.QNPGILHSVSGGLQSAVR.+3y16+2. (Light)	75.4	25.9
618.016	787.442	36	WNT1.QNPGILHSVSGGLQSAVR.+3y8. (Heavy)	75.4	25.9

616.674	787.442	36	WNT1.QNPGILHSVSGGLQSAVR.+3y8. (Light)	75.4	25.9
618.016	874.474	36	WNT1.QNPGILHSVSGGLQSAVR.+3y9. (Heavy)	75.4	25.9
616.674	874.474	36	WNT1.QNPGILHSVSGGLQSAVR.+3y9. (Light)	75.4	25.9
422.539	486.243	29	WNT2.CHGVSGSCTLR.+3b4. (Heavy)	61.1	19.8
421.197	482.218	29	WNT2.CHGVSGSCTLR.+3b4. (Light)	61.1	19.8
422.539	630.297	29	WNT2.CHGVSGSCTLR.+3b6. (Heavy)	61.1	19.8
421.197	626.271	29	WNT2.CHGVSGSCTLR.+3b6. (Light)	61.1	19.8
422.539	717.329	29	WNT2.CHGVSGSCTLR.+3b7. (Heavy)	61.1	21.8
421.197	713.304	29	WNT2.CHGVSGSCTLR.+3b7. (Light)	61.1	21.8
422.539	549.281	29	WNT2.CHGVSGSCTLR.+3y4. (Heavy)	61.1	19.8
421.197	549.281	29	WNT2.CHGVSGSCTLR.+3y4. (Light)	61.1	19.8
422.539	636.313	29	WNT2.CHGVSGSCTLR.+3y5. (Heavy)	61.1	23.8
421.197	636.313	29	WNT2.CHGVSGSCTLR.+3y5. (Light)	61.1	23.8
604.956	746.857	30.5	WNT2.CQDCLEALDVHTCK.+3y12+2. (Heavy)	73.7	25.2
602.272	744.845	30.5	WNT2.CQDCLEALDVHTCK.+3y12+2. (Light)	73.7	25.2
604.956	791.402	30.5	WNT2.CQDCLEALDVHTCK.+3y6. (Heavy)	73.7	30.2
602.272	787.377	30.5	WNT2.CQDCLEALDVHTCK.+3y6. (Light)	73.7	30.2
604.956	904.486	30.5	WNT2.CQDCLEALDVHTCK.+3y7. (Heavy)	73.7	30.2
602.272	900.461	30.5	WNT2.CQDCLEALDVHTCK.+3y7. (Light)	73.7	30.2
604.956	975.523	30.5	WNT2.CQDCLEALDVHTCK.+3y8. (Heavy)	73.7	30.2
602.272	971.498	30.5	WNT2.CQDCLEALDVHTCK.+3y8. (Light)	73.7	30.2
604.956	1104.566	30.5	WNT2.CQDCLEALDVHTCK.+3y9. (Heavy)	73.7	30.2
602.272	1100.541	30.5	WNT2.CQDCLEALDVHTCK.+3y9. (Light)	73.7	30.2
1010.556	1020.584	77.3	WNT2.ESAFVYAISSAGVVFAITR.+2y10. (Heavy)	103.6	52.4
1008.544	1020.584	77.3	WNT2.ESAFVYAISSAGVVFAITR.+2y10. (Light)	103.6	52.4
1010.556	1107.616	77.3	WNT2.ESAFVYAISSAGVVFAITR.+2y11. (Heavy)	103.6	52.4
1008.544	1107.616	77.3	WNT2.ESAFVYAISSAGVVFAITR.+2y11. (Light)	103.6	52.4
1010.556	1220.7	77.3	WNT2.ESAFVYAISSAGVVFAITR.+2y12. (Heavy)	103.6	51.4
1008.544	1220.7	77.3	WNT2.ESAFVYAISSAGVVFAITR.+2y12. (Light)	103.6	51.4
1010.556	1291.737	77.3	WNT2.ESAFVYAISSAGVVFAITR.+2y13. (Heavy)	103.6	51.4
1008.544	1291.737	77.3	WNT2.ESAFVYAISSAGVVFAITR.+2y13. (Light)	103.6	51.4
1010.556	1454.8	77.3	WNT2.ESAFVYAISSAGVVFAITR.+2y14. (Heavy)	103.6	50.4
1008.544	1454.8	77.3	WNT2.ESAFVYAISSAGVVFAITR.+2y14. (Light)	103.6	50.4
646.024	978.537	50.5	WNT3A.ESAFVHAIASAGVAFAVTR.+3y10. (Heavy)	77.4	31.8
644.683	978.537	50.5	WNT3A.ESAFVHAIASAGVAFAVTR.+3y10. (Light)	77.4	31.8
646.024	593.341	50.5	WNT3A.ESAFVHAIASAGVAFAVTR.+3y5. (Heavy)	77.4	26.8
644.683	593.341	50.5	WNT3A.ESAFVHAIASAGVAFAVTR.+3y5. (Light)	77.4	26.8
646.024	664.378	50.5	WNT3A.ESAFVHAIASAGVAFAVTR.+3y6. (Heavy)	77.4	26.8
644.683	664.378	50.5	WNT3A.ESAFVHAIASAGVAFAVTR.+3y6. (Light)	77.4	26.8
646.024	763.446	50.5	WNT3A.ESAFVHAIASAGVAFAVTR.+3y7. (Heavy)	77.4	25.8
644.683	763.446	50.5	WNT3A.ESAFVHAIASAGVAFAVTR.+3y7. (Light)	77.4	25.8

646.024	820.468	50.5	WNT3A.ESAFVHAIASAGVAFAVTR.+3y8. (Heavy)	77.4	23.8
644.683	820.468	50.5	WNT3A.ESAFVHAIASAGVAFAVTR.+3y8. (Light)	77.4	23.8
483.252	651.804	27.6	WNT3A.IGIQECQHQFR.+3y10+2. (Heavy)	65.6	22.7
481.91	651.804	27.6	WNT3A.IGIQECQHQFR.+3y10+2. (Light)	65.6	22.7
483.252	587.305	27.6	WNT3A.IGIQECQHQFR.+3y4. (Heavy)	65.6	26.7
481.91	587.305	27.6	WNT3A.IGIQECQHQFR.+3y4. (Light)	65.6	26.7
483.252	502.722	27.6	WNT3A.IGIQECQHQFR.+3y7+2. (Heavy)	65.6	22.7
481.91	502.722	27.6	WNT3A.IGIQECQHQFR.+3y7+2. (Light)	65.6	22.7
483.252	566.751	27.6	WNT3A.IGIQECQHQFR.+3y8+2. (Heavy)	65.6	21.7
481.91	566.751	27.6	WNT3A.IGIQECQHQFR.+3y8+2. (Light)	65.6	21.7
483.252	623.293	27.6	WNT3A.IGIQECQHQFR.+3y9+2. (Heavy)	65.6	21.7
481.91	623.293	27.6	WNT3A.IGIQECQHQFR.+3y9+2. (Light)	65.6	21.7
809.85	1139.493	21.9	WNT3A.SCAEGTAAICGCSSR.+2y11. (Heavy)	89	42
807.837	1139.493	21.9	WNT3A.SCAEGTAAICGCSSR.+2y11. (Light)	89	42
809.85	1268.536	21.9	WNT3A.SCAEGTAAICGCSSR.+2y12. (Heavy)	89	40
807.837	1268.536	21.9	WNT3A.SCAEGTAAICGCSSR.+2y12. (Light)	89	40
809.85	839.35	21.9	WNT3A.SCAEGTAAICGCSSR.+2y7. (Heavy)	89	41
807.837	839.35	21.9	WNT3A.SCAEGTAAICGCSSR.+2y7. (Light)	89	41
809.85	910.387	21.9	WNT3A.SCAEGTAAICGCSSR.+2y8. (Heavy)	89	42
807.837	910.387	21.9	WNT3A.SCAEGTAAICGCSSR.+2y8. (Light)	89	42
809.85	981.424	21.9	WNT3A.SCAEGTAAICGCSSR.+2y9. (Heavy)	89	42
807.837	981.424	21.9	WNT3A.SCAEGTAAICGCSSR.+2y9. (Light)	89	42
997.003	1078.531	41.9	WNT5A.ETAFTYAVSAAGVVNAMSR.+2y11. (Heavy)	102.6	48.2
994.991	1078.531	41.9	WNT5A.ETAFTYAVSAAGVVNAMSR.+2y11. (Light)	102.6	48.2
997.003	1177.599	41.9	WNT5A.ETAFTYAVSAAGVVNAMSR.+2y12. (Heavy)	102.6	47.2
994.991	1177.599	41.9	WNT5A.ETAFTYAVSAAGVVNAMSR.+2y12. (Light)	102.6	47.2
997.003	1248.636	41.9	WNT5A.ETAFTYAVSAAGVVNAMSR.+2y13. (Heavy)	102.6	49.2
994.991	1248.636	41.9	WNT5A.ETAFTYAVSAAGVVNAMSR.+2y13. (Light)	102.6	49.2
997.003	1411.7	41.9	WNT5A.ETAFTYAVSAAGVVNAMSR.+2y14. (Heavy)	102.6	50.2
994.991	1411.7	41.9	WNT5A.ETAFTYAVSAAGVVNAMSR.+2y14. (Light)	102.6	50.2
997.003	1512.748	41.9	WNT5A.ETAFTYAVSAAGVVNAMSR.+2y15. (Heavy)	102.6	48.2
994.991	1512.748	41.9	WNT5A.ETAFTYAVSAAGVVNAMSR.+2y15. (Light)	102.6	48.2
1260.107	1221.557	48	WNT5A.FNSPTTQDLVYIDPSPDYCVR.+2y10. (Heavy)	121.8	61.6
1258.094	1221.557	48	WNT5A.FNSPTTQDLVYIDPSPDYCVR.+2y10. (Light)	121.8	61.6
1260.107	1384.62	48	WNT5A.FNSPTTQDLVYIDPSPDYCVR.+2y11. (Heavy)	121.8	61.6
1258.094	1384.62	48	WNT5A.FNSPTTQDLVYIDPSPDYCVR.+2y11. (Light)	121.8	61.6
1260.107	1483.689	48	WNT5A.FNSPTTQDLVYIDPSPDYCVR.+2y12. (Heavy)	121.8	61.6
1258.094	1483.689	48	WNT5A.FNSPTTQDLVYIDPSPDYCVR.+2y12. (Light)	121.8	61.6
1260.107	993.446	48	WNT5A.FNSPTTQDLVYIDPSPDYCVR.+2y8. (Heavy)	121.8	63.6
1258.094	993.446	48	WNT5A.FNSPTTQDLVYIDPSPDYCVR.+2y8. (Light)	121.8	63.6
1260.107	1108.473	48	WNT5A.FNSPTTQDLVYIDPSPDYCVR.+2y9. (Heavy)	121.8	61.6

1258.094	1108.473	48	WNT5A.FNSPTTQDLVYIDPSPDYCVR.+2y9. (Light)	121.8	61.6
619.817	963.485	3.4	WNT5A.NESTGSLGTQGR.+2y10. (Heavy)	75.1	29.2
617.805	963.485	3.4	WNT5A.NESTGSLGTQGR.+2y10. (Light)	75.1	29.2
619.817	631.352	3.4	WNT5A.NESTGSLGTQGR.+2y6. (Heavy)	75.1	30.2
617.805	631.352	3.4	WNT5A.NESTGSLGTQGR.+2y6. (Light)	75.1	30.2
619.817	718.384	3.4	WNT5A.NESTGSLGTQGR.+2y7. (Heavy)	75.1	32.2
617.805	718.384	3.4	WNT5A.NESTGSLGTQGR.+2y7. (Light)	75.1	32.2
619.817	775.406	3.4	WNT5A.NESTGSLGTQGR.+2y8. (Heavy)	75.1	30.2
617.805	775.406	3.4	WNT5A.NESTGSLGTQGR.+2y8. (Light)	75.1	30.2
619.817	876.453	3.4	WNT5A.NESTGSLGTQGR.+2y9. (Heavy)	75.1	30.2
617.805	876.453	3.4	WNT5A.NESTGSLGTQGR.+2y9. (Light)	75.1	30.2

Appendix B. Peak areas for transitions detected in scheduled SRM analysis of dimethyl labeled H9 cell lysates.

Precursor m/z	Fragment m/z	RT (min)	Target Protein, Peptide, Fragment Ion, Label	Mean Peak Area	Standard Deviation of Mean Peak Area
582.795	476.246	29.1	ACTB.GYSFTTTAER.+2y4. (Heavy)	23811	9660
580.783	476.246	29.1	ACTB.GYSFTTTAER.+2y4. (Light)	20860	9751
582.795	577.294	29.1	ACTB.GYSFTTTAER.+2y5. (Heavy)	45451	21443
580.783	577.294	29.1	ACTB.GYSFTTTAER.+2y5. (Light)	41523	20064
582.795	678.342	29.1	ACTB.GYSFTTTAER.+2y6. (Heavy)	58962	19614
580.783	678.342	29.1	ACTB.GYSFTTTAER.+2y6. (Light)	90647	52141
582.795	825.41	29.1	ACTB.GYSFTTTAER.+2y7. (Heavy)	34110	14261
580.783	825.41	29.1	ACTB.GYSFTTTAER.+2y7. (Light)	54495	27176
582.795	912.442	29.1	ACTB.GYSFTTTAER.+2y8. (Heavy)	107325	46509
580.783	912.442	29.1	ACTB.GYSFTTTAER.+2y8. (Light)	182880	102798
911.978	1298.67	47.1	ACTB.SYELPDGQVITIGNER.+2y12. (Heavy)	4373888	435867
909.965	1298.67	47.1	ACTB.SYELPDGQVITIGNER.+2y12. (Light)	125124	12764
911.978	649.839	47.1	ACTB.SYELPDGQVITIGNER.+2y12+2. (Heavy)	5911726	716353
909.965	649.839	47.1	ACTB.SYELPDGQVITIGNER.+2y12+2. (Light)	129708	19544
911.978	706.381	47.1	ACTB.SYELPDGQVITIGNER.+2y13+2. (Heavy)	109338	11575
909.965	706.381	47.1	ACTB.SYELPDGQVITIGNER.+2y13+2. (Light)	150754	24616
911.978	475.226	47.1	ACTB.SYELPDGQVITIGNER.+2y4. (Heavy)	917033	77457
909.965	475.226	47.1	ACTB.SYELPDGQVITIGNER.+2y4. (Light)	968609	105112
911.978	689.358	47.1	ACTB.SYELPDGQVITIGNER.+2y6. (Heavy)	720522	64175
909.965	689.358	47.1	ACTB.SYELPDGQVITIGNER.+2y6. (Light)	935067	97949
1009.592	1323.818	38.1	ACTB.VAPEEHPVLLTEAPLNPK.+2y12. (Heavy)	245131	60316
1005.567	1319.793	38.1	ACTB.VAPEEHPVLLTEAPLNPK.+2y12. (Light)	312709	56804
1009.592	908.511	38.1	ACTB.VAPEEHPVLLTEAPLNPK.+2y16+2. (Heavy)	140185	35906
1005.567	906.499	38.1	ACTB.VAPEEHPVLLTEAPLNPK.+2y16+2. (Light)	173856	29472
1009.592	600.402	38.1	ACTB.VAPEEHPVLLTEAPLNPK.+2y5. (Heavy)	96814	19724
1005.567	596.377	38.1	ACTB.VAPEEHPVLLTEAPLNPK.+2y5. (Light)	118033	25860
1009.592	671.439	38.1	ACTB.VAPEEHPVLLTEAPLNPK.+2y6. (Heavy)	56786	14922
1005.567	667.414	38.1	ACTB.VAPEEHPVLLTEAPLNPK.+2y6. (Light)	75427	14720
1009.592	901.529	38.1	ACTB.VAPEEHPVLLTEAPLNPK.+2y8. (Heavy)	58846	14697
1005.567	897.504	38.1	ACTB.VAPEEHPVLLTEAPLNPK.+2y8. (Light)	86260	17821
669.362	914.459	53.2	AKT1.FYGAEIVSALDYLHSEK.+3b16+2. (Heavy)	6205	3392
666.679	912.446	53.2	AKT1.FYGAEIVSALDYLHSEK.+3b16+2. (Light)	8179	4550
669.362	1194.63	53.2	AKT1.FYGAEIVSALDYLHSEK.+3y10. (Heavy)	3605	2013
666.679	1190.605	53.2	AKT1.FYGAEIVSALDYLHSEK.+3y10. (Light)	14104	15996
669.362	1293.699	53.2	AKT1.FYGAEIVSALDYLHSEK.+3y11. (Heavy)	411	237

666.679	1289.674	53.2	AKT1.FYGAEIVSALDYLHSEK.+3y11. (Light)	605	616
669.362	832.446	53.2	AKT1.FYGAEIVSALDYLHSEK.+3y15+2. (Heavy)	7607	7444
666.679	830.433	53.2	AKT1.FYGAEIVSALDYLHSEK.+3y15+2. (Light)	32736	24227
669.362	913.977	53.2	AKT1.FYGAEIVSALDYLHSEK.+3y16+2. (Heavy)	2765	1162
666.679	911.965	53.2	AKT1.FYGAEIVSALDYLHSEK.+3y16+2. (Light)	3574	1579
1239.575	1209.538	50.3	AKT1.TFCGTPEYLAPEVLEDNDYGR.+2y10. (Heavy)	601	355
1237.563	1209.538	50.3	AKT1.TFCGTPEYLAPEVLEDNDYGR.+2y10. (Light)	3940	5865
1239.575	1306.591	50.3	AKT1.TFCGTPEYLAPEVLEDNDYGR.+2y11. (Heavy)	891	890
1237.563	1306.591	50.3	AKT1.TFCGTPEYLAPEVLEDNDYGR.+2y11. (Light)	538	479
1239.575	1377.628	50.3	AKT1.TFCGTPEYLAPEVLEDNDYGR.+2y12. (Heavy)	543	400
1237.563	1377.628	50.3	AKT1.TFCGTPEYLAPEVLEDNDYGR.+2y12. (Light)	449	189
1239.575	1490.712	50.3	AKT1.TFCGTPEYLAPEVLEDNDYGR.+2y13. (Heavy)	356	359
1237.563	1490.712	50.3	AKT1.TFCGTPEYLAPEVLEDNDYGR.+2y13. (Light)	252	161
1239.575	1080.496	50.3	AKT1.TFCGTPEYLAPEVLEDNDYGR.+2y9. (Heavy)	414	253
1237.563	1080.496	50.3	AKT1.TFCGTPEYLAPEVLEDNDYGR.+2y9. (Light)	435	212
426.221	646.35	27.6	AKT1.TFHVETPEER.+3b5. (Heavy)	5773	7659
424.879	642.325	27.6	AKT1.TFHVETPEER.+3b5. (Light)	4753	4376
426.221	747.397	27.6	AKT1.TFHVETPEER.+3b6. (Heavy)	771	583
424.879	743.372	27.6	AKT1.TFHVETPEER.+3b6. (Light)	1345	990
426.221	433.204	27.6	AKT1.TFHVETPEER.+3y3. (Heavy)	7046	6515
424.879	433.204	27.6	AKT1.TFHVETPEER.+3y3. (Light)	4928	4548
426.221	530.257	27.6	AKT1.TFHVETPEER.+3y4. (Heavy)	6113	3868
424.879	530.257	27.6	AKT1.TFHVETPEER.+3y4. (Light)	2624	2512
426.221	631.305	27.6	AKT1.TFHVETPEER.+3y5. (Heavy)	1956	2250
424.879	631.305	27.6	AKT1.TFHVETPEER.+3y5. (Light)	4015	4018
1030.466	1196.507	46.8	APC.NDSLSSLDFDDDDVDLSR.+2y10. (Heavy)	1374	742
1028.453	1196.507	46.8	APC.NDSLSSLDFDDDDVDLSR.+2y10. (Light)	1327	621
1030.466	1311.534	46.8	APC.NDSLSSLDFDDDDVDLSR.+2y11. (Heavy)	1069	760
1028.453	1311.534	46.8	APC.NDSLSSLDFDDDDVDLSR.+2y11. (Light)	1628	901
1030.466	1424.618	46.8	APC.NDSLSSLDFDDDDVDLSR.+2y12. (Heavy)	654	488
1028.453	1424.618	46.8	APC.NDSLSSLDFDDDDVDLSR.+2y12. (Light)	816	441
1030.466	934.411	46.8	APC.NDSLSSLDFDDDDVDLSR.+2y8. (Heavy)	2492	1472
1028.453	934.411	46.8	APC.NDSLSSLDFDDDDVDLSR.+2y8. (Light)	2526	1487
1030.466	1049.438	46.8	APC.NDSLSSLDFDDDDVDLSR.+2y9. (Heavy)	772	746
1028.453	1049.438	46.8	APC.NDSLSSLDFDDDDVDLSR.+2y9. (Light)	695	420
496.597	578.291	31.5	APC.NVSSLIATNEDHR.+3y10+2. (Heavy)	8510	5124
495.255	578.291	31.5	APC.NVSSLIATNEDHR.+3y10+2. (Light)	31302	24792
496.597	621.807	31.5	APC.NVSSLIATNEDHR.+3y11+2. (Heavy)	3275	2009
495.255	621.807	31.5	APC.NVSSLIATNEDHR.+3y11+2. (Light)	2559	993
496.597	771.338	31.5	APC.NVSSLIATNEDHR.+3y6. (Heavy)	19947	21637
495.255	771.338	31.5	APC.NVSSLIATNEDHR.+3y6. (Light)	2710	2669

496.597	842.375	31.5	APC.NVSSLIATNEDHR.+3y7. (Heavy)	1143	560
495.255	842.375	31.5	APC.NVSSLIATNEDHR.+3y7. (Light)	3538	3360
496.597	955.459	31.5	APC.NVSSLIATNEDHR.+3y8. (Heavy)	594	659
495.255	955.459	31.5	APC.NVSSLIATNEDHR.+3y8. (Light)	731	574
612.984	1206.623	28.7	APC.SAEDPVSEVPAVSQHPR.+3y11. (Heavy)	2275	2453
611.643	1206.623	28.7	APC.SAEDPVSEVPAVSQHPR.+3y11. (Light)	2316	#N/A
612.984	701.875	28.7	APC.SAEDPVSEVPAVSQHPR.+3y13+2. (Heavy)	8985	7192
611.643	701.875	28.7	APC.SAEDPVSEVPAVSQHPR.+3y13+2. (Light)	30922	26156
612.984	759.389	28.7	APC.SAEDPVSEVPAVSQHPR.+3y14+2. (Heavy)	4149	2378
611.643	759.389	28.7	APC.SAEDPVSEVPAVSQHPR.+3y14+2. (Light)	8030	4773
612.984	823.91	28.7	APC.SAEDPVSEVPAVSQHPR.+3y15+2. (Heavy)	2063	827
611.643	823.91	28.7	APC.SAEDPVSEVPAVSQHPR.+3y15+2. (Light)	3126	2280
612.984	891.48	28.7	APC.SAEDPVSEVPAVSQHPR.+3y8. (Heavy)	1986	1392
611.643	891.48	28.7	APC.SAEDPVSEVPAVSQHPR.+3y8. (Light)	8862	7501
683.997	783.381	33.1	AXN1.DAHEENPESILDEHVQR.+3y13+2. (Heavy)	1073	1041
682.656	783.381	33.1	AXN1.DAHEENPESILDEHVQR.+3y13+2. (Light)	1328	1045
683.997	783.374	33.1	AXN1.DAHEENPESILDEHVQR.+3y6. (Heavy)	1932	838
682.656	783.374	33.1	AXN1.DAHEENPESILDEHVQR.+3y6. (Light)	1149	682
683.997	896.458	33.1	AXN1.DAHEENPESILDEHVQR.+3y7. (Heavy)	3681	5087
682.656	896.458	33.1	AXN1.DAHEENPESILDEHVQR.+3y7. (Light)	1675	2111
683.997	1009.543	33.1	AXN1.DAHEENPESILDEHVQR.+3y8. (Heavy)	2397	1688
682.656	1009.543	33.1	AXN1.DAHEENPESILDEHVQR.+3y8. (Light)	1337	725
683.997	1096.575	33.1	AXN1.DAHEENPESILDEHVQR.+3y9. (Heavy)	1989	1253
682.656	1096.575	33.1	AXN1.DAHEENPESILDEHVQR.+3y9. (Light)	723	702
596.313	624.354	33.6	AXN1.SDIYLEYTR.+2b5. (Heavy)	1548	1088
594.301	620.329	33.6	AXN1.SDIYLEYTR.+2b5. (Light)	5071	5355
596.313	568.273	33.6	AXN1.SDIYLEYTR.+2y4. (Heavy)	3836	2482
594.301	568.273	33.6	AXN1.SDIYLEYTR.+2y4. (Light)	6692	6520
596.313	681.357	33.6	AXN1.SDIYLEYTR.+2y5. (Heavy)	1137	1105
594.301	681.357	33.6	AXN1.SDIYLEYTR.+2y5. (Light)	44080	37595
596.313	844.42	33.6	AXN1.SDIYLEYTR.+2y6. (Heavy)	1333	915
594.301	844.42	33.6	AXN1.SDIYLEYTR.+2y6. (Light)	2983	2700
596.313	957.504	33.6	AXN1.SDIYLEYTR.+2y7. (Heavy)	868	783
594.301	957.504	33.6	AXN1.SDIYLEYTR.+2y7. (Light)	1852	1783
829.368	1164.55	29.4	CDN1A.DCDALMAGCIQEAR.+2y10. (Heavy)	1799	1044
827.355	1164.55	29.4	CDN1A.DCDALMAGCIQEAR.+2y10. (Light)	1824	673
829.368	1235.587	29.4	CDN1A.DCDALMAGCIQEAR.+2y11. (Heavy)	733	637
827.355	1235.587	29.4	CDN1A.DCDALMAGCIQEAR.+2y11. (Light)	1067	814
829.368	833.393	29.4	CDN1A.DCDALMAGCIQEAR.+2y7. (Heavy)	878	654
827.355	833.393	29.4	CDN1A.DCDALMAGCIQEAR.+2y7. (Light)	1274	587
829.368	904.431	29.4	CDN1A.DCDALMAGCIQEAR.+2y8. (Heavy)	1254	990

827.355	904.431	29.4	CDN1A.DCDALMAGCIQEAR.+2y8. (Light)	1299	973
829.368	1051.466	29.4	CDN1A.DCDALMAGCIQEAR.+2y9. (Heavy)	3852	2105
827.355	1051.466	29.4	CDN1A.DCDALMAGCIQEAR.+2y9. (Light)	6697	4008
1196.065	1219.574	67.9	CDN1A.WNFDFVTETPLEGDFAWER.+2y10. (Heavy)	200	99
1194.053	1219.574	67.9	CDN1A.WNFDFVTETPLEGDFAWER.+2y10. (Light)	175	114
1196.065	1320.622	67.9	CDN1A.WNFDFVTETPLEGDFAWER.+2y11. (Heavy)	199	126
1194.053	1320.622	67.9	CDN1A.WNFDFVTETPLEGDFAWER.+2y11. (Light)	222	157
1196.065	1449.664	67.9	CDN1A.WNFDFVTETPLEGDFAWER.+2y12. (Heavy)	228	214
1194.053	1449.664	67.9	CDN1A.WNFDFVTETPLEGDFAWER.+2y12. (Light)	184	105
1196.065	1009.437	67.9	CDN1A.WNFDFVTETPLEGDFAWER.+2y8. (Heavy)	204	98
1194.053	1009.437	67.9	CDN1A.WNFDFVTETPLEGDFAWER.+2y8. (Light)	385	293
1196.065	1122.521	67.9	CDN1A.WNFDFVTETPLEGDFAWER.+2y9. (Heavy)	211	117
1194.053	1122.521	67.9	CDN1A.WNFDFVTETPLEGDFAWER.+2y9. (Light)	296	276
644.428	1057.692	30	CER1.TPASQGVILPIK.+2y10. (Heavy)	1817	1347
640.403	1053.667	30	CER1.TPASQGVILPIK.+2y10. (Light)	1758	917
644.428	714.543	30	CER1.TPASQGVILPIK.+2y6. (Heavy)	5763	3257
640.403	710.517	30	CER1.TPASQGVILPIK.+2y6. (Light)	6497	3613
644.428	771.564	30	CER1.TPASQGVILPIK.+2y7. (Heavy)	3270	2395
640.403	767.539	30	CER1.TPASQGVILPIK.+2y7. (Light)	8900	7083
644.428	899.623	30	CER1.TPASQGVILPIK.+2y8. (Heavy)	2588	1305
640.403	895.598	30	CER1.TPASQGVILPIK.+2y8. (Light)	155549	217025
644.428	986.655	30	CER1.TPASQGVILPIK.+2y9. (Heavy)	2316	994
640.403	982.63	30	CER1.TPASQGVILPIK.+2y9. (Light)	2401	2865
599.981	661.321	31	CER1.TVPFSQTITHEGCEK.+3y11+2. (Heavy)	3012	1224
597.298	659.309	31	CER1.TVPFSQTITHEGCEK.+3y11+2. (Light)	27629	31691
599.981	734.856	31	CER1.TVPFSQTITHEGCEK.+3y12+2. (Heavy)	6757	7123
597.298	732.843	31	CER1.TVPFSQTITHEGCEK.+3y12+2. (Light)	18320	21479
599.981	783.382	31	CER1.TVPFSQTITHEGCEK.+3y13+2. (Heavy)	9495	6430
597.298	781.369	31	CER1.TVPFSQTITHEGCEK.+3y13+2. (Light)	13878	8324
599.981	892.413	31	CER1.TVPFSQTITHEGCEK.+3y7. (Heavy)	3640	1743
597.298	888.388	31	CER1.TVPFSQTITHEGCEK.+3y7. (Light)	5604	4415
599.981	1106.545	31	CER1.TVPFSQTITHEGCEK.+3y9. (Heavy)	674	407
597.298	1102.52	31	CER1.TVPFSQTITHEGCEK.+3y9. (Light)	1904	1257
671.394	1210.655	33.1	CER1.VVVQNNLCFGK.+2y10. (Heavy)	18732	25749
667.368	1206.63	33.1	CER1.VVVQNNLCFGK.+2y10. (Light)	10319	11324
671.394	770.417	33.1	CER1.VVVQNNLCFGK.+2y6. (Heavy)	3229	1890
667.368	766.392	33.1	CER1.VVVQNNLCFGK.+2y6. (Light)	2365	1287
671.394	884.46	33.1	CER1.VVVQNNLCFGK.+2y7. (Heavy)	2268	1141
667.368	880.435	33.1	CER1.VVVQNNLCFGK.+2y7. (Light)	1185	972
671.394	1012.518	33.1	CER1.VVVQNNLCFGK.+2y8. (Heavy)	700	585
667.368	1008.493	33.1	CER1.VVVQNNLCFGK.+2y8. (Light)	1537	1627

671.394	1111.587	33.1	CER1.VVVQNNLCFGK.+2y9. (Heavy)	1431	1297
667.368	1107.562	33.1	CER1.VVVQNNLCFGK.+2y9. (Light)	1193	768
692.034	779.508	39.8	CTNB1.HAVVNLINYQDDAELATR.+3b7. (Heavy)	37010	9418
690.692	775.482	39.8	CTNB1.HAVVNLINYQDDAELATR.+3b7. (Light)	22185	5583
692.034	893.551	39.8	CTNB1.HAVVNLINYQDDAELATR.+3b8. (Heavy)	15112	4977
690.692	889.525	39.8	CTNB1.HAVVNLINYQDDAELATR.+3b8. (Light)	12683	4037
692.034	1295.586	39.8	CTNB1.HAVVNLINYQDDAELATR.+3y11. (Heavy)	11808	1711
690.692	1295.586	39.8	CTNB1.HAVVNLINYQDDAELATR.+3y11. (Light)	11236	1801
692.034	890.421	39.8	CTNB1.HAVVNLINYQDDAELATR.+3y8. (Heavy)	21974	5749
690.692	890.421	39.8	CTNB1.HAVVNLINYQDDAELATR.+3y8. (Light)	20260	4445
692.034	1018.48	39.8	CTNB1.HAVVNLINYQDDAELATR.+3y9. (Heavy)	12219	3428
690.692	1018.48	39.8	CTNB1.HAVVNLINYQDDAELATR.+3y9. (Light)	10287	3178
725.424	1058.567	27.8	CTNB1.LLNDEDQVVVNK.+2b9. (Heavy)	2003	2923
721.398	1054.542	27.8	CTNB1.LLNDEDQVVVNK.+2b9. (Light)	1118	924
725.424	1191.615	27.8	CTNB1.LLNDEDQVVVNK.+2y10. (Heavy)	2951	3346
721.398	1187.59	27.8	CTNB1.LLNDEDQVVVNK.+2y10. (Light)	3525	4927
725.424	833.503	27.8	CTNB1.LLNDEDQVVVNK.+2y7. (Heavy)	1491	1588
721.398	829.478	27.8	CTNB1.LLNDEDQVVVNK.+2y7. (Light)	1317	751
725.424	962.545	27.8	CTNB1.LLNDEDQVVVNK.+2y8. (Heavy)	1113	1013
721.398	958.52	27.8	CTNB1.LLNDEDQVVVNK.+2y8. (Light)	1125	1115
725.424	1077.572	27.8	CTNB1.LLNDEDQVVVNK.+2y9. (Heavy)	1140	1134
721.398	1073.547	27.8	CTNB1.LLNDEDQVVVNK.+2y9. (Light)	1459	783
757.419	1082.599	55	CTNB1.NEGVATYAAAVLFR.+2y10. (Heavy)	4078	1853
755.407	1082.599	55	CTNB1.NEGVATYAAAVLFR.+2y10. (Light)	2840	1553
757.419	1181.668	55	CTNB1.NEGVATYAAAVLFR.+2y11. (Heavy)	81653	19636
755.407	1181.668	55	CTNB1.NEGVATYAAAVLFR.+2y11. (Light)	5213	2900
757.419	1238.689	55	CTNB1.NEGVATYAAAVLFR.+2y12. (Heavy)	173870	34095
755.407	1238.689	55	CTNB1.NEGVATYAAAVLFR.+2y12. (Light)	5790	2424
757.419	910.515	55	CTNB1.NEGVATYAAAVLFR.+2y8. (Heavy)	4979	1507
755.407	910.515	55	CTNB1.NEGVATYAAAVLFR.+2y8. (Light)	5809	2598
757.419	1011.562	55	CTNB1.NEGVATYAAAVLFR.+2y9. (Heavy)	2888	1492
755.407	1011.562	55	CTNB1.NEGVATYAAAVLFR.+2y9. (Light)	2343	1257
390.856	550.267	27.6	DKK1.DHHQASNSSR.+3b4. (Heavy)	3224	3061
389.515	546.242	27.6	DKK1.DHHQASNSSR.+3b4. (Light)	4578	3510
390.856	463.226	27.6	DKK1.DHHQASNSSR.+3y4. (Heavy)	4102	2730
389.515	463.226	27.6	DKK1.DHHQASNSSR.+3y4. (Light)	15484	13706
390.856	550.258	27.6	DKK1.DHHQASNSSR.+3y5. (Heavy)	3578	3632
389.515	550.258	27.6	DKK1.DHHQASNSSR.+3y5. (Light)	2527	1485
390.856	621.295	27.6	DKK1.DHHQASNSSR.+3y6. (Heavy)	1630	1059
389.515	621.295	27.6	DKK1.DHHQASNSSR.+3y6. (Light)	2441	1169
390.856	443.71	27.6	DKK1.DHHQASNSSR.+3y8+2. (Heavy)	24542	35315

389.515	443.71	27.6	DKK1.DHHQASNSSR.+3y8+2. (Light)	11286	11556
522.586	625.273	27	DKK1.NGICVSSDQNHFR.+3y10+2. (Heavy)	1576	1109
521.244	625.273	27	DKK1.NGICVSSDQNHFR.+3y10+2. (Light)	5900	5832
522.586	681.815	27	DKK1.NGICVSSDQNHFR.+3y11+2. (Heavy)	1517	636
521.244	681.815	27	DKK1.NGICVSSDQNHFR.+3y11+2. (Light)	2154	2521
522.586	903.407	27	DKK1.NGICVSSDQNHFR.+3y7. (Heavy)	953	468
521.244	903.407	27	DKK1.NGICVSSDQNHFR.+3y7. (Light)	1512	1150
522.586	990.439	27	DKK1.NGICVSSDQNHFR.+3y8. (Heavy)	681	535
521.244	990.439	27	DKK1.NGICVSSDQNHFR.+3y8. (Light)	992	145
522.586	545.257	27	DKK1.NGICVSSDQNHFR.+3y9+2. (Heavy)	1832	1741
521.244	545.257	27	DKK1.NGICVSSDQNHFR.+3y9+2. (Light)	4294	4877
688.289	1169.45	20.9	DKK1.SSDCASGLCCAR.+2y10. (Heavy)	#N/A	#N/A
686.276	1169.45	20.9	DKK1.SSDCASGLCCAR.+2y10. (Light)	37	3
688.289	736.323	20.9	DKK1.SSDCASGLCCAR.+2y6. (Heavy)	75	50
686.276	736.323	20.9	DKK1.SSDCASGLCCAR.+2y6. (Light)	55	28
688.289	823.355	20.9	DKK1.SSDCASGLCCAR.+2y7. (Heavy)	65	52
686.276	823.355	20.9	DKK1.SSDCASGLCCAR.+2y7. (Light)	70	27
688.289	894.392	20.9	DKK1.SSDCASGLCCAR.+2y8. (Heavy)	105	#N/A
686.276	894.392	20.9	DKK1.SSDCASGLCCAR.+2y8. (Light)	79	56
688.289	1054.423	20.9	DKK1.SSDCASGLCCAR.+2y9. (Heavy)	#N/A	#N/A
686.276	1054.423	20.9	DKK1.SSDCASGLCCAR.+2y9. (Light)	62	32
651.328	1069.476	17	DVL1.LSSSTEQSTSSR.+2y10. (Heavy)	#N/A	#N/A
649.315	1069.476	17	DVL1.LSSSTEQSTSSR.+2y10. (Light)	#N/A	#N/A
651.328	665.321	17	DVL1.LSSSTEQSTSSR.+2y6. (Heavy)	35	12
649.315	665.321	17	DVL1.LSSSTEQSTSSR.+2y6. (Light)	41	10
651.328	794.364	17	DVL1.LSSSTEQSTSSR.+2y7. (Heavy)	#N/A	#N/A
649.315	794.364	17	DVL1.LSSSTEQSTSSR.+2y7. (Light)	20	3
651.328	895.412	17	DVL1.LSSSTEQSTSSR.+2y8. (Heavy)	22	0
649.315	895.412	17	DVL1.LSSSTEQSTSSR.+2y8. (Light)	21	2
651.328	982.444	17	DVL1.LSSSTEQSTSSR.+2y9. (Heavy)	#N/A	#N/A
649.315	982.444	17	DVL1.LSSSTEQSTSSR.+2y9. (Light)	22	#N/A
487.964	608.859	26.2	DVL1.NVLSNRPVHAYK.+3y10+2. (Heavy)	5974	3412
485.281	606.846	26.2	DVL1.NVLSNRPVHAYK.+3y10+2. (Light)	6844	7199
487.964	658.393	26.2	DVL1.NVLSNRPVHAYK.+3y11+2. (Heavy)	2865	2546
485.281	656.38	26.2	DVL1.NVLSNRPVHAYK.+3y11+2. (Light)	2714	2276
487.964	746.45	26.2	DVL1.NVLSNRPVHAYK.+3y6. (Heavy)	1544	1041
485.281	742.425	26.2	DVL1.NVLSNRPVHAYK.+3y6. (Light)	2485	4118
487.964	508.801	26.2	DVL1.NVLSNRPVHAYK.+3y8+2. (Heavy)	4612	7189
485.281	506.788	26.2	DVL1.NVLSNRPVHAYK.+3y8+2. (Light)	1640	1786
487.964	552.317	26.2	DVL1.NVLSNRPVHAYK.+3y9+2. (Heavy)	7451	8767
485.281	550.304	26.2	DVL1.NVLSNRPVHAYK.+3y9+2. (Light)	103705	181753

608.015	1173.693	26	DVL1.SQASATAPGLPPPHPTTK.+3y11. (Heavy)	110	155
605.332	1169.668	26	DVL1.SQASATAPGLPPPHPTTK.+3y11. (Light)	89	162
608.015	752.427	26	DVL1.SQASATAPGLPPPHPTTK.+3y15+2. (Heavy)	1308	795
605.332	750.414	26	DVL1.SQASATAPGLPPPHPTTK.+3y15+2. (Light)	1235	1177
608.015	787.946	26	DVL1.SQASATAPGLPPPHPTTK.+3y16+2. (Heavy)	324	269
605.332	785.933	26	DVL1.SQASATAPGLPPPHPTTK.+3y16+2. (Light)	719	968
608.015	809.482	26	DVL1.SQASATAPGLPPPHPTTK.+3y7. (Heavy)	679	611
605.332	805.457	26	DVL1.SQASATAPGLPPPHPTTK.+3y7. (Light)	20453	25104
608.015	906.535	26	DVL1.SQASATAPGLPPPHPTTK.+3y8. (Heavy)	762	409
605.332	902.509	26	DVL1.SQASATAPGLPPPHPTTK.+3y8. (Light)	605	393
621.389	984.603	29.5	FRAT1.APGPLAAAVPADK.+2y10. (Heavy)	2204	2133
617.364	980.578	29.5	FRAT1.APGPLAAAVPADK.+2y10. (Light)	1704	1894
621.389	1041.624	29.5	FRAT1.APGPLAAAVPADK.+2y11. (Heavy)	1881	1213
617.364	1037.599	29.5	FRAT1.APGPLAAAVPADK.+2y11. (Light)	5260	4523
621.389	632.392	29.5	FRAT1.APGPLAAAVPADK.+2y6. (Heavy)	6542	6977
617.364	628.366	29.5	FRAT1.APGPLAAAVPADK.+2y6. (Light)	9810	8637
621.389	703.429	29.5	FRAT1.APGPLAAAVPADK.+2y7. (Heavy)	15762	9784
617.364	699.404	29.5	FRAT1.APGPLAAAVPADK.+2y7. (Light)	4177	2696
621.389	774.466	29.5	FRAT1.APGPLAAAVPADK.+2y8. (Heavy)	4519	2564
617.364	770.441	29.5	FRAT1.APGPLAAAVPADK.+2y8. (Light)	3347	2473
752.01	1116.729	50.3	FRAT1.LLQQLVLSGNLIK.+2y10. (Heavy)	1763	1766
747.984	1112.704	50.3	FRAT1.LLQQLVLSGNLIK.+2y10. (Light)	8911	8347
752.01	1244.787	50.3	FRAT1.LLQQLVLSGNLIK.+2y11. (Heavy)	1174	585
747.984	1240.762	50.3	FRAT1.LLQQLVLSGNLIK.+2y11. (Light)	14337	25305
752.01	776.518	50.3	FRAT1.LLQQLVLSGNLIK.+2y7. (Heavy)	2066	1174
747.984	772.493	50.3	FRAT1.LLQQLVLSGNLIK.+2y7. (Light)	4067	2018
752.01	875.586	50.3	FRAT1.LLQQLVLSGNLIK.+2y8. (Heavy)	1817	1154
747.984	871.561	50.3	FRAT1.LLQQLVLSGNLIK.+2y8. (Light)	4430	3051
752.01	988.67	50.3	FRAT1.LLQQLVLSGNLIK.+2y9. (Heavy)	1266	836
747.984	984.645	50.3	FRAT1.LLQQLVLSGNLIK.+2y9. (Light)	2014	1481
660.675	1100.55	30.4	FZD1.FPVHGAGELCVGQNTSDK.+3b10. (Heavy)	680	349
657.991	1096.524	30.4	FZD1.FPVHGAGELCVGQNTSDK.+3b10. (Light)	1376	580
660.675	940.519	30.4	FZD1.FPVHGAGELCVGQNTSDK.+3b9. (Heavy)	2526	1924
657.991	936.494	30.4	FZD1.FPVHGAGELCVGQNTSDK.+3b9. (Light)	5015	4757
660.675	781.399	30.4	FZD1.FPVHGAGELCVGQNTSDK.+3y7. (Heavy)	2154	1591
657.991	777.374	30.4	FZD1.FPVHGAGELCVGQNTSDK.+3y7. (Light)	2005	1348
660.675	880.467	30.4	FZD1.FPVHGAGELCVGQNTSDK.+3y8. (Heavy)	1901	1331
657.991	876.442	30.4	FZD1.FPVHGAGELCVGQNTSDK.+3y8. (Light)	1566	994
660.675	1040.498	30.4	FZD1.FPVHGAGELCVGQNTSDK.+3y9. (Heavy)	1385	1073
657.991	1036.473	30.4	FZD1.FPVHGAGELCVGQNTSDK.+3y9. (Light)	1724	852
547.78	576.308	22.7	FZD1.GGFPGGAGASER.+2b7. (Heavy)	439	599

545.767	572.283	22.7	FZD1.GGFPGGAGASER.+2b7. (Light)	262	186
547.78	590.289	22.7	FZD1.GGFPGGAGASER.+2y6. (Heavy)	225	228
545.767	590.289	22.7	FZD1.GGFPGGAGASER.+2y6. (Light)	186	97
547.78	647.311	22.7	FZD1.GGFPGGAGASER.+2y7. (Heavy)	519	645
545.767	647.311	22.7	FZD1.GGFPGGAGASER.+2y7. (Light)	3399	3623
547.78	704.332	22.7	FZD1.GGFPGGAGASER.+2y8. (Heavy)	522	409
545.767	704.332	22.7	FZD1.GGFPGGAGASER.+2y8. (Light)	631	661
547.78	801.385	22.7	FZD1.GGFPGGAGASER.+2y9. (Heavy)	167	#N/A
545.767	801.385	22.7	FZD1.GGFPGGAGASER.+2y9. (Light)	965	788
544.307	658.353	42.2	FZD1.VPSYLNYHFLGEK.+3y10+2. (Heavy)	4042	2908
541.624	656.34	42.2	FZD1.VPSYLNYHFLGEK.+3y10+2. (Light)	5971	2623
544.307	701.869	42.2	FZD1.VPSYLNYHFLGEK.+3y11+2. (Heavy)	3701	2230
541.624	699.856	42.2	FZD1.VPSYLNYHFLGEK.+3y11+2. (Light)	12139	1722
544.307	750.395	42.2	FZD1.VPSYLNYHFLGEK.+3y12+2. (Heavy)	6180	2558
541.624	748.383	42.2	FZD1.VPSYLNYHFLGEK.+3y12+2. (Light)	81899	14524
544.307	625.386	42.2	FZD1.VPSYLNYHFLGEK.+3y5. (Heavy)	4372	2398
541.624	621.361	42.2	FZD1.VPSYLNYHFLGEK.+3y5. (Light)	6978	3550
544.307	1039.551	42.2	FZD1.VPSYLNYHFLGEK.+3y8. (Heavy)	951	475
541.624	1035.526	42.2	FZD1.VPSYLNYHFLGEK.+3y8. (Light)	488	241
739.919	1133.635	24.5	GLI3.GQQEQPEGTTLVK.+2y10. (Heavy)	168	13
735.894	1129.61	24.5	GLI3.GQQEQPEGTTLVK.+2y10. (Light)	414	326
739.919	1261.694	24.5	GLI3.GQQEQPEGTTLVK.+2y11. (Heavy)	155	30
735.894	1257.668	24.5	GLI3.GQQEQPEGTTLVK.+2y11. (Light)	161	#N/A
739.919	779.481	24.5	GLI3.GQQEQPEGTTLVK.+2y7. (Heavy)	497	251
735.894	775.456	24.5	GLI3.GQQEQPEGTTLVK.+2y7. (Light)	298	166
739.919	876.534	24.5	GLI3.GQQEQPEGTTLVK.+2y8. (Heavy)	404	343
735.894	872.509	24.5	GLI3.GQQEQPEGTTLVK.+2y8. (Light)	368	251
739.919	1004.592	24.5	GLI3.GQQEQPEGTTLVK.+2y9. (Heavy)	1362	1645
735.894	1000.567	24.5	GLI3.GQQEQPEGTTLVK.+2y9. (Light)	247	133
486.952	762.448	28	GLI3.IKPDEDLPSPGAR.+3b6. (Heavy)	2414	1846
484.268	754.398	28	GLI3.IKPDEDLPSPGAR.+3b6. (Light)	4925	3112
486.952	875.532	28	GLI3.IKPDEDLPSPGAR.+3b7. (Heavy)	819	535
484.268	867.482	28	GLI3.IKPDEDLPSPGAR.+3b7. (Light)	1520	1207
486.952	577.278	28	GLI3.IKPDEDLPSPGAR.+3y11+2. (Heavy)	5315	3681
484.268	577.278	28	GLI3.IKPDEDLPSPGAR.+3y11+2. (Light)	6321	5971
486.952	584.315	28	GLI3.IKPDEDLPSPGAR.+3y6. (Heavy)	6794	3590
484.268	584.315	28	GLI3.IKPDEDLPSPGAR.+3y6. (Light)	15094	12531
486.952	812.426	28	GLI3.IKPDEDLPSPGAR.+3y8. (Heavy)	1107	1117
484.268	812.426	28	GLI3.IKPDEDLPSPGAR.+3y8. (Light)	2091	1446
774.438	1116.637	44.3	GLI3.TSPNSLVTILNNSR.+2y10. (Heavy)	602	130
772.426	1116.637	44.3	GLI3.TSPNSLVTILNNSR.+2y10. (Light)	1751	1282

774.438	1230.68	44.3	GLI3.TSPNSLVTILNNSR.+2y11. (Heavy)	468	213
772.426	1230.68	44.3	GLI3.TSPNSLVTILNNSR.+2y11. (Light)	320	220
774.438	817.453	44.3	GLI3.TSPNSLVTILNNSR.+2y7. (Heavy)	1293	941
772.426	817.453	44.3	GLI3.TSPNSLVTILNNSR.+2y7. (Light)	1293	374
774.438	916.521	44.3	GLI3.TSPNSLVTILNNSR.+2y8. (Heavy)	1053	928
772.426	916.521	44.3	GLI3.TSPNSLVTILNNSR.+2y8. (Light)	847	485
774.438	1029.605	44.3	GLI3.TSPNSLVTILNNSR.+2y9. (Heavy)	438	253
772.426	1029.605	44.3	GLI3.TSPNSLVTILNNSR.+2y9. (Light)	480	299
663.751	1116.681	50.6	GSK3B.DIKPQNLLLDPDTAVLK.+3y10. (Heavy)	1139	2072
659.726	1112.656	50.6	GSK3B.DIKPQNLLLDPDTAVLK.+3y10. (Light)	863	540
663.751	865.039	50.6	GSK3B.DIKPQNLLLDPDTAVLK.+3y15+2. (Heavy)	2469	1251
659.726	861.014	50.6	GSK3B.DIKPQNLLLDPDTAVLK.+3y15+2. (Light)	1676	1226
663.751	775.486	50.6	GSK3B.DIKPQNLLLDPDTAVLK.+3y7. (Heavy)	9639	6552
659.726	771.461	50.6	GSK3B.DIKPQNLLLDPDTAVLK.+3y7. (Light)	2971	1875
663.751	890.513	50.6	GSK3B.DIKPQNLLLDPDTAVLK.+3y8. (Heavy)	4419	2516
659.726	886.488	50.6	GSK3B.DIKPQNLLLDPDTAVLK.+3y8. (Light)	2605	1947
663.751	1003.597	50.6	GSK3B.DIKPQNLLLDPDTAVLK.+3y9. (Heavy)	2333	1797
659.726	999.572	50.6	GSK3B.DIKPQNLLLDPDTAVLK.+3y9. (Light)	2465	1198
712.687	977.428	23	GSK3B.IQAAASTPTNATAASDANTGDR.+3y10. (Heavy)	643	457
711.345	977.428	23	GSK3B.IQAAASTPTNATAASDANTGDR.+3y10. (Light)	519	470
712.687	1078.476	23	GSK3B.IQAAASTPTNATAASDANTGDR.+3y11. (Heavy)	82	#N/A
711.345	1078.476	23	GSK3B.IQAAASTPTNATAASDANTGDR.+3y11. (Light)	498	99
712.687	748.322	23	GSK3B.IQAAASTPTNATAASDANTGDR.+3y7. (Heavy)	244	207
711.345	748.322	23	GSK3B.IQAAASTPTNATAASDANTGDR.+3y7. (Light)	195	91
712.687	835.354	23	GSK3B.IQAAASTPTNATAASDANTGDR.+3y8. (Heavy)	197	242
711.345	835.354	23	GSK3B.IQAAASTPTNATAASDANTGDR.+3y8. (Light)	229	160
712.687	906.391	23	GSK3B.IQAAASTPTNATAASDANTGDR.+3y9. (Heavy)	185	57
711.345	906.391	23	GSK3B.IQAAASTPTNATAASDANTGDR.+3y9. (Light)	329	213
751.945	1087.608	37.1	GSK3B.VIGNGSFGVVYQAK.+2y10. (Heavy)	1541	1209
747.919	1083.583	37.1	GSK3B.VIGNGSFGVVYQAK.+2y10. (Light)	17113	10383
751.945	1258.673	37.1	GSK3B.VIGNGSFGVVYQAK.+2y12. (Heavy)	1557	988
747.919	1254.648	37.1	GSK3B.VIGNGSFGVVYQAK.+2y12. (Light)	838	322
751.945	796.487	37.1	GSK3B.VIGNGSFGVVYQAK.+2y7. (Heavy)	1217	933
747.919	792.461	37.1	GSK3B.VIGNGSFGVVYQAK.+2y7. (Light)	1043	708
751.945	943.555	37.1	GSK3B.VIGNGSFGVVYQAK.+2y8. (Heavy)	1646	1283
747.919	939.53	37.1	GSK3B.VIGNGSFGVVYQAK.+2y8. (Light)	900	667
751.945	1030.587	37.1	GSK3B.VIGNGSFGVVYQAK.+2y9. (Heavy)	3715	2345
747.919	1026.562	37.1	GSK3B.VIGNGSFGVVYQAK.+2y9. (Light)	1042	768
772.39	1164.531	30	HES1.FLSTCEGVNTEVR.+2y10. (Heavy)	1002	794
770.377	1164.531	30	HES1.FLSTCEGVNTEVR.+2y10. (Light)	1166	975
772.39	1251.563	30	HES1.FLSTCEGVNTEVR.+2y11. (Heavy)	3239	2704

770.377	1251.563	30	HES1.FLSTCEGVNTEVR.+2y11. (Light)	2395	2193
772.39	774.41	30	HES1.FLSTCEGVNTEVR.+2y7. (Heavy)	2338	1232
770.377	774.41	30	HES1.FLSTCEGVNTEVR.+2y7. (Light)	4047	3788
772.39	903.453	30	HES1.FLSTCEGVNTEVR.+2y8. (Heavy)	2129	1563
770.377	903.453	30	HES1.FLSTCEGVNTEVR.+2y8. (Light)	3082	2842
772.39	1063.484	30	HES1.FLSTCEGVNTEVR.+2y9. (Heavy)	1070	984
770.377	1063.484	30	HES1.FLSTCEGVNTEVR.+2y9. (Light)	2689	1908
498.302	507.307	8	HES1.LGSQAGEAAK.+2y5. (Heavy)	11	#N/A
494.277	503.282	8	HES1.LGSQAGEAAK.+2y5. (Light)	16	7
498.302	578.345	8	HES1.LGSQAGEAAK.+2y6. (Heavy)	11	#N/A
494.277	574.32	8	HES1.LGSQAGEAAK.+2y6. (Light)	16	8
498.302	706.403	8	HES1.LGSQAGEAAK.+2y7. (Heavy)	18	6
494.277	702.378	8	HES1.LGSQAGEAAK.+2y7. (Light)	#N/A	#N/A
498.302	793.435	8	HES1.LGSQAGEAAK.+2y8. (Heavy)	11	0
494.277	789.41	8	HES1.LGSQAGEAAK.+2y8. (Light)	11	0
498.302	850.457	8	HES1.LGSQAGEAAK.+2y9. (Heavy)	41	37
494.277	846.432	8	HES1.LGSQAGEAAK.+2y9. (Light)	64	51
722.412	1318.782	27.1	HES1.NSSSPVAATPASVNTTPDKPK.+3y12. (Heavy)	464	272
718.386	1310.731	27.1	HES1.NSSSPVAATPASVNTTPDKPK.+3y12. (Light)	5139	7363
722.412	781.455	27.1	HES1.NSSSPVAATPASVNTTPDKPK.+3y15+2. (Heavy)	1610	1018
718.386	777.43	27.1	HES1.NSSSPVAATPASVNTTPDKPK.+3y15+2. (Light)	2120	1791
722.412	879.516	27.1	HES1.NSSSPVAATPASVNTTPDKPK.+3y17+2. (Heavy)	6225	6103
718.386	875.491	27.1	HES1.NSSSPVAATPASVNTTPDKPK.+3y17+2. (Light)	7550	10137
722.412	923.032	27.1	HES1.NSSSPVAATPASVNTTPDKPK.+3y18+2. (Heavy)	771	579
718.386	919.007	27.1	HES1.NSSSPVAATPASVNTTPDKPK.+3y18+2. (Light)	650	157
722.412	966.548	27.1	HES1.NSSSPVAATPASVNTTPDKPK.+3y19+2. (Heavy)	610	229
718.386	962.523	27.1	HES1.NSSSPVAATPASVNTTPDKPK.+3y19+2. (Light)	871	439
417.577	524.78	26.2	HEY1.LGSAHPEAPALR.+3y10+2. (Heavy)	2100	1501
416.235	524.78	26.2	HEY1.LGSAHPEAPALR.+3y10+2. (Light)	1382	1327
417.577	553.291	26.2	HEY1.LGSAHPEAPALR.+3y11+2. (Heavy)	2954	1657
416.235	553.291	26.2	HEY1.LGSAHPEAPALR.+3y11+2. (Light)	1795	1192
417.577	527.33	26.2	HEY1.LGSAHPEAPALR.+3y5. (Heavy)	1247	153
416.235	527.33	26.2	HEY1.LGSAHPEAPALR.+3y5. (Light)	2971	2697
417.577	753.425	26.2	HEY1.LGSAHPEAPALR.+3y7. (Heavy)	612	209
416.235	753.425	26.2	HEY1.LGSAHPEAPALR.+3y7. (Light)	1019	585
417.577	445.746	26.2	HEY1.LGSAHPEAPALR.+3y8+2. (Heavy)	5511	3587
416.235	445.746	26.2	HEY1.LGSAHPEAPALR.+3y8+2. (Light)	10660	10262
478.598	810.477	24.2	HEY1.LVSHLNNYASQR.+3b7. (Heavy)	205	89
477.256	806.452	24.2	HEY1.LVSHLNNYASQR.+3b7. (Light)	353	193
478.598	595.289	24.2	HEY1.LVSHLNNYASQR.+3y10+2. (Heavy)	356	284
477.256	595.289	24.2	HEY1.LVSHLNNYASQR.+3y10+2. (Light)	945	949

478.598	644.823	24.2	HEY1.LVSHLNNYASQR.+3y11+2. (Heavy)	695	324
477.256	644.823	24.2	HEY1.LVSHLNNYASQR.+3y11+2. (Light)	1432	1078
478.598	624.31	24.2	HEY1.LVSHLNNYASQR.+3y5. (Heavy)	847	506
477.256	624.31	24.2	HEY1.LVSHLNNYASQR.+3y5. (Light)	1186	1423
478.598	965.48	24.2	HEY1.LVSHLNNYASQR.+3y8. (Heavy)	281	224
477.256	965.48	24.2	HEY1.LVSHLNNYASQR.+3y8. (Light)	412	283
847.469	1072.527	58	HEY1.YLSIIEGLDASDPLR.+2y10. (Heavy)	4484	2722
845.457	1072.527	58	HEY1.YLSIIEGLDASDPLR.+2y10. (Light)	1389	598
847.469	1185.611	58	HEY1.YLSIIEGLDASDPLR.+2y11. (Heavy)	970	579
845.457	1185.611	58	HEY1.YLSIIEGLDASDPLR.+2y11. (Light)	1078	525
847.469	1385.727	58	HEY1.YLSIIEGLDASDPLR.+2y13. (Heavy)	692	428
845.457	1385.727	58	HEY1.YLSIIEGLDASDPLR.+2y13. (Light)	792	506
847.469	886.463	58	HEY1.YLSIIEGLDASDPLR.+2y8. (Heavy)	983	820
845.457	886.463	58	HEY1.YLSIIEGLDASDPLR.+2y8. (Light)	1021	641
847.469	943.484	58	HEY1.YLSIIEGLDASDPLR.+2y9. (Heavy)	2060	1433
845.457	943.484	58	HEY1.YLSIIEGLDASDPLR.+2y9. (Light)	941	688
561.801	589.33	27.8	INHBA.EGSDLSVVER.+2y5. (Heavy)	3940	2890
559.788	589.33	27.8	INHBA.EGSDLSVVER.+2y5. (Light)	14650	9092
561.801	702.414	27.8	INHBA.EGSDLSVVER.+2y6. (Heavy)	66474	41149
559.788	702.414	27.8	INHBA.EGSDLSVVER.+2y6. (Light)	43850	25604
561.801	817.441	27.8	INHBA.EGSDLSVVER.+2y7. (Heavy)	1766	852
559.788	817.441	27.8	INHBA.EGSDLSVVER.+2y7. (Light)	1641	1308
561.801	904.473	27.8	INHBA.EGSDLSVVER.+2y8. (Heavy)	2034	1226
559.788	904.473	27.8	INHBA.EGSDLSVVER.+2y8. (Light)	2448	1639
561.801	961.495	27.8	INHBA.EGSDLSVVER.+2y9. (Heavy)	2072	1726
559.788	961.495	27.8	INHBA.EGSDLSVVER.+2y9. (Light)	2658	1800
654.008	767.398	29.2	INHBA.HPQGSLDTGEEAEEVGLK.+3b7. (Heavy)	8974	10135
651.325	763.373	29.2	INHBA.HPQGSLDTGEEAEEVGLK.+3b7. (Light)	14986	16127
654.008	925.468	29.2	INHBA.HPQGSLDTGEEAEEVGLK.+3b9. (Heavy)	1749	1036
651.325	921.442	29.2	INHBA.HPQGSLDTGEEAEEVGLK.+3b9. (Light)	2077	1769
654.008	706.428	29.2	INHBA.HPQGSLDTGEEAEEVGLK.+3y6. (Heavy)	4974	8265
651.325	702.403	29.2	INHBA.HPQGSLDTGEEAEEVGLK.+3y6. (Light)	5673	5106
654.008	777.465	29.2	INHBA.HPQGSLDTGEEAEEVGLK.+3y7. (Heavy)	2987	2424
651.325	773.44	29.2	INHBA.HPQGSLDTGEEAEEVGLK.+3y7. (Light)	3105	1106
654.008	906.508	29.2	INHBA.HPQGSLDTGEEAEEVGLK.+3y8. (Heavy)	1777	852
651.325	902.483	29.2	INHBA.HPQGSLDTGEEAEEVGLK.+3y8. (Light)	1621	1144
491.817	588.391	30	INHBA.SELLLSEK.+2b5. (Heavy)	7133	4569
487.792	584.365	30	INHBA.SELLLSEK.+2b5. (Light)	25824	33718
491.817	508.328	30	INHBA.SELLLSEK.+2y4. (Heavy)	10791	8208
487.792	504.303	30	INHBA.SELLLSEK.+2y4. (Light)	8500	7563
491.817	621.412	30	INHBA.SELLLSEK.+2y5. (Heavy)	11239	9245

487.792	617.387	30	INHBA.SELLLSEK.+2y5. (Light)	24206	18452
491.817	734.496	30	INHBA.SELLLSEK.+2y6. (Heavy)	9327	16701
487.792	730.471	30	INHBA.SELLLSEK.+2y6. (Light)	12454	9613
491.817	863.539	30	INHBA.SELLLSEK.+2y7. (Heavy)	1653	1163
487.792	859.513	30	INHBA.SELLLSEK.+2y7. (Light)	2041	1582
640.882	679.408	30	LFTY1.EHLGPLASGAHK.+2b6. (Heavy)	2870	2288
636.857	675.382	30	LFTY1.EHLGPLASGAHK.+2b6. (Light)	5085	2969
640.882	444.287	30	LFTY1.EHLGPLASGAHK.+2y4. (Heavy)	5674	4523
636.857	440.262	30	LFTY1.EHLGPLASGAHK.+2y4. (Light)	27378	22316
640.882	531.319	30	LFTY1.EHLGPLASGAHK.+2y5. (Heavy)	2409	1161
636.857	527.294	30	LFTY1.EHLGPLASGAHK.+2y5. (Light)	3056	2446
640.882	602.356	30	LFTY1.EHLGPLASGAHK.+2y6. (Heavy)	6018	3794
636.857	598.331	30	LFTY1.EHLGPLASGAHK.+2y6. (Light)	4389	2671
640.882	435.261	30	LFTY1.EHLGPLASGAHK.+2y9+2. (Heavy)	2309	1939
636.857	433.248	30	LFTY1.EHLGPLASGAHK.+2y9+2. (Light)	2287	1837
734.445	783.455	44	LFTY1.LPPNSELVQAVLR.+2b7. (Heavy)	1823	388
732.433	779.43	44	LFTY1.LPPNSELVQAVLR.+2b7. (Light)	1246	718
734.445	1128.637	44	LFTY1.LPPNSELVQAVLR.+2y10. (Heavy)	611	352
732.433	1128.637	44	LFTY1.LPPNSELVQAVLR.+2y10. (Light)	713	355
734.445	798.52	44	LFTY1.LPPNSELVQAVLR.+2y7. (Heavy)	1409	1070
732.433	798.52	44	LFTY1.LPPNSELVQAVLR.+2y7. (Light)	1013	794
734.445	927.562	44	LFTY1.LPPNSELVQAVLR.+2y8. (Heavy)	667	401
732.433	927.562	44	LFTY1.LPPNSELVQAVLR.+2y8. (Light)	806	573
734.445	1014.594	44	LFTY1.LPPNSELVQAVLR.+2y9. (Heavy)	640	431
732.433	1014.594	44	LFTY1.LPPNSELVQAVLR.+2y9. (Light)	1697	2400
656.916	1152.71	40.5	LFTY1.QPLLLQVSVQR.+2y10. (Heavy)	74917	42010
654.904	1152.71	40.5	LFTY1.QPLLLQVSVQR.+2y10. (Light)	137282	102665
656.916	716.405	40.5	LFTY1.QPLLLQVSVQR.+2y6. (Heavy)	5802	4447
654.904	716.405	40.5	LFTY1.QPLLLQVSVQR.+2y6. (Light)	6719	4542
656.916	829.489	40.5	LFTY1.QPLLLQVSVQR.+2y7. (Heavy)	2453	1593
654.904	829.489	40.5	LFTY1.QPLLLQVSVQR.+2y7. (Light)	4873	3155
656.916	942.573	40.5	LFTY1.QPLLLQVSVQR.+2y8. (Heavy)	2420	1205
654.904	942.573	40.5	LFTY1.QPLLLQVSVQR.+2y8. (Light)	1049	876
656.916	1055.657	40.5	LFTY1.QPLLLQVSVQR.+2y9. (Heavy)	7578	4648
654.904	1055.657	40.5	LFTY1.QPLLLQVSVQR.+2y9. (Light)	1628	1100
456.273	504.271	3.3	NANOG.NSNGVTQK.+2b5. (Heavy)	216	121
452.248	500.246	3.3	NANOG.NSNGVTQK.+2b5. (Light)	185	66
456.273	507.344	3.3	NANOG.NSNGVTQK.+2y4. (Heavy)	323	195
452.248	503.319	3.3	NANOG.NSNGVTQK.+2y4. (Light)	185	87
456.273	564.365	3.3	NANOG.NSNGVTQK.+2y5. (Heavy)	149	81
452.248	560.34	3.3	NANOG.NSNGVTQK.+2y5. (Light)	183	105

456.273	678.408	3.3	NANOG.NSNGVTQK.+2y6. (Heavy)	98	51
452.248	674.383	3.3	NANOG.NSNGVTQK.+2y6. (Light)	171	98
456.273	765.44	3.3	NANOG.NSNGVTQK.+2y7. (Heavy)	173	76
452.248	761.415	3.3	NANOG.NSNGVTQK.+2y7. (Light)	529	292
836.437	1205.594	41.8	NANOG.TVFSSTQLCVLNDR.+2y10. (Heavy)	780	510
834.425	1205.594	41.8	NANOG.TVFSSTQLCVLNDR.+2y10. (Light)	1038	905
836.437	1292.626	41.8	NANOG.TVFSSTQLCVLNDR.+2y11. (Heavy)	557	58
834.425	1292.626	41.8	NANOG.TVFSSTQLCVLNDR.+2y11. (Light)	1109	917
836.437	889.456	41.8	NANOG.TVFSSTQLCVLNDR.+2y7. (Heavy)	814	264
834.425	889.456	41.8	NANOG.TVFSSTQLCVLNDR.+2y7. (Light)	1507	735
836.437	1017.515	41.8	NANOG.TVFSSTQLCVLNDR.+2y8. (Heavy)	801	802
834.425	1017.515	41.8	NANOG.TVFSSTQLCVLNDR.+2y8. (Light)	648	334
836.437	1118.562	41.8	NANOG.TVFSSTQLCVLNDR.+2y9. (Heavy)	1049	1070
834.425	1118.562	41.8	NANOG.TVFSSTQLCVLNDR.+2y9. (Light)	1189	725
789.102	1196.719	58.7	NANOG.YLSLQQMQELSNILNLSYK.+3y10. (Heavy)	402	152
786.419	1192.694	58.7	NANOG.YLSLQQMQELSNILNLSYK.+3y10. (Light)	430	326
789.102	1325.761	58.7	NANOG.YLSLQQMQELSNILNLSYK.+3y11. (Heavy)	1269	2295
786.419	1321.736	58.7	NANOG.YLSLQQMQELSNILNLSYK.+3y11. (Light)	394	230
789.102	928.99	58.7	NANOG.YLSLQQMQELSNILNLSYK.+3y15+2. (Heavy)	730	483
786.419	926.977	58.7	NANOG.YLSLQQMQELSNILNLSYK.+3y15+2. (Light)	549	273
789.102	1029.048	58.7	NANOG.YLSLQQMQELSNILNLSYK.+3y17+2. (Heavy)	1205	2336
786.419	1027.035	58.7	NANOG.YLSLQQMQELSNILNLSYK.+3y17+2. (Light)	827	609
789.102	1083.635	58.7	NANOG.YLSLQQMQELSNILNLSYK.+3y9. (Heavy)	1304	1255
786.419	1079.609	58.7	NANOG.YLSLQQMQELSNILNLSYK.+3y9. (Light)	762	648
958	1242.655	46	NODAL.GQPSSPSPLAYMLSLYR.+2y10. (Heavy)	1112	487
955.988	1242.655	46	NODAL.GQPSSPSPLAYMLSLYR.+2y10. (Light)	438	312
958	1329.687	46	NODAL.GQPSSPSPLAYMLSLYR.+2y11. (Heavy)	427	289
955.988	1329.687	46	NODAL.GQPSSPSPLAYMLSLYR.+2y11. (Light)	409	242
958	1426.74	46	NODAL.GQPSSPSPLAYMLSLYR.+2y12. (Heavy)	209	95
955.988	1426.74	46	NODAL.GQPSSPSPLAYMLSLYR.+2y12. (Light)	243	140
958	1513.772	46	NODAL.GQPSSPSPLAYMLSLYR.+2y13. (Heavy)	126	#N/A
955.988	1513.772	46	NODAL.GQPSSPSPLAYMLSLYR.+2y13. (Light)	180	66
958	1032.518	46	NODAL.GQPSSPSPLAYMLSLYR.+2y8. (Heavy)	529	361
955.988	1032.518	46	NODAL.GQPSSPSPLAYMLSLYR.+2y8. (Light)	384	235
787.447	1183.578	30	NODAL.TKPLSMLYVDNGR.+2y10. (Heavy)	805	916
783.421	1183.578	30	NODAL.TKPLSMLYVDNGR.+2y10. (Light)	665	390
787.447	1280.63	30	NODAL.TKPLSMLYVDNGR.+2y11. (Heavy)	#N/A	#N/A
783.421	1280.63	30	NODAL.TKPLSMLYVDNGR.+2y11. (Light)	1646	849
787.447	836.426	30	NODAL.TKPLSMLYVDNGR.+2y7. (Heavy)	1039	310
783.421	836.426	30	NODAL.TKPLSMLYVDNGR.+2y7. (Light)	958	749
787.447	983.461	30	NODAL.TKPLSMLYVDNGR.+2y8. (Heavy)	1830	1628

783.421	983.461	30	NODAL.TKPLSMLYVDNGR.+2y8. (Light)	793	501
787.447	1070.494	30	NODAL.TKPLSMLYVDNGR.+2y9. (Heavy)	1305	1681
783.421	1070.494	30	NODAL.TKPLSMLYVDNGR.+2y9. (Light)	1262	548
591.827	606.358	31	NODAL.VPSTCCAPVK.+2y5. (Heavy)	2477	1438
587.802	602.333	31	NODAL.VPSTCCAPVK.+2y5. (Light)	4482	3417
591.827	766.389	31	NODAL.VPSTCCAPVK.+2y6. (Heavy)	9100	8185
587.802	762.364	31	NODAL.VPSTCCAPVK.+2y6. (Light)	3415	2183
591.827	867.436	31	NODAL.VPSTCCAPVK.+2y7. (Heavy)	2823	2086
587.802	863.411	31	NODAL.VPSTCCAPVK.+2y7. (Light)	2266	1869
591.827	954.469	31	NODAL.VPSTCCAPVK.+2y8. (Heavy)	1996	1049
587.802	950.443	31	NODAL.VPSTCCAPVK.+2y8. (Light)	6317	7662
591.827	1051.521	31	NODAL.VPSTCCAPVK.+2y9. (Heavy)	5421	5650
587.802	1047.496	31	NODAL.VPSTCCAPVK.+2y9. (Light)	5625	5442
686.342	1211.529	43.6	NOTC1.FEEPVVLPDLDDQTDHR.+3y10. (Heavy)	2436	1951
685.001	1211.529	43.6	NOTC1.FEEPVVLPDLDDQTDHR.+3y10. (Light)	13616	17751
686.342	712.344	43.6	NOTC1.FEEPVVLPDLDDQTDHR.+3y12+2. (Heavy)	2041	928
685.001	712.344	43.6	NOTC1.FEEPVVLPDLDDQTDHR.+3y12+2. (Light)	3591	4895
686.342	761.878	43.6	NOTC1.FEEPVVLPDLDDQTDHR.+3y13+2. (Heavy)	1424	787
685.001	761.878	43.6	NOTC1.FEEPVVLPDLDDQTDHR.+3y13+2. (Light)	2262	1212
686.342	810.405	43.6	NOTC1.FEEPVVLPDLDDQTDHR.+3y14+2. (Heavy)	1447	1070
685.001	810.405	43.6	NOTC1.FEEPVVLPDLDDQTDHR.+3y14+2. (Light)	2424	2159
686.342	874.926	43.6	NOTC1.FEEPVVLPDLDDQTDHR.+3y15+2. (Heavy)	1125	1062
685.001	874.926	43.6	NOTC1.FEEPVVLPDLDDQTDHR.+3y15+2. (Light)	1015	800
655.866	646.315	42.3	NOTC1.GSIVYLEIDNR.+2y5. (Heavy)	64694	29189
653.854	646.315	42.3	NOTC1.GSIVYLEIDNR.+2y5. (Light)	33977	14088
655.866	759.4	42.3	NOTC1.GSIVYLEIDNR.+2y6. (Heavy)	3959	2235
653.854	759.4	42.3	NOTC1.GSIVYLEIDNR.+2y6. (Light)	7049	3457
655.866	922.463	42.3	NOTC1.GSIVYLEIDNR.+2y7. (Heavy)	2458	1646
653.854	922.463	42.3	NOTC1.GSIVYLEIDNR.+2y7. (Light)	4593	3409
655.866	1021.531	42.3	NOTC1.GSIVYLEIDNR.+2y8. (Heavy)	2722	1715
653.854	1021.531	42.3	NOTC1.GSIVYLEIDNR.+2y8. (Light)	3419	978
655.866	1134.615	42.3	NOTC1.GSIVYLEIDNR.+2y9. (Heavy)	5156	1662
653.854	1134.615	42.3	NOTC1.GSIVYLEIDNR.+2y9. (Light)	4289	1593
824.939	1287.68	45	NOTC1.NGGTCDLLTLTEYK.+2y10. (Heavy)	758	238
820.914	1283.655	45	NOTC1.NGGTCDLLTLTEYK.+2y10. (Light)	774	844
824.939	1388.728	45	NOTC1.NGGTCDLLTLTEYK.+2y11. (Heavy)	7735	3748
820.914	1384.703	45	NOTC1.NGGTCDLLTLTEYK.+2y11. (Light)	583	526
824.939	899.539	45	NOTC1.NGGTCDLLTLTEYK.+2y7. (Heavy)	2285	1213
820.914	895.513	45	NOTC1.NGGTCDLLTLTEYK.+2y7. (Light)	2476	1563
824.939	1012.623	45	NOTC1.NGGTCDLLTLTEYK.+2y8. (Heavy)	2799	2047
820.914	1008.598	45	NOTC1.NGGTCDLLTLTEYK.+2y8. (Light)	1064	863

824.939	1127.65	45	NOTC1.NGGTCDLLTLTEYK.+2y9. (Heavy)	1549	604
820.914	1123.625	45	NOTC1.NGGTCDLLTLTEYK.+2y9. (Light)	1163	801
365.565	463.322	26.2	P53.LGFLHSGTAK.+3b4. (Heavy)	3470	1488
362.882	459.297	26.2	P53.LGFLHSGTAK.+3b4. (Light)	1037	872
365.565	495.307	26.2	P53.LGFLHSGTAK.+3y5. (Heavy)	1036	869
362.882	491.282	26.2	P53.LGFLHSGTAK.+3y5. (Light)	731	223
365.565	632.366	26.2	P53.LGFLHSGTAK.+3y6. (Heavy)	544	432
362.882	628.341	26.2	P53.LGFLHSGTAK.+3y6. (Light)	1316	1872
365.565	446.763	26.2	P53.LGFLHSGTAK.+3y8+2. (Heavy)	2646	2655
362.882	444.751	26.2	P53.LGFLHSGTAK.+3y8+2. (Light)	734	413
365.565	475.274	26.2	P53.LGFLHSGTAK.+3y9+2. (Heavy)	1086	1109
362.882	473.261	26.2	P53.LGFLHSGTAK.+3y9+2. (Light)	2938	2165
700.749	839.602	54.4	P53.RPILTIITLEDSSGNLLGR.+3b7. (Heavy)	1246	866
699.407	835.576	54.4	P53.RPILTIITLEDSSGNLLGR.+3b7. (Light)	1910	1985
700.749	1047.506	54.4	P53.RPILTIITLEDSSGNLLGR.+3y10. (Heavy)	2679	2733
699.407	1047.506	54.4	P53.RPILTIITLEDSSGNLLGR.+3y10. (Light)	1864	1378
700.749	716.405	54.4	P53.RPILTIITLEDSSGNLLGR.+3y7. (Heavy)	5253	3496
699.407	716.405	54.4	P53.RPILTIITLEDSSGNLLGR.+3y7. (Light)	1856	1433
700.749	803.437	54.4	P53.RPILTIITLEDSSGNLLGR.+3y8. (Heavy)	1308	957
699.407	803.437	54.4	P53.RPILTIITLEDSSGNLLGR.+3y8. (Light)	3577	1871
700.749	918.464	54.4	P53.RPILTIITLEDSSGNLLGR.+3y9. (Heavy)	6835	2548
699.407	918.464	54.4	P53.RPILTIITLEDSSGNLLGR.+3y9. (Light)	160536	61571
702.886	831.385	28.5	P53.SVTCTYSPALNK.+2b7. (Heavy)	1246	866
698.861	827.36	28.5	P53.SVTCTYSPALNK.+2b7. (Light)	1910	1985
702.886	1186.607	28.5	P53.SVTCTYSPALNK.+2y10. (Heavy)	2679	2733
698.861	1182.582	28.5	P53.SVTCTYSPALNK.+2y10. (Light)	1864	1378
702.886	824.481	28.5	P53.SVTCTYSPALNK.+2y7. (Heavy)	5253	3496
698.861	820.456	28.5	P53.SVTCTYSPALNK.+2y7. (Light)	1856	1433
702.886	925.529	28.5	P53.SVTCTYSPALNK.+2y8. (Heavy)	1308	957
698.861	921.504	28.5	P53.SVTCTYSPALNK.+2y8. (Light)	3577	1871
702.886	1085.56	28.5	P53.SVTCTYSPALNK.+2y9. (Heavy)	6835	2548
698.861	1081.535	28.5	P53.SVTCTYSPALNK.+2y9. (Light)	160536	61571
573.854	968.539	44	PO5F1.FEALQLSFK.+2b8. (Heavy)	2844	1272
569.829	964.514	44	PO5F1.FEALQLSFK.+2b8. (Light)	15455	5875
573.854	654.412	44	PO5F1.FEALQLSFK.+2y5. (Heavy)	10167	2837
569.829	650.387	44	PO5F1.FEALQLSFK.+2y5. (Light)	3611	2333
573.854	767.496	44	PO5F1.FEALQLSFK.+2y6. (Heavy)	3295	1439
569.829	763.471	44	PO5F1.FEALQLSFK.+2y6. (Light)	3905	1991
573.854	838.533	44	PO5F1.FEALQLSFK.+2y7. (Heavy)	4649	2124
569.829	834.508	44	PO5F1.FEALQLSFK.+2y7. (Light)	7975	2881
573.854	967.576	44	PO5F1.FEALQLSFK.+2y8. (Heavy)	4567	2301

569.829	963.551	44	PO5F1.FEALQLSFK.+2y8. (Light)	49186	7871
747.4	1219.61	23	PO5F1.LEQNPEESQDIK.+2y10. (Heavy)	82	#N/A
743.375	1215.585	23	PO5F1.LEQNPEESQDIK.+2y10. (Light)	203	95
747.4	751.413	23	PO5F1.LEQNPEESQDIK.+2y6. (Heavy)	395	379
743.375	747.388	23	PO5F1.LEQNPEESQDIK.+2y6. (Light)	470	267
747.4	880.456	23	PO5F1.LEQNPEESQDIK.+2y7. (Heavy)	#N/A	#N/A
743.375	876.431	23	PO5F1.LEQNPEESQDIK.+2y7. (Light)	126	91
747.4	977.509	23	PO5F1.LEQNPEESQDIK.+2y8. (Heavy)	112	4
743.375	973.484	23	PO5F1.LEQNPEESQDIK.+2y8. (Light)	130	49
747.4	1091.552	23	PO5F1.LEQNPEESQDIK.+2y9. (Heavy)	93	#N/A
743.375	1087.527	23	PO5F1.LEQNPEESQDIK.+2y9. (Light)	139	51
1028.001	1293.641	34.1	PO5F1.WVEEADNNENLQEICK.+2y10. (Heavy)	453	209
1023.975	1289.615	34.1	PO5F1.WVEEADNNENLQEICK.+2y10. (Light)	673	333
1028.001	1408.667	34.1	PO5F1.WVEEADNNENLQEICK.+2y11. (Heavy)	317	363
1023.975	1404.642	34.1	PO5F1.WVEEADNNENLQEICK.+2y11. (Light)	332	250
1028.001	1479.705	34.1	PO5F1.WVEEADNNENLQEICK.+2y12. (Heavy)	243	178
1023.975	1475.679	34.1	PO5F1.WVEEADNNENLQEICK.+2y12. (Light)	469	197
1028.001	1065.555	34.1	PO5F1.WVEEADNNENLQEICK.+2y8. (Heavy)	572	425
1023.975	1061.53	34.1	PO5F1.WVEEADNNENLQEICK.+2y8. (Light)	437	274
1028.001	1179.598	34.1	PO5F1.WVEEADNNENLQEICK.+2y9. (Heavy)	296	176
1023.975	1175.573	34.1	PO5F1.WVEEADNNENLQEICK.+2y9. (Light)	501	271
752.937	1064.573	31.7	PTC1.LPTPSPEPPPSVVR.+2y10. (Heavy)	636	333
750.925	1064.573	31.7	PTC1.LPTPSPEPPPSVVR.+2y10. (Light)	972	731
752.937	1161.626	31.7	PTC1.LPTPSPEPPPSVVR.+2y11. (Heavy)	920	772
750.925	1161.626	31.7	PTC1.LPTPSPEPPPSVVR.+2y11. (Light)	809	642
752.937	1262.674	31.7	PTC1.LPTPSPEPPPSVVR.+2y12. (Heavy)	1130	905
750.925	1262.674	31.7	PTC1.LPTPSPEPPPSVVR.+2y12. (Light)	1390	1779
752.937	880.489	31.7	PTC1.LPTPSPEPPPSVVR.+2y8. (Heavy)	1010	874
750.925	880.489	31.7	PTC1.LPTPSPEPPPSVVR.+2y8. (Light)	1723	1239
752.937	977.541	31.7	PTC1.LPTPSPEPPPSVVR.+2y9. (Heavy)	4641	4913
750.925	977.541	31.7	PTC1.LPTPSPEPPPSVVR.+2y9. (Light)	878	634
704.671	786.384	28.2	PTC1.TEYDPHTHVYYTTAEPR.+3y13+2. (Heavy)	2936	1413
703.329	786.384	28.2	PTC1.TEYDPHTHVYYTTAEPR.+3y13+2. (Light)	2819	1727
704.671	843.897	28.2	PTC1.TEYDPHTHVYYTTAEPR.+3y14+2. (Heavy)	1252	658
703.329	843.897	28.2	PTC1.TEYDPHTHVYYTTAEPR.+3y14+2. (Light)	1765	838
704.671	925.429	28.2	PTC1.TEYDPHTHVYYTTAEPR.+3y15+2. (Heavy)	811	472
703.329	925.429	28.2	PTC1.TEYDPHTHVYYTTAEPR.+3y15+2. (Light)	2655	1777
704.671	837.41	28.2	PTC1.TEYDPHTHVYYTTAEPR.+3y7. (Heavy)	1661	1048
703.329	837.41	28.2	PTC1.TEYDPHTHVYYTTAEPR.+3y7. (Light)	871	712
704.671	1000.473	28.2	PTC1.TEYDPHTHVYYTTAEPR.+3y8. (Heavy)	2514	951
703.329	1000.473	28.2	PTC1.TEYDPHTHVYYTTAEPR.+3y8. (Light)	2617	2253

661.365	679.87	27.7	PTC1.TYVEVVHQSVAQNSTQK.+3y12+2. (Heavy)	1661	1530
658.681	677.857	27.7	PTC1.TYVEVVHQSVAQNSTQK.+3y12+2. (Light)	3268	2963
661.365	729.404	27.7	PTC1.TYVEVVHQSVAQNSTQK.+3y13+2. (Heavy)	1137	736
658.681	727.392	27.7	PTC1.TYVEVVHQSVAQNSTQK.+3y13+2. (Light)	4284	4965
661.365	793.925	27.7	PTC1.TYVEVVHQSVAQNSTQK.+3y14+2. (Heavy)	1222	720
658.681	791.913	27.7	PTC1.TYVEVVHQSVAQNSTQK.+3y14+2. (Light)	2367	1998
661.365	843.46	27.7	PTC1.TYVEVVHQSVAQNSTQK.+3y15+2. (Heavy)	3618	4172
658.681	841.447	27.7	PTC1.TYVEVVHQSVAQNSTQK.+3y15+2. (Light)	6171	8053
661.365	808.446	27.7	PTC1.TYVEVVHQSVAQNSTQK.+3y7. (Heavy)	1207	587
658.681	804.421	27.7	PTC1.TYVEVVHQSVAQNSTQK.+3y7. (Light)	2303	1899
662.032	690.851	38.1	SFRP1.FYTKPPQCVDIPADLR.+3y12+2. (Heavy)	3381	4600
659.349	690.851	38.1	SFRP1.FYTKPPQCVDIPADLR.+3y12+2. (Light)	1700	1406
662.032	770.926	38.1	SFRP1.FYTKPPQCVDIPADLR.+3y13+2. (Heavy)	826	577
659.349	768.914	38.1	SFRP1.FYTKPPQCVDIPADLR.+3y13+2. (Light)	1024	570
662.032	821.45	38.1	SFRP1.FYTKPPQCVDIPADLR.+3y14+2. (Heavy)	1480	803
659.349	819.438	38.1	SFRP1.FYTKPPQCVDIPADLR.+3y14+2. (Light)	1579	1145
662.032	902.982	38.1	SFRP1.FYTKPPQCVDIPADLR.+3y15+2. (Heavy)	917	636
659.349	900.969	38.1	SFRP1.FYTKPPQCVDIPADLR.+3y15+2. (Light)	2804	2424
662.032	799.431	38.1	SFRP1.FYTKPPQCVDIPADLR.+3y7. (Heavy)	1349	644
659.349	799.431	38.1	SFRP1.FYTKPPQCVDIPADLR.+3y7. (Light)	1280	991
626.662	795.892	45.3	SFRP1.SEAIIEHLCASEFALR.+3b14+2. (Heavy)	3398	3048
625.321	793.88	45.3	SFRP1.SEAIIEHLCASEFALR.+3b14+2. (Light)	6101	4652
626.662	666.822	45.3	SFRP1.SEAIIEHLCASEFALR.+3y11+2. (Heavy)	2317	2328
625.321	666.822	45.3	SFRP1.SEAIIEHLCASEFALR.+3y11+2. (Light)	2360	2108
626.662	723.364	45.3	SFRP1.SEAIIEHLCASEFALR.+3y12+2. (Heavy)	19293	23448
625.321	723.364	45.3	SFRP1.SEAIIEHLCASEFALR.+3y12+2. (Light)	16059	18132
626.662	953.451	45.3	SFRP1.SEAIIEHLCASEFALR.+3y8. (Heavy)	2181	2444
625.321	953.451	45.3	SFRP1.SEAIIEHLCASEFALR.+3y8. (Light)	2564	2598
626.662	1066.535	45.3	SFRP1.SEAIIEHLCASEFALR.+3y9. (Heavy)	1365	1593
625.321	1066.535	45.3	SFRP1.SEAIIEHLCASEFALR.+3y9. (Light)	1602	739
413.263	429.312	31.2	SFRP1.SQYLLTAIHK.+3y3. (Heavy)	10321	10353
410.58	425.287	31.2	SFRP1.SQYLLTAIHK.+3y3. (Light)	42335	38654
413.263	500.349	31.2	SFRP1.SQYLLTAIHK.+3y4. (Heavy)	2076	2261
410.58	496.324	31.2	SFRP1.SQYLLTAIHK.+3y4. (Light)	15996	8904
413.263	601.397	31.2	SFRP1.SQYLLTAIHK.+3y5. (Heavy)	2773	1368
410.58	597.372	31.2	SFRP1.SQYLLTAIHK.+3y5. (Light)	4761	2755
413.263	714.481	31.2	SFRP1.SQYLLTAIHK.+3y6. (Heavy)	1481	838
410.58	710.456	31.2	SFRP1.SQYLLTAIHK.+3y6. (Light)	2926	1787
413.263	495.818	31.2	SFRP1.SQYLLTAIHK.+3y8+2. (Heavy)	5389	3201
410.58	493.805	31.2	SFRP1.SQYLLTAIHK.+3y8+2. (Light)	5953	4699
938.096	1168.633	41.5	SFRP2.DSLQCTCEEMNDINAPYLVMGQK.+3y10. (Heavy)	8428	3038

935.413	1164.608	41.5	SFRP2.DSLQCTCEEMNDINAPYLVMGQK.+3y10. (Light)	8753	2452
938.096	1281.717	41.5	SFRP2.DSLQCTCEEMNDINAPYLVMGQK.+3y11. (Heavy)	646	296
935.413	1277.692	41.5	SFRP2.DSLQCTCEEMNDINAPYLVMGQK.+3y11. (Light)	1790	399
938.096	1038.473	41.5	SFRP2.DSLQCTCEEMNDINAPYLVMGQK.+3y17+2. (Heavy)	750	335
935.413	1036.46	41.5	SFRP2.DSLQCTCEEMNDINAPYLVMGQK.+3y17+2. (Light)	692	416
938.096	983.553	41.5	SFRP2.DSLQCTCEEMNDINAPYLVMGQK.+3y8. (Heavy)	963	589
935.413	979.528	41.5	SFRP2.DSLQCTCEEMNDINAPYLVMGQK.+3y8. (Light)	979	397
938.096	1054.59	41.5	SFRP2.DSLQCTCEEMNDINAPYLVMGQK.+3y9. (Heavy)	1278	762
935.413	1050.565	41.5	SFRP2.DSLQCTCEEMNDINAPYLVMGQK.+3y9. (Light)	828	392
882.514	1133.669	53.6	SFRP2.EVLEQAGAWIPLVMK.+2y10. (Heavy)	3463	3625
878.489	1129.644	53.6	SFRP2.EVLEQAGAWIPLVMK.+2y10. (Light)	6234	5917
882.514	1261.728	53.6	SFRP2.EVLEQAGAWIPLVMK.+2y11. (Heavy)	736	388
878.489	1257.702	53.6	SFRP2.EVLEQAGAWIPLVMK.+2y11. (Light)	3462	2549
882.514	934.573	53.6	SFRP2.EVLEQAGAWIPLVMK.+2y7. (Heavy)	845	550
878.489	930.548	53.6	SFRP2.EVLEQAGAWIPLVMK.+2y7. (Light)	4431	5013
882.514	1005.61	53.6	SFRP2.EVLEQAGAWIPLVMK.+2y8. (Heavy)	1059	960
878.489	1001.585	53.6	SFRP2.EVLEQAGAWIPLVMK.+2y8. (Light)	3431	2081
882.514	1062.632	53.6	SFRP2.EVLEQAGAWIPLVMK.+2y9. (Heavy)	2121	1303
878.489	1058.607	53.6	SFRP2.EVLEQAGAWIPLVMK.+2y9. (Light)	1235	744
444.931	594.323	30.1	SFRP2.LPNLLGHETMK.+3y10+2. (Heavy)	119515	55316
442.248	592.311	30.1	SFRP2.LPNLLGHETMK.+3y10+2. (Light)	10624	5882
444.931	556.295	30.1	SFRP2.LPNLLGHETMK.+3y4. (Heavy)	9164	6349
442.248	552.27	30.1	SFRP2.LPNLLGHETMK.+3y4. (Light)	9422	5198
444.931	750.375	30.1	SFRP2.LPNLLGHETMK.+3y6. (Heavy)	17247	9213
442.248	746.35	30.1	SFRP2.LPNLLGHETMK.+3y6. (Light)	7230	5192
444.931	863.459	30.1	SFRP2.LPNLLGHETMK.+3y7. (Heavy)	909	658
442.248	859.434	30.1	SFRP2.LPNLLGHETMK.+3y7. (Light)	1117	964
444.931	545.797	30.1	SFRP2.LPNLLGHETMK.+3y9+2. (Heavy)	4250	2746
442.248	543.784	30.1	SFRP2.LPNLLGHETMK.+3y9+2. (Light)	3842	2407
814.463	1252.687	47.5	SHH.ELTPNYNPDIIFK.+2y10. (Heavy)	610	341
810.438	1248.662	47.5	SHH.ELTPNYNPDIIFK.+2y10. (Light)	840	589
814.463	1353.735	47.5	SHH.ELTPNYNPDIIFK.+2y11. (Heavy)	733	577
810.438	1349.71	47.5	SHH.ELTPNYNPDIIFK.+2y11. (Light)	560	419
814.463	878.528	47.5	SHH.ELTPNYNPDIIFK.+2y7. (Heavy)	1300	1205
810.438	874.503	47.5	SHH.ELTPNYNPDIIFK.+2y7. (Light)	781	467
814.463	1041.592	47.5	SHH.ELTPNYNPDIIFK.+2y8. (Heavy)	1023	569
810.438	1037.567	47.5	SHH.ELTPNYNPDIIFK.+2y8. (Light)	877	805
814.463	1155.635	47.5	SHH.ELTPNYNPDIIFK.+2y9. (Heavy)	13883	20771
810.438	1151.609	47.5	SHH.ELTPNYNPDIIFK.+2y9. (Light)	674	482
660.427	966.609	33.5	SHH.LAHALLAALAPAR.+2y10. (Heavy)	1848	893

658.414	966.609	33.5	SHH.LAHALLAALAPAR.+2y10. (Light)	2123	999
660.427	1103.668	33.5	SHH.LAHALLAALAPAR.+2y11. (Heavy)	15405	8384
658.414	1103.668	33.5	SHH.LAHALLAALAPAR.+2y11. (Light)	2559	1472
660.427	669.404	33.5	SHH.LAHALLAALAPAR.+2y7. (Heavy)	2560	1375
658.414	669.404	33.5	SHH.LAHALLAALAPAR.+2y7. (Light)	1732	703
660.427	782.488	33.5	SHH.LAHALLAALAPAR.+2y8. (Heavy)	31412	15568
658.414	782.488	33.5	SHH.LAHALLAALAPAR.+2y8. (Light)	2673	1469
660.427	895.572	33.5	SHH.LAHALLAALAPAR.+2y9. (Heavy)	1153	753
658.414	895.572	33.5	SHH.LAHALLAALAPAR.+2y9. (Light)	1373	343
652.003	780.874	29.4	SHH.SGGCFPGSATVHLEQGGTK.+3b15+2. (Heavy)	1300	1251
649.319	778.862	29.4	SHH.SGGCFPGSATVHLEQGGTK.+3b15+2. (Light)	8064	4608
652.003	658.859	29.4	SHH.SGGCFPGSATVHLEQGGTK.+3y13+2. (Heavy)	2686	2732
649.319	656.846	29.4	SHH.SGGCFPGSATVHLEQGGTK.+3y13+2. (Light)	2311	997
652.003	707.385	29.4	SHH.SGGCFPGSATVHLEQGGTK.+3y14+2. (Heavy)	2419	2725
649.319	705.373	29.4	SHH.SGGCFPGSATVHLEQGGTK.+3y14+2. (Light)	18091	11863
652.003	780.92	29.4	SHH.SGGCFPGSATVHLEQGGTK.+3y15+2. (Heavy)	1338	1725
649.319	778.907	29.4	SHH.SGGCFPGSATVHLEQGGTK.+3y15+2. (Light)	6996	5227
652.003	901.504	29.4	SHH.SGGCFPGSATVHLEQGGTK.+3y8. (Heavy)	2715	1944
649.319	897.479	29.4	SHH.SGGCFPGSATVHLEQGGTK.+3y8. (Light)	2998	1799
928.526	1045.655	49	SMO.DYVLCQANVTIGLPTK.+2y10. (Heavy)	687	327
924.5	1041.63	49	SMO.DYVLCQANVTIGLPTK.+2y10. (Light)	626	170
928.526	1173.714	49	SMO.DYVLCQANVTIGLPTK.+2y11. (Heavy)	441	279
924.5	1169.689	49	SMO.DYVLCQANVTIGLPTK.+2y11. (Light)	424	136
928.526	1333.745	49	SMO.DYVLCQANVTIGLPTK.+2y12. (Heavy)	652	229
924.5	1329.719	49	SMO.DYVLCQANVTIGLPTK.+2y12. (Light)	387	198
928.526	1446.829	49	SMO.DYVLCQANVTIGLPTK.+2y13. (Heavy)	390	289
924.5	1442.804	49	SMO.DYVLCQANVTIGLPTK.+2y13. (Light)	1304	997
928.526	974.618	49	SMO.DYVLCQANVTIGLPTK.+2y9. (Heavy)	574	380
924.5	970.593	49	SMO.DYVLCQANVTIGLPTK.+2y9. (Light)	1546	1301
762.892	1144.578	31	SMO.FNSSGQCEVPLVR.+2y10. (Heavy)	997	755
760.88	1144.578	31	SMO.FNSSGQCEVPLVR.+2y10. (Light)	1366	708
762.892	1231.61	31	SMO.FNSSGQCEVPLVR.+2y11. (Heavy)	821	821
760.88	1231.61	31	SMO.FNSSGQCEVPLVR.+2y11. (Light)	2059	1326
762.892	872.466	31	SMO.FNSSGQCEVPLVR.+2y7. (Heavy)	1499	721
760.88	872.466	31	SMO.FNSSGQCEVPLVR.+2y7. (Light)	1238	963
762.892	1000.524	31	SMO.FNSSGQCEVPLVR.+2y8. (Heavy)	1362	748
760.88	1000.524	31	SMO.FNSSGQCEVPLVR.+2y8. (Light)	641	442
762.892	1057.546	31	SMO.FNSSGQCEVPLVR.+2y9. (Heavy)	986	956
760.88	1057.546	31	SMO.FNSSGQCEVPLVR.+2y9. (Light)	1601	1214
616.32	913.449	16.9	SMO.GAASSGNATGPGPR.+2y10. (Heavy)	#N/A	#N/A
614.307	913.449	16.9	SMO.GAASSGNATGPGPR.+2y10. (Light)	41	34

616.32	1000.481	16.9	SMO.GAASSGNATGPGPR.+2y11. (Heavy)	#N/A	#N/A
614.307	1000.481	16.9	SMO.GAASSGNATGPGPR.+2y11. (Light)	32	22
616.32	1071.518	16.9	SMO.GAASSGNATGPGPR.+2y12. (Heavy)	68	67
614.307	1071.518	16.9	SMO.GAASSGNATGPGPR.+2y12. (Light)	65	45
616.32	769.395	16.9	SMO.GAASSGNATGPGPR.+2y8. (Heavy)	#N/A	#N/A
614.307	769.395	16.9	SMO.GAASSGNATGPGPR.+2y8. (Light)	29	12
616.32	826.417	16.9	SMO.GAASSGNATGPGPR.+2y9. (Heavy)	29	12
614.307	826.417	16.9	SMO.GAASSGNATGPGPR.+2y9. (Light)	#N/A	#N/A
749.914	951.541	28	SUFU.GIETDGSNLSGVSAK.+2y10. (Heavy)	5368	3245
745.888	947.516	28	SUFU.GIETDGSNLSGVSAK.+2y10. (Light)	2368	2696
749.914	1066.568	28	SUFU.GIETDGSNLSGVSAK.+2y11. (Heavy)	1574	951
745.888	1062.543	28	SUFU.GIETDGSNLSGVSAK.+2y11. (Light)	1396	922
749.914	1167.615	28	SUFU.GIETDGSNLSGVSAK.+2y12. (Heavy)	2264	1510
745.888	1163.59	28	SUFU.GIETDGSNLSGVSAK.+2y12. (Light)	1354	564
749.914	1296.658	28	SUFU.GIETDGSNLSGVSAK.+2y13. (Heavy)	1132	691
745.888	1292.633	28	SUFU.GIETDGSNLSGVSAK.+2y13. (Light)	575	#N/A
749.914	807.487	28	SUFU.GIETDGSNLSGVSAK.+2y8. (Heavy)	3372	2347
745.888	803.462	28	SUFU.GIETDGSNLSGVSAK.+2y8. (Light)	2345	1477
646.066	1115.727	38.8	SUFU.GLEINSKPVLPPINPQR.+3b10. (Heavy)	10225	9258
643.382	1107.677	38.8	SUFU.GLEINSKPVLPPINPQR.+3b10. (Light)	5824	8164
646.066	746.451	38.8	SUFU.GLEINSKPVLPPINPQR.+3y13+2. (Heavy)	2798	1680
643.382	744.438	38.8	SUFU.GLEINSKPVLPPINPQR.+3y13+2. (Light)	6742	6532
646.066	802.993	38.8	SUFU.GLEINSKPVLPPINPQR.+3y14+2. (Heavy)	1582	896
643.382	800.98	38.8	SUFU.GLEINSKPVLPPINPQR.+3y14+2. (Light)	2020	964
646.066	724.41	38.8	SUFU.GLEINSKPVLPPINPQR.+3y6. (Heavy)	5441	4648
643.382	724.41	38.8	SUFU.GLEINSKPVLPPINPQR.+3y6. (Light)	17332	22087
646.066	821.463	38.8	SUFU.GLEINSKPVLPPINPQR.+3y7. (Heavy)	2036	1358
643.382	821.463	38.8	SUFU.GLEINSKPVLPPINPQR.+3y7. (Light)	47486	60552
745.034	976.467	50.9	SUFU.VHEFTGTDGPSGFGFELTFR.+3b9. (Heavy)	682	366
743.692	972.442	50.9	SUFU.VHEFTGTDGPSGFGFELTFR.+3b9. (Light)	1942	1425
745.034	812.43	50.9	SUFU.VHEFTGTDGPSGFGFELTFR.+3y6. (Heavy)	2624	2013
743.692	812.43	50.9	SUFU.VHEFTGTDGPSGFGFELTFR.+3y6. (Light)	1300	718
745.034	869.452	50.9	SUFU.VHEFTGTDGPSGFGFELTFR.+3y7. (Heavy)	721	639
743.692	869.452	50.9	SUFU.VHEFTGTDGPSGFGFELTFR.+3y7. (Light)	671	512
745.034	1016.52	50.9	SUFU.VHEFTGTDGPSGFGFELTFR.+3y8. (Heavy)	1390	1158
743.692	1016.52	50.9	SUFU.VHEFTGTDGPSGFGFELTFR.+3y8. (Light)	1384	849
745.034	1073.542	50.9	SUFU.VHEFTGTDGPSGFGFELTFR.+3y9. (Heavy)	722	331
743.692	1073.542	50.9	SUFU.VHEFTGTDGPSGFGFELTFR.+3y9. (Light)	1044	679
614.321	746.407	37.6	TDGF1.DDSIWPQEEPAIRPR.+3y12+2. (Heavy)	1308	1193
612.979	746.407	37.6	TDGF1.DDSIWPQEEPAIRPR.+3y12+2. (Light)	1898	1494
614.321	789.923	37.6	TDGF1.DDSIWPQEEPAIRPR.+3y13+2. (Heavy)	1447	1309

612.979	789.923	37.6	TDGF1.DDSIWPQEEPAIRPR.+3y13+2. (Light)	1523	801
614.321	847.436	37.6	TDGF1.DDSIWPQEEPAIRPR.+3y14+2. (Heavy)	5918	7002
612.979	847.436	37.6	TDGF1.DDSIWPQEEPAIRPR.+3y14+2. (Light)	11517	20480
614.321	838.489	37.6	TDGF1.DDSIWPQEEPAIRPR.+3y7. (Heavy)	2522	1130
612.979	838.489	37.6	TDGF1.DDSIWPQEEPAIRPR.+3y7. (Light)	6122	8927
614.321	1095.591	37.6	TDGF1.DDSIWPQEEPAIRPR.+3y9. (Heavy)	4601	3170
612.979	1095.591	37.6	TDGF1.DDSIWPQEEPAIRPR.+3y9. (Light)	2088	1306
812.967	1195.706	69	TDGF1.FSYSVIWIMAISK.+2y10. (Heavy)	212	87
808.941	1191.681	69	TDGF1.FSYSVIWIMAISK.+2y10. (Light)	166	89
812.967	1358.769	69	TDGF1.FSYSVIWIMAISK.+2y11. (Heavy)	107	68
808.941	1354.744	69	TDGF1.FSYSVIWIMAISK.+2y11. (Light)	42	14
812.967	896.521	69	TDGF1.FSYSVIWIMAISK.+2y7. (Heavy)	291	268
808.941	892.496	69	TDGF1.FSYSVIWIMAISK.+2y7. (Light)	166	112
812.967	1009.605	69	TDGF1.FSYSVIWIMAISK.+2y8. (Heavy)	255	155
808.941	1005.58	69	TDGF1.FSYSVIWIMAISK.+2y8. (Light)	175	108
812.967	1108.674	69	TDGF1.FSYSVIWIMAISK.+2y9. (Heavy)	320	199
808.941	1104.649	69	TDGF1.FSYSVIWIMAISK.+2y9. (Light)	277	240
500.292	570.344	23.5	TDGF1.TPELPPSAR.+2b5. (Heavy)	1108	664
498.28	566.318	23.5	TDGF1.TPELPPSAR.+2b5. (Light)	535	356
500.292	527.294	23.5	TDGF1.TPELPPSAR.+2y5. (Heavy)	1094	1034
498.28	527.294	23.5	TDGF1.TPELPPSAR.+2y5. (Light)	437	419
500.292	640.378	23.5	TDGF1.TPELPPSAR.+2y6. (Heavy)	424	261
498.28	640.378	23.5	TDGF1.TPELPPSAR.+2y6. (Light)	649	485
500.292	769.42	23.5	TDGF1.TPELPPSAR.+2y7. (Heavy)	377	214
498.28	769.42	23.5	TDGF1.TPELPPSAR.+2y7. (Light)	188	118
500.292	866.473	23.5	TDGF1.TPELPPSAR.+2y8. (Heavy)	143	63
498.28	866.473	23.5	TDGF1.TPELPPSAR.+2y8. (Light)	251	188
713.422	1136.643	44.4	WIF1.ASVVQVGFPCLGK.+2y10. (Heavy)	1153	666
709.397	1132.618	44.4	WIF1.ASVVQVGFPCLGK.+2y10. (Light)	1461	887
713.422	753.427	44.4	WIF1.ASVVQVGFPCLGK.+2y6. (Heavy)	1657	1123
709.397	749.401	44.4	WIF1.ASVVQVGFPCLGK.+2y6. (Light)	4692	3615
713.422	810.448	44.4	WIF1.ASVVQVGFPCLGK.+2y7. (Heavy)	2529	1526
709.397	806.423	44.4	WIF1.ASVVQVGFPCLGK.+2y7. (Light)	4300	4552
713.422	909.516	44.4	WIF1.ASVVQVGFPCLGK.+2y8. (Heavy)	779	443
709.397	905.491	44.4	WIF1.ASVVQVGFPCLGK.+2y8. (Light)	1027	397
713.422	1037.575	44.4	WIF1.ASVVQVGFPCLGK.+2y9. (Heavy)	3484	3038
709.397	1033.55	44.4	WIF1.ASVVQVGFPCLGK.+2y9. (Light)	1713	804
728.307	910.37	29.5	WIF1.TCQQAECPGGCR.+2b7. (Heavy)	2666	1178
726.295	906.344	29.5	WIF1.TCQQAECPGGCR.+2b7. (Light)	5647	3023
728.307	1162.473	29.5	WIF1.TCQQAECPGGCR.+2y10. (Heavy)	1308	1111
726.295	1162.473	29.5	WIF1.TCQQAECPGGCR.+2y10. (Light)	6387	4786

728.307	835.319	29.5	WIF1.TCQQAECPGGCR.+2y7. (Heavy)	2004	1409
726.295	835.319	29.5	WIF1.TCQQAECPGGCR.+2y7. (Light)	4416	3721
728.307	906.356	29.5	WIF1.TCQQAECPGGCR.+2y8. (Heavy)	2610	1793
726.295	906.356	29.5	WIF1.TCQQAECPGGCR.+2y8. (Light)	4463	2615
728.307	1034.414	29.5	WIF1.TCQQAECPGGCR.+2y9. (Heavy)	1935	1516
726.295	1034.414	29.5	WIF1.TCQQAECPGGCR.+2y9. (Light)	1793	1300
913.044	1134.655	73	WIF1.VLIGFEEDILIVSEGK.+2y10. (Heavy)	380	292
909.019	1130.63	73	WIF1.VLIGFEEDILIVSEGK.+2y10. (Light)	236	141
913.044	1263.698	73	WIF1.VLIGFEEDILIVSEGK.+2y11. (Heavy)	218	180
909.019	1259.673	73	WIF1.VLIGFEEDILIVSEGK.+2y11. (Light)	211	132
913.044	1410.766	73	WIF1.VLIGFEEDILIVSEGK.+2y12. (Heavy)	146	87
909.019	1406.741	73	WIF1.VLIGFEEDILIVSEGK.+2y12. (Light)	98	66
913.044	1467.788	73	WIF1.VLIGFEEDILIVSEGK.+2y13. (Heavy)	116	73
909.019	1463.763	73	WIF1.VLIGFEEDILIVSEGK.+2y13. (Light)	101	90
913.044	1005.613	73	WIF1.VLIGFEEDILIVSEGK.+2y9. (Heavy)	277	229
909.019	1001.588	73	WIF1.VLIGFEEDILIVSEGK.+2y9. (Light)	218	170
1079.968	1239.491	38.7	WNT1.ACNSSSPALDGCELLCCGR.+2y10. (Heavy)	272	159
1077.955	1239.491	38.7	WNT1.ACNSSSPALDGCELLCCGR.+2y10. (Light)	296	153
1079.968	1352.576	38.7	WNT1.ACNSSSPALDGCELLCCGR.+2y11. (Heavy)	363	269
1077.955	1352.576	38.7	WNT1.ACNSSSPALDGCELLCCGR.+2y11. (Light)	294	208
1079.968	1423.613	38.7	WNT1.ACNSSSPALDGCELLCCGR.+2y12. (Heavy)	243	157
1077.955	1423.613	38.7	WNT1.ACNSSSPALDGCELLCCGR.+2y12. (Light)	248	147
1079.968	1067.443	38.7	WNT1.ACNSSSPALDGCELLCCGR.+2y8. (Heavy)	3569	4746
1077.955	1067.443	38.7	WNT1.ACNSSSPALDGCELLCCGR.+2y8. (Light)	460	255
1079.968	1124.465	38.7	WNT1.ACNSSSPALDGCELLCCGR.+2y9. (Heavy)	271	260
1077.955	1124.465	38.7	WNT1.ACNSSSPALDGCELLCCGR.+2y9. (Light)	385	328
670.703	1085.57	53.4	WNT1.ETAFIFAITSAGVTHSVAR.+3y11. (Heavy)	1244	913
669.362	1085.57	53.4	WNT1.ETAFIFAITSAGVTHSVAR.+3y11. (Light)	801	402
670.703	708.883	53.4	WNT1.ETAFIFAITSAGVTHSVAR.+3y14+2. (Heavy)	1903	816
669.362	708.883	53.4	WNT1.ETAFIFAITSAGVTHSVAR.+3y14+2. (Light)	3578	4492
670.703	765.425	53.4	WNT1.ETAFIFAITSAGVTHSVAR.+3y15+2. (Heavy)	12970	18311
669.362	765.425	53.4	WNT1.ETAFIFAITSAGVTHSVAR.+3y15+2. (Light)	22196	32111
670.703	838.96	53.4	WNT1.ETAFIFAITSAGVTHSVAR.+3y16+2. (Heavy)	1337	582
669.362	838.96	53.4	WNT1.ETAFIFAITSAGVTHSVAR.+3y16+2. (Light)	2395	1518
670.703	874.478	53.4	WNT1.ETAFIFAITSAGVTHSVAR.+3y17+2. (Heavy)	2273	951
669.362	874.478	53.4	WNT1.ETAFIFAITSAGVTHSVAR.+3y17+2. (Light)	3529	4428
618.016	1060.575	36	WNT1.QNPGILHSVSGGLQSAVR.+3y11. (Heavy)	19455	9672
616.674	1060.575	36	WNT1.QNPGILHSVSGGLQSAVR.+3y11. (Light)	11551	6526
618.016	655.862	36	WNT1.QNPGILHSVSGGLQSAVR.+3y13+2. (Heavy)	1951	1292
616.674	655.862	36	WNT1.QNPGILHSVSGGLQSAVR.+3y13+2. (Light)	1609	1076
618.016	789.442	36	WNT1.QNPGILHSVSGGLQSAVR.+3y16+2. (Heavy)	5901	4378

616.674	789.442	36	WNT1.QNPGILHSVSGGLQSAVR.+3y16+2. (Light)	7174	3795
618.016	787.442	36	WNT1.QNPGILHSVSGGLQSAVR.+3y8. (Heavy)	2981	4815
616.674	787.442	36	WNT1.QNPGILHSVSGGLQSAVR.+3y8. (Light)	10926	17916
618.016	874.474	36	WNT1.QNPGILHSVSGGLQSAVR.+3y9. (Heavy)	3163	1694
616.674	874.474	36	WNT1.QNPGILHSVSGGLQSAVR.+3y9. (Light)	2914	2104
422.539	486.243	29	WNT2.CHGVSGSCTLR.+3b4. (Heavy)	8003	3935
421.197	482.218	29	WNT2.CHGVSGSCTLR.+3b4. (Light)	62773	157898
422.539	630.297	29	WNT2.CHGVSGSCTLR.+3b6. (Heavy)	2582	2064
421.197	626.271	29	WNT2.CHGVSGSCTLR.+3b6. (Light)	1537	1439
422.539	717.329	29	WNT2.CHGVSGSCTLR.+3b7. (Heavy)	1052	1631
421.197	713.304	29	WNT2.CHGVSGSCTLR.+3b7. (Light)	1566	990
422.539	549.281	29	WNT2.CHGVSGSCTLR.+3y4. (Heavy)	5791	4583
421.197	549.281	29	WNT2.CHGVSGSCTLR.+3y4. (Light)	2806	1576
422.539	636.313	29	WNT2.CHGVSGSCTLR.+3y5. (Heavy)	22317	13235
421.197	636.313	29	WNT2.CHGVSGSCTLR.+3y5. (Light)	1965	1449
604.956	746.857	30.5	WNT2.CQDCLEALDVHTCK.+3y12+2. (Heavy)	5998	2988
602.272	744.845	30.5	WNT2.CQDCLEALDVHTCK.+3y12+2. (Light)	4664	3280
604.956	791.402	30.5	WNT2.CQDCLEALDVHTCK.+3y6. (Heavy)	10899	11394
602.272	787.377	30.5	WNT2.CQDCLEALDVHTCK.+3y6. (Light)	4463	3458
604.956	904.486	30.5	WNT2.CQDCLEALDVHTCK.+3y7. (Heavy)	9573	10542
602.272	900.461	30.5	WNT2.CQDCLEALDVHTCK.+3y7. (Light)	8104	7580
604.956	975.523	30.5	WNT2.CQDCLEALDVHTCK.+3y8. (Heavy)	1134	917
602.272	971.498	30.5	WNT2.CQDCLEALDVHTCK.+3y8. (Light)	1345	1099
604.956	1104.566	30.5	WNT2.CQDCLEALDVHTCK.+3y9. (Heavy)	1007	781
602.272	1100.541	30.5	WNT2.CQDCLEALDVHTCK.+3y9. (Light)	4244	3994
1010.556	1020.584	77.3	WNT2.ESAFVYAISSAGVVFAITR.+2y10. (Heavy)	143	83
1008.544	1020.584	77.3	WNT2.ESAFVYAISSAGVVFAITR.+2y10. (Light)	145	85
1010.556	1107.616	77.3	WNT2.ESAFVYAISSAGVVFAITR.+2y11. (Heavy)	181	96
1008.544	1107.616	77.3	WNT2.ESAFVYAISSAGVVFAITR.+2y11. (Light)	169	91
1010.556	1220.7	77.3	WNT2.ESAFVYAISSAGVVFAITR.+2y12. (Heavy)	83	65
1008.544	1220.7	77.3	WNT2.ESAFVYAISSAGVVFAITR.+2y12. (Light)	90	62
1010.556	1291.737	77.3	WNT2.ESAFVYAISSAGVVFAITR.+2y13. (Heavy)	151	113
1008.544	1291.737	77.3	WNT2.ESAFVYAISSAGVVFAITR.+2y13. (Light)	105	74
1010.556	1454.8	77.3	WNT2.ESAFVYAISSAGVVFAITR.+2y14. (Heavy)	112	32
1008.544	1454.8	77.3	WNT2.ESAFVYAISSAGVVFAITR.+2y14. (Light)	162	104
646.024	978.537	50.5	WNT3A.ESAFVHAIASAGVAFAVTR.+3y10. (Heavy)	2093	903
644.683	978.537	50.5	WNT3A.ESAFVHAIASAGVAFAVTR.+3y10. (Light)	1717	1328
646.024	593.341	50.5	WNT3A.ESAFVHAIASAGVAFAVTR.+3y5. (Heavy)	3249	2312
644.683	593.341	50.5	WNT3A.ESAFVHAIASAGVAFAVTR.+3y5. (Light)	3011	1611
646.024	664.378	50.5	WNT3A.ESAFVHAIASAGVAFAVTR.+3y6. (Heavy)	2015	1522
644.683	664.378	50.5	WNT3A.ESAFVHAIASAGVAFAVTR.+3y6. (Light)	3095	1794

646.024	763.446	50.5	WNT3A.ESAFVHAIASAGVAFAVTR.+3y7. (Heavy)	3020	1883
644.683	763.446	50.5	WNT3A.ESAFVHAIASAGVAFAVTR.+3y7. (Light)	2139	1059
646.024	820.468	50.5	WNT3A.ESAFVHAIASAGVAFAVTR.+3y8. (Heavy)	3815	3093
644.683	820.468	50.5	WNT3A.ESAFVHAIASAGVAFAVTR.+3y8. (Light)	5634	4016
483.252	651.804	27.6	WNT3A.IGIQECQHQFR.+3y10+2. (Heavy)	8945	10061
481.91	651.804	27.6	WNT3A.IGIQECQHQFR.+3y10+2. (Light)	8140	6325
483.252	587.305	27.6	WNT3A.IGIQECQHQFR.+3y4. (Heavy)	2132	1409
481.91	587.305	27.6	WNT3A.IGIQECQHQFR.+3y4. (Light)	5848	3726
483.252	502.722	27.6	WNT3A.IGIQECQHQFR.+3y7+2. (Heavy)	12367	11934
481.91	502.722	27.6	WNT3A.IGIQECQHQFR.+3y7+2. (Light)	4488	2241
483.252	566.751	27.6	WNT3A.IGIQECQHQFR.+3y8+2. (Heavy)	2939	2126
481.91	566.751	27.6	WNT3A.IGIQECQHQFR.+3y8+2. (Light)	7593	6772
483.252	623.293	27.6	WNT3A.IGIQECQHQFR.+3y9+2. (Heavy)	3353	1732
481.91	623.293	27.6	WNT3A.IGIQECQHQFR.+3y9+2. (Light)	4619	3912
809.85	1139.493	21.9	WNT3A.SCAEGTAAICGCSSR.+2y11. (Heavy)	113	#N/A
807.837	1139.493	21.9	WNT3A.SCAEGTAAICGCSSR.+2y11. (Light)	169	103
809.85	1268.536	21.9	WNT3A.SCAEGTAAICGCSSR.+2y12. (Heavy)	56	1
807.837	1268.536	21.9	WNT3A.SCAEGTAAICGCSSR.+2y12. (Light)	2	#N/A
809.85	839.35	21.9	WNT3A.SCAEGTAAICGCSSR.+2y7. (Heavy)	252	194
807.837	839.35	21.9	WNT3A.SCAEGTAAICGCSSR.+2y7. (Light)	57	#N/A
809.85	910.387	21.9	WNT3A.SCAEGTAAICGCSSR.+2y8. (Heavy)	171	57
807.837	910.387	21.9	WNT3A.SCAEGTAAICGCSSR.+2y8. (Light)	490	508
809.85	981.424	21.9	WNT3A.SCAEGTAAICGCSSR.+2y9. (Heavy)	339	246
807.837	981.424	21.9	WNT3A.SCAEGTAAICGCSSR.+2y9. (Light)	9127	11601
997.003	1078.531	41.9	WNT5A.ETAFTYAVSAAGVVNAMSR.+2y11. (Heavy)	562	208
994.991	1078.531	41.9	WNT5A.ETAFTYAVSAAGVVNAMSR.+2y11. (Light)	518	214
997.003	1177.599	41.9	WNT5A.ETAFTYAVSAAGVVNAMSR.+2y12. (Heavy)	445	422
994.991	1177.599	41.9	WNT5A.ETAFTYAVSAAGVVNAMSR.+2y12. (Light)	258	204
997.003	1248.636	41.9	WNT5A.ETAFTYAVSAAGVVNAMSR.+2y13. (Heavy)	380	316
994.991	1248.636	41.9	WNT5A.ETAFTYAVSAAGVVNAMSR.+2y13. (Light)	333	219
997.003	1411.7	41.9	WNT5A.ETAFTYAVSAAGVVNAMSR.+2y14. (Heavy)	409	232
994.991	1411.7	41.9	WNT5A.ETAFTYAVSAAGVVNAMSR.+2y14. (Light)	213	81
997.003	1512.748	41.9	WNT5A.ETAFTYAVSAAGVVNAMSR.+2y15. (Heavy)	206	122
994.991	1512.748	41.9	WNT5A.ETAFTYAVSAAGVVNAMSR.+2y15. (Light)	129	28
1260.107	1221.557	48	WNT5A.FNSPTTQDLVYIDPSPDYCVR.+2y10. (Heavy)	883	581
1258.094	1221.557	48	WNT5A.FNSPTTQDLVYIDPSPDYCVR.+2y10. (Light)	332	270
1260.107	1384.62	48	WNT5A.FNSPTTQDLVYIDPSPDYCVR.+2y11. (Heavy)	303	207
1258.094	1384.62	48	WNT5A.FNSPTTQDLVYIDPSPDYCVR.+2y11. (Light)	158	91
1260.107	1483.689	48	WNT5A.FNSPTTQDLVYIDPSPDYCVR.+2y12. (Heavy)	212	140
1258.094	1483.689	48	WNT5A.FNSPTTQDLVYIDPSPDYCVR.+2y12. (Light)	354	172
1260.107	993.446	48	WNT5A.FNSPTTQDLVYIDPSPDYCVR.+2y8. (Heavy)	473	266

1258.094	993.446	48	WNT5A.FNSPTTQDLVYIDPSPDYCVR.+2y8. (Light)	311	244
1260.107	1108.473	48	WNT5A.FNSPTTQDLVYIDPSPDYCVR.+2y9. (Heavy)	372	170
1258.094	1108.473	48	WNT5A.FNSPTTQDLVYIDPSPDYCVR.+2y9. (Light)	436	257
619.817	963.485	3.4	WNT5A.NESTGSLGTQGR.+2y10. (Heavy)	71	50
617.805	963.485	3.4	WNT5A.NESTGSLGTQGR.+2y10. (Light)	185	104
619.817	631.352	3.4	WNT5A.NESTGSLGTQGR.+2y6. (Heavy)	169	65
617.805	631.352	3.4	WNT5A.NESTGSLGTQGR.+2y6. (Light)	133	70
619.817	718.384	3.4	WNT5A.NESTGSLGTQGR.+2y7. (Heavy)	285	267
617.805	718.384	3.4	WNT5A.NESTGSLGTQGR.+2y7. (Light)	161	99
619.817	775.406	3.4	WNT5A.NESTGSLGTQGR.+2y8. (Heavy)	114	46
617.805	775.406	3.4	WNT5A.NESTGSLGTQGR.+2y8. (Light)	241	150
619.817	876.453	3.4	WNT5A.NESTGSLGTQGR.+2y9. (Heavy)	39	26
617.805	876.453	3.4	WNT5A.NESTGSLGTQGR.+2y9. (Light)	306	135

Curriculum Vitae

Name

Kevin Kania

Education

The University of Western Ontario
London, Ontario, Canada
Masters' in Biochemistry
2010-Present

The University of Western Ontario
London, Ontario, Canada
Bachelor of Medical Sciences
Honors Specialization in Biochemistry
2005-2009

Honours and Awards

Developmental Biology Student Award
University of Western Ontario
2011

Continuing Admission Scholarship
University of Western Ontario
2005-2009

Work Experience

Teaching Assistant
Biochemistry 4420a
The University of Western Ontario
2011-2013

Presentations

Kania, K.G., Postovit, L., Lajoie, G.A. Targeted Proteomics in Human Pluripotent Stem Cells. (2013) *Poster Presentation.* Oncology Research and Education Day. London, ON

Kania, K.G., Postovit, L., Lajoie, G.A. Targeted Proteomics in Human Pluripotent Stem Cells. (2013) *Poster Presentation.* London Health Research Day. London, ON

Kania, K.G., Postovit, L., Lajoie, G.A. Targeted Proteomics in Human Pluripotent Stem Cells. (2012) *Poster Presentation.* Developmental Biology Research Day.

Kania, K.G., Postovit, L., Lajoie, G.A. Targeted Proteomics in Human Pluripotent Stem Cells. (2012) *Poster Presentation.* Till and McCulloch Meetings. Montreal, QC.

Kania, K.G., Postovit, L., Lajoie, G.A. Detecting Low Abundance Proteins in Human Embryonic Stem Cells by Mass Spectrometry. (2011) *Poster Presentation.* Canadian Conference on Epigenetics. London, ON.